Declaration

I Nicola Isabel Barnard declare that the dissertation hereby submitted by me for the Magister Scientiae degree at the University of the Free State is my own independent work and has not previously been submitted by me at another university/faculty. I further more cede copyright of the dissertation in favour of the University of the Free State.

Signed:..... Date:.....

Synthesis, structural aspects and electrochemistry of ferrocene-containing betadiketonato titanium(IV) complexes with biomedical applications

Nicola Isabel Barnard

A dissertation submitted in accordance with the requirements for the degree

Magister Scientiae

In the

Department of Chemistry

Faculty of Natural and Agricultural Sciences

At the

University of the Free State

Date

May 2006

Supervisor

Prof. J.C. Swarts

Acknowledgements

In the name of Jesus Christ, my Lord and saviour. The Holy Spirit, may its light shine out from within me. All praise to God my gracious father without whom nothing is possible.

I would like to thank all my friends, family and colleagues for their support, friendship and guidance through the good times and the bad. Special appreciation must be made to the following people: My mother, Raelene Barnard, moomin you are truly an extraordinary person, my inspiration and my rock. My boyfriend, Luke Marais, for the many late nights and long days he has spent helping and supporting me. Elizabeth Erasmus, whose experience and willingness to share knowledge has been invaluable. Finally, my supervisor Jannie Swarts, probably the most intelligent, energetic, truly dedicated man I will ever meet. For your efforts and understanding I cannot thank you enough.

I feel I must also send a prayer to my late grandfather, Raymond Charles Goosen. As well as my dear father Jacobus Abraham Barnard, who passed away during the course of this study. They brought me into this world with every advantage, taught me courage, to embrace life and most importantly the wonder of love. May you rest in peace and in happiness.

I wish to acknowledge the National Research Foundation for their financial support during the course of this study. The CANSA Association of South Africa is also recognised for funding provided for this research.

Thank you.

Nicola Isabel Barnard

Table of contents

oooooooooooooooooooOOOooooooooooooooooo

List of abbreviations

A	absorbance
Å	angstrom
acac$^-$	2,4-pentanedionato, acetylacetonato
biphen^{2-}	2,2-biphenyldiolato
bipy	2,2-bipyridine
bzac$^-$	1-phenyl-1,3-butanedionato, benzoylacetonato
CH_3CN	acetonitrile
CH_3OH	methanol
cisplatin	*cis*-diamminedichlororplatinum(II)
CO	carbon monoxide or carbonyl
CoLo	human colorectral cell line
Cp	cyclopentadienyl $(C_5H_5)^-$
CV	cyclic voltammetry
δ	chemical shift
Hdbm	dibenzoylmethane
DCM	dichloromethane
DMSO	dimethyl sulfoxide
D_O	diffusion coefficient of the oxidized specie
D_R	diffusion coefficient of the reduced specie
ε	molecular extinction coefficient
E	applied potential
$E^{0/}$	formal reduction potential
E_{pa}	peak anodic potential
E_{pc}	peak cathodic potential
ΔE_p	separation of peak anodic and peak cathodic potentials
Et	ethyl

Fc	ferrocene or ferrocenyl (Note: strictly ferrocene should be Hfc and fc ferrocenyl, but it is customary in electrochemistry to abbreviate the ferrocene/ferrocenium couple as Fc/Fc^+. In this document this notation will be accepted as the current form.)
fca$^-$	1-ferrocenoyl-1,3-butanedionato, ferrocenoylacetonato
ΔG^*	free energy of activation
Hacac	2,4-pentanedinel, acetylacetone
Hbzac	1-phenyl-1,3-butanedione, benzoylacetone
HeLa	human cervix epitheloid cancer cell line
hfaa$^-$	1,1,1,5,5,5-hexafluoro-2,4-pentanedionato, hexafluoroacetylacetonato
Hfca	1-ferrocenoyl-1,3-butanedione, ferrocenoylacetone
Hmaa	1-methoxy-1,3-butanedione, methyl acetoacetone
HSacac	4-thioxopenatan-2-one, thioacetylacetone
Htfaa	1,1,1-trifluoro-2,4-pentanedione, trifluoroacetylacetone
Htfba	1-phenyl-3-trifluorobutanedione, trifluorobenzoylacetone
IC_{50}	mean drug concentration causing 50% cell death
i_{pa}	peak anodic current
i_{pc}	peak cathodic current
k	rate constant
k_{obs}	observed rate constant
L	ligand
LDA	lithium diisopropylamide
LSV	linear sweep voltammetry
M	central metal atom
maa$^-$	1-methoxy-1,3-butanediolato, methyl acetoacetonato
Mc	metallocenyl, $(C_5H_5)_2M^{2+}$
$McCl_2$	metallocene dichloride
Me	methyl

n	number of electrons
NHE	normal hydrogen electrode
^{1}H NMR	nuclear magnetic resonance spectroscopy
Ph	phenyl (C_6H_5)
phen	1,10-phenanthroline
pK_a	-log K_a, K_a = acid dissociation constant
ppm	parts per million
Pr^i	isopropyl
S	solvent
SCE	standard calomel electrode
SHE	standard hydrogen electrode
SW	Oster Young square wave voltammetry
T	temperature
$TBAFP_6$	tetrabuthylammonium hexafluorophosphate
Tc	titanocenyl, biscyclopentadienyltitanium(IV), $(C_5H_5)_2Ti^{2+}$
$TcCl_2$	titanocene dichloride, dichlorobiscyclopentadienyltitanium(IV)
$tfaa^-$	1,1,1-trifluoro-2,4-pentanediolato, trifluoroacetylacetonato
$tfba^-$	1-phenyl-3,3,3-trifluorobutanediolato, trifluorobenzoylacetonato
THF	tetrahydrofuran
X	halogen
χ_R	group electronegativity (Gordy scale) of R-group

List of Structures

Precursors

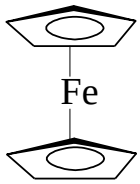

[1] Ferrocene (Fc)

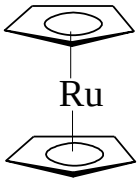

[2] Ruthenocene (Rc)

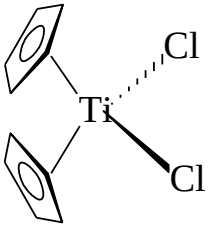

[3] Titanocene dichloride $[Cp_2TiCl_2]$

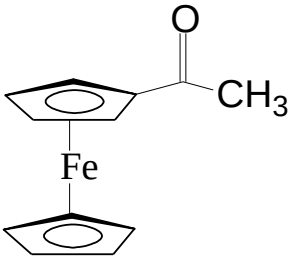

[4] Acetylferrocene

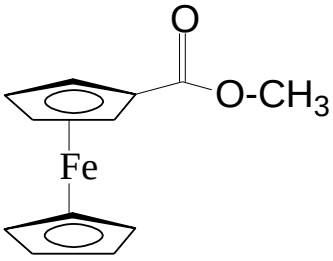

[5] Methyl ferrocenoate

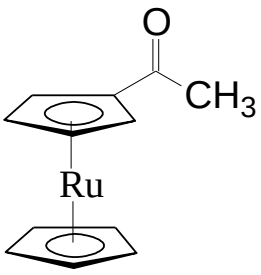

[6] Acetylruthenocene

Ferrocene-containing β-diketones

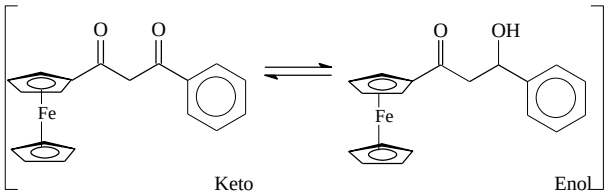

[7] [$FcCOCH_2COPh$]

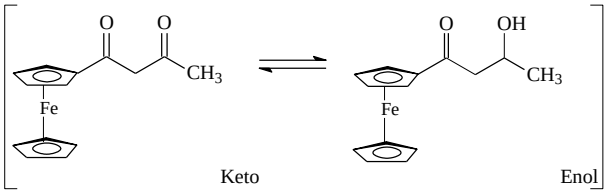

[8] [$FcCOCH_2COCH_3$]

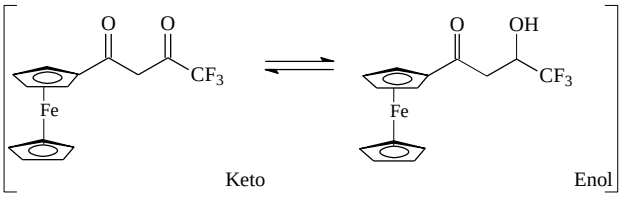

[9] [$FcCOCH_2COCF_3$]

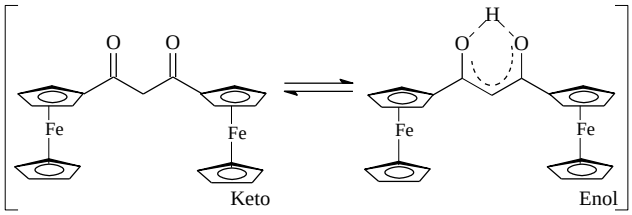

[10] [$FcCOCH_2COFc$]

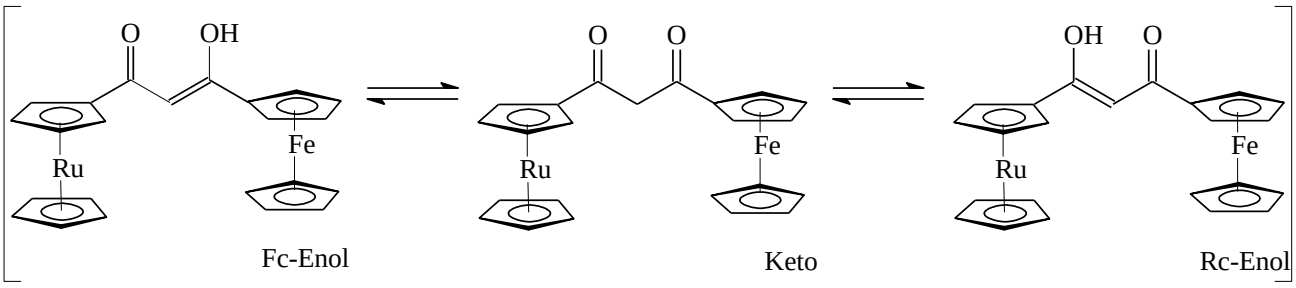

[11] [$FcCOCH_2CORc$]

Mono-β-diketonato titanium(IV) salts

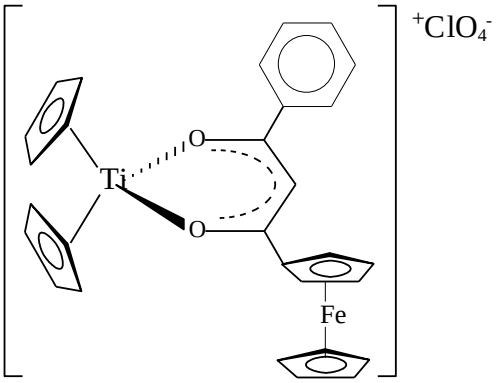

[12] $[Cp_2Ti(FcCOCHCOPh)ClO_4$

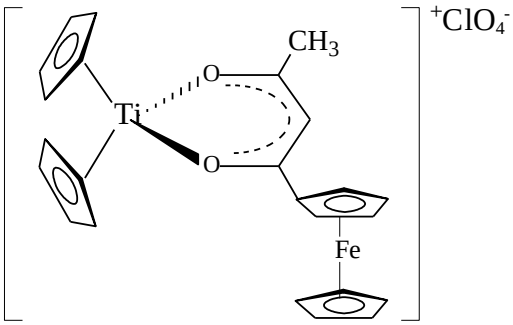

[13] $[Cp_2Ti(FcCOCHCOCH_3)ClO_4]$

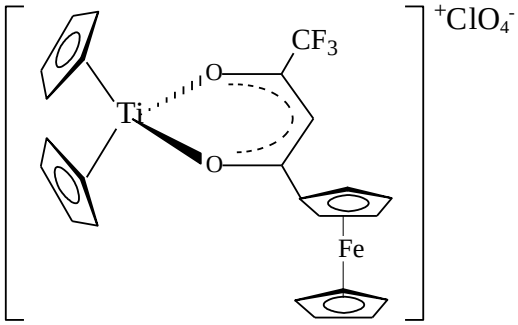

[14] $[Cp_2Ti(FcCOCHCOCF_3)ClO_4]$

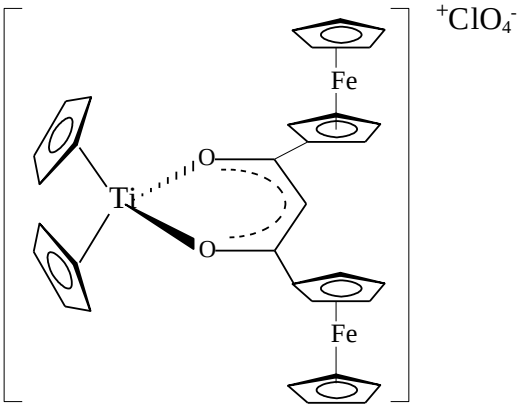

[15] $[Cp_2Ti(FcCOCHCOFc)ClO_4]$

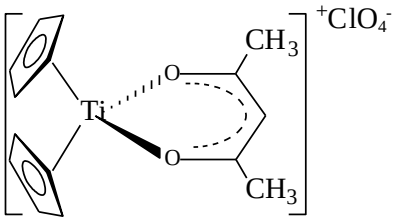

[16] $[Cp_2Ti(CH_3COCHCOCH_3)ClO_4]$

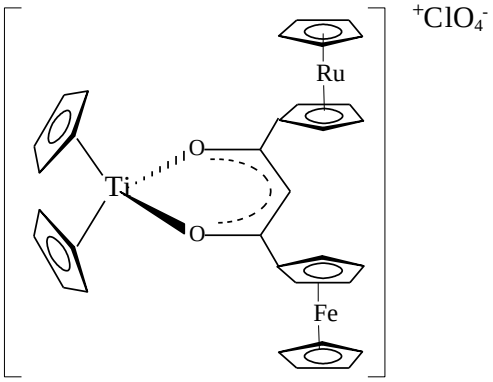

[17] $[Cp_2Ti(FcCOCHCORc)ClO_4]$

Dichlorobis-β-diketonato titanium(IV) complexes

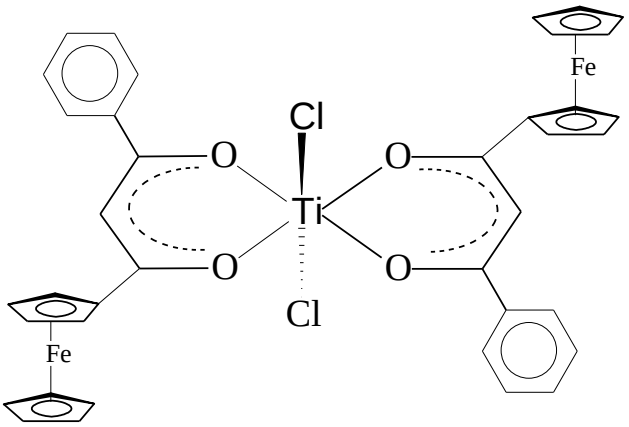

[18] $[(FcCOCHCOPh)_2TiCl_2]$

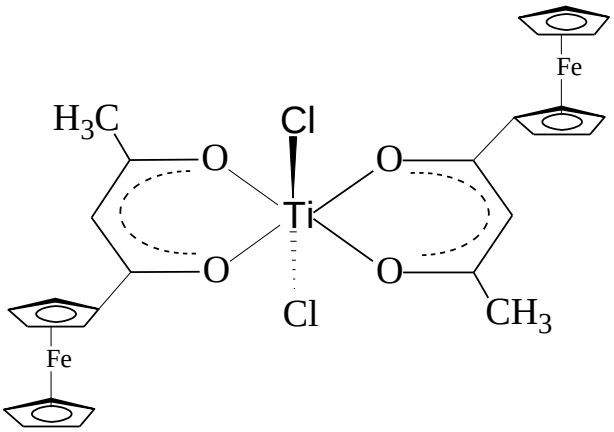

[19] $[(FcCOCHCOCH_3)_2TiCl_2]$

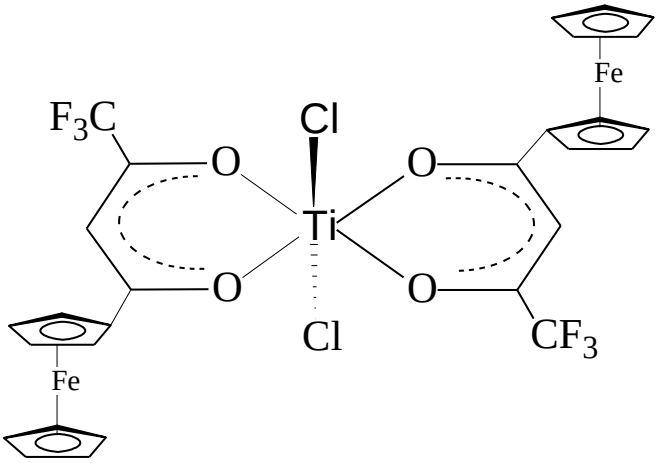

[20] $[(FcCOCHCOCF_3)_2TiCl_2]$

Di(1-oxyethyl-1-ferrocenyl)bis(β-diketonato)titanium(IV) complexes

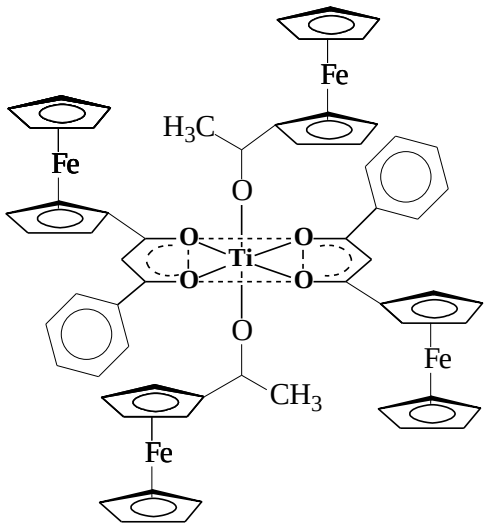

[21] $[(FcCOCHCOPh)_2Ti(O\text{-}CH\text{-}(CH_3)\text{-}Fc)_2]$

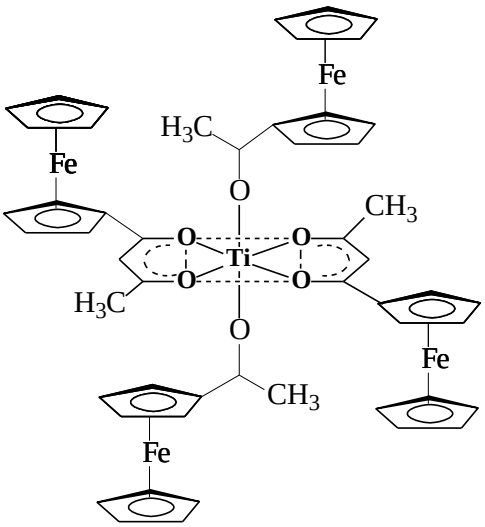

[22] $[(FcCOCHCOCH_3)_2Ti(O\text{-}CH\text{-}(CH_3)\text{-}Fc)_2]$

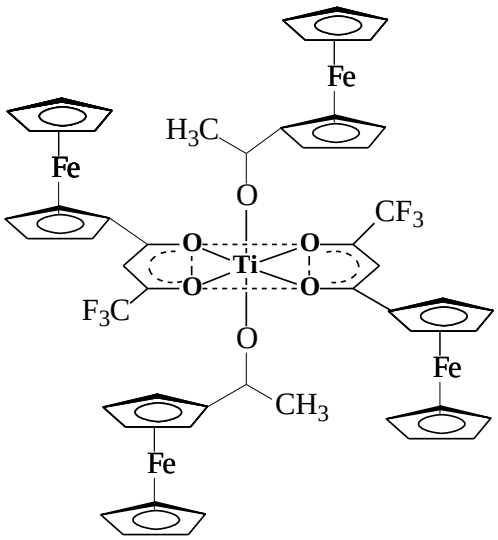

[23] $[(FcCOCHCOCF_3)_2Ti(O\text{-}CH\text{-}(CH_3)\text{-}Fc)_2]$

Supporting electrolytes

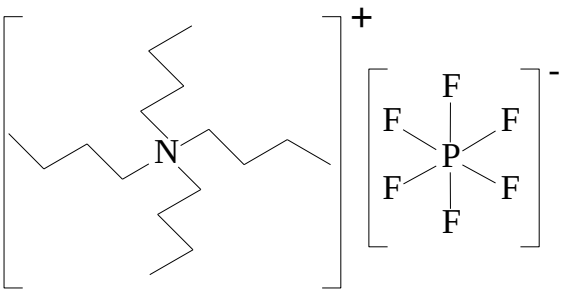

[24] tetra-n-butylammonium hexafluorophosphate

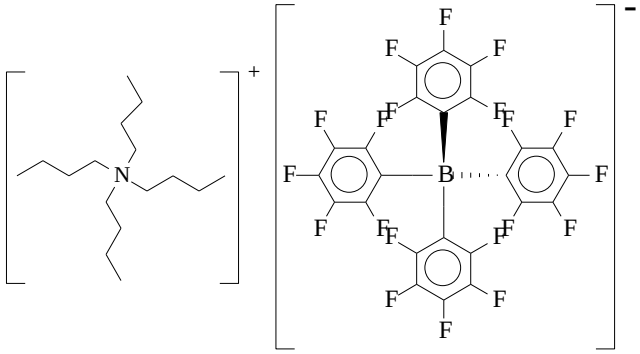

[25] $[N(^{n}Bu)_4B(C_6F_5)_4]$ (BARF)

Chapter 1

Introduction and aims of study

1.1. Introduction

1.1.1. Metallocenes

After the initial discovery of the first ever metallocene, ferrocene [dicyclopentadienyl iron(II)], Sir Geoffrey Wilkinson and Fischer shared the Nobel Prize for chemistry in 1973, for their work in developing metallocenes as a whole new class of compounds.[1]

There are currently many different areas of study involving the chemistry of metallocenes. These include organic synthesis,[2] metallocenes as catalysts or catalytic components in a variety of reactions,[1] as flame-retardants,[3] smoke suppressants and intriguingly in medical applications.[4-8]

1.1.2. Metallocenes as catalysts

Metallocenes have been called the single most important development in catalyst technology. In 1957 Giulio Natta reported the polymerization of ethylene using titanocene dichloride as catalyst. Polymerization was accomplished in the presence of the co-catalyst, trimethyl aluminium. Metallocene-based catalysts have especially revolutionised the immense polyolefin industry. The key to the success of metallocenes as catalysts lies in the ease by which the structure of the catalyst complex may be modified to yield linear and stereochemically controlled polymers.

Ferrocene itself and its derivatives have been the topic of numerous studies and have found application as colour pigments, high burning rate catalysts in solid fuels, liquid fuel combustion catalysts and as smoke suppressants.[9]

1.1.3. Antineoplastic activity of metallocenes

An exciting new field in which metallocenes can be utilised has been developing after the discovery that certain metallocene derivatives show pronounced antineoplastic activity.

In 1979 the antitumor properties of titanocene dichloride, [Cp_2TiCl_2] **[3]**, were reported by Köpf and co-workers.[10] [Cp_2TiCl_2] as a cancer therapeutic agent is currently in phase II clinical trials. All the dihalides of titanocene and a number of other transition metals have displayed (hydrophobic, organometallic) anti-tumour activity.[11] In addition these cytotoxic activities have been demonstrated against numerous cancerous cell lines. Many other titanocene derivatives also exhibit antineoplastic properties.[12-14] Titanium tends to accumulate in nucleic acid rich regions of tumour cells; titanocene dichloride has also been shown to inhibit DNA and RNA synthesis. Formation of metallocene-DNA complexes has been implicated in the mechanism of these compounds anti-tumour properties.[15,16]

Ferrocene is another metallocene which has shown promise in a number of biomedical applications, including as a mediator in glucose biosensoring.[17] Another medical application for ferrocene derivatives has been identified with reports that some of these compounds demonstrate antineoplastic activity against a number of cell lines which are resistant to classical anti-tumour drugs.[18] In 1984 Köpf-Maier *et al*[19] was the first to show that the ferricenium species have appreciable activity against cancer. In follow up studies, Neuse and co-workers[20] found ferrocenylacetic acid induced good to excellent cure rates against various *in vitro* human tumour clonogenic assays. Most recently, Osella and co-workers have determined the mechanism of action of the ferrocenyl moiety in chemotherapy to be one of electron transfer.[21]

The vastly different chemical and hydrolytic stability of each of the metallocenes points to a unique mechanism of action for each metallocene *in vivo.*[16]

1.1.4. Problems associated with chemotherapeutic drugs

Many drawbacks are associated with current cancer therapies and many potentially useful antineoplastic materials suffer from negative side effects which limit or exclude their use in clinical chemotherapy. Some of the problems, which this study has concentrated on and tried to address, are:

Poor aqueous solubility: As the human body consists of approximately 70% water, aqueous solubility has obvious administration and absorption advantages.

By developing antineoplastic compounds with high aqueous solubility, the body's own circulatory system (blood) may be utilised for distribution of the drug within the patient.[22]

Drug resistance: The metastatic nature of cancer cells leads to drug resistance after continued dosage.[23] In addition, multiple administrations of more than one type of antineoplastic drug (multidrug regiments with differing mechanisms, intracellular sites of action, and toxicities) sometimes lead to multidrug resistance.

Combining more than one antineoplastic moiety into one compound will allow simultaneous administration of a number of anti-tumour drugs and may have the additional advantage of showing synergistic effects between the antineoplastic moieties.

Toxicity: Probably the most important limiting factor for most anti-cancer drugs is the narrow therapeutic index between cell kill of cancer cells and that of normal cells. That is to say current chemotherapeutic agents are unable to distinguish between cancer cells and healthy cells.[24]

Development of antineoplastic materials with highly selective absorption by cancerous cells would be greatly advantageous.

A compound which is able to overcome these problems and which encompasses the suggested advantages would indeed be a giant leap forward in the continuing battle against cancer.

1.2. Aims of study

With this background, the following goals were set for this study:

1. Synthesis of the five ferrocene-containing β-diketones, [$FcCOCH_2COR$] where R = CH_3, CF_3, C_6H_5, Fc, Rc.

   Here Fc and Rc are the ferrocenyl $(C_5H_5)Fe(C_5H_4)$ and ruthenocenyl $(C_5H_5)Ru(C_5H_4)$ group respectively. Cp = $C_5H_5^-$ = cyclopentadienyl ring.

2. Synthesis of the new sp^3 hybridised titanocenyl complexes $[Cp_2Ti(FcCOCHCOR)]^+ClO_4^-$. The β-diketonato ligands are those derived from goal 1. The resulting complexes are unique in that they incorporate two different metallocene centres within the same molecule. Their ionic character will also help improve aqueous compatibility.

3. Synthesis and characterisation of the mixed metal, octahedral, titanium(IV) complexes $[(FcCOCHCOR)_2TiCl_2]$ and $[(FcCOCHCOR)_2Ti(O\text{-}CH\text{-}(CH_3)\text{-}Fc)_2]$ with R = C_6H_5 (Ph), CH_3, CF_3.

4. Electrochemical characterisation of the synthesised complexes utilising cyclic, square wave and linear sweep voltammetry. The results will allow the determination of the formal reduction potentials of the redox active ferrocenyl and titanocenyl centres. It will also highlight any intramolecular communication between the redox active metal centres.

5. Single crystal, crystallographic characterisation of [$FcCOCH_2CORc$] **[11]** and $[Cp_2Ti(FcCOCHCOCH_3)]^+ClO_4^-$ **[13]**, as representative examples of each of the classes of compounds from goal 1 and 2.

6. Cytotoxicity studies of the titanium complexes $[Cp_2Ti(FcCOCHCOR)]^+ClO_4^-$, to determine any antineoplastic activity they may possess, as well as highlighting any synergistic effects which the antineoplastic ferrocenyl and titanocenyl groups may exhibit.

1.3. References

[1] G. Wilkinson, Editor, *Comprehensive Organometallic Chemistry*, vol. 3, Pergamon Press, Oxford, 1982, p. 475-545 and references therein.

[2] G. Wilkinson, Editor, *Comprehensive Organometallic Chemistry*, vol. 3, Pergamon Press, Oxford, 1982, p. 273-278 and references therein.

[3] E.W. Neuse, J.R. Woodhouse, G. Montaudo and S. Puglisi, *Appl. Organomet. Chem.*, 53, **2** (1988).

[4] E.W. Neuse and F. Kanzawa, *Appl. Organomet. Chem.*, 19, **4** (1990).

[5] P. Köpf-Maier, S. Grabowski, J. Liegener and H. Köpf, *Inorg. Chim. Acta*, 99 , **108** (1985).

[6] E. Meléndez, *Crit. Rev. Oncol.*, 309, **42** (2002).

[7] P. Köpf-Maier, M. Leitner and H. Köpf, *J. Inorg. Nucl. Chem.*, 1789 , **42** (1980).

[8] P. Köpf-Maier, M. Leitner, R. Voigtlander and H. Köpf, *Z. Naturforsch.*, 1174, **34C** (1979).

[9] W.C. du Plessis, T.G. Vosloo and J.C. Swarts, *J. Chem. Soc., Dalton Trans.*, 2507 (1998).

[10] H. Köpf and P. Köpf Meier, *Angew. Chem.*, 477, **18** (1979).

[11] B.K. Keppler and M.E. Heim, *Drugs of the Future*, 638, **3** (1988).

[12] P. Köpf-Maier and H. Köpf, *Struct. Bonding*, 103, **70** (1988).

[13] P.Köpf-Maier and H. Köpf, *Chem. Rev.*, 1137, **87** (1987).

[14] P. Köpf-Maier, *Eur. J. Clin. Pharmacol.*, 1, **47** (1994).

[15] M. Guo, H. Sun, H.J. McArdle, L. Gambling and P.J. Sadler, *Biochemistry*, 10023, **39** (2000).

[16] M.M. Harding and G. Mokdsi, *Curr. Med. Chem.*, 1289, **7** (2000).

[17] N.J. Long, *Metallocenes: An Introduction to Sandwich Complexes*, Blackwell Science, London, p. 258 (1998).

[18] P. Köpf, *Naturforsch. C. Biochem. Biophys. Biol. Virol*, 843, **40** (1985).

[19] P. Köpf-Maier and H. Köpf and E. W. Neuse, *J Cancer Res. Clin. Oncol.*, 336, **108** (1984).

[20] E. W. Neuse and F. Kanzawa, *Appl. Organomet. Chem.*, 19, **4** (1990).

[21] D. Osella, M. Ferrali, P. Zanello, F. Laschi, M. Fontani, C. Nervi and G. Cavigiolio, *Inorg. Chim. Acta*, 42, **306** (2000).

[22] J.C. Swarts, *Macromol. Symp,*. 123, **186** (2002).

[23] W. Wolf, R.C. Manaka, *J. Chem. Hemotol. Oncol.*, 79, **7** (1977).

[24] R. Duncan, J. Kopecek, *Adv. Polym. Sci.*, 51, **57** (1984).

Chapter 2

Literature Survey

2.1. Introduction

Organometallic chemistry is a rapidly emerging field of interest as highlighted by the recently held International Symposium on Bioorganometallic Chemistry, Paris (France) July 2002, as well as recent review articles in journals such as the *Journal of Organometallic Chemistry* and *Organometallics.*[1]

Many of these compounds have been reported to show significant antineoplastic activity and this chemotherapeutic activity is currently the topic of numerous studies both locally in South Africa and internationally.

As this research program is focused on the synthesis, characterization and biomedical application of new ferrocene-containing betadiketonato (β-diketonato) complexes of titanium(IV), a literature survey of typical ferrocene and titanium chemistry and related topics is relevant.

2.2. The Chemistry of β-diketones

2.2.1. Synthesis

β-diketones may be formed by a Claisen condensation reaction. The reaction involves the replacement of an α–hydrogen atom of a ketone by an acyl group. Under appropriate conditions the ketone can be acetylated with an ester, acid anhydride or an acid chloride to form the desired β-diketone.[2] Although Lewis acids such as BF_3 can be used to promote β-diketone formation, the strong electron donating properties of a ferrocenyl group lowers the acidity of the methyl hydrogen atoms of acetylferrocene **[4]**, which in turn necessitates the use of strong bases to produce reasonable yields. These bases include metal amides such as potassium amide used by Hauser and co-workers to prepare various ferrocene containing β-diketones in liquid ammonia as solvent.[3] Alkoxides including sodium methoxide were utilised by Weinmayer as basic initiator in diethyl ether,[4] while Cullen *et al* favoured the use of the sterically hindered base lithium diisopropylamide ($LiNPr^i_2$) in their preparations.[5]

An adaptation of the method of Cullen *et al* was later reported to produce the most favourable results for ferrocene - containing β-diketones, producing higher yields in faster reactions.[6] Ketone acylation with esters probably involves a three-step ionic mechanism.[2] The basic condensation of acetone with ethyl acetate utilising sodium ethoxide is shown as a representative example in **Scheme 2.1.**

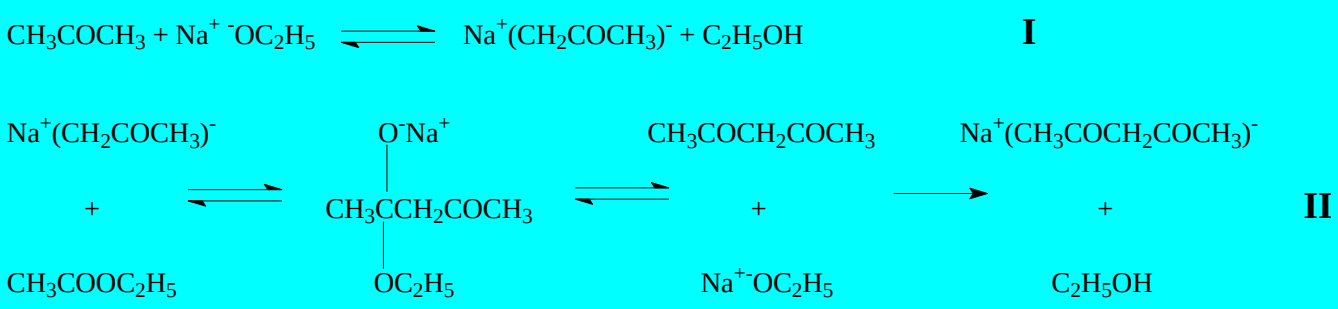

Scheme 2.1. Basic condensation of acetone with ethyl acetate utilising sodium ethoxide as initiator.

The first step involves the removal of an α–hydrogen from the ketone to form the acetonato anion. (**I** in **Scheme 2.1.**).

The second step may be formulated as the addition of the acetonato anion to the cabonyl carbon of ethyl acetate.

This is followed by the release of the ethoxide ion to form acetylacetone. The pK_a of β-diketones are so low (e.g. pK_a of [$CH_3COCH_2COCH_3$] = 8.95) that it is invariably isolated as the salt (the final step in **Scheme 2.1.**) and must be regenerated by acidification.

With the ethoxide anion as initiator, the equilibrium in the first step of **Scheme 2.1** is probably on the side of the unchanged ketone (i.e. to the left). However when a much stronger base ($NaNH_2$) is used, an equivalent of ketone is converted essentially completely to its anion and ammonia, NH_3. Ammonia(g) is liberated at the end of the reaction rather than ethanol, C_2H_5OH.

A common side effect associated with β-diketone synthesis is self-aldol condensation, especially in the case of acetylferrocene. This reaction is discussed in greater detail in paragraph 2.8.2. The effect can be minimised provided the added base is never the limiting reagent. The final product is then isolated via column chromatography.[6]

2.2.2. Keto-enol tautomerism

Although typically presented in ketonic form, most β-diketones exist as keto and enol isomers which are in equilibrium with each other. The enol isomer is stabilized by a hydrogen bridge and may exist as two tautomers as shown in **Scheme 2.2.** The conversion kinetics from one enol form to the other is normally very fast, with a rate constant approaching $10^6.s^{-1}$. Utilizing ^{17}O NMR, Kwon and Moon also observed that the equilibrium constant (K_{enol}) is highly dependant on the character and position of the R groups.[7]

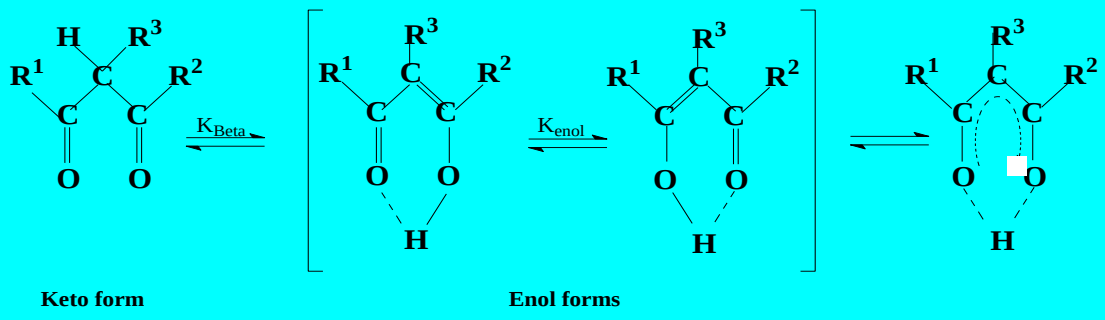

Scheme 2.2. Schematic representation of tautomerism of β-diketones with the enol form showing pseudo aromatic character.

The hydrogen atom of the CHR^3 group in the keto form is very acidic because of the adjacent, electron withdrawing, C=O groups. Observed pK_a values for several β-diketones are listed in **Table 2.1.** The keto-enol tautomerism of a wide variety of β-diketones has been studied extensively over the years.[8-13] It has been generally accepted that the enolic form is favoured in non-polar solvents, and simultaneous conjugation and chelation through hydrogen bonding is responsible for the stability of the enol tautomer.

Table 2.1. pKa values and % enol isomers of various β-diketones of the form R^1COCH_2COR.[2]

β-diketone	**R^1**	**R^2**	**pKa**	**% Enol**
Hacac	CH_3	CH_3	8.95[6]	91
Htfaa	CH_3	CF_3	6.30[14]	>99
Hba	CH_3	C_6H_5	8.55[6]	92
Hdbm	C_6H_5	C_6H_5	9.35[14]	>99
Hhfaa	CF_3	CF_3	4.43[14]	100
Hfca	Fc	CH_3	10.01[6]	77.5[15]
Hfctfa	Fc	CF_3	6.53[6]	95.1[15]
Hbfcm	Fc	C_6H_5	10.41[6]	91.2[15]
Hdfcm	Fc	Fc	13.10[6]	67.1[15]

The proportion of enol tautomers in β-diketones generally increases when an electron withdrawing group is substituted for hydrogen at an α-position relative to a carbonyl group or when the ligands contain an aromatic ring,[16] whereas substitution of a bulky group (such as an alkyl) at the α-position tends to bring about a large decrease in enol proportion.[17]

Concerning β-diketones with a ferrocenyl group, enolisation in solution was found to be predominantly away from the arromatic ferrocenyl group.[6] A resonance driving force appears to control the conversion from β-diketone into an enolic isomer. This resonance driving force implies that formation of different canonical forms of a specific isomer will lower the energy of this specific isomer enough to allow it to dominate over other isomers which might be favoured by electronic effects (see **Scheme 2.3**).

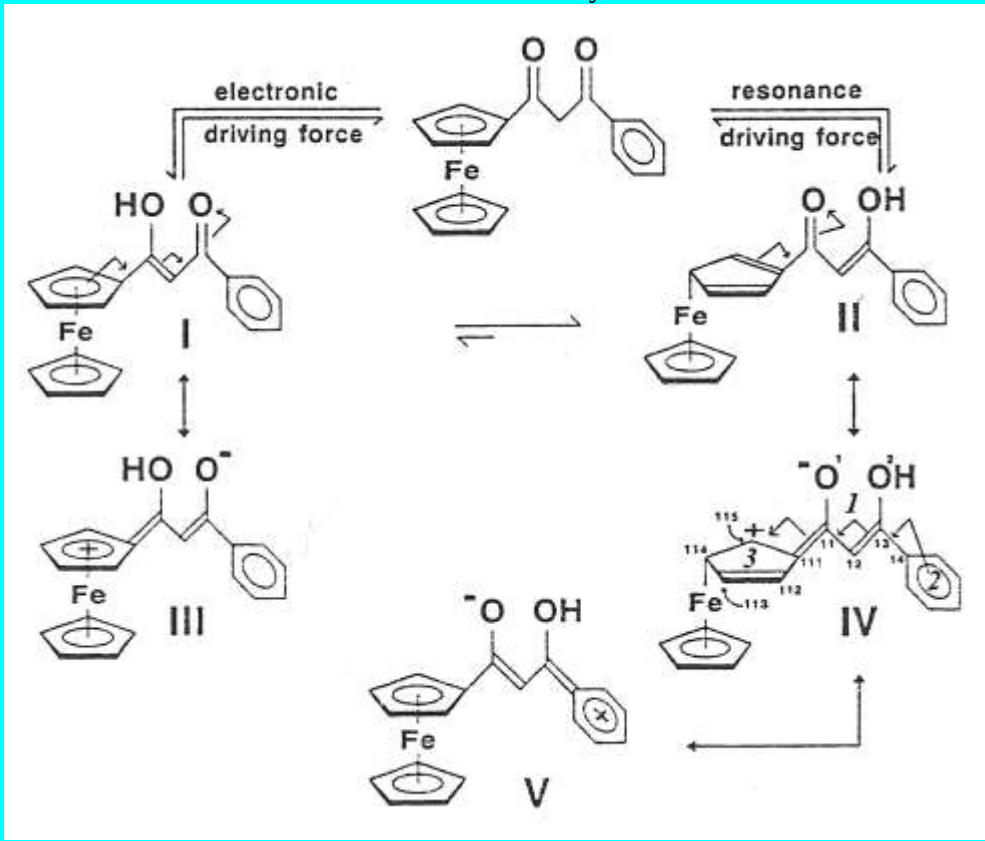

Scheme 2.3. Electronic considerations in terms of R group electronegativity, χ_R (χ_{methyl} = 2.34, $\chi_{ferrocenyl}$ = 1.87), favour I as the enol form for [$FcCOCH_2COPh$]. However, structure II was shown by crystallography and NMR spectroscopy to be dominant, implying the equilibrium between I and II lies far to the right because resonance stabilisation is the main driving force.[15] According to the resonance driving force related structures (zwitterions IV and V) stabilise structure II much more effectively than zwitterion III stabilises I. (From W.C. du Plessis, T.G. Vosloo and J.C. Swarts, *J. Chem. Soc., Dalton Trans.*, 2507 (1998).

Kinetic investigations for simple ferrocene-containing β-diketones found that the rate of conversion from keto to enol isomers is very slow ($t_{½}$ = 4.4 hours for [$FcCOCH_2COCH_3$]). Many β-diketones are isolated as the solid Li salt [R^1-CO-$CHLi^+$-CO-R^2] from solution. Liberation of the free β-diketone is achieved by acidification. The lithium salt exists predominantly as a keto isomer, therefore the first product obtained from the synthetic procedure is also the keto isomer. If the ^{1}H NMR is obtained within minutes after acidification, the keto isomer will appear to be dominant. Several days later enough time would have elapsed to allow conversion of the keto form to the equilibrium keto content, with ^{1}H NMR showing enol dominance. It is interesting to note that in the solid state the enol form is the only stable isomer for the ferrocene-containing β-diketones. In solution, the equilibrium position has up to 32% keto isomer content.[15]

2.3. Ferrocene Chemistry

2.3.1. Introduction

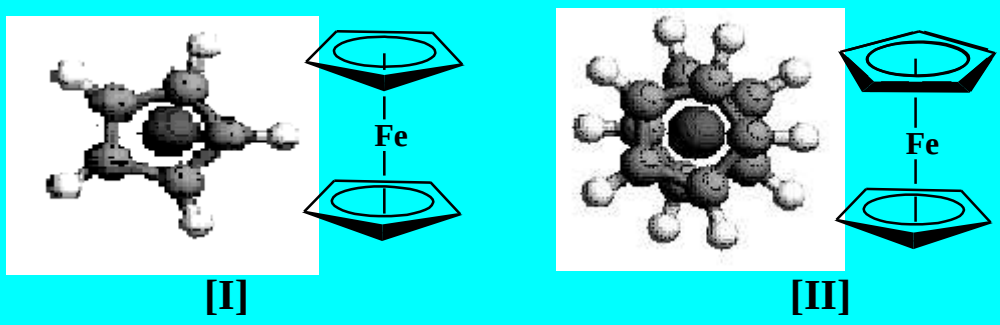

[I] [II]

Figure 2.1. **F**errocene**[1]**, shown in the eclipsed D_{5h} conformation **[I]**, can also exist in the staggered D_{5d} conformation **[II]**.

The geometry of ferrocene is quite remarkable in that it possesses a sandwiched structure in which two cyclopentadienyl rings lie parallel to one another with an iron(II) cation buried in the π-electron cloud between them. Further co-ordination of the Fe(II) centre occurs grudgingly.

Ferrocene **[1]**, is readily oxidised with hydrogen peroxide[18] or other oxidising agents to the ferricenium cation **[B]**. The reverse reaction, reduction of the ferrocenium cation to neutral ferrocene, is mediated by NADH,[19] metalloproteins[20] and other strong reducing agents (See **Scheme 2.4**). The ferrocenium cation itself is an ion-radical species of appreciable stability, which interacts readily with free radical precursors and a variety of biologically important electron donor compounds as well as with other nucleophiles.[21] The low formal reduction potential of ferrocene in water ($E^{0/}$ = 0.127 V *vs*. saturated SCE at 25°C[22]) makes it prone to biologically controlled oxidation-reduction processes. The ferrocenium cation undergoes recombination reactions with free radicals which, after proton elimination, leads to substituted, uncharged (i.e. reduced) ferrocene compounds **[C]**.[23]

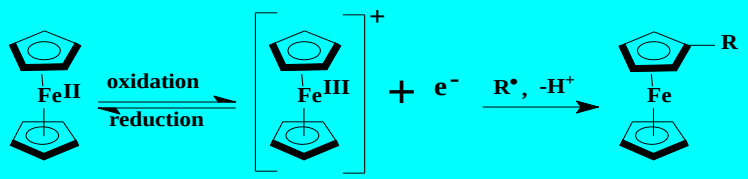

[1] [B] [C]

Scheme 2. 4. Oxidation of ferrocene **[1]** to give the ferrocenium cation **[B]** which can undergo reductive coupling with radicals, R•, to give substituted ferrocenes **[C].**

2.3.2. The chemistry of ferrocene

The chemistry of ferrocene and its derivatives has been well documented.[24-28] Only selected reaction features related to this study will be discussed below.

Most ferrocene-containing compounds may be prepared from only a few different starting materials. All are easily prepared from ferrocene**[1]** and are sufficiently versatile to be converted to many derivatives.

Considering one of the goals of this study, which is the co-ordination of the ferrocenyl moiety onto a second metallocene center (titanocene dichloride), one of the objectives was to synthesise a series of substituted ferrocenes containing reactive side groups capable of undergoing coordination reactions with titanocene dichloride. A fair amount of information on these types of compounds is available, some examples of which are shown in **Scheme 2.5**.

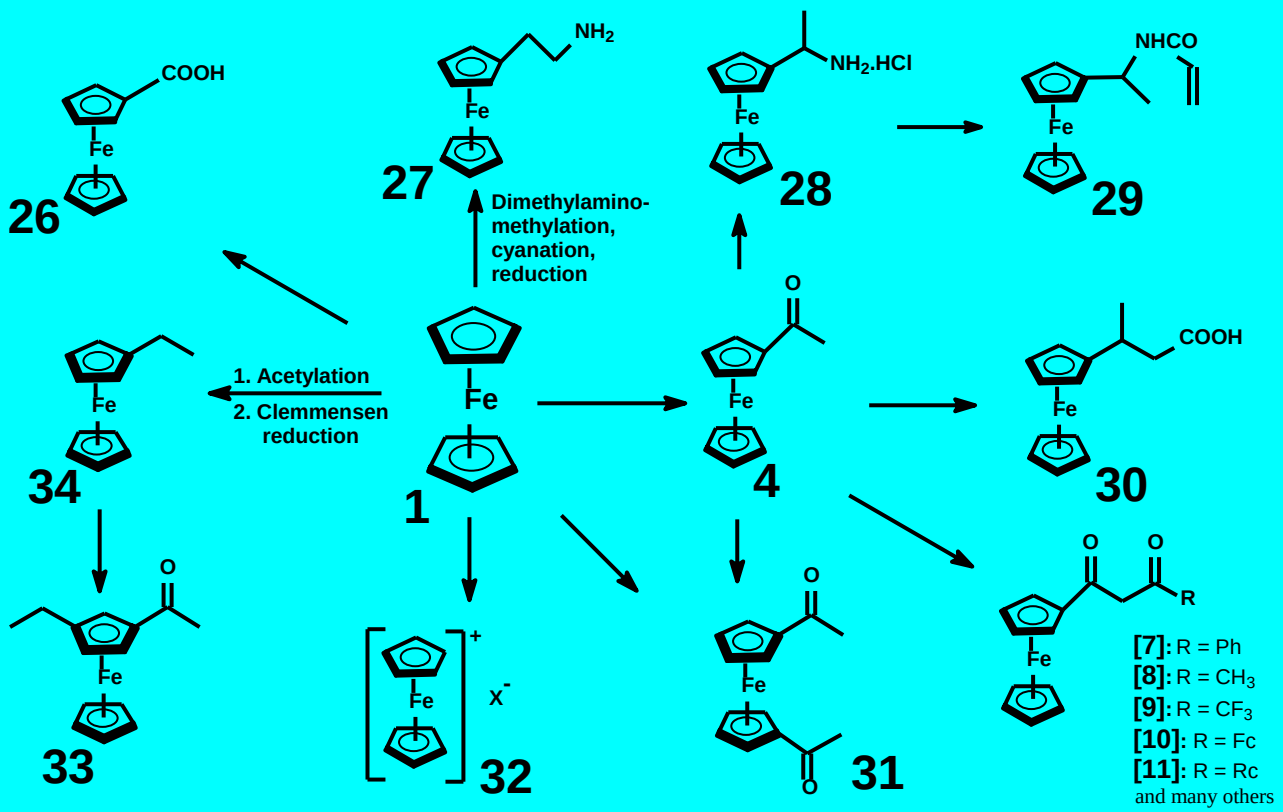

Scheme 2. 5. Chemistry of ferrocene**[1]**. $X^- = [CCl_3COO]^-.2CCl_3COOH$ in **[32]**.

The enhanced aromatic reactivity of ferrocene, over benzene, makes possible a wide range of electrophilic substitution reactions which can often be effected under mild conditions.[23,29]

Ferrocene is much more reactive towards Friedel-Crafts acylation,[30-33] in for example the preparation of acetylferrocene **[4]**, than either benzene or anisole.

Hydrogen substitution of already mono-substituted ferrocenes may or may not proceed with ease, depending on whether the existing substituent is an electron donating, such as alkyl, or an electron-withdrawing substituent, such as acetyl. Electron donating substituents activate the ferrocene complex, and substitution takes place preferentially on the substituted cyclopentadienyl ring, as shown in the acetylation of ethylferrocene **[34]** to give **[33]**. Electron-withdrawing groups de-activate the complex, leading almost exclusively to the heteroannular 1,1'-substituted products.[34] This is demonstrated by the acylation of acetylferrocene **[4]** to give 1,1'-diacetylferrocene **[31]**.

Acyl ferrocenes are extremely useful synthetic intermediates *en route* to other ferrocenes.[35] These compounds are capable of undergoing a large variety of reactions such as Clemmensen reduction to substituted alkanes, lithium aluminium hydride reduction to alcohols and a whole variety of common ketone condensation reactions. Foremost of these, with respect to this study, may be cited the Claisen condensation of acetylferrocene with an appropriate ester to give the β-diketones **[7] – [11]** as well as many others.[36]

Ferrocenoic acid **[26]** has been prepared in many ways,[29] the most important being carbonation of lithioferrocene,[37,38] or by oxidation of acetylferrocene[29,39] **[4]** and by the 2-chlorobenzoyl-chloride method.[40] 3-Ferrocenylbutanoic acid **[30]** was obtained by the Reformatsky reaction between acetylferrocene and malonic acid, followed by catalytic hydrogenation of the obtained intermediate 3-ferrocenyl-3-methylacrylic acid.[41]

Reductive amination of acetylferrocene **[4]** with cyanoborohydride, in the presence of ammonium acetate followed by treatment with HCl, gave 1-ferrocenylethylamine hydrochloride **[28]**.[42,43] Conversion of **[28]** to N-(1-ferrocenylethyl)acrylamide **[29]** was achieved by allowing neutralised **[28]** to react with acryloyl chloride in the presence of triethylamine.[44]

The preparation of amine functionality slightly removed from the ferrocenyl moiety by a methylene spacer is demonstrated by the synthesis ferrocenylethylamine **[27]**, which is accomplished by the reduction of ferrocenylacetonitrile with $LiAlH_4$,[45] obtained from ferrocenylmethyl(trimethylammonium)iodide.[46-48] Finally, ferrocenium salts **[32]** were prepared and isolated by Neuse and others by oxidation reactions, *inter alia* for biological testing.[49]

2.4. Titanocene Chemistry

2.4.1. Introduction

Titanocene(IV) dichloride possesses a unique chemical structure where substituents may be interchanged at two different positions (**Figure 2.2**). Diverse physical, chemical and biological properties can therefore be introduced to the molecule, while still maintaining a tetrahedral structure about the central titanium atom. Various substituents can be introduced into the cyclopentadienyl ring prior to forming the metallocene dihalide (position A). In this way the cyclopentadienyl rings can be modified in a virtually unlimited number of ways in order to influence the electronic properties, steric and coordination environment of the titanium centre by a static intramolecular communication to the cyclopentadienyl rings bearing the side chains. As the alteration of the cyclopentadienyl ring is not part of this study, no further discussion will be given on this topic.

In the second approach to substituted titanocene derivitives, different ligands can replace the two Cl^- ions coordinated to the central metal atom (position B).[50] It was the intention of this study to explore the effects of modifying these points to coordinate ligands, which provide a second metal centre.

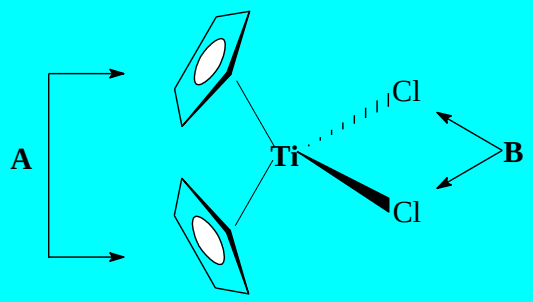

Figure 2.2. Structural flexibility of titanocene(IV) dichloride for chemical design.

2.4.2. The synthesis and chemistry of titanocene(IV) dichloride

The normal starting point for metallocene synthesis is the 'cracking' of dicyclopentadiene. This involves a retro Diels-Alder reaction to produce the monomeric and fairly unstable cyclopentadiene (Cp or C_5H_6). Because it is a weak acid (pK_a = 15), it can be deprotonated by alkali metals. Sodium cyclopentadienide (NaCp) is the preferred reagent for metallocene synthesis. In the final step of metallocene synthesis, the Cp from NaCp is reacted with a metal salt or metal halide (**Scheme 2.6**). Another method which may be employed is the 'co-condensation method'. It is possible to use vapours of transition metals as routine reagents in synthesis and catalysis,[51] as well as using a metal salt and cyclopentadiene.

If the salt anion (such as Cl^- in $FeCl_2$) has poor basicity and cannot deprotonate cyclopentadiene, an auxiliary base can be utilised to generate the cyclopentadienyl anions *in situ*.[52] Alternatively, a reducing agent is required.

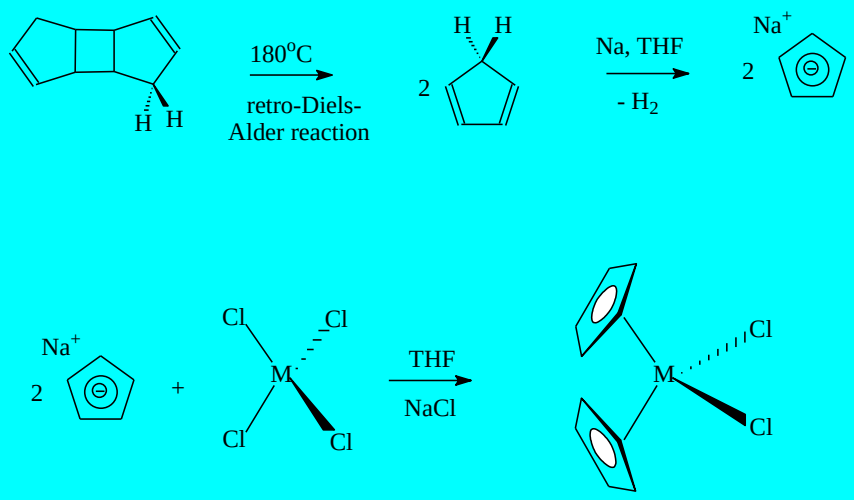

Scheme 2.6. Synthesis of metallocenes using a metal salt and cyclopentadienyl reagents, M = Ti, Zr or Hf.

The chloride ligands on the central metal atom of the titanocene dichloride can be exchanged for any other halide or pseudohalide ligand without the loss of any anti-tumour activity.[53] Specific complexes do however have different anticancer activity, the Cl^- complexes having the lowest IC_{50} values. From a medical point of view and with the goals of this study in mind, this is therefore the preferred site of molecular modification.

The chemistry of titanocene dichloride is well documented.[54] A few relevant reactions are represented in **scheme 2.7.**

Reduction of titanocene dichloride ($[Cp_2TiCl_2]$) **[3]** to dicarbonyldi(cyclopentadienyl)titanium(II) **[35]** can occur *via* several methods, including the aid of an activated magnesium amalgam in a carbon monoxide atmosphere.[55] A more recent method of reductive carbonylation, which is currently used in catalytic processes, is the exposure of Ti(IV) to CO and $AlCl_3$ in an ionic liquid like 1-ethyl-3-methylimidazolium chloride ($AlCl_3$-EMIC) melt.[56]

An important point to note is that the titanium in $[Cp_2Ti(CO)_2]$ **[35]** has an oxidation state of II. Titanium(III) dicarbonyl complexes are known and have a formula of $[CpTi(CO)_2]^+$.[56] The rest of the complexes discussed in this section are in the (IV) oxidation state.

Compound **[36]**, the dithio titanocene complex, can be obtained by reacting **[3]** with 2 mole of a mercaptan, RSH. Titanocene dichloride has a marked tendency to react with thiols.[57, 58] The same compound **[36]** may be prepared by oxidative addition of alkyl and aryl disulphides to **[35]**.[59]

Reaction of methyl lithium with **[3]** yields bis(cyclopentadienyl)dimethyltitanium(IV),[60,61] which is a very useful precursor to a large variety of titanium(IV) complexes.

When equimolar amounts of most alcohols are allowed to react with **[3]** in the presence of a base such as $(Et)_3N$, a preferential cleavage of the cyclopentadienyl ring over the chloride ligand, to yield the monoalkoxide **[38]** occurs.[62] Forcing conditions yield the di- and tetraalkoxides.[62] Dialcohols (such as 1,2-benzenediol) normally react by splitting off one Cp-ring and one Cl^- ion.[63] Under apropriate conditions, such as in the presence of sodamide ($NaNH_2$), displacement of both Cl^- ions is achieved to yield **[39]** as the product.[64]

Depending on reaction conditions, two types of titanium(IV) β-diketonates, **[40]** and **[41]** can be formed. As an integral part of this study titanium(IV) β-diketonates will be discussed in greater detail in paragraph 2.5.2.

Air-stable titanocene salt complexes **[42]** were synthesized by reacting titanocene dichloride **[3]** with phosphorous- or sulphur-based β-amino acid complexes in atmospheric conditions.[65] Each complex of **[42]** contains two identical ligands with a terminal ammonium chloride group and either the phosphorous- or sulphur-based ester groups bonded directly to the titanium centre.

Complex **[43]** was synthesised to functionalise the titanium complex to have a suitable site (R) to anchor to a monomeric or polymeric drug carrier.[66]

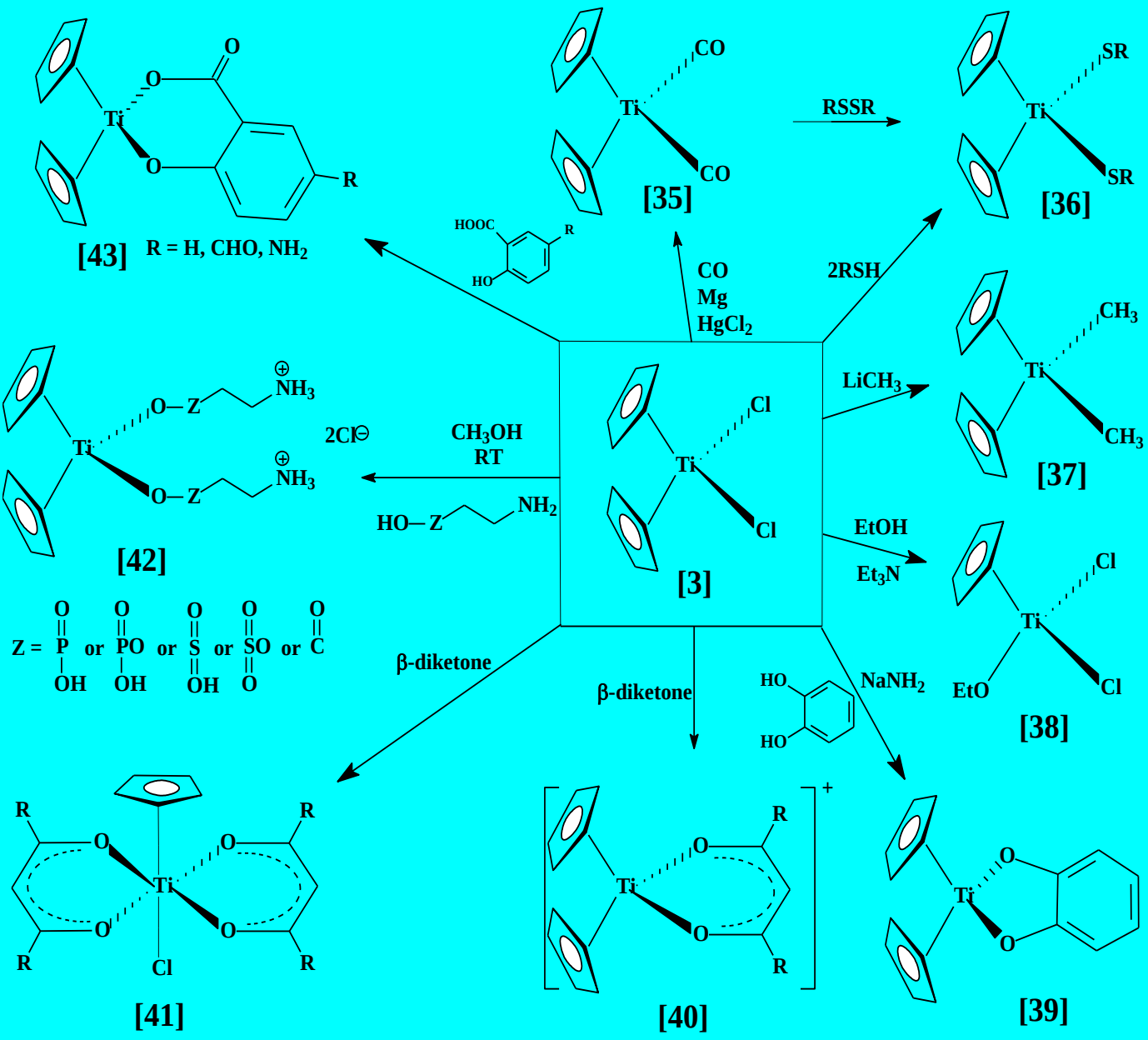

Scheme 2.7. Common reactions of titanocene dichloride [Cp_2TiCl_2] **[3]**.

2.5. Chemistry of metal β-diketonato complexes

2.5.1. Introduction

Under appropriate conditions the enolic hydrogen atom of a β-diketonato ligand can be replaced by a metal cation to produce a six-membered pseudo-aromatic chelating ring (six-membered metallocyclic ring), see **Scheme 2.8.**

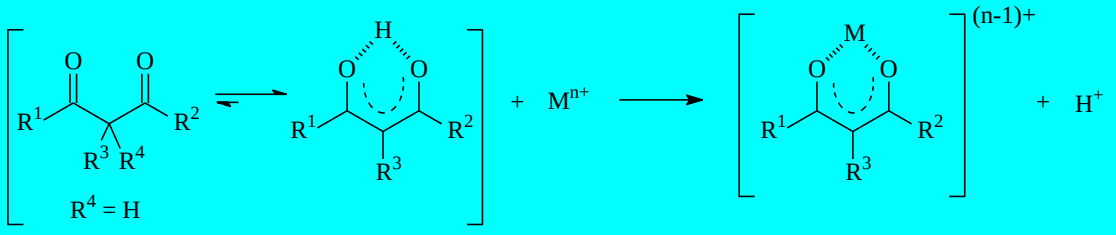

Scheme 2.8. Formation of a six-membered pseudo-aromatic chelating ring of metal β-diketonates.

Mono, bis, tris and even tetrakis β-diketonato metal complexes are known.[67]

In mono-β-diketonato metal(III) and metal (IV) complexes, the β-diketonato ligands are bidentate with the configuration about the metal (Ti^{IV} for this study) approximately tetrahedral.[68] Doyle and Tobias prepared a series of titanocene(IV)-β-diketonato complexes. Most complexes of titanium tend to be sensitive to atmospheric oxygen. Stability to oxygen generally follows this simple pattern.

(least O_2 stable) $Ti^{II} < Ti^{III} < Ti^{IV}$ (most O_2 stable)

Ti^{II} and Ti^{III} complexes are converted to TiO_2 upon exposure to air. Ti^{IV} complexes are therefore better suited to experimentation, biomedical application and storage purposes. Even so, many Ti^{IV} complexes exist only for short times in air before ligands are exchanged and ultimately TiO_2 is liberated.

The bis-β-diketonato titanium complexes have an octahedral-coordination and can exist both in the *trans*- and *cis*-configuration (**Figure 2.3**). The *cis*-configuration is the most stable isomer for most cases, even though the *trans*-configuration may sometimes be preferred due to steric reasons.[69] The higher stability of the *cis*-configuration is attributed to the π-back donation into the three metal *d*-orbitals d_{xy}, d_{xz} and d_z^2, whereas for the *trans*-configuration only two *d*-orbitals (d_{xy} and d_{xz}) are occupied.[70]

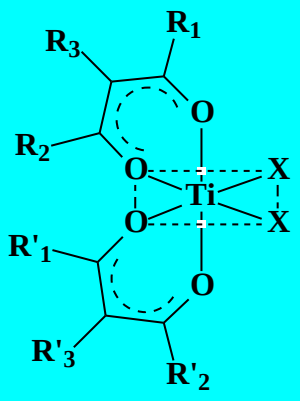

[44]

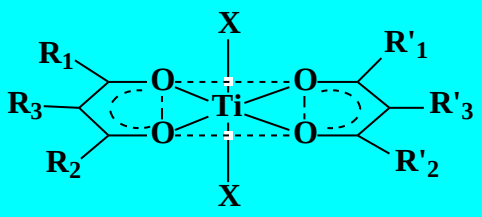

[45]

Figure 2.3. Structure of the bis-β-diketonato titanium complexes, [Ti(β-diketonato)$_2$X$_2$], in the *cis*- **[44]** and *trans*-conformations **[45]**, X = OR, Cl or Cp$^-$. It should be noted that in the cited literature $R_1 = R_2$, therefor only one *cis* and one *trans* conformation is possible.

2.5.2. Mono-β-diketonato titanium(IV) complexes

The synthesis of titanium(IV) complexes is usually based on an anion metathesis reaction, which is driven by precipitation of one of the products.

Titanocene dichloride dissolves in water with aquation to give cationic species, some polynuclear complexes also exist (**Scheme 2.9**). Either one of the cationic species **[46]**, **[47]** or **[48]** can be treated with $AgClO_4$ to form the perchlorate salt. According to Doyle and Tobias,[71] addition of the β-diketone displaces the perchlorate ligands to produce the titanocene(IV)-β-diketonato complexes shown in **Scheme 2.10.** It is important to note that even with very high concentrations of the chelating ligand it is impossible to obtain the bis-chelate. The complexes undoubtedly have a wedge-like sandwich structure with tetrahedral coordination about the titanium centre, which is the same coordination as for titanocene dichloride.[72] The ease of preparation of these mono-β-diketonate complexes results from the very low solvation energy of the complex cation.

This study is focused on expanding the available library of $[Cp_2Ti(\beta\text{-diketonato})]^+$ complexes to include mixed metal complexes of the type $[Cp_2Ti(FcCOCHCOR)]^+ClO_4^-$, with Fc = ferrocenyl and to probe any communication that might exist between the two metal centres, Ti and Fe.

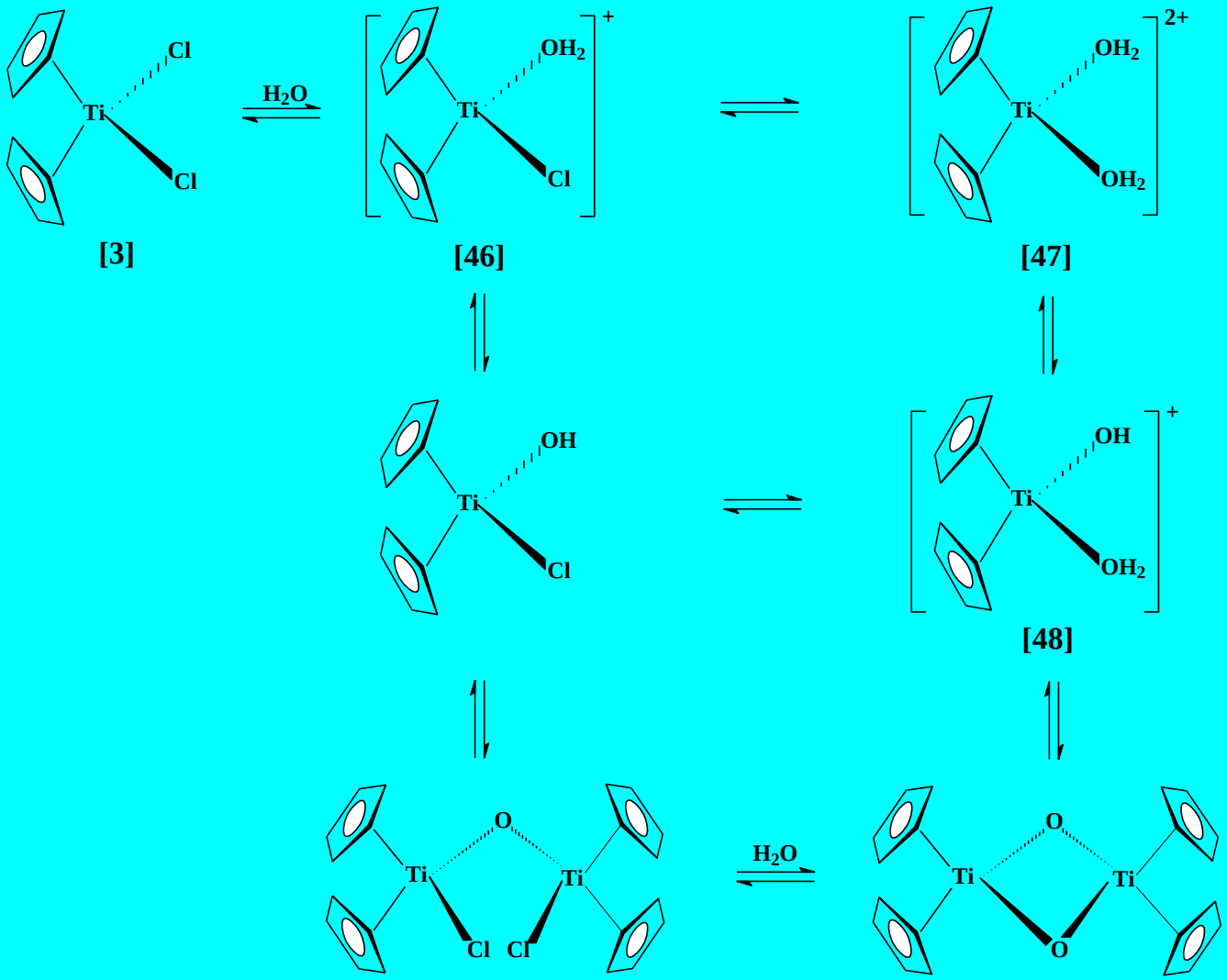

Scheme 2.9. Aqueous chemistry of titanocene dichloride **[3]**.

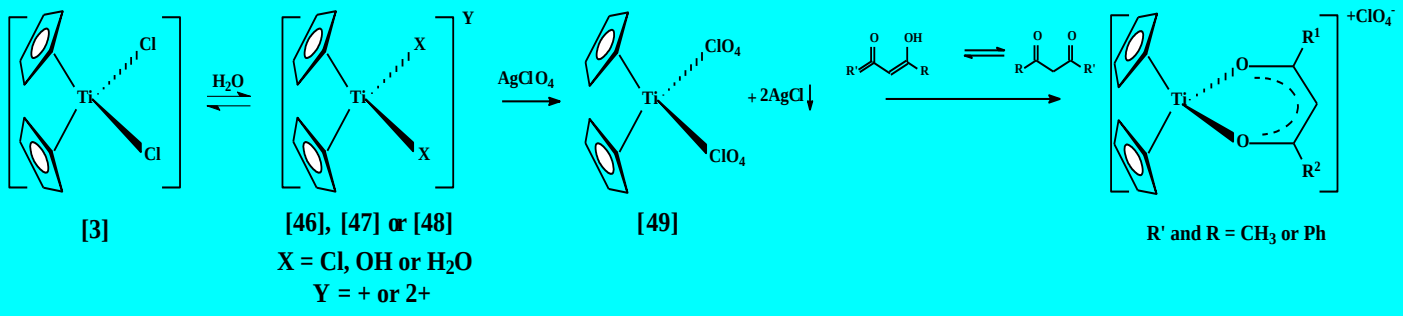

Scheme 2.10. Reaction and formation of the titanocene(IV)-β-diketonato complexes.[71] The authors of this publication list **[49]** as the structure in the $AgClO_4$ reaction, however, a structure in which the ClO_4 groups have been replaced with the H_2O groups and in which ClO_4^- act as two counter anions would be more correct (see **Chapter 3**, page 63, **Scheme 3.4**).

2.6. Electroanalytical chemistry

2.6.1. Introduction

Cyclic voltammetry is possibly the simplest and most versatile electroanalytical technique for the study of electro-active species. The effectiveness of cyclic voltammetry lies in its ability to probe redox behaviour of these species over a wide potential range,[73] in a relatively short amount of time. It is a simple and direct method for the measurement of the formal reduction potentials of a reaction. Thermodynamic and kinetic information may be obtained in one experiment,[74] therefore both reduction potential and heterogeneous electron transfer rates can be measured. The rate and nature of a chemical reaction coupled to the electron transfer step can also be studied.

A redox couple may or may not be electrochemically reversible. By electrochemical reversibility, it is meant that the rate of electron transfer between the electrode and substrate is fast enough to maintain the concentration of the oxidised and reduced species in equilibrium at the electrode surface. For this study cyclic voltammetric experiments where performed to illustrate possible communication between the different metal centres, especially between Ti and Fe in complexes of the type $[Cp_2Ti(FcCOCHCOR)]^+ClO_4^-$.

2.6.2. The basic cyclic voltammetry experiment

Cyclic voltammetry involves the measurement of the resulting current, between a working electrode and an auxilliary electrode when the potential of the working electrode is oscillated in an unstirred solution. The potential of the small, static, working electrode is controlled relative to a reference electrode. Numerous reference electrodes are available, most commonly used are the saturated calomel electrode (SCE) or a silver/silver chloride electrode (Ag/AgCl). The controlled potential, applied over these two electrodes, can be viewed as an excitation signal. This signal is a linear potential scanning with a triangular waveform. The experiment starts at an initial potential, E_i, proceeding to a predetermined limit switching potential, $E_{\lambda 1}$, where the direction of the scan is reversed (**Figure 2.4**).

The scan may be terminated at any stage, or a second cycle as indicated by the broken line, can be initiated. Single or multiple cycles can be measured. The scanning rate as indicated by the slope, may vary between ± 15 $mV.s^{-1}$ to 40000 $mV.s^{-1}$.

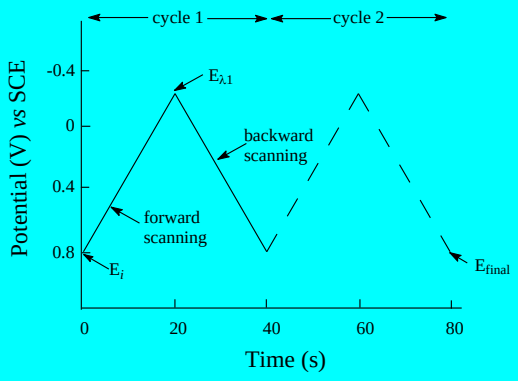

Figure 2.4. Typical excitation signal for cyclic voltammetry – a triangular potential waveform.

For a typical cyclic voltammogram, the current response (vertical axis) is plotted as a function of the applied potential (horizontal axis), see **Figure 2.5.** Differences between the successive scans are important in obtaining and understanding information about the mechanism of reactions.

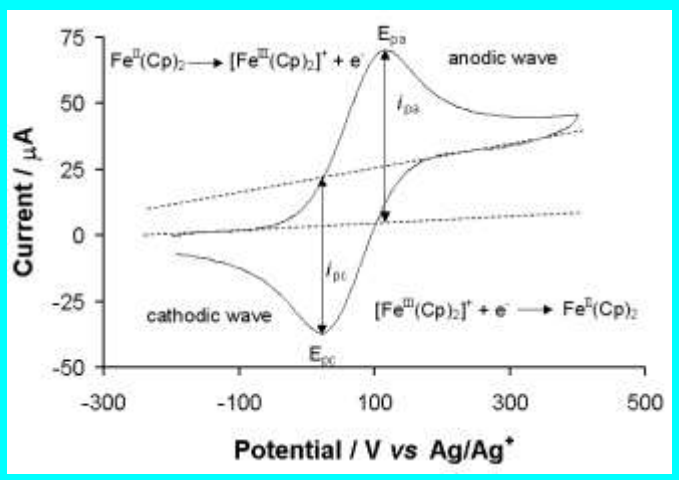

Figure 2.5. Cyclic voltammogram of a 3.0 $mmol.dm^{-3}$ ferrocene measured in 0.1 $mol.dm^{-3}$ tetrabutylammonium hexafluorophosphate/acetonitrile on a glassy carbon electrode at 25˚C, scan rate 100$mV.s^{-1}$.

2.6.3. Important parameters of cyclic voltammetry

The most important parameters of cyclic voltammetry are the peak anodic potentials (E_{pa}), peak cathodic potential (E_{pc}), the magnitudes of the peak anodic current (i_{pa}) and peak cathodic current (i_{pc}) (**Figure 2.5**).

The formal reduction potential for an electrochemically reversible redox couple is midway between the two peak potentials.

Equation 2.1. $$E^{0/} = (E_{pa} + E_{pc})/2$$

This $E^{0/}$ is an estimate of the polarographic $E_{1/2}$ value, provided that the diffusion constants of the oxidised and reduced species are equal. The polarographic $E_{1/2}$ value can be calculated from $E^{0/}$ *via*

Equation 2.2. $$E_{1/2} = E^{0/} + (RT/nF) \ln (D_R/D_O)$$

where D_R = diffusion coefficient of the reduced specie and D_O = diffusion coefficient of the oxidised specie. In cases where $D_R/D_O = 1$, $E_{1/2} = E^{0/}$.

Theoretically an electrochemical couple is considered electrochemically reversible when the difference in peak potentials (ΔE_p) is 59 mV at 25˚C for a one electron transfer process. In practice (within the context of this research program) due to electrode imperfections, a redox couple with a ΔE_p value up to 90 mV will still be considered as electrochemically reversible. Peak separation increases due to slow electron transfer kinetics at the electrode surface.

The number of electrons (n) transferred in the electrode reaction for a reversible couple can be determined from the separation between the peak potentials from Equation 2.3.

Equation 2.3. $$\Delta E_p = E_{pa} - E_{pc} \approx 59 \text{ mV}/n$$

The peak current, i_p, is described by the Randle-Sevcik equation.

Equation 2.4. $$i_p = (2.69 \times 10^5) n^{3/2} A D^{1/2} v^{1/2} C$$

i_p = peak current (Ampere), *n* = amount of electrons per molecule, A = working electrode surface (cm^2), C = concentration ($mol.cm^{-3}$), *v* = Scan rate ($V.s^{-1}$) and D = Diffusion coefficient ($cm^2.s^{-1}$).

The values of i_{pa} and i_{pc} should be identical for a reversible redox couple, implying:

Equation 2.5. $$i_{pc}/i_{pa} = 1$$

Systems may also be quasi-reversible or irreversible (**Figure 2.6.**). An electrochemically quasi-reversible couple is where both the oxidation and reduction processes takes place, but the electrochemical kinetics are slow and $\Delta E_p > 59$ mV (practically 90 mV $\leq \Delta E_p \leq \pm$ 150 mV). A chemically irreversible system is one where only oxidation or reduction is possible.[75] Electrochemical irreversibility is typified, within the context of this thesis, by $\Delta E_p \geq 150$ mV, $i_{pc}/i_{pa} = 0$. For quasi-reversible or irreversible systems, Equations 2.1, 2.3 and 2.4 are not applicable.

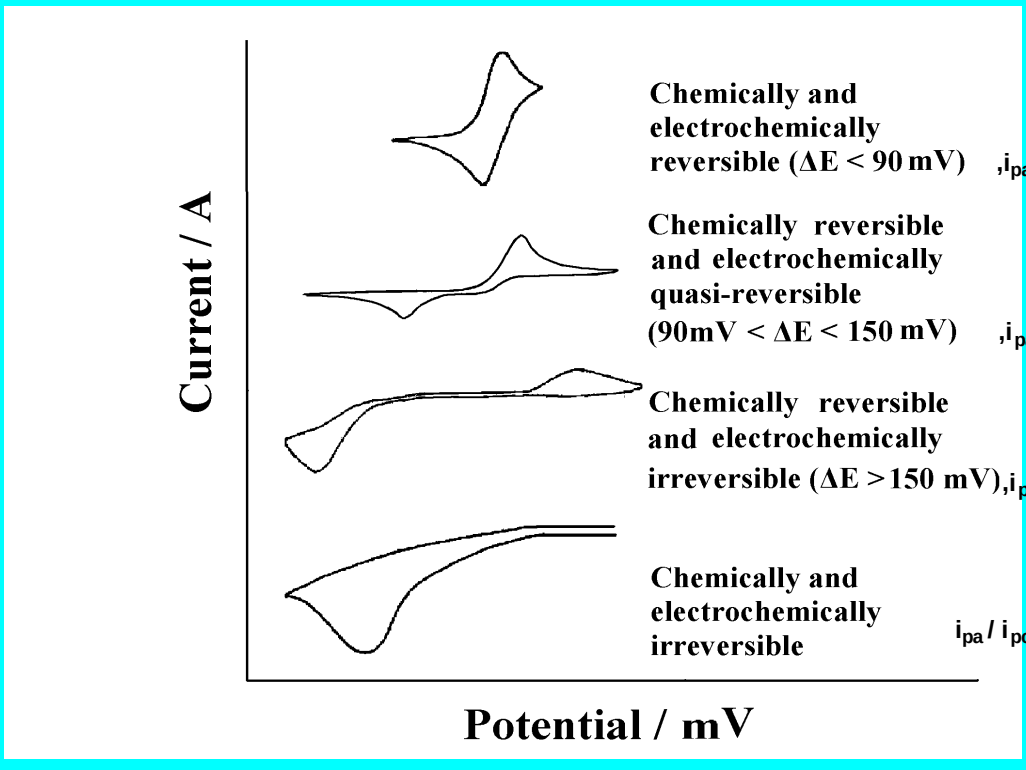

Figure 2.6. A schematic representation of the cyclic voltammograms expected for electrochemically reversible, quasi-reversible and irreversible systems. Quasi irreversibility will be associated with $1 < i_{pa}/i_{pc} < 0$.

2.6.4. Solvents, supporting electrolytes and reference electrodes

A suitable medium consisting of a solvent containing a supporting electrolyte is needed for electrochemical phenomena to occur.[76] The electrochemical specie under investigation must be soluble to the extent of at least 1 x 10^{-4} mol.dm^{-3} and the electrolyte concentration must be at least 10 times greater. An ideal solvent should possess electrochemical and chemical inertness over a wide potential range and should preferably be unable to solvate the electrochemical specie. Solvents that are often used are acetonitrile (CH_3CN) and tetrahydrofuran (THF), commonly used in anodic studies. Dichloromethane (DCM) is used when a strictly non-coordinating solvent is required.

The purpose of a supporting electrolyte is to increase the conductivity of the medium and to carry most of the current. Tetrabutylammonium hexafluorophosphate ($TBAPF_6$) is the most widely used supporting electrolyte in organic solvents.

Recent developments in the expansion of new supporting electrolytes and the use of nontraditional solvents have increased options in electrochemical studies. It has been demonstrated by Ohrenberg and Geiger that by using the noncoordinating solvent α-α-α- trifluorotoluene (or (trifluoromethyl)benzene) and the electrolyte tetrabutylammonium tetrakispentafluorophenylborate $[N(Bu)_4][B(C_6F_5)_4]$ reversible electrochemistry could be obtained for nickelocene.[77] The analysis of the cobaltocene Co (III) /Co (II) couple also yielded previously unknown reversible electrochemistry.

LeSuer and Geiger showed that the use of the non-coordinating supporting electrolyte $[N(Bu)_4][B(C_6F_5)_4]$ improves electrochemistry compared to measurement in the presence of the weak coordinating electrolyte tertrabutylammonium hexafluorophosphate.[78] It was shown that with the use of this electrolyte, electrochemistry could be conducted in solvents of low dielectric strength (in, for example, *t*-butyl methyl ether). It was also shown that the peak separation between two very close oxidation peaks can be better analyzed with the use of this electrolyte. This can be seen in **Figure 2.7** where the CV of the triferrocenyl compound $[Fe(\eta\text{-}C_5H_4)_2]_3(SiMe_2)_2$ is shown.

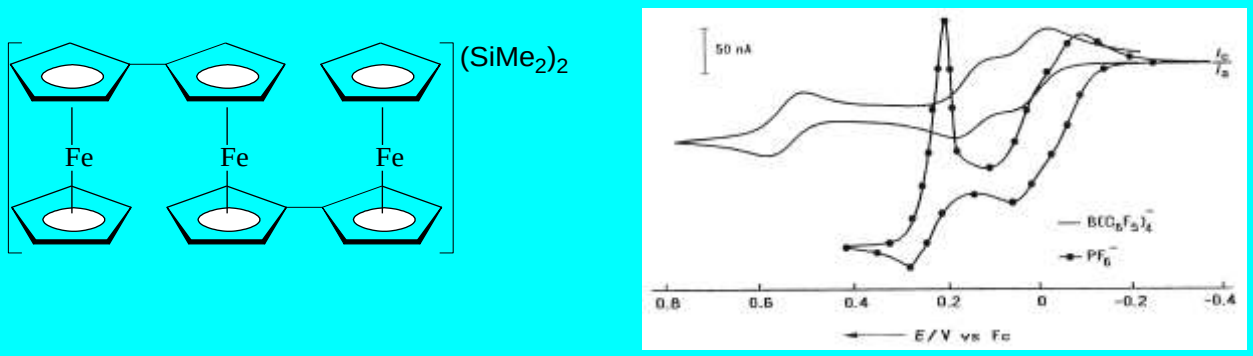

Figure 2.7. Electrochemistry of $[Fe(\eta\text{-}C_5H_4)_2]_3$ (structure included left) $(SiMe_2)_2$ (1.0 mM) in the presence of the electrolyte $[NBu_4][B(C_6F5)_4]$ and the electrolyte $[NBu_4][PF_6]$ versus a Ag/AgCl reference electrode. Solvent dichloromethane. Scan rate 0.2 V s-1. (from R.J. le Suer and W.E. Geiger, *Angew. Chem*., Int. Ed. Engl., 2000, 39, 248)

Measured potential data was previously specified commonly *vs* the normal hydrogen electrode (NHE) or a saturated calomel electrode (SCE) reference electrode. With non-aqueous solvents, a system like Ag/Ag^+ (0.01 mol dm^{-3} $AgNO_3$ in CH_3CN) was preferred. IUPAC now recommend that all electrochemical data is reported *vs* an internal standard. In organic media the Fc/Fc^+ couple is a convenient internal standard.[79, 80] The Fc/Fc^+ couple $E^{0/} = 0.400$ V *vs* NHE.[81] NHE and SCE are used for measurements in aqueous solutions. In many instances electrochemical measurements of organometallic compounds in water are impossible due to insolubility or instability.

2.6.5. Cyclic voltammetry of ferrocene

The reversible electron transfer process involving the ferrocenyl moiety has led to many well documented electrochemical studies both in organic and aqueous media. The reversibility and high rate of electron transfer of the ferrocenyl moiety often leads to $\Delta E_p = E_{pa} - E_{pc}$ close to 59 mV and i_{pc}/i_{pa} ratios approaching unity.[82] Ferrocene, with a formal reduction potential of 400 mV *vs* NHE,[81] can be used in CV experiments as an internal reference system in a wide range of non-aqueous solvents,[80] or when using different reference electrodes.[79] Different formal reduction potentials for Fc in solvents such as THF, DCM and CH_3CN referred to the same reference electrode have been recorded. Irrespective of the shift in $E^{0/}$ (Fc/Fc^+) in different solvents, the formal reduction potential of another compound (e.g. $[IrCl_2(FcCOCH_2COCF_3)(COD)]$) *vs* Fc/Fc^+ as an internal standard, remains unchanged.[83]

When ferrocene is bounded in a complex like a β-diketone ($FcCOCH_2COR$), the $E^{0/}$ value of the ferrocenyl couple is influenced by the group electronegativity of the R group (see **Figure 2.8, Table 2.3**).[15] This shift in formal reduction potential is attributable to good communication between the ferrocenyl ligand and the R group *via* the backbone of the pseudo-aromatic β-diketone core. With increasing electronegativity of the R group on the β-diketone, the $E^{0/}$ value of the Fc/Fc^+ couple also increases since electron-density is withdrawn from it by R. There is also a linear relationship between the pK_a of the β-diketone and the $E^{0/}$ value of the Fc/Fc^+ couple, with increasing pK_a there is a decrease in the $E^{0'}$ value for the Fc/Fc^+ couple.

As shown in **Figure 2.8** and **Table 2.3**, [$FcCOCH_2COFc$] (Hdfcm), with two ferrocenyl ligands bounded to it, showed different oxidation and reduction peaks for the different Fc moieties.[84-86] The observed inequalities are due to the improbability of both ferrocenyl groups in the same molecule simultaneously coming into contact with the electrode.[6,15]

Firstly, one ferrocenyl group is oxidised according to the reaction:

$$FcCOCH_2COFc \rightarrow FcCOCH_2COFc^+ + e^- \quad ;E^{0/} = 0.187V \textit{ vs.} Fc/Fc^+$$

The group electronegativity of a Fc^+ group ($\chi_{Fc+} = 2.82$) is larger than that of the Fc group ($\chi_{Fc} = 1.87$) and therefore much more electron withdrawing. The second Fc group in [$FcCOCH_2COFc^+$] which must be oxidised is now (by conjugation) experiencing a stronger electron withdrawing effect, making it more difficult to oxidise.

$$FcCOCH_2COFc^+ \rightarrow Fc^+COCH_2COFc^+ + e^- \quad ;E^{0/} = 0.297V \textit{ vs.} Fc/Fc^+$$

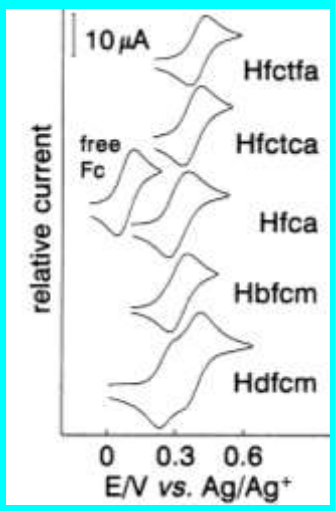

Figure 2.8. Cyclic voltammograms of 2 mmol dm^{-3} solutions of ferrocene (Fc) and ferrocene-containing β-diketones of the type [$FcCOCH_2COR$], where R = CF_3 (Hfctfa), CCl_3 (Hfctca), CH_3 (Hfca), Ph (Hbfcm) and Fc (Hdfcm), measured in 0.1 mol dm^{-3} $TBAPF_6/CH_3CN$ at a scan rate of 50 mV s^{-1} on a Pt working electrode at 25.0(1)°C *versus* Ag/Ag^+.

Table 2.3. $E^{0/}$ (formal reduction potentials) *vs* Ag/Ag^+, ΔEp; and i_{pa}/i_{pc} (peak anodic/cathodic current ratios), of the β-diketones of the type $FcCOCH_2COR$ R = CF_3, CCl_3, CH_3, Ph and Fc group electronegativities of the R groups on the β-diketones and pK_a values of the β-diketones.

β-diketones	**R groups on the β-diketones**	**$E^{0/}$ *vs* Ag/Ag^+ / mV[15]**	**Group electronegativities of the R groups[15]**	**ΔEp /mV**	**i_{pa}/i_{pc}**	**pK_a of the β-diketones[6]**
Hfctfa	CF_3	0.394	3.01	74	0.96	6.53
Hfctca	CCl_3	0.370	2.76	78	0.98	7.15
Hfca	CH_3	0.313	2.34	86	0.99	10.01
Hbfcm	Ph	0.306	2.21	73	0.97	10.41
Hdfcm	Fc	0.265; 0.374	Fc = 1.87 Fc^+ = 2.82	66 72	1.00 0.98	13.10 6.80

2.6.6. Cyclic voltammetry of ruthenocene

For the purposes of this study a third metallocene (ruthenocene) was introduced into a few complexes. A brief background of the electrochemistry of this compound is therefore relevant, in that it will help explain our findings. In the past, oxidation of ruthenocene was thought to proceed via a $2e^-$ irreversible process.[87] However, this result was observed by using tetrabutylammonium perchlorate as supporting electrolyte, which has weak coordinating properties. Later studies utilising a noncoordinating electrolyte in a noncoordinating solvent showed that a $1e^-$ reversible electrochemical process occurs.[88] Tetrabutylammonium tetrakis[3,5-bis(trifluoromethyl)phenyl]borate $[NBu_4][B(C_6F_5)_4]$ was used as the electrolyte. A reduction potential of 1.03V was obtained for ruthenocene *versus* an aqueous AgCl/Ag (1.0M KCl) reference electrode. The CV is shown in **Figure 2.9.**

A quasi-reversible $1e^-$ oxidation of ruthenocene in Lewis acid-base molten salts was demonstrated when a mixture of 0.8:1 AlCl3: 1-butylpyridinium chloride was used as the solvent.[89] See **Figure 2.10.**

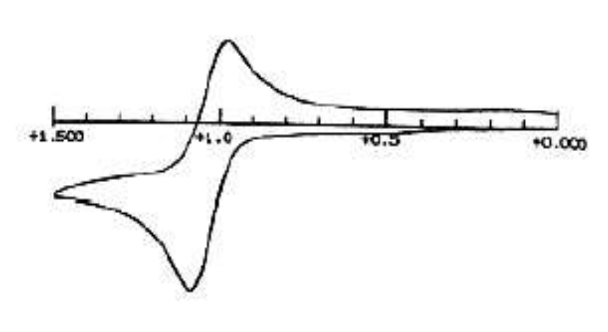

Figure 2.9. The $1e^-$ reversible electrochemistry of ruthenocene (0.5mM), in 0.1M $[NBu_4][B(C_6F_5)_4]$ in dichloromethane. Scan rate = 100mV/s (from M.G. Hill, W.M. Lamanna and K.R. Mann, *Inorg. Chem*., 4687, **30**, 1991).

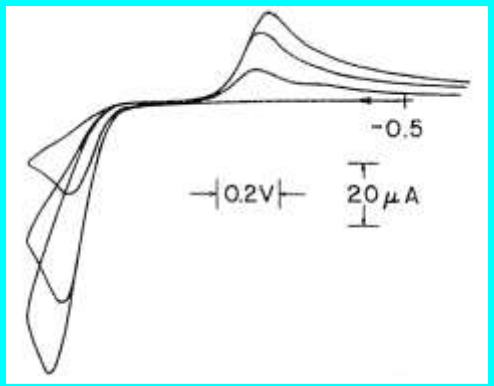

Figure 2.10. The quasi-reversible $1e^-$ oxidation of ruthenocene (22.2mM) in Lewis acid-base molten salts (from R.J. Gale and R. Job, *Inorg. Chem*., 20, **42**, 1981).

Electrochemistry of ruthenocene-substituted derivatives appears to deviate from that of the parent metallocene compound. Recent studies by Jacob and co-workers found that the electrochemistry of a newly synthesised novel ruthenocene surfactant is irreversible.[90] Two oxidation peaks (at 0.74 V and 0.91 V) but no reduction peak, even at very high scan rates were observed for the compound dodecyl dimethyl(methylruthenocenyl)-ammonium bromide in an 0.1M NaCl aqueous solution. Irreversible electrochemistry was also found by Sato and co-workers for their binuclear ruthenocene compounds.[91] They showed that for the compound 1,4-bis(ruthenocenyl)benzene the two oxidation potentials were 0.42V and 0.56V *versus* the Fc/Fc^+ couple, the reduction peak occurred at 0.28V. The CV of the binuclear compound is shown in **Figure 2.11.**

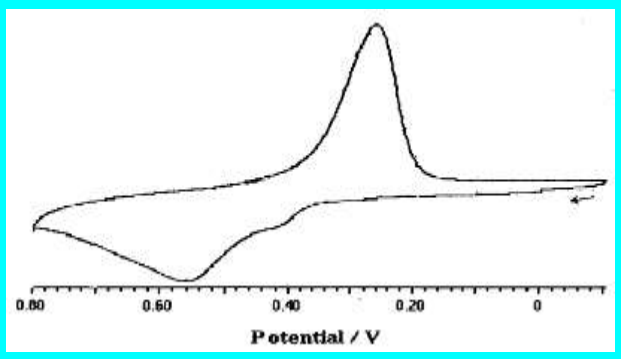

Figure 2.11. Irreversible electrochemistry of 1,4-bis(ruthenocenyl)benzene in dichloromethane utilising a glassy carbon electrode. Scan rate 0.1 $V.s^{-1}$. Supporting electrolyte $TBAClO_4$ (from M. Sato, G. Maruyama, A. Tanemura, *J. Org.Met. Chem*., 655, **23**, 2002).

It has been postulated in several papers that the bis(ruthenocenium) dication $[RuCp_2]_2^{2+}$ may play an important role in ruthenocene rodox processes. Electrochemical preparation of the bis(ruthenocenium) dication was reported by Geiger and co-workers. According to their findings, oxidadation of ruthenocene (**(1)** in **Scheme 2.12**) in $CH_2Cl_2/[NBu_4][B(C_6F_5)_4]$, gives the dimeric dication $[(RuCp_2)_2]^{2+}$ (**(2^{2+}) Scheme 2.12**), in equilibrium with the 17-electron ruthenocenium ion (**(1^{1+})**). At room temperature this rapid equilibrium accounts for the quazi-reversible observations. The bis(ruthenocenium) dication undergoes an irreversible two-electron cathodic reaction at E_{pc} ca. 0 V to generate neutral ruthenocene.[92]

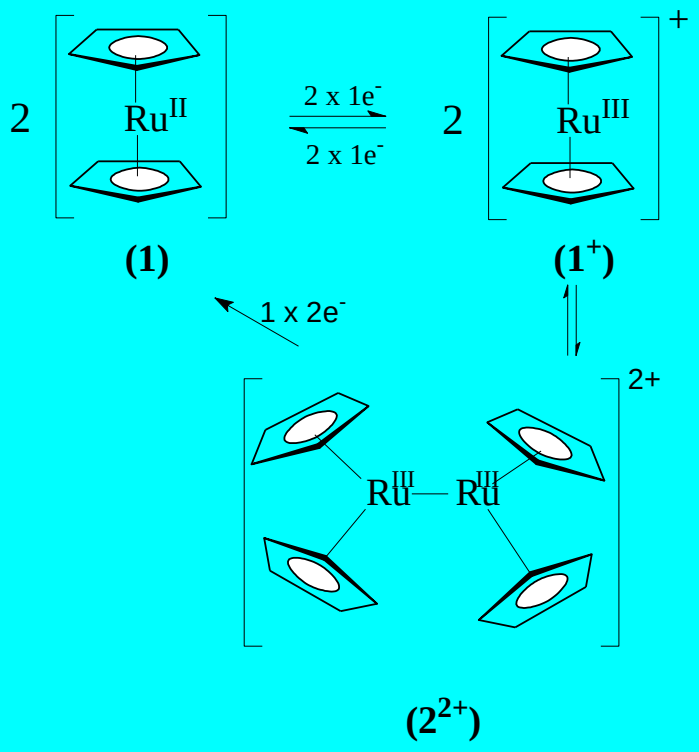

Scheme 2.11. Schematic representation of oxidation/reduction equilibriums for ruthenocene.

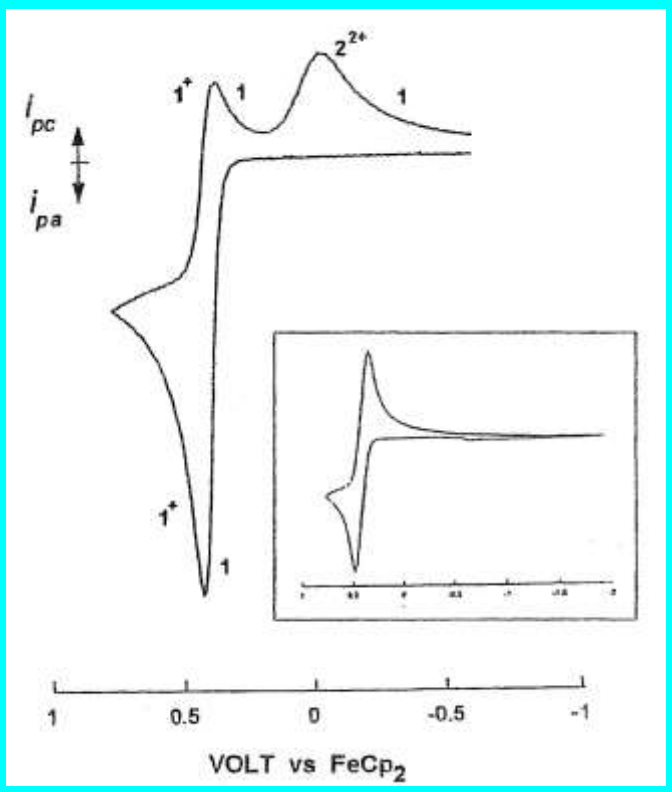

Figure 2.12. Cyclic voltammogram of 2 mM [$RuCp_2$] in CH_2Cl_2/0.1 M [NBu_4][$B(C_6F_5)_4$] at 2 mm (*d*) glassy carbon electrode. T = 243K, v = 0.2 v.s^{-1}. Inset gives scan under same conditions at ambient temperature. (From S. Trupia, A. Nafady and W.E. Geiger, *Inorg. Chem.*, 5480, **42** (2003).

2.6.7. Cyclic voltammetry of titanocene

The redox properties of titanocene dichloride are strongly dependant on the solvent. THF and DCM reveal quasi-reversible redox character with i_{pa}/i_{pc} = 0.65-0.95 and ΔE_p = 90-100 mV. In CH_3CN a small re-oxidation peak, strongly shifted to the positive direction with ΔE_p = 400 mV, was observed (**Table 2.4**).[93] This effect may be interpreted within the framework of a 'square scheme', where the electrochemical reduction step is accompanied by the rapid substitution of a chloride ligand by a solvent molecule (**Scheme 2.12**). The back electron transfer follows the same reaction path for weakly coordinating media (THF, DCM) whereas this process is shifted to a more positive potential in the case of strong coordinating solvents (CH_3CN).

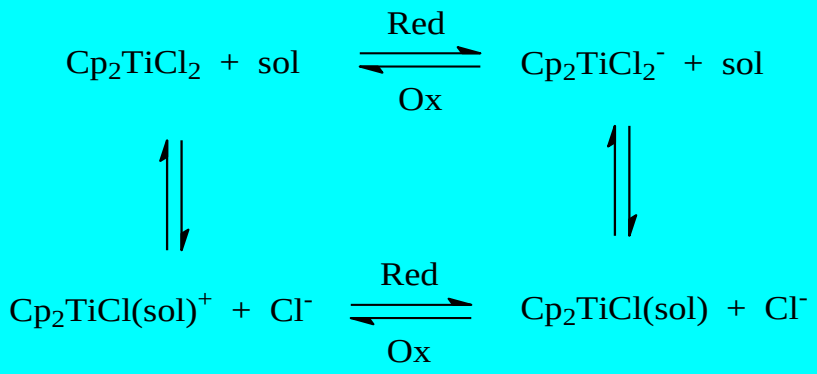

Scheme 2.12. The 'square scheme' illustrating the oxidation and reduction of titanocene dichloride (sol = solvent).

Typical $E^{0/}$ for titanocene(IV) dichloride have been reported elsewhere.[93-95] Electrochemical characterisation of a titanocene(IV) dichloride derivative, $[Cl_2TiCpC_5H_4(CH_2)_3NC_4H_4]$, revealed that the reduction and oxidation resemble the behaviour of the unsubstituted titanocene(IV) dichloride (**Table 2.4**).[96] Reduction of this complex demonstrates a dependence on the solvent complexation ability, which gives rise to the quasi-reversible behaviour found in THF and DCM. In CH_3CN irreversibility was found. Here once again the Ti^{4+}/Ti^{3+} transition leads to the substitution of one of the Cl^- ions by a solvent molecule.

Table 2.4. Redox potentials in solutions *vs* Ag/Ag^+ and SCE (Pt electrode and supporting electrolyte 0.2 M *n*-Bu_4NPF_6) of Fc, $[Cp_2TiCl_2]$ and $[Cl_2TiCpC_5H_4(CH_2)_3NC_4H_4]$ $[(Cp_2TiCl_2)_3Py]$.[96]

Substance	**Solution**	**$E^{0/}$ *vs* Ag/Ag^+ / V**	**$E^{0/}$ *vs* SCE / V**	**$E^{0/}$ *vs* Fc/Fc^+ / V**	**i_{pa}/i_{pc}**	**ΔE_p / V**
Fc	THF	0.20	0.53	0.00	1.0	100
	DCM	0.21	0.43	0.00	1.0	100
	CH_3CN	0.10	0.43	0.00	1.0	80
$[Cp_2TiCl_2]$	THF	-1.08	-0.76	-1.28	0.-90-0.95	90
	DCM	-0.95	-0.73	-1.16	0.65-0.75	100
	CH_3CN	-0.80	-0.47	-0.90	-	400
$[(Cp_2TiCl_2)_3Py$	THF	-1.12	-0.79	-1.32	0.7-0.9	95
	DCM	-0.98	-0.76	-1.19	0.65-0.8	115
	CH_3CN	-0.845	-0.525	-0.945	-	425

As can be seen from **Table 2.4**, the $E^{0/}$ values as well as the reversibility (ΔE_p) of the complexes are highly dependent on the nature of the solvent and the supporting electrolyte used.[97]

These results are confirmed by electrochemical studies of another titanocene derivative, di(propylthiotetramethylcyclopentadienyl)titanium dichloride,[97] $[(C_5Me_4SCH_2CH_2CH_3)_2TiCl_2]$, whose electrochemical behaviour is analogous to that of titanocene dichloride. The first reduction step of $[(C_5Me_4SCH_2CH_2CH_3)_2TiCl_2]$ depends strongly on the nature of the solvent and the supporting electrolyte.

2.6.8. Cyclic voltammetry of titanocene β-diketonato complexes

Electrochemical data obtained from the dicyclopentadienyl titanium(III)-β-diketonato complex [Ti(III)Cp_2(LL')], where LL' = $acac^-$ or $bzac^-$, shows that both the metal as well as the β-diketonato ligand are electrochemically active (**Figure 2.12**).[98] The Ti(III) can be reversibly oxidized in a one electron process, at a potential which is apparently independent of the β-diketonato ligand. [$TiCp_2$(acac)] $E^{0/}$ = -0.86 V and [$TiCp_2$(bzac)] $E^{0/}$ = -0.85 V *vs* Fc/Fc^+ in butyronitrile (0.2 M NBu_4PF_6). The author of this publication attributed the negligible influence of the β-diketonato ligand to the existence of a highly localized centred frontier orbital which dominates the redox chemistry. The peaks at ± -2.5 V are attributed to the β-diketonato ligand. The observations of a reversible Ti^{3+}/Ti^{4+} couple is extraordinary in that it represents one of the few cases where this couple displays an electrochemically reversible system. The reason for this is probably the fact that [Cp_2Ti^{III}(β)] and [Cp_2Ti^{IV}(β)]$^+$ are structurally isomorphous. No structural changes occur during oxidation of Ti(III) or reduction of Ti(IV).

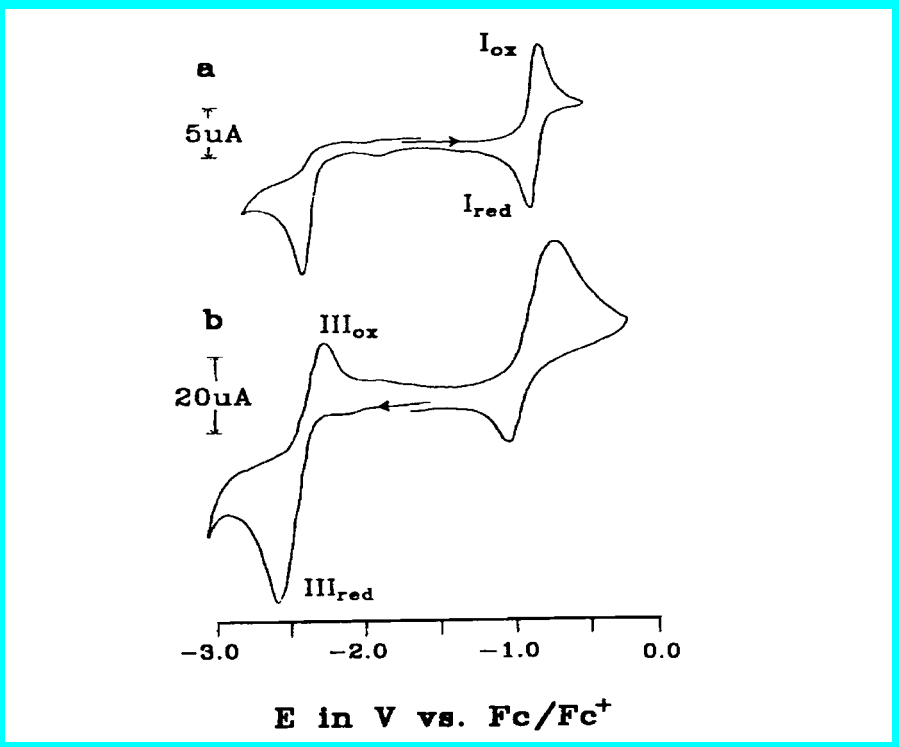

Figure 2.12. CV of [Cp_2Ti (bzac)] (2 mM) obtained in butyronitrile (0.2 M NBu_4PF_6) at scan rate 200 mV/s with **a)** 1 mm Pt disk electrode at 22˚C and **b)** a 5 mm glassy carbon disk electrode at -50˚C.[98]

2.7. Biological aspects

2.7.1. Introducton

Apart from radical surgery, the two major techniques used for the treatment of cancer are radiotherapy and chemotherapy. Both methods can induce disabling and life-threatening side effects, mainly because they destroy normal and healthy tissues indiscriminately.[99] For this reason many potentially good chemotherapeutic drugs often find limited clinical use. Cisplatin, $[Pt(NH_3)_2Cl_2]$, the most succesful metal-containing chemotherapeutic drug to date is an excellent example of this. Detrimental and dose limiting properties of cisplatin include *inter alia* lack of aqueous solubility, high toxicity, anorexia, high rate of excretion from the body, development of drug resistance and most importantly, the inability to distinguish between healthy and cancerous cells.[100] To overcome these negative effects in cancer chemotherapy, new antineoplastic materials are constantly being synthesised and evaluated. New methods of delivering an active drug to a cancerous growth are being developed[101] and combination therapy has been investigated in the hope of finding synergistic effects.

2.7.2. Cytotoxicity and mechanism of action of ferrocene and ferrocene derivatives

In 1984 Köpf-Maier and co-workers[102] were the first to show that ferricenium species have appreciative activity against cancer. In particular it was found that the ferricenium salts have an ID_{100} (ID = inhibiting dosage) value of 480 mg/kg test animal (mice). The compounds also give a TI value of 2.0 (TI = therapeutic index) which is the same as cisplatin (TI = 2.0). The optimum dosage of cisplatin (7 mg/kg mass of test animals) is, however, much less.

In contrast to the ferricenium salt, ferrocene itself was found to be totally inactive, presumably due to its total lack of aqueous solubility.

In follow up studies, Neuse and co-workers[103] found ferrocenylacetic acid induced good to excellent cure rates against human adenocarcinoma, squamous cell carcinoma and large-cell carcinoma of the lung in *in vitro* human tumour clonogenic assays. The latest research on the cytotoxic capabilities of ferrocene compounds has been performed at the University of the Free State.

It was reported in 2001,[36] for example, that 3-ferrocenylbutanoic acid (**[30]** in **scheme 2.5**) is one order of magnitude more active against Murine EMT-6 cancer cells when anchored on the water-soluble polymer as compared to its cytotoxicity as a free monomeric drug. In addition, from this laboratory was filed a patent (December 2000) which described the cytotoxic properties of ferrocene-containing β-diketones and their rhodium and iridium complexes. In particular it was found that the IC_{50}-values of the [FcCOCH2COCF$_3$] (Hfctfa) complex was much more favourable than that of cisplatin, especially against platinum resistant cell lines such as COR L23, a sensitive large human lung cell carcinoma. The therapeutic index (TI) of these compounds also exceeds 8 compared to the 2 for cisplatin.

Osella and co-workers have recently determined the mechanism of action of the ferrocenyl moiety in chemotherapy.[104] The process is based on electron transfer. First the Fe^{II}-containing ferrocenyl group needs to be activated by oxidation to a Fe^{III}-containing ferricenium species by redox-active enzymes in a particular body compartment. The ferricenium species then interacts with water and oxygen to generate a hydroxyl radical ($OH^{\bullet}$). The hydroxyl radical then cleaves the DNA strands, resulting in cell death. Electrochemical and biological studies[8,9] indicate that ferrocenyl derivatives with formal reduction potential larger than ca. 0.216 V *vs* a saturated calomel electrode (SCE) are inactive in cytotoxicity experiments. Ferrocenyl oxidation by redox enzymes in the cell becomes thermodynamically impossible in compounds with higher positive formal reduction potentials. Such ferrocenyl derivatives then become, for all practical purposes, inactive.

2.7.3. Cytotoxicity of ruthenocene

The radiopharmaceutical acetyl-(^{103}Ru)-ruthenocene has been used in the investigation of the affinity of acetylruthenocene for the adrenal glands of mice. This labelled compound was prepared by heating acetyl ferrocene with ^{103}-ruthenium trichloride. The compound was shown to have an affinity for regions of the adrenal gland where adrogen and glucocorticoid syntheses occur.[105] A study was then performed illustrating effects of hormones on the localization of acetylruthenocene. It was found that if the hormones can be controlled, then the acetyl ruthenocene target can also be controlled *in vivo*.[106]

2.7.4. Cytotoxicity of titanocene(IV) dichloride and other titanocene derivatives

Titanocene derivatives and bis(β-diketonato)titanium(IV) appear to offer an alternative for cancer chemotherapy over platinum compounds. These complexes do not follow the rationale and mechanism of action of the platinum complexes.[53]

Diacido titanium complexes of type $[Cp_2TiX_2]$, where X = carboxylates, phenolates, dithiolenes and thiophenolates have shown anti-proliferative action.[107] Other mono-substituted complexes of the formula $[Cp_2TiClX]$, where X = 1,3,5-trichlorophenolate, 1-aminothiophenolate, 1-methylphenolate and selenophenolate, also exhibit similar anti-tumour activity.[107, 108]

Replacement, ranging from mono- to deca-substitution, of H atoms of the Cp rings $[C_5H_5^-]$ for CH_3, C_2H_5 and $[N(CH_3)_2]$ groups was aimed at improving the anti-tumour activity of cyclopentadienyl metal or metallocenyl complexes. This modification of the Cp ligand on $(C_5H_5)Ti^{2+}$ showed a dramatic reduction in the anti-tumour activity, as the degree of H substitution increases.[107]

Whereas substitution on the cyclopentadienyl ring(s) with carbomethoxy has shown increased anti-tumour action.[109]

Several ionic titanocene complexes of general formula $[Cp_2TiXL]^+Y^-$ or $[Cp_2TiL_2]^{2+}\bullet 2[Y^-]$, where X is an anionic ligand and L is a neutral ligand, have been tested for anti-proliferative action.

These species offer higher solubility in water than the neutral titanocene dihalides. A few representative examples of this type of complex are $[Cp_2Ti(bipy)][CF_3SO_3]_2$, $[Cp_2Ti(phen)][CF_3SO_3]_2$, $[Cp_2Ti[o\text{-}S(NHCH_3)C_6H_4]^+I^-$ and $[Cp_2Ti(Cl)NCCH_3]^+[FeCl_4]^-$.[110,111]

Budotitane (**Figure 2.13**) belongs to the class of bis(β-diketonato)metal complexes.[112] The [M(β-diketonato)$_2$X$_2$] complexes are highly susceptible to hydrolysis and are relatively difficult to dissolve in water. Variation of the R groups (entries A-D in **Table 2.5**) of the β-diketonato ligands in [M(β-diketonato)$_2$X$_2$] complexes may increase the anti-tumour activity. Anti-tumour activity is independent of the leaving group X.[113] From examinations of the extent to which aromatic groups (E-H in **Table 2.5**) on the β-diketonato ligand changes the anti-cancer efficiency of the [M(β-diketonato)$_2$X$_2$] complexes, it is evident that when phenyl groups stand in direct conjugation to the metal enolate pseudo-aromatic ring, the anti-tumour activity increases dramatically (entries G-H). Variations on the phenyl ring (entries I-L) also affect the anti-tumour properties of the complexes. The introduction of methyl groups on the phenyl ring (I) does not alter anti-tumour activity, whereas methoxy, chlorine and nitro groups reduce anti-tumour activity (entries J-L).

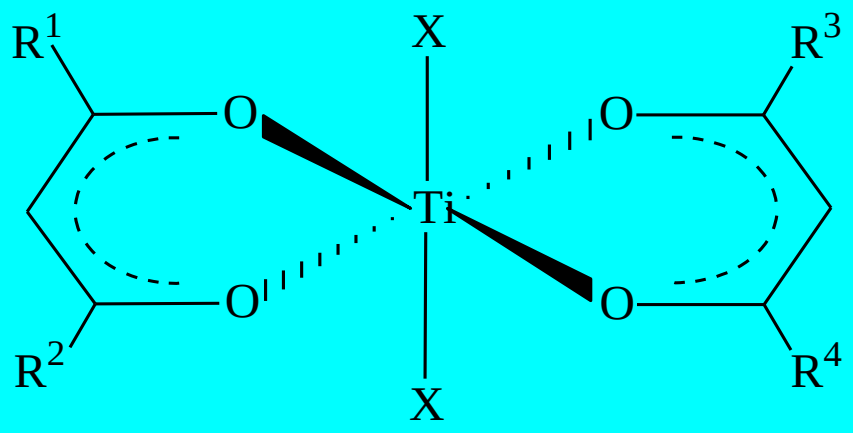

Variations of X, R^1, R^2, R^3 and R^4 are shown in Table 2.12.

Figure 2.13. Structure of budotitane.

Table 2.5. Anti-tumour activity of Ti(β-diketonato)$_2$X$_2$. T/C(%) = (median survival time of treated animal / median survival time of control animal) x 100. Larger T/C values indicate cancer diseased mice lived longer when treated with the indicated drug.

Number	β-diketonato	X	T/C(%)
A	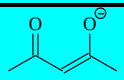	OEt	90-100
B	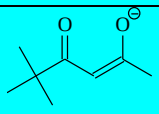	OEt	130-170
C	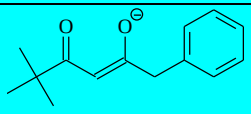	OEt	150-200
D	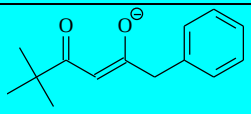	Cl	150-200
E	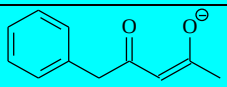	OEt	130-170
F	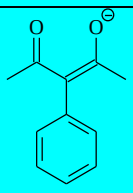	OEt	200-250
G	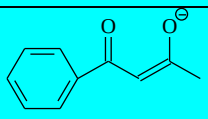	OEt	>300
H	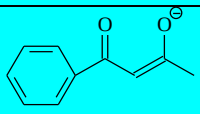	Cl	>300
I	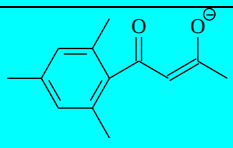	Cl	>300
J	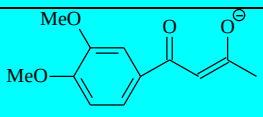	Cl	150-200
K	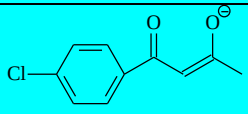	Cl	150-200
L	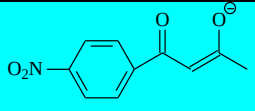	Cl	100-120

Another parameter in changing the activity of the [M(β-diketonato)$_2$X$_2$] type of complexes is variation of the central metal atom. In this case the titanium and zirconium derivatives with the benzoylacetonato ligand produced the highest activity, followed by a marked decrease in the order Hf > Mo > Sn > Ge for the other metals tested (**Table 2.6**).[113]

Table 2.6. Anti-tumour activity of [M(bzac)$_2$X$_2$] complexes, with M as indicated. T/C(%) = (median survival time of treated animal / median survival time of control animal) x 100.

M	T/C(%)
Ti	>300
Zr	>300
Hf	200-250
Mo	150-200
Sn	120-150
Ge	100-110

This study had as its goal the synthesis of new air stable and hydrolysis stable complexes of the type [Cp$_2$Ti (FcCOCHCOR)]$^+$ClO$_4^-$ and testing their activity against cancer cells.

2.8. Structural aspects

2.8.1. Introduction

Certain structural aspects of the various compounds related to this study have already been briefly discussed in previous sections. This segment will concentrate mainly on crystallographic details and associated literature.

2.8.2. Crystallography of ferrocene and ferrocene-containing β-diketones

Crystal structures (**Figure 2.14)** and data for selected β-diketones are summarised in **Table 2.7.**

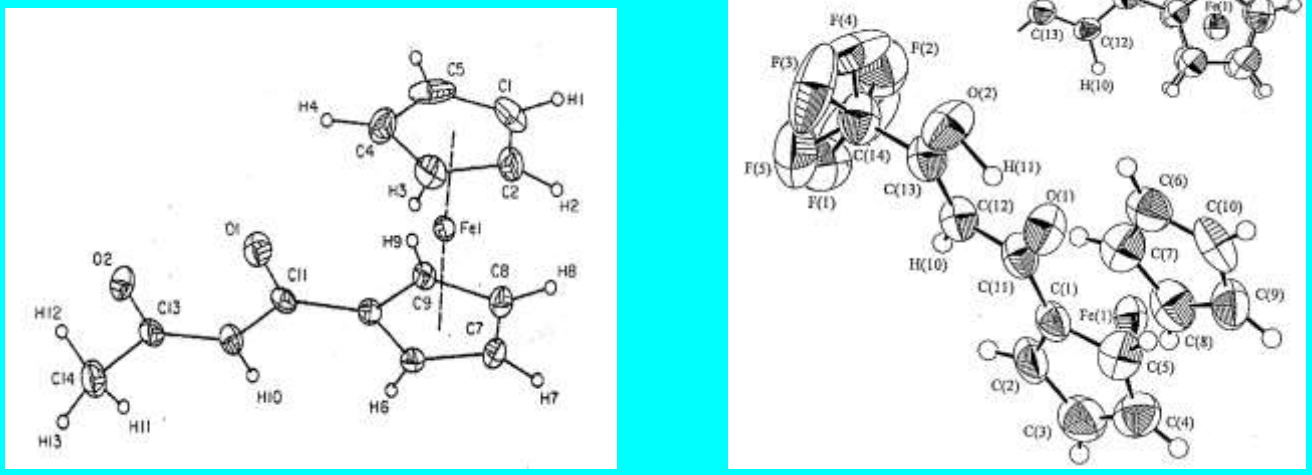

(A) **(B)**

Figure 2.14. Perspective view of the molecules, showing the atom numbering scheme of: **(A)** 1-ferrocenyl-3-hydroxy-but-2-en-1-one or ferrocenoylacetone [$FcCOCH_2COCH_3$] and **(B)** Ferrocenoyltrifluoroacetone [$FcCOCH_2COCF_3$]. The view from above, down the C_5 ferrocenyl axis (top right structure **B**) highlights the eclipsed conformation of the ferrocenyl group and the assymetric enolisation of the molecule.

Table 2.7. Selected crystallographic data for β-diketones, including the typical range of bond lengths in enolized 1,3-diketones. T = triclinic, M = monoclinic, and O = orthorhombic crystal system.

β-diketone	keto or enol	C=O bond length /Å	C-O (enol) bond length /Å	C=C bond length between carbonyl groups /Å	C-C bond length between carbonyl groups /Å	O….O bond length /Å	Crystal system
Hacac [$CH_3COCH_2COCH_3$]	asym enol	1.238	1.331	1.338	1.412	2.535	T
Hfca[114] [$FcCOCH_2COCH_3$]	asym enol	1.287(6)	1.307(6)	1.373(7)	1.406(7)	2.462	O
Hbfcm [$FcCOCH_2COPh$]	asym enol	1.284(4)	1.303(4)	1.372(4)	1.406(4)	2.464(8)	M
Hfctfa [$FcCOCH_2COCF_3$]	Asym enol	1.277(5)	1.297(5)	1.348(6)	1.432(6)	2.549(6)	M

Most of the β-diketones isolated in the solid state, are in the enol form. There are two extreme forms of intramolecular hydrogen bonding namely, symmetric and asymmetric hydrogen bonding. In asymmetric enolization, the enolic hydrogen is bound much more tightly to one oxygen atom than to the other. Symmetric hydrogen bonds as well as markedly asymmetric hydrogen bonds have been observed in examples having identical or different substituents.[114] The fine balance between symmetric and asymmetric hydrogen bonding is indicated by the occurrence of symmetric and asymmetric forms in two polymorphs of the same compound Hdbm [$PhCOCH_2COPh$].[115]

In free [$FcCOCH_2COCF_3$] (Hfctfa) the trifluoromethyl group is disordered. Hfctfa, like [$FcCOCH_2COCH_3$] (Hfca) and [$FcCOCH_2COPh$] (Hbfcm), are enolised asymmetrically in a direction away from the ferrocenyl group, despite the large difference in group electronegativities of the ferrocenyl and the trifluoromethyl groups. This clearly indicates resonance driving forces will always carry priority over electronic driving forces to determine which enol form of a β-diketone possessing aromatic side groups is favoured. The cyclopentadienyl rings of the ferrocenyl group deviate only 2.17(1)° from an eclipsed conformation although the energy barrier to cyclopentadienyl rotation in ferrocene (which includes conversion from the eclipsed to the staggered conformation) is very small (4 $\pm$ 1 kJ mol^{-1}).[114]

This approximately eclipsed formation of the ferrocenyl group is evident in most β-diketones of this type. However, as has been previously mentioned, a staggered conformation is also possible (paragraph 2.3.1., **Figure 2.1**). It is even possible to observe both conformations within different molecules of the same compound, as was the case with (η^4-1,5-Cyclooctadiene)(1-ferrocenyl-1,3-butanedionatoκ^2O,O')rhodium (1), (**Figure 2.15**).[116] Two crystallographically independant molecules A and B are present in the same unit cell (see **Figure 2.16**).

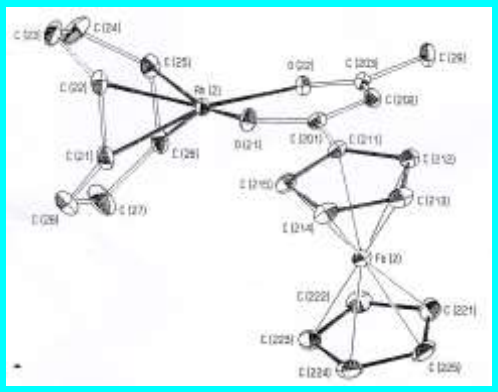

Figure 2.15. Persrective view and atom labelling of molecule B of (η^4-1,5-Cyclooctadiene)(1-ferrocenyl-1,3-butanedionatoκ^2O,O')rhodium (1), H atoms ommited for clarity. The numbering scheme in A and B is identical exept for the first digit which is 1 for A and 2 for B. See also **Figure 2.16.** (From J.C. Swarts, T.G. Vosloo, J.G. Leipoldt and G.J. Lamprecht, *Acta Cryst.*, 763-765, **C49** (1993).

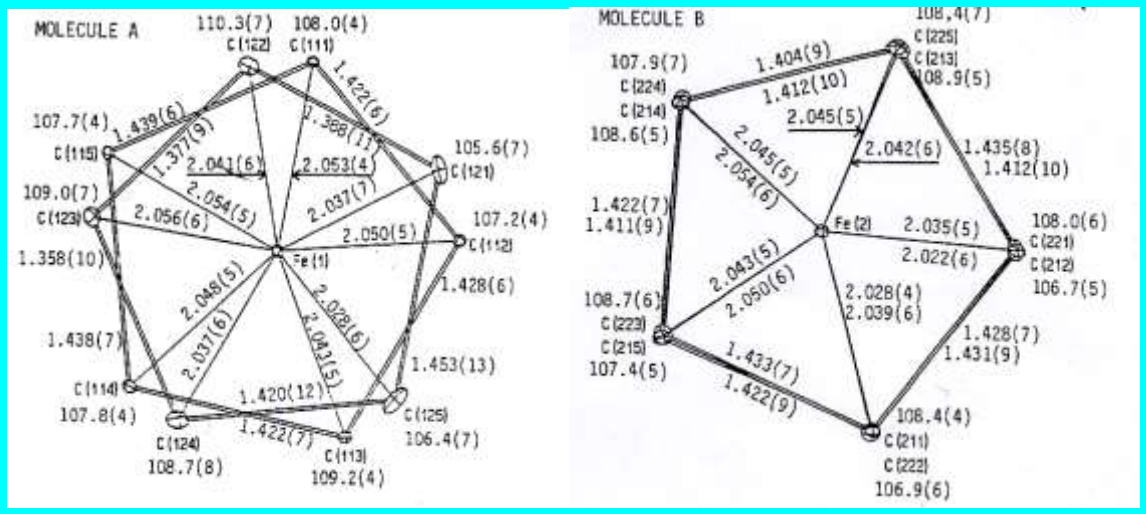

Figure 2.16. A veiw from the top of the ferrocenyl groups of (η^4-1,5-Cyclooctadiene)(1-ferrocenyl-1,3-butanedionatoκ^2O,O')rhodium (1). The bond angles (º) which are indicated above or below each atom refer to the angle between two adjacent sides of the five membered Cp rings. The upper printed bond lengths (Å) shown in each bond in molecule B are associated with atoms C(21*j*), While the lower printed bond lengths are associated with atoms C(22*j*); *j* = 1,2,...,5. (From J.C. Swarts, T.G. Vosloo, J.G. Leipoldt and G.J. Lamprecht, *Acta Cryst.*, 763-765, **C49** (1993).

Another interesting case is that of (E)-1,3-diferrocenyl-2-buten-1-one-water (4/1), (**Figure 2.17**).

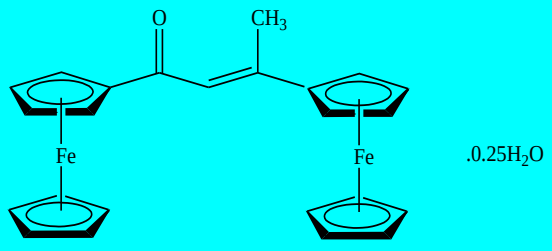

Figure 2.17. Simplified structure of (E)-1,3-diferrocenyl-2-buten-1-one-water (4/1), self-condensation product of acetylferrocene.

The compound results from the self-condensation of acetylferrocene due to incomplete enolate formation, a consequence of the high reactivity of the enolate moiety of acetylferrocene towards electrophilic centers. Two independent $[Fe_2(C_5H_5)_2(C_{14}H_{12}O)]$ molecules (A and B shown in **Figure 2.18.**) are found in the asymmetric unit. Pairs of one of these molecules form dimers linked by hydrogen bonds *via* a water molecule occupying either of two sites related by a center of symmetry.[117]

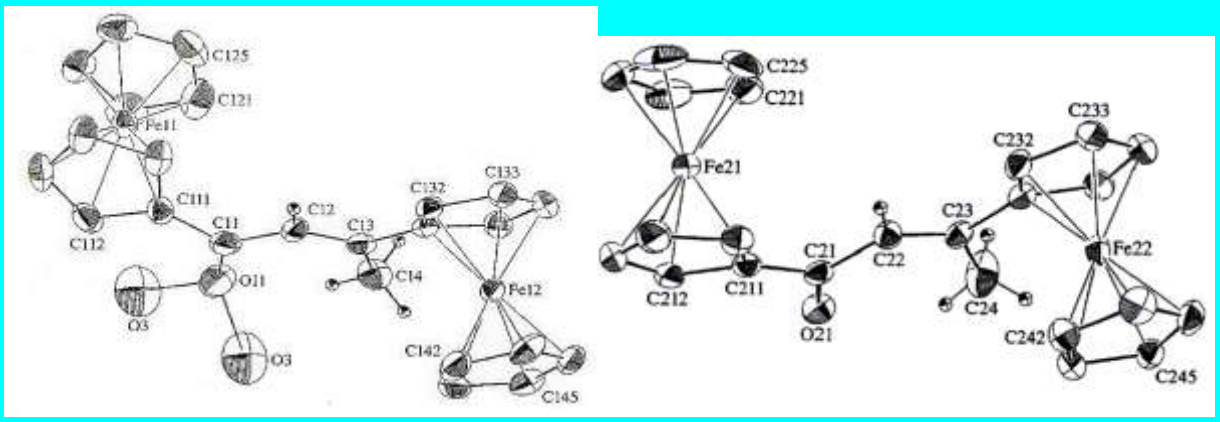

(A) **(B)**

Figure 2.18. The structures of molecules **(A)** (The primed atom is generated through the center of symmetry) and **(B)** of (E)-1,3-diferrocenyl-2-buten-1-one-water (4/1**,** showing the numbering scheme and displacement ellipsoids of 30% probability. (From J.J.C. Erusmus, G.J. Lamprecht, J.C. Swarts, A. Roodt and A. Oskarsson, *Acta Cryst*, 3000-3002, **C52** (1996).

An interesting question which can now be raised, is weather such dimerisation is possible if one of the ferrocenyl groups is replaced by, for example, a ruthenocenyl moiety.

2.9. Conclusion

What follows in this thesis is the discussion of results from a study on various ferrocene-containing β-diketonato titanium(IV) complexes by the author (Chapter 3). Experimental detail of this study (Chapter 4) and a summery of results and future perspectives are given in Chapter 5.

2.10. References

[1] R. Meyer, S. Brink, C.E.J. van Rensburg. G.K. Jooné, H. Gorls and S. Lotz, *J. Organomet. Chem.*, 117, **690** (2005).

[2] C.R. Hauser, F.W. Swamer and J.T. Adams, *Organic reactions*, John Wiley and sons, New York, 59, **8** (1954).

[3] H.G. Walker Jr, J.J. Sanderson and C.R. Hauser, *J. Am. Chem. Soc.*, 4109, **75** (1953).

[4] V. Weinmayr, *Naturwissenschaften*, 311, **45** (1958).

[5] W.R. Cullen, S.J. Rettig and E.B. Wickenheiser, *J. Mol. Catal.*, 251, **66** (1991).

[6] W.C. du Plessis, T.G. Vosloo and J.C. Swarts, *J. Chem. Soc., Dalton Trans.*, 2507 (1998).

[7] S. Moon and Y. Kwon, *Magn. Reson.Chem.*, 89, **39** (2001).

[8] J.B. Conant and A.F. Thompson Jr, *J, Am. Chem. Soc.*, 4039, **54** (1932).

[9] G.W. Wheland, *Advanced Organic Chemistry* 3rd Ed., John Wiley and sons, New York, 59, **8** (1960).

[10] R.J. Irving and M.A.V. Rriberio de Silva, *J. Chem. Soc. Dalton*, 798 (1975).

[11] S. Bratoz, D. Hadzi and G. Rossmy, *Trans. Faraday Soc.*, 464, **52** (1956).

[12] H.S. Jarrett, M.S. Sadler and J.N. Shoolery, *J. Chem. Phys.*, 2092, **21** (1953).

[13] L.W. Reeves, *Can. J. Chem.*, 1351, **35** (1957).

[14] J.G. Leipoldt and E.C. Grobler, *Transition Met. Chem.(Wienheim Ger.)*, 110, **11** (1986).

[15] W.C. (Ina) du Plessis, W.L. Davis, S.J. Cronje and J.C. Swarts, *Inorg. Chim. Acta*, 97, **314** (2001).

[16] J.D. Park, H.A. Brown and J.R. Lachen, *J. Am. Chem. Soc.*, 4753, **75** (1953).

[17] G. Klose, p. Thomas, E. Uhlemann and J. Marki, *Tetrahedron*, 2695, **22** (1966).

[18] R. Epton, M. E. Hobson and G. Marr, *J. Organomet. Chem.*, 231, **149** (1978).

[19] B. Carlson, L. L. Miller, P. Neta and J. Grodkowski, *J. Am. Chem. Soc.*, 7233, **106** (1984).

[20] J.R. Pladziewicz and M.S. Brenner, *Inorg. Chem.*, 3629, **26** (1987).

[21] V.A. Nefedov and L. K. Tarygina, *Russ. J. Org. Chem. (Eng. Transl.)*, 1960, **12** (1976).

[22] S. Sahami and M. J. Weaver, *J. Solution Chem.*, 199, **10** (1981).

[23] M. Rosenblum, *Chemistry of the Iron Group Metallocenes*, Part I, Wiley-Interscince, New York, pp 201-208 (1965).

[24] E.W. Neuse and H. Rosenberg in *Reviews in Macromolecular Chemistry*; eds. K. F. O'Driscoll and M. Shen, Marcel Dekker, New York, **5** (1970).

[25] D.E. Bublitz and K.L. Rinehart Jr., *Organic Reactions*, 1, **17** (1969).

[26] G. Wilkinson, *Comprehensive Organometallic Chemistry*, Pergamon Press, Oxford, **4**, ch. 31 and **8**, ch. 59 (1988).

[27] D.W. Mago, P. D. Shaw and M.D. Rausch, *Chem. Ind. (London)*, 1388 (1957).

[28] R.W. Fish and M. Rosenblum, *J. Org. Chem.*, 1253, **30** (1965).

[29] D.E. Bublitz and K.L. Rinehart Jr., *Organic Reactions*, 1, **17** (1969).

[30] V. Hofmann, H. Ringsdorf and G. Maucevic, *Makromol. Chem.*,1929, **176** (1975).

[31] M. Rosenblum, A.K. Barnejee, N. Danieli, R. W. Fisch and V. Schlatter, *J. Am. Chem. Soc.*, 316, **85** (1963).

[32] K. Schögl, *Mh. Chem.*, 601, **88** (1957).

[33] K. Schögl and H. Egger, *Mh. Chem.*, 376, **94** (1963).

[34] A. Benkeser, Y. Nagai and J. Hooz, *J. Am. Chem. Soc.*, 1450, **86** (1964).

[35] G.R. Buell, W.E. McEwen and J. Kleinberg, *J. Am. Chem. Soc.*, 40, **84** (1962).

[36] W.C. du Plessiss, J.J.C. Erasmus, G.J. Lamprecht, J. Conradie, T.S. Cameron, M.A.S. Aquino and J.C. Swarts, *Can. J. Chem.*, 378, **77** (1999).

[37] R.A. Benkeser, D. Goggin and G. Schroll, *J. Am. Chem. Soc.*, 4025, **76** (1954).

[38] D. Seyferth and J.F. Helling, *Chem. Ind. (London)*, 1568, (1961).

[39] A.N. Nesmeyanov, V.A. Sazonova and V.N. Drozd, *Izv. Akad. Nauk USSR, Odt. Khim. Nauk*, 45, (1962).

[40] P.C. Reeves, *Org. Synth.*, 28, **56** (1977).

[41] P. Da Re and E. Sianesi, *Experientia*, 648, **21(11)** (1965).

[42] V. Hofmann, H. Ringsdorf and G. Maucevic, *Makromol. Chem.*,1929, **176** (1975).

[43] R.F. Hudson and G.E. Moss, *J. Chem. Soc.*, 5157, (1962).

[44] E.W. Neuse and A.G. Perlwitz in *Polyamides as Drug Carriers: Water-Soluble Polymers*; eds. S.W. Shalaby, C.L. McCormick and G. B. Butler, *American Chemical Society*, Washington DC, ch. 25, pp 395-404 (1991).

[45] D. Lednicer, J.K. Linsay and C.R. Hauser, *J. Org. Chem.*, 653, **23** (1958).

[46] J.K. Lindsay and C.R. Hauser, *J. Org. Chem.*, 355, **22** (1957).

[47] D. Seyferth, H. P. Hoffman, R. Burton and J.F. Helling, *Inorg. Chem.*, 227, **1** (1962).

[48] D.E. Bublitz and K.L. Rinehart, *Org. Reactions*, 21, (1968).

[49] P. Köpf-Maier, H. Köpf and E.W. Neuse, *J. Cancer Res. Clin. Oncol.*, 336, **108** (1984)

[50] H. Köpf and P. Köpf-Maier, *in Platinum, Gold and other Metal Chemotherapeutic Agents (A.C.S. Symp. Ser)*, 315, **209** (1983) and references therein.

[51] P.L. Timms and T.W. Turney, *Adv. Organomet. Chem.*, 53 , **15** (1977).

[52] G. Wilkinson, Editor, *Comprehensive Organometallic Chemistry*, vol. **I** and **II**, Pergamon Press, Oxford (1982) and references therein.

[53] E. Meléndez, *Crit. Rev. Oncol.*, 309, **42** (2002).

[54] G. Wilkinson, Editor, *Comprehensive Organometallic Chemistry*, vol. **3**, Pergamon Press, Oxford, pp. 271-547 (1982) and references therein.

[55] J.M. Shreeve, Editor, *Inorganic Synthesis*, John Wiley & Sons, New York, 147, **24** (1986).

[56] R.T. Carlin and J. Fuller, *Inorg. Chim. Acta*, 189 , **225** (1997).

[57] H. Köpf and M. Smichmidt, *Z. Anorg. Allg. Chem.*, 139 , **340** (1965).

[58] S.A. Giddings, *Inorg. Chem.*, 849, **6** (1967); R.B. King and C.A. Eggers, *Inorg. Chem.*, 340, **7** (1968).

[59] G. Fachinetti and C. Floriani, *J. Chem. Soc., Dalton Trans.*, 2433 (1974).

[60] P. Köpf-Maier, M. Leitner and H. Köpf, *J. Inorg. Nucl. Chem.*, 1789, **42** (1980).

[61] P.C. Wailes, H. Weigold and A.P. Bell, *J. Organomet. Chem*, 181, **33** (1971).

[62] P.C. Bharara, *J. Organomet. Chem.*, 199, **121** (1976).

[63] R. Choukroun and Gervais, *J. Chem. Soc., Dalton Trans.*, 1800 (1980).

[64] K. Andrä, *J. Organomet. Chem.*, 567, **11 (**1968).

[65] S.A. Shackelford, D.F. Shellhamer and V.L. Heasley, *Tetrahedron Lett.*, 6333, **40** (1999).

[66] M.G. Meirim, E.W. Neuse, M. Rhemtula and S. Schmitt, *Trans. Met. Chem.*, 272, **13** (1988).

[67] T.J. Pinnavalia and R.C. Fay, *Inorg. Chem.*, 502, **7** (1968).

[68] D.A. White, *J. Inorg. Nucl. Chem.*, 691, **33** (1971).

[69] R.C. Fay and R.N. Lowry, *Inorg, Chem.*,1512 (1967).

[70] D.C. Bradley and C.E. Holloway, *J. Chem. Soc., Chem. Commun.*, 284 (1965).

[71] G. Doyle and R.S. Tobias, *Inorg. Chem.*, 1111, **6** (1967).

[72] N.V. Alekseev and I.A. Ronova, *Zh. Strukt. Khim.*, 103 , **7** (1966).

[73] P.T. Kissinger and W.R. Heineman, *J. Chem. Educ.*, 702 , **60** (1983).

[74] D.H. Evans, K.M. O'Connell, R.A. Peterson and M.J. Kelly, *J. Chem. Educ.*, 290, **60** (1983).

[75] P.A. Christensen and A. Hamnett, *Techniques and Mechanisms in Electrochemistry*, Blackie Academic & Professional, London, pp. 55-67, 170-175 (1994).

[76] J.J. Van Benschoten, J.Y. Lewis, W.R. Heineman, D.A. Roston and P.T. Kissinger, *J. Chem. Educ.*, 772, **60(9)** (1983).

[77] R.J. Le Suer and W.E. Geiger, *Angew.Chem.,Int.Ed.Engl.*, 248, **39** (2000).

[78] L. Pospišil, B.T. King and J. Michl, *Electrochim.Acta*, 103, **44** (1998).

[79] R.R. Gagné, C.A. Koval and G.C. Lisensky, *Inorg. Chem.*, 2855, **19** (1980).

[80] G. Gritzener and J. Kuta, *Pure and Appl. Chem.*, 461, **56** (1984).

[81] H.M. Koepp, H. Wendt and H. Stehlow, *Z. Electrochem.*, 483, **64** (1960).

[82] D.H Evans, K.M. O'Connell, R.A. Peterson and M.J. Kelly, *J. Chem. Edu.*, 291, **60** (1983); P.T. Kissinger and W.R. Heineman, *J. Chem. Edu.*, 702, **60** (1983); J.J. van Benschoten, J.Y. Lewis and W.R. Heineman, *J. Chem. Edu.*, 772, **60** (1983); D.T. Sawyer and J.L. Roberts Jr., *Experimental Electrochemistry for Chemists*, Wiley, New York, pp 118 (1974).

[83] J. Conradie, Ph.D. Study, University of the Orange Free State, R.S.A. (1999).

[84] C. LaVanda, D.O. Cowan, C. Leitch and K. Bechgaard, *J. Amer. Chem. Soc.*, 6788, **96** (1974).

[85] W.H. Morrison, Jr., S. Krogsrud and D.N. Hendrickson, *Inorg. Chem.*, 1998, **12** (1973).

[86] G.M. Brown, T.J. Meyer, D.O. Cowan, C. LeVanda, F. Kaufman, P.V. Roling and M.D. Rausch, *Inorg. Chem.*, 506, **14** (1975).

[87] M.G. Hill, W.M. Lamanna and K.R. Mann, *Inorg.Chem.*, 4687, **30** (1991).

[88] R.J. Gale and R. Job, *Inorg.Chem.*, 42, **20** (1981).

[89] C. Jacob, A.Y. Safronov, S. Wilson, H.A.O. Hill and T.F. Booth, *J.Electroanal.Chem.*, 161, **427** (1997).

[90] M. Sato, G. Maruyama and A. Tanemura, *J.Organomet.Chem.*, 23, **655** (2002).

[91] C. Ohrenberg and W.E. Geiger, *Inorg.Chem.*, 2948, **39** (2000).

[92] S. Trupia, A. Nafady and W.E. Geiger, *Inorg. Chem.*, 5480, **42** (2003).

[93] J. Langmaier, Z. Samec, V. Varga, M. Horacek, R. Choukroun and K. Mach, *J. Organomet. Chem.*, 323, **584** (1999).

[94] G.V. Loukova and V.V. Strelets, *J. Organomet. Chem.*, 203, **606** (2003).

[95] N. El Murr, A. Chaloyard and J. Tirouflet, *J. Chem. Soc. Chem. Comm* , 446 (1980).

[96] M.A Vorotyntsev, M. Casalta, E. Pousson, L. Roullier, G. Boni and C. Moise, *Electrochim, Acta*, 4017, **46** (2001).

[97] A. Vallat, R. Roulier and C. Bourdon, *J. Electroanal. Chem.*, 75, **542** (2003).

[98] A.M. Bond, R. Colton, U. Englert, H. Hűgel and F. Merken, *Inorg. Chim. Acta*, 117, **235** (1995).

[99] S.G. Bown, *J. Photochem. Photobiol. B:Biol.*, 12, **6** (1990).

[100] J.C. Swarts, D.M. Swarts, D.M. Maree, E.W. Neuse, C. La Madeleine and J. E. van Lier, *Anticancer Research*, **21**, p 2033 (2001).

[101] J.C. Swarts, E.W. Neuse, A.G. Perlwitz, A.S. Stephanou and G.J. Lamprecht, *Angew. Makromol. Chem.*, 123, **207** (1993).

[102] P. Köpf-Maier and H. Köpf and E. W. Neuse, *J Cancer Res. Clin. Oncol.*, 336, **108** (1984).

[103] E. W. Neuse and F. Kanzawa, *Appl. Organomet. Chem.*, 19, **4** (1990).

[104] D. Osella, M. Ferrali, P. Zanello, F. Laschi, M. Fontani, C. Nervi and G. Cavigiolio, *Inorg. Chim. Acta*, 42, **306** (2000).

[105] J. Shani, T. Livshitz and M. Wenzel, *Int.J.Nucl.Med.Bio.*, 13, **12** (1985).

[106] J.C. Swarts, D.M. Swarts, D.D. Maree, E.W. Neuse, C. La Madeleine and J.E. Van Lier, *Anticancer Res.*, 1-5, **20** (2000).

[107] P. Köpf-Maier and H. Köpf, *Struct. Bonding*, 103, **70** (1988).

[108] P. Köpf-Maier, T.P. Klapötke and H. Köpf, *Inorg. Chim. Acta*, 119, **153** (1988).

[109] J.R. Boyles, M.C. Baird, B.G. Campling and N. Jain, *J. Inorg. Biochem.*, 159, **84** (2001).

[110] P. Köpf-Maier, *Eur. J. Clin. Pharmacol.*, 1, **47** (1994).

[111] P. Köpf-Maier and H. Köpf, *Chem. Rev.*, 1137, **87** (1987).

[112] M.J. Blandamer and J. Burgess, *Coord. Chem. Rev.*, 93, **31** (1980).

[113] B.K. Keppler and M.E. Heim, *Drugs of the Future*, 638, **3** (1988).

[114] W. Bell, J.A Crayston, C. Glidewell, M.A. Mazid, and B. Hursthouse, *J. Organomet. Chem.*, 115, **434** (1992).

[114] A. Haaland and J. Nilsson, *J. Chem. Soc. Chem. Commun.*, **88** (1968).

[115] M.C. Etter, D.A. Jahn and Z. Urbañczyk-Lipkowska, *Acta Cryst.*, 260, **C43** (1987).

[116] J.C. Swarts, T.G. Vosloo, J.G. Leipoldt and G.J. Lamprecht, *Acta Cryst.*, 763, **C49** (1993).

[117] J.J.C. Erasmus, G.J. Lamprecht, J.C. Swarts, A. Roodt and A. Oskarsson, *Acta Cryst*, 3000-3002, **C52** (1996).

Chapter 3

Results and Discussion

3.1. Introduction

The synthesis and characterisation of new ferrocenyl-titanocenyl organometallic compounds of the type $[Cp_2Ti(FcCOCHCOR)]^+ClO_4^-$, $[(FcCOCHCOR)_2TiCl_2]$ and $[(FcCOCHCOR)_2Ti(O\text{-}CH\text{-}(CH_3)\text{-}Fc)_2]$, with Fc = $(C_5H_5)Fe(C_5H_4)^-$, are described in this chapter. Manipulation of the electron density on the iron and titanium centres was achieved by changing the R-group on the ferrocene-containing β-diketone [$FcCOCH_2COR$] from Fc with group electronegativity, χ_{Fc} = 1.87 on the Gordy scale, to the highly electronegative group CF_3 with χ_{CF3} = 3.01. Characterisation methods of these compounds included techniques such as proton nuclear magnetic resonance (^{1}H NMR), cyclic voltammetry as well as single crystal crystallographic structural determinations. The change in electron density on the central coordinating titanium metal is reflected in formal reduction potentials obtained with voltammetric methods. Cytotoxic properties of selected compounds on cancer cells are also presented.

3.2. Synthesis and identification of compounds

3.2.1. Synthesis of ferrocene-containing β-diketones

Acetylferrocene **[4]** and acetylruthenocene **[6]** were prepared by treating ferrocene **[1]** and ruthenocene **[2]** respectively with acetic anhydride. The reaction was performed in the presence of phosphoric acid. To ensure maximum yields the internal reaction temperature was kept between 100 and 105˚C, reaction time for acetylferrocene was also increased (see **Chapter 4**, paragraph 4.3.1). Acetylferrocene [$FcOCH_3$] **[4]** was prepared in yields of 84% whilst the maximum yield obtained for [$RcOCH_3$] **[6]** was 36%. En route to the target β-diketones an adaptation of the method of Cullen *et al.*[1] to a one-pot procedure was utilised. Abstraction of a methyl proton of acetylferrocene was achieved with the strong, sterically hindered base, lithium diisopropylamide ($LiNPr^i_2$). The resulting lithium salt of acetylferrocene then underwent a Claisen condensation reaction with a range of

monocarboxylic esters to afford the following β-diketones: 1-ferrocenyl-3-phenyl-1,3-propanedione ([$FcCOCH_2COPh$], **[7]**); 1-ferrocenylbutane-1,3-dione ([$FcCOCH_2COCH_3$], **[8]**) and 1-ferrocenyl-4,4,4-trifluorobutane-1,3-dione, ([$FcCOCH_2COCF_3$], **[9]**).

A self-aldol condensation product of acetylferrocene, 1,3-diferrocenylbut-2-en-1-one ([$FcC(CH_3)CHCOFc$], **[X]**) was obtained in all β-diketone synthesis as a by-product. Formation of the by-product was minimised by ensuring that the added base was never the limiting reagent[2] (see **Scheme 3.1**). Rigorous Schlenk conditions were maintained and flash column chromatography of the crude product was needed to separate the β-diketones from the dehydrated self-aldol condensation product **[X]**.

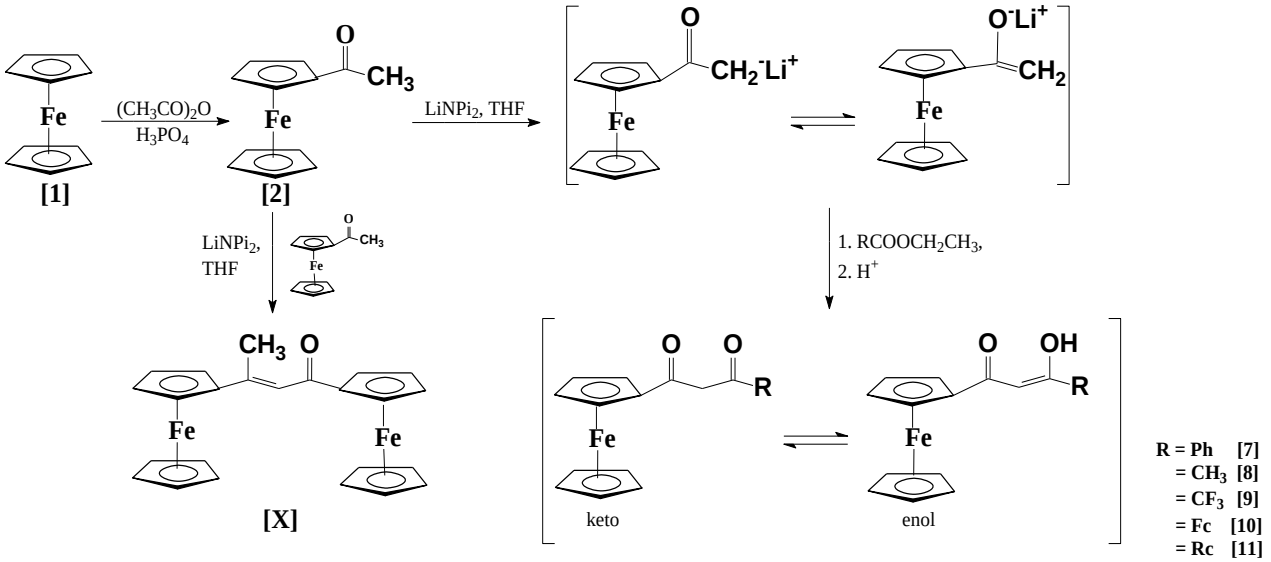

Scheme 3.1. Claisen condensation of acetylferrocene **[2]** with an appropriate ester gives β-diketones [$FcCOCH_2COR$], where R = Ph **[7]**, CH_3 **[8]**, CF_3 **[9]**, Fc **[10]** and Rc **[11]**. Self-aldol condensation of acetylferrocene leads to the side product **[X]**.

1,3-diferrocenylpropane-1,3-dione ([$FcCOCH_2COFc$], **[10]**) and 1-ferrocenyl-3-ruthenocenylpropane-1,3-dione ([$FcCOCH_2CORc$], **[11]**) required preparation of the precursor methylferrocenoate **[4]**, **Scheme 3.2.** Firstly ferrocene is treated in a Freidel Crafts reaction medium with 2-chlorobenzoyl chloride. The product (2-chlorobenzoyl)ferrocene was then treated with the strong base, potassium *tert*-butoxide. Acidification of the crude reaction mixture gave ferrocenecarboxylic acid [$FcCO_2H$] in

63% yield, based on the original amount of ferrocene used. All products in this three-step procedure are distinctively coloured and progress is therefore easily followed. In the Friedel Crafts reaction, addition of anhydrous aluminium chloride to a solution of ferrocene in DCM, produces a deep blue colour, while the product, (2-chlorobenzoyl)ferrocene, is a dark red solid. In the second step, synthesis of ferrocenecarboxylic acid is seen as a colour change from dark a red solution, fading to tan and finally giving the acid as mustard coloured powder. Ferrocenoic acid is then methylated in the presence of H_2SO_4 to give methylferrocenoate (light yellow) with yields in excess of 80%, see **Scheme 3.2.**

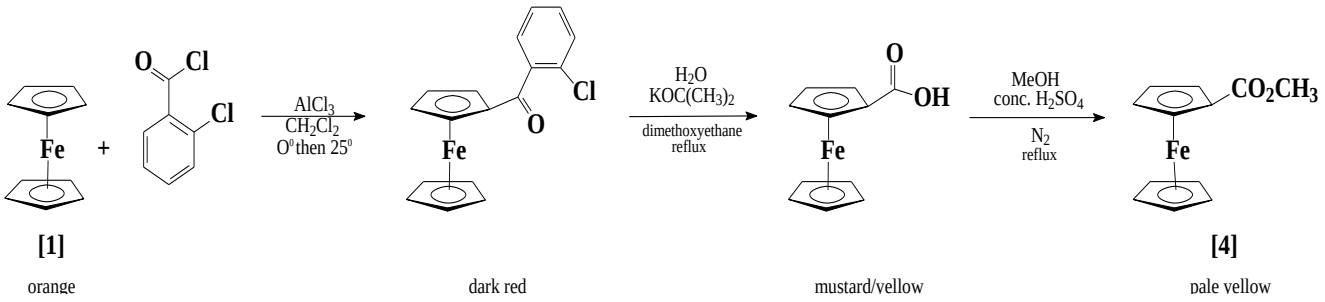

Scheme 3.2. Multi-step synthesis of methylferrocenoate *via* ferrocenecarboxilic acid.

Methylferrocenoate was then reacted with acetylferrocene and acetylruthenocene respectively to give β-diketones **[10]** and **[11]**. Reaction conditions are essentially the same as for the other β-diketones although yields for theses two compounds were found to be much lower (most likely due to steric effects). The synthesis of [$FcCOCH_2COFc$] and [$FcCOCH_2CORc$] are shown in **Scheme 3.3**, see also **Table 3.1.**

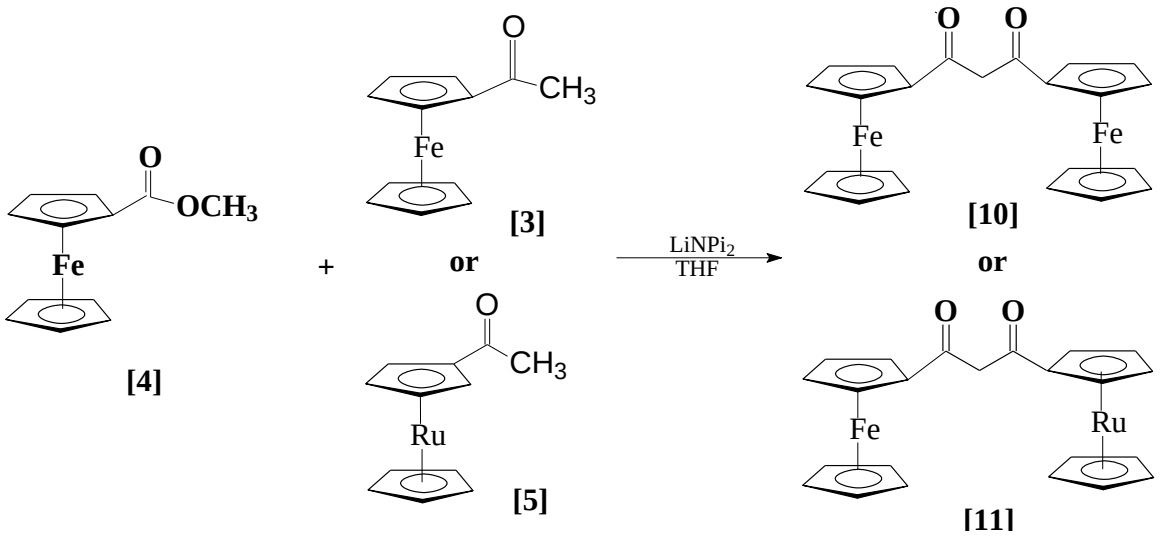

Scheme 3.3. Synthesis of bi-nuclear β-diketones, [$FcCOCH_2COFc$], **[10]** and [$FcCOCH_2CORc$], **[11]**.

As mentioned in chapter 2, β-diketones in solution and in the vapour phase[3] exist in equilibrium mixtures of enol and keto tautomers (see **Scheme 3.1**). ^{1}H NMR studies indicate, by comparing the relative intensities of the CH_2 (keto) and CH (enol) signals in solution, that the enol form dominates.[2,4] Due to resonance driving forces, enolisation in solution, occurs predominantly in the direction away from the aromatic ferrocenyl side group.[2]

After storage of the solid-state β-Diketones for approximately two months, ^{1}H NMR showed that the enol isomer not only dominated, but was in fact the only isomer present. This is due to the enol form having lower crystal energy than the keto form. When such a sample is dissolved in chloroform, an equilibrium sets in between the keto and enol forms according to the reaction

$$\mathbf{Fc\text{-}CO\text{-}CH_2\text{-}CO\text{-}R} \underset{}{\overset{K_c}{\rightleftharpoons}} \mathbf{Fc\text{-}CO\text{-}CH{=}C(OH)\text{-}R}$$

This equilibrium is characterised by an equilibrium constant K_c, which is summarised in **Table 3.1.**

Table 3.1. Percentage yields and equilibrium values for selected β-diketones as well as colour of solid product.

β-Diketone	**Yield (%)**	**Equilibrium value Keto $\rightleftharpoons$ enol (K_c)[a]**	**Colour**
[$FcCOCH_2COPh$]	30	10.4	Pink/red
[$FcCOCH_2COCH_3$]	35	3.4	Orange/red
[$FcCOCH_2COCF_3$]	40	30.0	Purple/red or maroon
[$FcCOCH_2COFc$]	26	2.0	Red/brown
[$FcCOCH_2CORc$]	12	1.94[b]	Tan

a) K_c values taken from W.C. (Ina) du Plessis, W.L. Davis, S.J. Cronje and J.C. Swarts, *Inorg. Chim. Acta*, 97-104, **314** (2001).

b) K.C. Kemp, J.C. Swarts, Unpublished results (2004).

3.2.2. Titanium complexes

Tetrahedral mono-β-diketonato titanium(IV) complexes of the type $[Cp_2Ti(\beta\text{-diketonato})]^+ClO_4^-$, as well as, octahedral bis-β-diketonato titanium(IV) complexes of the type $[(\beta\text{-diketonato})_2TiCl_2]$ and $[(FcCOCHCOR)_2Ti(O\text{-}CH\text{-}(CH)\text{-}Fc)_2]$ were synthesized.

3.2.2.1. Mono-β-diketonato titanium(IV) salts

A variety of new $[Cp_2Ti(\beta\text{-diketonato})]^+ClO_4^-$ complexes **[12]** – **[16]**, (see **Table 3.2**) were synthesized according to the general procedure as described by Doyle and Tobias.[5] Synthesis is initiated by dissolving titanocene dichloride ($[Cp_2TiCl_2]$) in water. During this time the two Cl^- groups of $[Cp_2TiCl_2]$ are replaced with water molecules giving several cationic species (see **Chapter 2**, page 30, **Scheme 2.9**) one of which is **[47]** (**Scheme 3.4**).

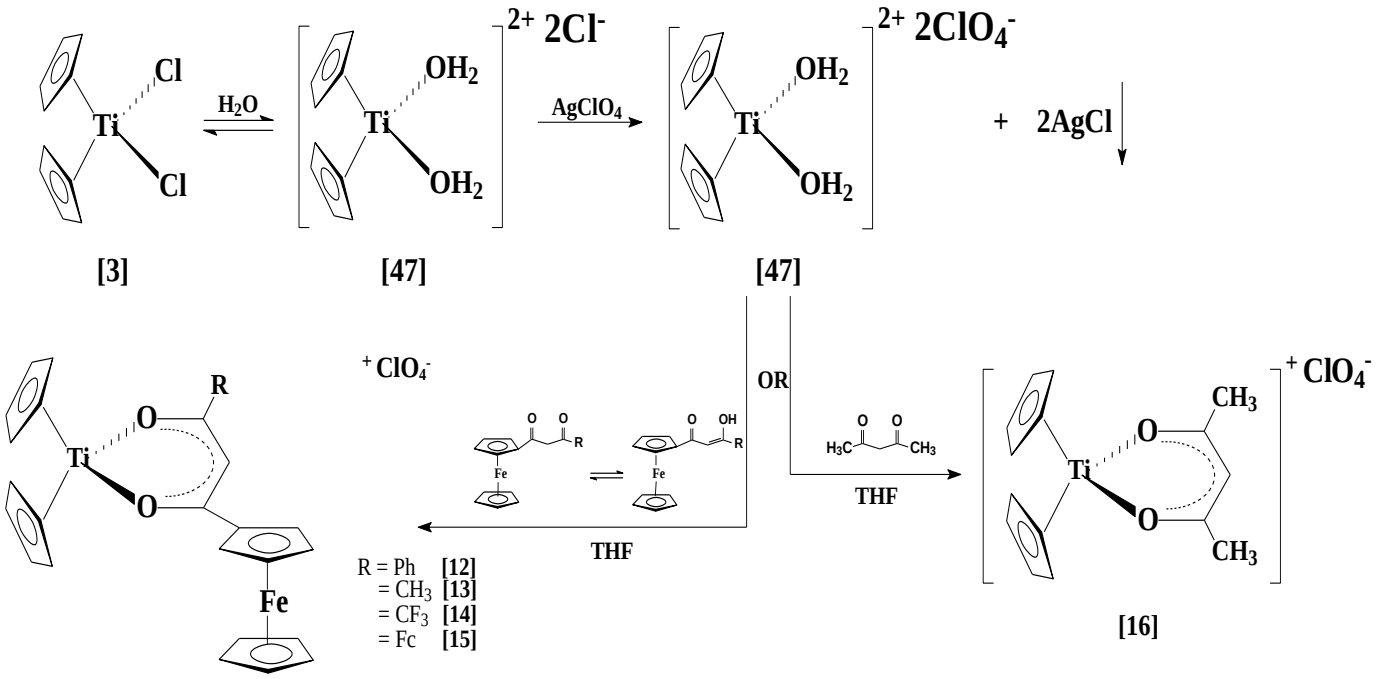

Scheme 3.4. Synthesis of mono-β-diketonato titanium(IV) salts of the type $[Cp_2Ti(\beta\text{-diketonato})]^+ClO_4^-$, where R = Ph **[12]**, CH_3 **[13]**, CF_3 **[14]**, Fc **[15]** as well as $[Cp_2Ti(H_3CCOCHCOCH_3)]^+ClO_4^-$ **[16]**. The aquated species **[47]** is but one of several such species which may exist in solution.

Addition of silver perchlorate [$AgClO_4$] removes all Cl^- by precipitating AgCl, while the aquated perchlorate titanium salt remains in solution. The aquation equilibrium reaction is driven to completion by this precipitation of silver chloride. Replacement of the Cl^- groups is done to enhance the next step of the synthesis, i.e. coordination of the β-diketonato ligand onto the titanium centre. This is because H_2O is a much better leaving group than Cl^-. The final product is an ionic species with ClO_4^- as the counter ion (**Scheme 3.4**). Due to the dominance of the enol tautomer of β-diketonates in solution a base or hydrogen acceptor is not required for the reaction.[2]

In the case of $[Cp_2Ti(FcCOCHCORc)]^+ClO_4^-$ **[17]**, i.e. where R = ruthenocene, the synthesis described above failed, with side reactions dominating. To obtain $[Cp_2Ti(FcCOCHCORc)]^+ClO_4^-$, a β-diketone exchange reaction was utilised (**Scheme 3.5.)**. It was found that this β-diketone exchange reaction is only synthetically viable when the incoming β-diketone contains pendant side groups which are less electronegative than those of the leaving ligand. Here $\chi_{Fc} = 1.87$, $\chi_{Rc} = 1.94$[6] while $\chi_{CH3} = 2.34$. The crystal structure of $[Cp_2Ti(FcCOCHCOCH_3)]^+ClO_4^-$ reported in this study (paragraph 3.3.2) provides an explanation as to the efficiency of this type of reaction (see **Chapter 3**, page 83, **Scheme 3.15**).

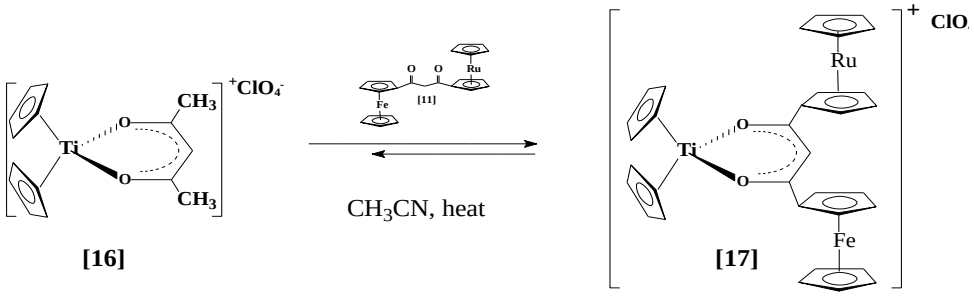

Scheme 3.5. Synthesis of $[Cp_2Ti(FcCOCHCORc)]^+ClO_4^-$ **[17]**.

Table 3.2. Synthesised Mono-β-diketonato titanocenyl complexes.

Ti complex	No.	Colour	Remark
$[Cp_2Ti(FcCOCHCOPh)]^+ClO_4^-$	**[12]**	Purple	New
$[Cp_2Ti(FcCOCHCOCH_3)]^+ClO_4^-$	**[13]**	Red-brown	New
$[Cp_2Ti(FcCOCHCOCF_3)]^+ClO_4^-$	**[14]**	Navy blue	New
$[Cp_2Ti(FcCOCHCOFc)]^+ClO_4^-$	**[15]**	Purple-brown	New
$[Cp_2Ti(CH_3COCHCOCH_3)]^+ClO_4$	**[16]**	Grey-red	Known[5]
$[Cp_2Ti(FcCOCHCORc)\ ]^+ClO_4^-$	**[17]**	Tan	New

All the mono-β-diketonato titanium(IV) salts are insoluble in water, hexane and ether, but soluble in organic solvents such as chloroform, dichloromethane, acetone and ethanol. Dissolving the product in ethanol causes decomposition of the product by the splitting off one of the cyclopentadienyl rings.[7]

The mono-β-diketonato titanocenyl compounds from **Table 3.2** have been found to be reasonably stable in the solid state and have (so far) been stored for up to two years without significant decomposition. The complexes are also reasonably stable in solution. After standing two days in acetone or acetonitrile only slight decomposition was detected. Slow coordination, with the solvent (acetone or acetonitrile) is thought to be the reason for the observed spectral changes (see **Figure 3.1)**.

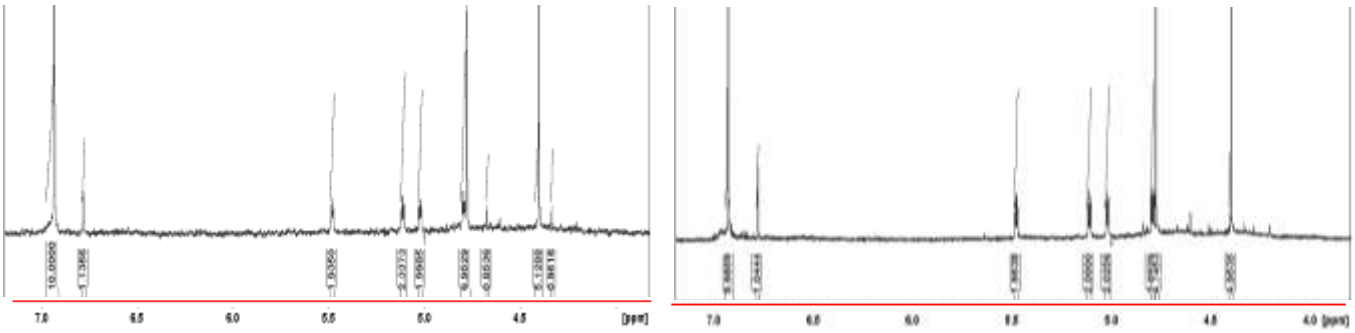

(A) **(B)**

Figure 3.1. ^{1}H NMR spectra of $[Cp_2Ti(FcCOCHCORc)]^{+}ClO_4^{-}$ (acetone-d_6). **A)** After 10 minutes in solution. **B)** After two hours in solution. Arrows highlight changes over time. These changes are not ascribed to aqueous decomposition, due to the stability of these complexes towards water, see **Chapter 4** synthetic details.

^{1}H NMR spectra of acetone-d_6 solutions of all the mono-β-diketonato titanium(IV) salt complexes $[Cp_2Ti(FcCOCHCOR)]^{+}ClO_4^{-}$ are easily interpreted (**Figure 3.2**). Three general signal(sets) are observable: Titanium bound cyclopentadienyl (Cp) protons; a methine proton from the β-diketonato ligand and finally the ferrocene signals. The titanium bound cyclopentadienyl protons (Cp_2 = 10 protons) resonate at a relatively low field (~7.0 ppm) due to the electropositivness of the Ti^{4+} centre. The β-diketonato methine proton ($[FcCOC\mathbf{H}COR]^{-}$ = 1 proton) resonates at a slightly higher field between 6.0 and 7.0 ppm, which is still in the aromatic region. This is due to the pseudo-aromatic system generated by the coordination of the β-diketonato ligand to titanium(IV). Three peaks, two less

intense signals (2 x ½ x C_5H_4(Cp) = 2 x 2 protons) of the substituted cycoplentadienyl ring of ferrocene and one longer signal of greater intensity (Cp = 5 protons), are characteristic of the ferrocenyl group. The ferrocenyl "trio" are found between 4.0 and 6.0 ppm. The remaining signals belong to the R-group of the β-diketonato ligand i.e. R = Ph, CH_3, CF_3, Rc or Fc. If R = Fc the ferrocenyl signals integrate double the usual amount of protons. Varying the R-group causes shifts in the exact position of the first three described signals. These shifts are due to electronic communication through C-C bonds *via* conjugation. Depending on the electron donating or electron withdrawing properties of the β-diketonato R-group, the signals may be moved either up or down field (**Table 3.3**).

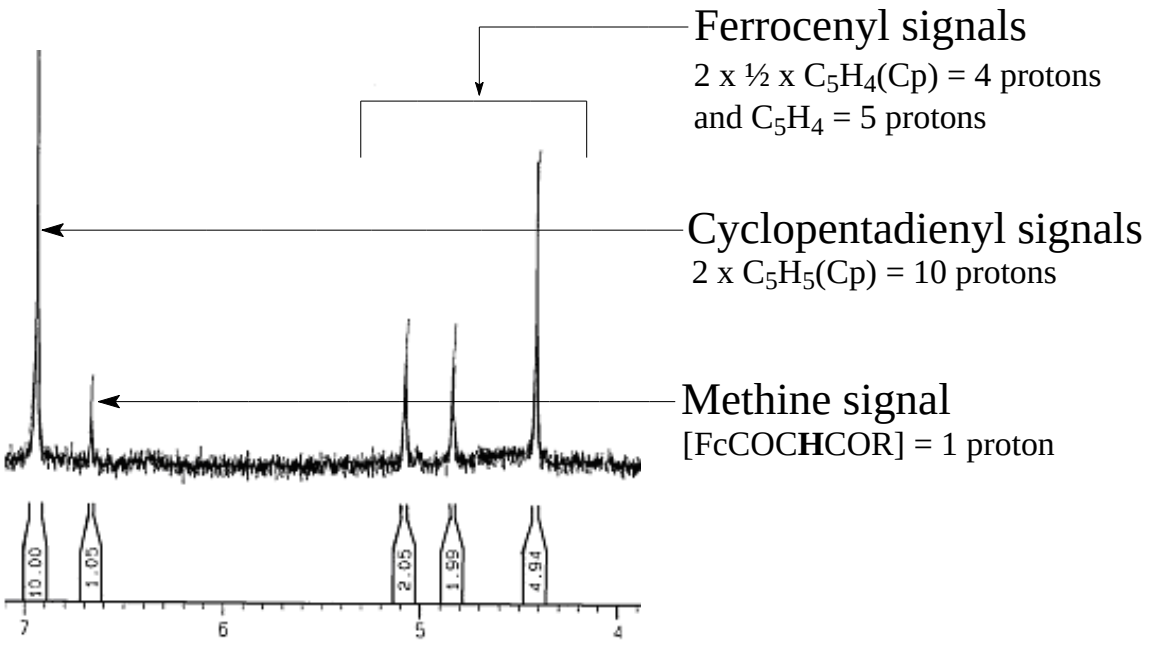

Figure 3.2. Typical ^{1}H NMR signals of $[Cp_2Ti(FcCOCHCOR)]^+ClO_4^-$ complexes.

Table 3.3. Difference in methine ^{1}H NMR peak positions (in acetone-d_6) and synthetic yields of the mono-β-diketonato titanocenyl complexes of the type $[Cp_2Ti(FcCOCHCOR)]^+ClO_4^-$. Group electronegativity, χ_R, and the pK_a of the free β-diketones are also listed.

No.	R group	Yield	^{1}H NMR position of the methine proton / ppm	χ_R [a] / Gordy scale	$X_{Fc}(1.87) + \chi_R$	pK_a of the free β-diketone[2]
[12]	Ph	35%	7.31	2.21	4.08	10.41
[13]	CH_3	46%	6.68	2.34	4.21	10.01
[14]	CF_3	35%	6.90	3.01	4.88	6.53
[15]	Fc	25%	6.87	1.87	3.74	13.10

[17]	Rc	20%	6.78	1.94[6]	3.81	>13.00[6]

a) χ_R (Gordy scale) apparent group electronegativity values.[2, 6]

In general, an increase in percentage yield of the $[Cp_2Ti(\beta\text{-diketonato})]^+ClO_4^-$ complexes is observed as the group electronegativity of the R-groups of the β-diketonato ligand increases (see **Figure 3.4**).

As the ruthenocene-containing complex **[17]** was produced *via* a different synthetic rout than **[12]** - **[15]**, it is not considered in the percentage yield relationship (coordinates have been included separately).

From the graph (**Figure 3.3**) the expected yield of $[Cp_2Ti(FcCOCHCOCF_3)]^+ClO_4^-$ **[14]** is about 72%, yet, much lower yields are found in practice. This poor yield of the CF_3–containing complex may be due to very strong Ti-F bond strength (569 $kJ.mol^{-1}$).[8] It is considered possible that the $[CpTi(H_2O)_2]^+ClO_4^-$ will break some of the C-F bonds (bond strength = 552 $kJ\ mol^{-1}$)[8] of the β-diketone $[FcCOCH_2COCF_3]$. This decomposition of the β-diketone will decrease yields in the synthesis of compound **[14]**.

There does not seem to be a direct relationship between χ_R and ^1H NMR position of the β-diketonato methine proton or the pK_a of the free β-diketone (**Table3.3**). The general trend is that as χ_R increases, the methine ^1H NMR peak moves to a higher field position. The methine signals are found in the aromatic region due to the pseudo-aromatic metallocyclic ring to which they are bound.

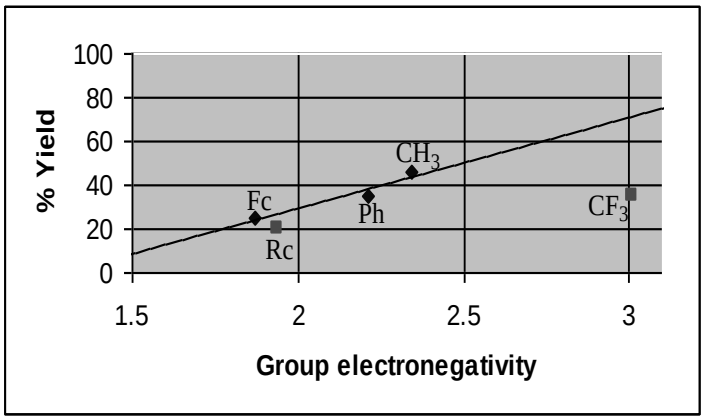

Figure 3.3. Relationship between percentage yield (%) of the $[Cp_2Ti(\beta\text{-diketonato})]^+ClO_4^-$ complexes and the group electronegativities (Gordy scale) of the R-groups on the β-diketonato ligands.

Synthesis of $[Cp_2Ti(FcCOCHCOR)]^+$ cations are complicated by the insolubility of the β-diketones in water. This problem was overcome by means of mixed solvent systems utilising H_2O as solvent for titanocene species and THF for β-diketone solutions. Aquation of titanocene dichloride is essential for a successful reaction. Synthesis of $[Cp_2Ti(\beta\text{-diketonate})]^+ClO_4^-$ complexes (**Scheme 2.10.**, paragraph 2.5.2., pg 30) is therefore more accurately described by **Scheme 3.3.** The synthetic procedure (**Chapter 4**) describes the use of a slight molar shortage (1 %) of $AgClO_4$ compared to the required volume to remove all Cl^-. This protocol was adapted because it was found that any excesses of silver perchlorate caused reaction failure. The final modification to the procedure of Doyle and Tobias was the addition of inert atmospheric reaction conditions i.e. reactions were performed under N_2 to increase yields.

3.2.2.2. Dichlorobis-β-diketonato titanium(IV) complexes

The reactions of three β-diketones [$FcCOCH_2COR$], where R = Ph, CH_3 and CF_3 with titanium(IV) tetrachloride were studied. The complexes were synthesised according to the general procedure as described by Fay and Lowry.[9] The procedure involves dissolving the β-diketone (2 eq) in dichloromethane. $TiCl_4$ (1 eq.), also dissolved in DCM, is added giving an instant colour change from the reddish β-diketone solutions to dark green suspension. The reaction is then driven to completion by the addition of heat (see **Scheme 3.6**). All the bis-β-diketonato titanium complexes are exceptionally moisture sensitive during all stages of preparation. Extreme care must therefore be taken to ensure all glassware and solvents are utterly dry. Dry hexane is used to precipitate the product, which had to be collected by filtration under a nitrogen stream to prevent decomposition by humidity. Original reaction conditions used chloroform as the solvent, but higher yields were obtained with DCM. Dichloromethane also proved easier to work with than chloroform. A lower boiling point

helped in controlling the speed of evaporation, as well as minimising other problems caused by $CHCl_3$ fumes.

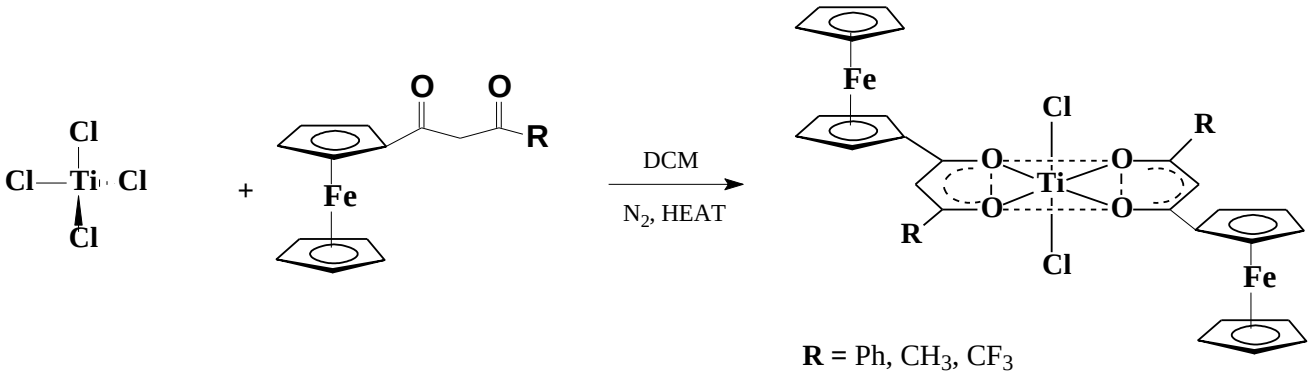

Scheme 3.6. Synthesis of dichlorobis-β-diketonato titanium(IV) complexes of the type $[(FcCOCHCOR)_2TiCl_2]$, where R = Ph, CH_3 and CF_3.

Table 3.4. Percentage yields and colours of synthesised dichlorobis-β-diketonato titanium(IV) complexes, as well as group elecronegativity of the R-group on the β-diketone.

Complex	No.	Yield (%)	χ_R (Gordy scale)	Colour
$[(FcCOCHCOPh)_2TiCl_2]$	**[18]**	79	2.21	Bottle green
$[(FcCOCHCOCH_3)_2TiCl_2]$	**[19]**	78	2.34	Emerald green
$[(FcCOCHCOCF_3)_2TiCl_2]$	**[20]**	72	3.01	Dark blue/green

As seen in **Table 3.4** the yields obtained for the bisβ-diketonato complexes were quite proficient. **Figure 3.4** presents the relationship between % yield of the complexes and the group electronegativity (χ_R) of the R-group on the β-diketone. From the figure it is evident that there is a direct relationship between these two properties. That is, with increasing electronegativity (electron withdrawing character) there is an unequivocal decrease in product yield. Ti(IV) is also very electronegative

(deficient in electrons) and will therefore preferably complex with electron rich ligands, which has a stabilising effect on Ti-O-C bonds and therefore the complexes to which they are bound.

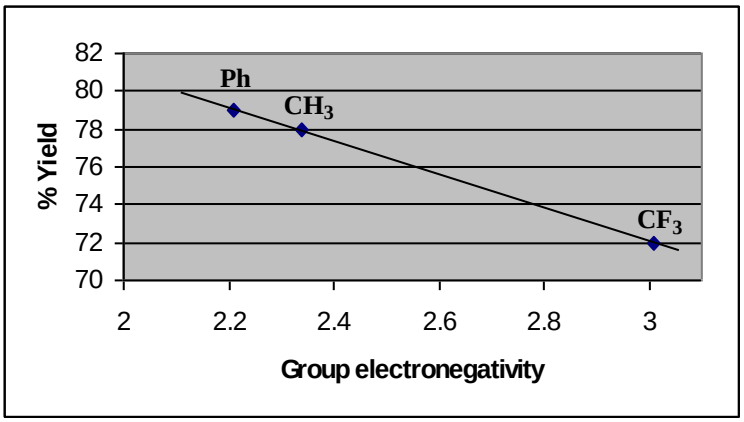

Figure 3.4. Relationship between percentage yield (%) and the group electronegativity (of the R-groups on the β-diketonato ligands, Gordy scale) for bis-β-diketonato titanium(IV) complexes of the type [(β-diketonato)$_2$TiCl$_2$] where R = Ph **[18]**, CH_3 **[19]** and CF_3 **[20]**.

Cleaning the products **[18]** – **[20]**, of side reaction products and excess starting materials proved to be a challenging task. Once again, sensitivity to atmospheric moisture presented problems. These were overcome by working as fast as possible. Recrystallisation was performed under an argon blanket and all vessels were sealed immediately and stored under dry conditions. The final product is also stored in sealed containers under argon in a silica gel dessicator to prevent decomposition for up to six months.

^{1}H NMR spectra of the dichlorobis-β-diketonato titanium(IV) complexes were performed in acetone-d^6 solutions. The spectra are not as easily interpreted as those of the mono-β-diketonato titanocene complexes. Interpretation of the spectra becomes difficult, as singlet signals for the various groups are not seen. Instead multiplets, which integrate to the correct amount of protons, are observed. In this way the multiplet methine (2 x [FcCOC**H**COR]$^-$ = 2 protons) and ferrocenyl (4 x Fc = 18 protons) signals are assigned (**Figure 3.5**).

The various signals for these complexes resonate at slightly higher fields than their mono- β-diketonato counterparts. This is due to the cationic nature of the mono-β-diketonato complexes (electron deficient) in contrast to the neutral bis-β-diketonato complexes (abundant electrons). The *raison d'être*

for the multiplet signals is attributed to a mixture of a number of different possible isomers of the complexes (see **Scheme 3.7**), which cause different interactions through space.

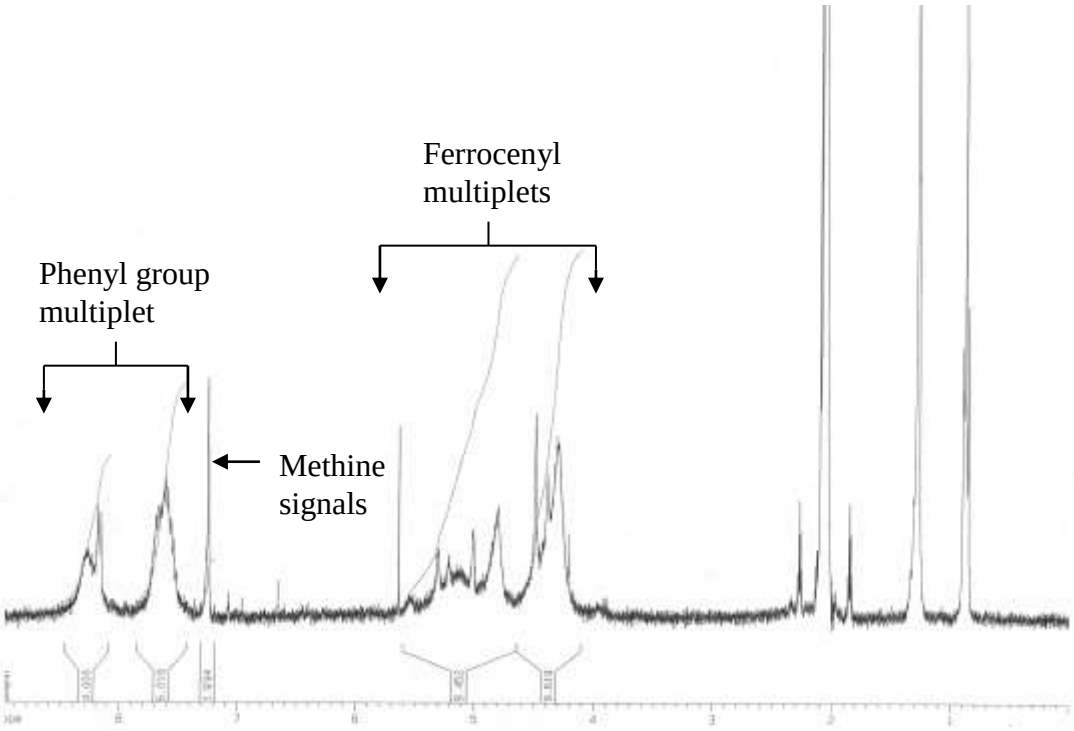

Figure 3.5. Typical ^{1}H NMR signals for $[(FcCOCHCOR)_2TiCp_2]$ complexes ($[FcCOCHCOPh)TiCp_2]$ **[20]** is given here as a representative example.

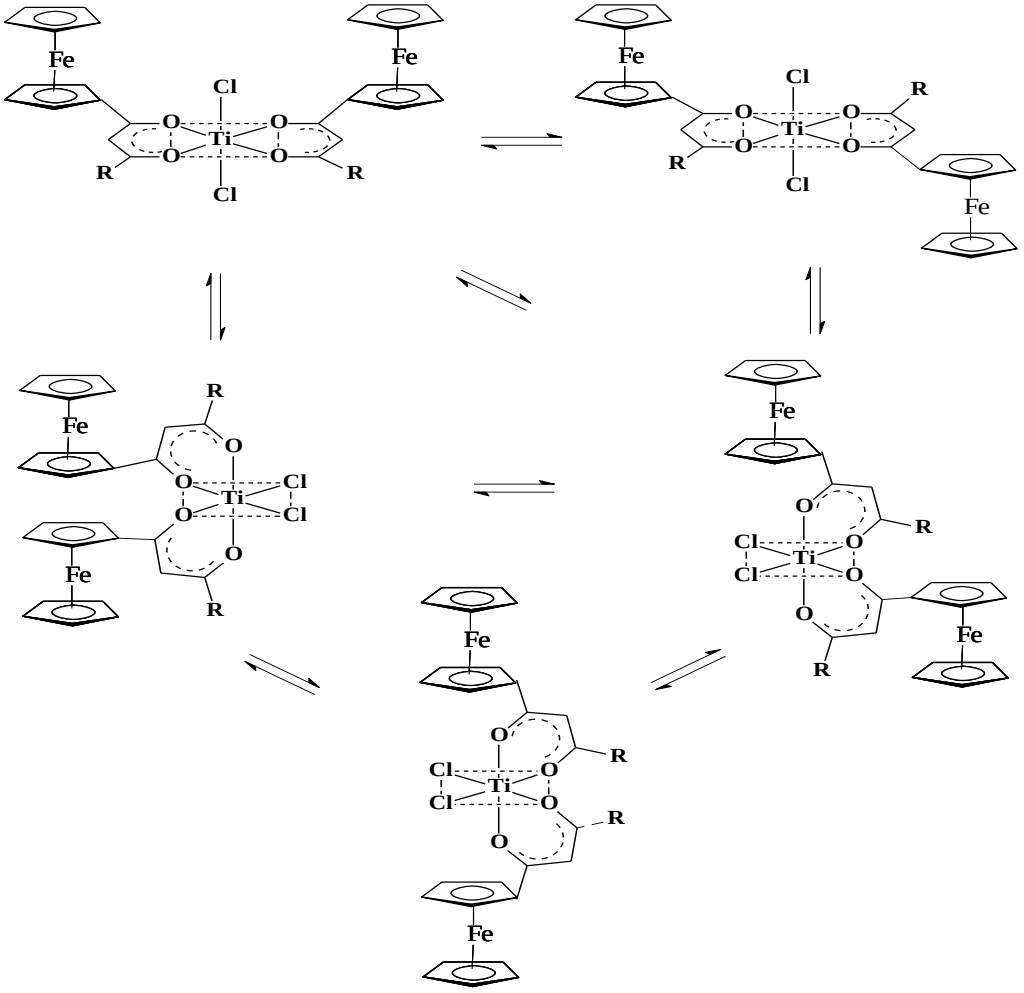

Scheme 3.7. Five of the possible isomers for dichlorobis-β-diketonato titanium(IV) complexes.

3.2.2.3. Di(1-oxyethyl-1-ferrocenyl)bis(β-diketonato)titanium(IV) complexes

The ferrocenyl alcohol, 1-ferrocenylethan-1-ol ([$FcCH_3(CH)OH$]), was added to the dichlorobis-β-diketonato titanium(IV) complexes to replace the chloride ligands.

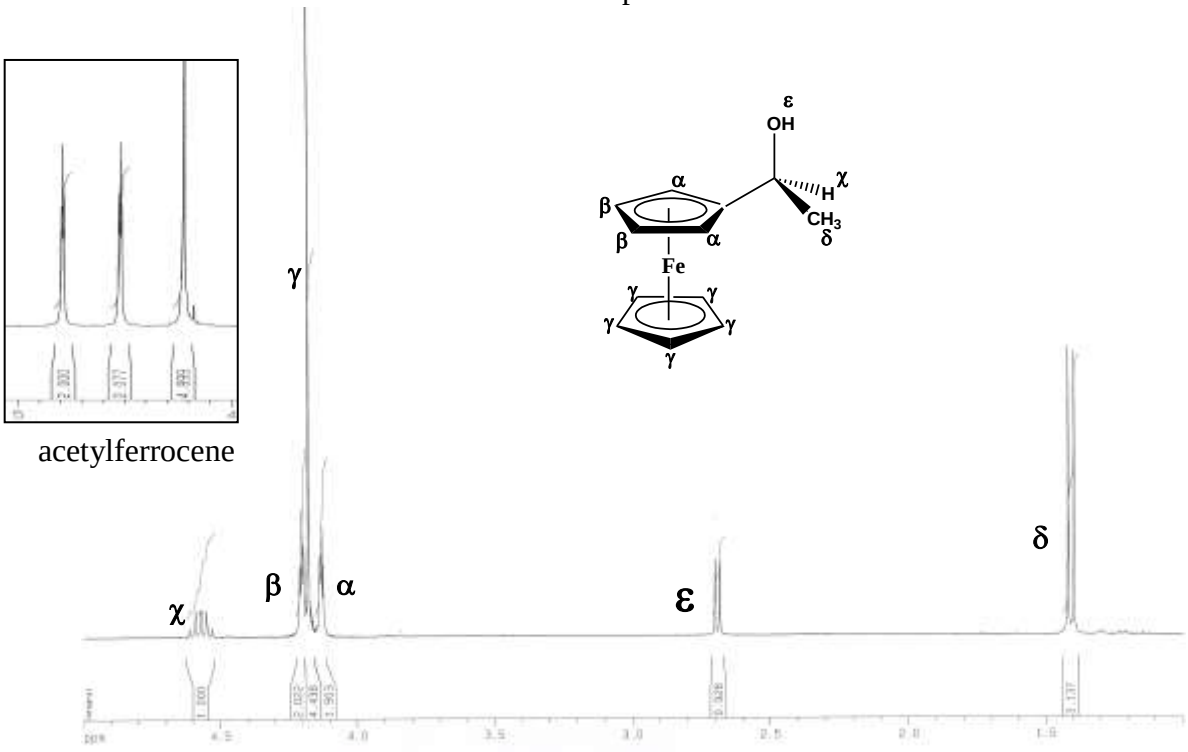

Figure 3.6. ^{1}H NMR spectra of 1-ferrocenylethan-1-ol [$FcCH_3(CH)OH$] in $CDCl_3$ (Insert shows ferrocenyl signals for ^{1}H NMR spectra of acetylferrocene [$(C_5H_5)Fe(C_5H_4)COCH_3$)]).

In the case of acetylferrocene (see insert in **Figure 3.6**) the -$COCH_3$ group is electron withdrawing, resulting in the characteristic ferrocenyl 2 x triplet signals (2 x ½ $(C_5H_4)^{2-}$ = 2 protons each) at lower field than the singlet ($(C_5H_5)^-$ = 5 protons). Interesting to note, is how the ferrocene signals of 1-ferrocenylethan-1-ol have changed. The [$CH(OH)CH_3$] group is electron donating, which moves the entire ferrocenyl signal set to a higher field. This effect is experienced more strongly by the H atoms adjacent to the substituent group (Hα) causing the triplet to shift to a higher field (up field of the singlet) at 4.13 ppm. The signal of the (Hβ) protons remains down field of the C_5H_5 singlet (Hγ) but much closer than the corresponding acetylferrocene signal. The methyl (Hδ) signal displays as a doublet at 1.4 ppm, while the hydroxyl (OH, ε) also displays as a doublet at 2.7 ppm. The methine proton (Hχ) neighbours the CH_3 and OH groups and the ^{1}H NMR signal displays as a quartet of doublets, at 4.63 ppm, with some signals overlapping.

Three di(1-oxyethyl-1-ferrocenyl)bis(β-diketonato)titanium(IV) complexes of the type [$(FcCOCHCOR)_2Ti(O\text{-}CH(CH_3)\text{-}Fc)_2$], where R = Ph **[21]**, CH_3 **[22]** and CF_3 **[23]**, were synthesised

from the reaction between **[18]**, **[19]** and **[20]** and 1-ferrocenylethane-1-ol. The synthesis of these compounds is illustrated in **Scheme 3.8.**

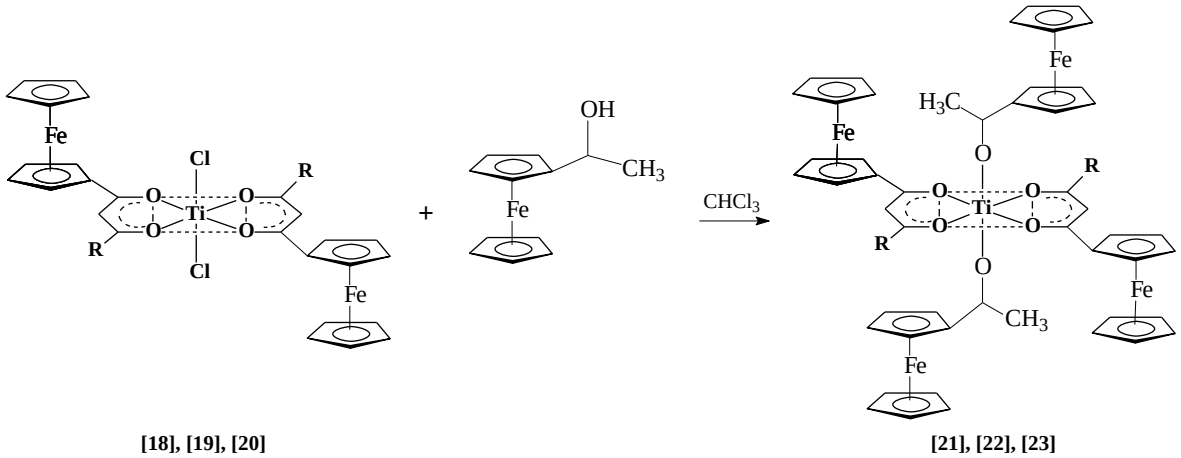

[18], [19], [20] **[21], [22], [23]**

Scheme 3.8. Synthesis of the $[(FcCOCHCOR)_2Ti(O\text{-}CH(CH_3)\text{-}Fc)_2]$ complexes, where R = Ph **[21]**, CH_3 **[22]** and CF_3 **[23]**.

Table 3.5. Yields obtained for the synthesis of the di(1-oxyethyl-1-ferrocenyl)bis(β-diketonato)titanium(IV) complexes with different R-groups.

Compound	**R group**	**% Yield**	**χ_R (Gordy scale)**	**Colour**
[21]	Ph	29	2.21	Green/black
[22]	CH_3	38	2.34	Dark green
[23]	CF_3	45	3.01	Blue/black

As can be seen from the data in **Table 3.5**, there appears to be a relationship between the group electronegativity of the R-group on the β-diketonato ligand and the yield obtained. The general trend is observed in **Figure 3.7.** That is, as the group electronegativity increases the yield also increases. These results are in contrast to those found for the dichlorobis-β-diketonato titanium(IV) complexes, and may be explained by an increase in the positive character of the titanium centre as χ_R increases. This makes the chloro-complexes better electrophiles and the titanium centre more susceptible to nucleophilic attack by the ferrocene-containing alcohol.

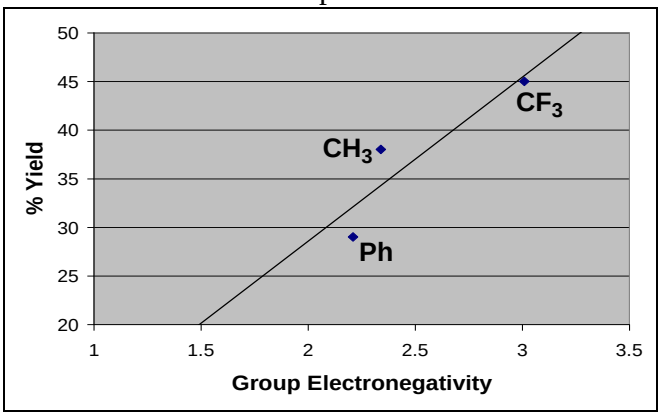

Figure 3.7. Graph of group electronegativity *vs.* % Yield of the $[(FcCOCHCOR)_2Ti(O\text{-}CH\text{-}(CH)\text{-}Fc)_2]$ complexes.

The ^1H NMR spectra of acetonitrile-*d* (CD_3CN) solutions of the di(1-oxyethyl-1-ferrocenyl)bis(β-diketonato)titanium(IV)complexes, $[(FcCOCHCOR)_2Ti(O\text{-}CH\text{-}(CH)\text{-}Fc)_2]$ are once again quite difficult to interpret (see **Figure 3.8**). The ferrocene signals for the β-diketonato ligand as well as the alcohol can not be resolved at all. Instead a broad multiplet is observed between 4.2 -5.6 ppm. The multiplet integrates for the correct number of protons, namely 36. The ferrocene-based multiplet, as well as the multiplets observed for the other protons, are attributed to different possible isomers for the complexes as well as different isomers R/S for 1-ferrocenylethan-1-ol. The isomers cause different interactions through space and are comparable to those shown in **Scheme 3.7.**

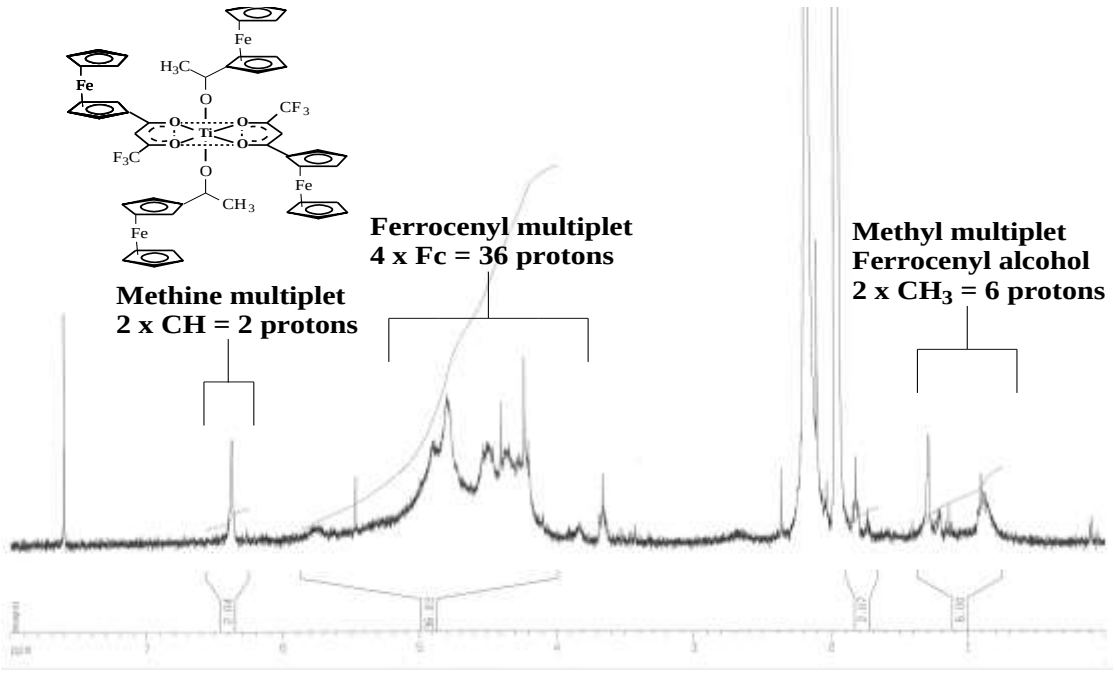

Figure 3.8. ^1H NMR of $[(FcCOCHCOCF_3)_2Ti(O\text{-}CH(CH_3)\text{-}Fc)_2]$ **[22]** in *d*-acetonitrile. Insert: One of the isomeric structures of **[22]**.

3.3. Structural determinations

The single crystal structures of [FcCOCHCORc] **[11]** and $[(Cp)_2Ti(FcCOCHCOCH_3)]^+ClO_4^-$ **[18]** were solved by Dr. A.J. Muller of the Department of Chemistry, University of the Free State. He is gratefully acknowledged for determining and solving these crystal structures.

3.3.1. Crystal structure of 1-ferrocenyl-3-ruthenocenylpropane-1,3-dione, [FcCOCH$_2$CORc], [11]

A perspective view of [FcCOCH$_2$CORc] showing atom labelling is presented in **Figure 3.9**. Crystal data for the structure is summarized in **Table 3.6**, bond lengths and angles may be found in **Tables 3.7** and **3.8.**

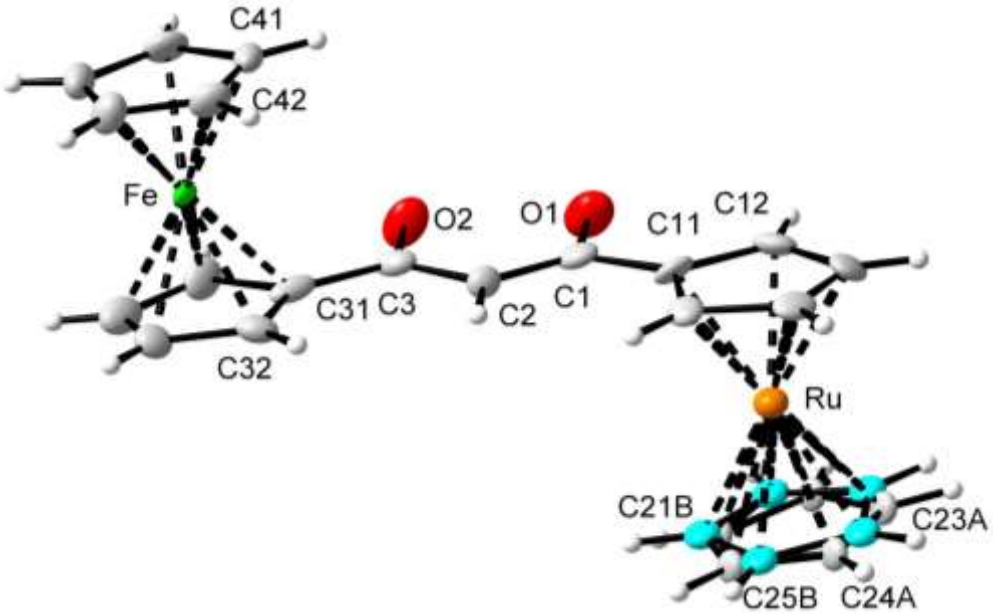

Figure 3.9. Perspective view of 1-ferrocenyl-3-ruthenocenylpropane-1,3-Dione ([FcCOCH$_2$CORc], **[11]**), showing the numbering scheme and displacement ellipsoids of 30% probability. All shown hydrogen atoms are theoretically placed. The OH hydrogen for this structure could not be found from the density map, implying it is not exclusively localised on either O(1) or O(2).

Figure 3.10. Sandwich distances for solid state unsubstituted ferrocene and ruthenocene.[10]

As shown in **Figure 3.10** the sandwich distance for unsubstituted ferrocene is 3.32 Å. The corresponding distance in [FcCOCH$_2$CORc] has increased to 3.339 Å. For unsubstituted ruthenocene a sandwich distance of 3.68 Å is reported.[10] Within compound **[11]** this distance is equal to 3.600 Å.

Typical C-C and C=C bond lengths are 1.54 Å and 1.34 Å respectively.[11] The bonds C(1)-C(2) [1.340(16) Å] and C(2)-C(3) [1.382(17) Å] do not differ significantly and their relative "shortness" is indicative of double bond character. Characteristic bond lengths for C-O bonds are 1.43 Å and for C=O this distance is 1.20 Å. Bond lengths O(1)-C(1) [1.283(16) Å] and O(2)-C(3) [1.285(15) Å] therefore also display double bond character. The fact that these bonds are equal in length indicates that [$FcCOCH_2CORc$] displays (random) symmetric enolisation. This is only possible if enolisation is ca. 50% on the ferrocenyl side and 50% on the ruthenocenyl side. It follows that the enol H atom is localised between O(1) and O(2), with no clear preference for either oxygen.

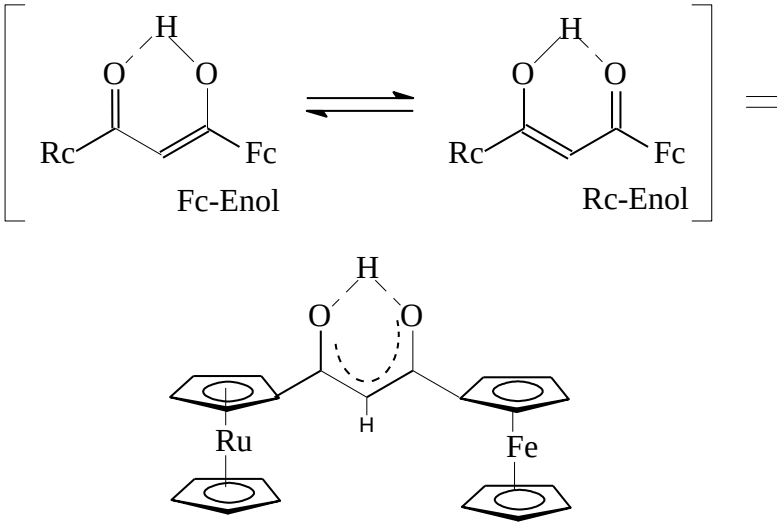

Scheme 3.9. Equilibrium between enolic forms of [$FcCOCH_2CORc$] favours no particular end isomer implying the Fc_{enol} and Rc_{enol} make an approximately equal contribution to the overall structure.

An O(1)-O(2) distance of 2.42 Å is also consistant with the enolic structure of 1-ferrocenyl-3-ruthenocenylpropane-1,3-dione. β-Diketones in the keto form typically have O-O distances of *ca.* 3.05Å.[12] Unlike in the solid state, it was established by ^{1}H NMR that both enol forms as well as the keto form of [$FcCOCH_2CORc$] exist in $CDCl_3$ solution (see **Chapter 4**, Paragraph 4.3.2.5 and **Spectrum 8, Appendix A**). A theoretical bond angle value of 120° is expected for carbon sp^2 hybridization. C(1)-C(2)-C(3) [122.9(13)°] deviates only slightly from this value.

The bonds C(1)-C(11) [1.471(17) Å] and C(3)-C(31) [1.455(18) Å] are almost equal and are both shorter than a typical C-C bond (1.54 Å), indicating appreciable conjugation between the pseudo-aromatic β-diketonato core to the ferrocenyl and ruthenocenyl side groups.

The tortion angle defined by O(2)-C(3)-C(31)-C(35) [4.8(17)°] also shows effective conjugation of the aromatic ferrocenyl moiety to the pseudo-aromatic β-diketonato plane. Evidence of the effective congugation of the ruthenocenyl moiety is given by tortion angle O(1)-C(1)-C(11)-C(15) = 2.4(11)°. Conjugation can take place in at least two ways. This is demonstrated by the formation of canonical forms **III** and **IV** of the two theoretically possible enol forms **I** and **II** of [$FcCOCH_2COPh$] (**Chapter 2**, page 20, **Scheme 2.3**). As the group electronegativity of ferrocene (χ_{Fc} 1.87) and ruthenocene (χ_{Rc} 1.94) are very similar and resonance driving forces are applicable to both metallocenes, the existence of equal amounts of both enol forms (**Scheme 3.9**) of compound **[11]** is explained.

The cyclopentadienyl rings of the ferrocenyl group deviated by only 1.5° from an eclipsed conformation, as measured from the tortion angle C(31) - *C(31-35) - *C(41-45) - C(41) (**Figure 3.11**). Here, *C(31-35) represents the centroid of the Cp ring defined by atoms C(31)-C(35), while *C(41-45) represents the centroid of the Cp ring defined by atoms C(41)-C(45).

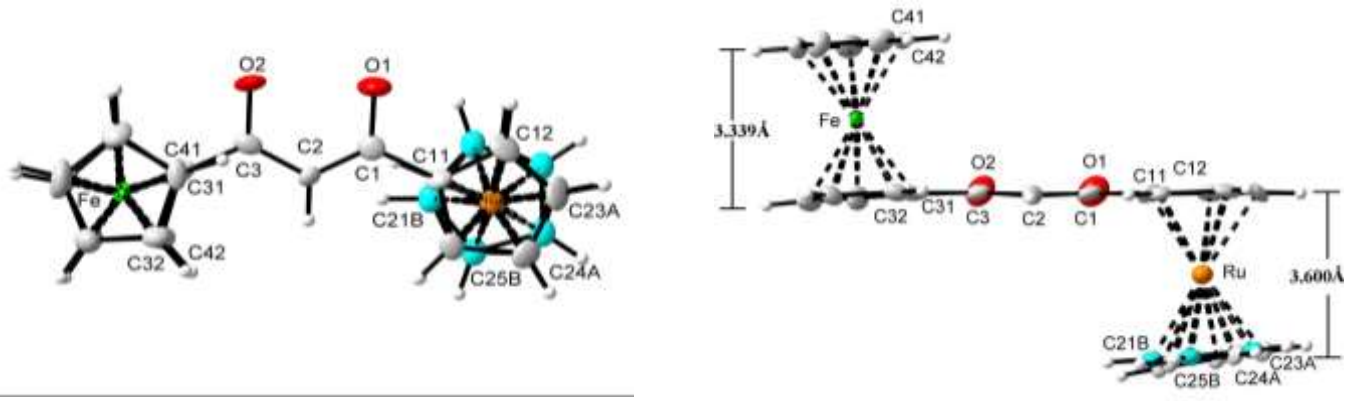

Figure 3.11. Perspective views of [(FcCOCHCORc] **[11]** Left: Over view, highlighting the eclipsed conformation of the ferrocenyl cyclopentadienyl rings. Right: Side view, emphasising planarity of compound **[11]**.

For the ruthenocenyl portion two conformations of the Cp rings were found. The un-coordinated cyclopentadienyl ring shows very high thermal vibration, giving rise to a "vibrational thermal disorder", two positions can therefore be identified. The one structure is almost eclipsed (Cp rings deviate 6.5° from eclipsed conformation) and the other is a gauche conformation (deviation from eclipsed Cp ring conformation is 13.4°), see **Figure 3.12**.

* Centroid of cyclopentadienyl ring for the given numbers.

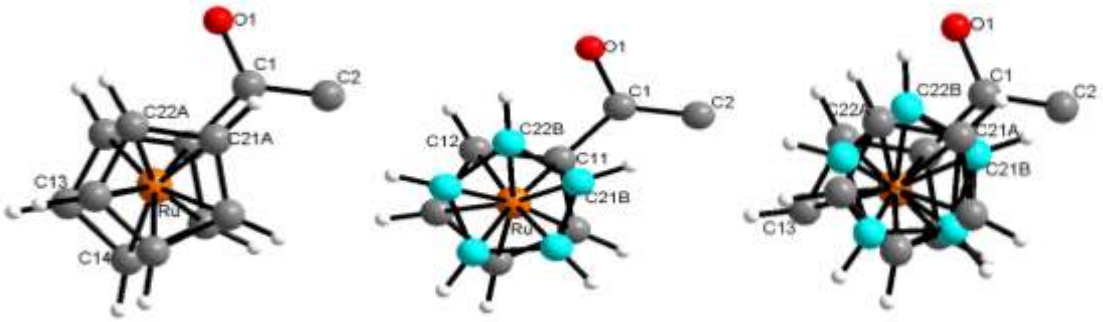

(A) **(B)** **(C)**

Figure 3.12. A partial view of [(FcCOCHCORc] **[11]**, highlighting the **(A)** eclipsed conformation, **(B)** gauche conformation and **(C)** combined conformations of the cyclopentadienyl rings of the ruthenocenyl fragment.

Table 3.6. Crystal data and structure refinement for 1-ferrocenyl-3-ruthenocenylpropane-1,3-dione, [$FcCOCH_2CORc$], **[11]**.

Empirical formula	$C_{23}H_{19}FeO_2Ru$	**Theta range for data collection**	1.71 to 27.50°.
Formula weight	484.30 $g.mol^{-1}$	**Index ranges**	-31<=h<=33, -55<=k<=61, -4<=l<=7
Temperature	293(2)K	**Reflections collected**	10258
Crystal size	0.34 x 0.18 x 0.03 mm^3	**Independent reflections**	3346 [R(int) = 0.0997]
Crystal system	Orthorhombic	**Completeness to theta = 27.50°**	99.7 %
Space group	F dd2	**Absorption correction**	Semi-empirical from equivalents
Unit cell dimensions	a = 26.076(5) Å α= 90°. b = 47.524(10) Å β= 90°. c = 5.9115(12) Å γ = 90°.	**Max. and min. transmission**	0.9681 and 0.5912
		Refinement method	Full-matrix least-squares on F^2
Volume	7326(3) $Å^3$	**Data / restraints / parameters**	3346 / 27 / 243
Density (calculated)	1.756 Mg/m^3	**Goodness-of-fit on F^2**	1.032
Z	16	**Final R indices[I>2sigma(I)]**	R1 = 0.0619, wR2 = 0.1366
Absorption coefficient	1.632 mm^{-1}	**R indices (all data)**	R1 = 0.1174, wR2 = 0.1594
***F*(000)**	3888	**Largest diff. peak and hole**	0.982 and -0.756 $e.Å^{-3}$
Wavelength	0.71073 Å	**Crystal size**	0.36 x 0.03 x 0.02 mm^3

Table 3.7. Bond lengths (Å) and angles (º) for [$FcCOCH_2CORc$] **[11]**. The standard deviation of the last decimal is given in parentheses.

Bond	Length(Å)	Bond	Length(Å)	Bond	Length(Å)
O(1)-C(1)	1.283(16)	C(22A)-C(23A)	1.41(2)	C(32)-C(33)	1.372(16)
O(2)-C(3)	1.285(15)	C(22A)-H(22A)	0.93	C(32)-H(32)	0.93
C(1)-C(2)	1.340(16)	C(23A)-C(24A)	1.401(19)	C(33)-C(34)	1.33(2)
C(1)-C(11)	1.471(17)	C(23A)-H(23A)	0.93	C(33)-H(33)	0.93
C(2)-C(3)	1.382(17)	C(24A)-C(25A)	1.406(19)	C(34)-C(35)	1.40(2)
C(2)-H(2)	0.93	C(24A)-H(24A)	0.93	C(34)-H(34)	0.93
C(3)-C(31)	1.455(18)	C(25A)-H(25A)	0.93	C(35)-H(35)	0.93
C(11)-C(15)	1.44(2)	C(21B)-C(25B)	1.40(2)	C(41)-C(42)	1.378(18)
C(11)-C(12)	1.439(17)	C(21B)-C(22B)	1.406(18)	C(41)-C(45)	1.433(18)
C(12)-C(13)	1.409(19)	C(21B)-H(21B)	0.93	C(41)-H(41)	0.93
C(12)-H(12)	0.93	C(22B)-C(23B)	1.408(17)	C(42)-C(43)	1.334(17)
C(13)-C(14)	1.42(2)	C(22B)-H(22B)	0.93	C(42)-H(42)	0.93
C(13)-H(13)	0.93	C(23B)-C(24B)	1.405(18)	C(43)-C(44)	1.42(2)
C(14)-C(15)	1.456(17)	C(23B)-H(23B)	0.93	C(43)-H(43)	0.93
C(14)-H(14)	0.93	C(24B)-C(25B)	1.398(18)	C(44)-C(45)	1.41(2)
C(15)-H(15)	0.93	C(24B)-H(24B)	0.93	C(44)-H(44)	0.93
C(21A)-C(22A)	1.396(19)	C(25B)-H(25B)	0.93	C(45)-H(45)	0.93
C(21A)-C(25A)	1.40(2)	C(31)-C(32)	1.391(19)		
C(21A)-H(21A)	0.93	C(31)-C(35)	1.473(17)		

Table 3.8. Selected angles (º) for [$FcCOCH_2CORc)]^+ClO_4^-$ **[11]**. The standard deviation of the last decimal is given in parentheses.

Atoms	Angle	Atoms	Angle	Atoms	Angle
C(1)-C(2)-C(3)	122.9(13)	O(2)-C(3)-C(2)	118.1(12)	C(25B)-C(21B)-C(22B)	107.8(13)
O(1)-C(1)-C(2)	119.8(12)	O(2)-C(3)-C(31)	117.4(12)	C(25B)-C(21B)-H(21B)	126.1
O(1)-C(1)-C(11)	114.5(12)	C(15)-C(11)-C(12)	107.2(11)	C(34)-C(33)-C(32)	111.1(14)
C(2)-C(1)-C(11)	125.7(13)	C(2)-C(3)-C(31)	124.4(13)	C(44)-C(45)-H(45)	128.1
C(1)-C(2)-C(3)	122.9(13)	C(15)-C(11)-C(1))	127.4(12	**Tortion Angles**	
C(1)-C(2)-H(2)	118.5	C(21A)-C(25A)-H(25A)	125.9	O(2)-C(3)-C931)-C(35)	4.8(17)°
C(3)-C(2)-H(2)	118.5	C(24A)-C(25A)-H(25A)	125.9	O(1)-C(1)-C(11)-C(15)	177.6(11)

3.3.2. Structural determination of 1-Ferrocenoyl-1,3-butanedionato-κ^2O,O'-bis (η^5-cyclopentadienyl) titanium(IV) perchlorate, [$Cp_2Ti(FcCOCHCOCH_3)ClO_4$] [18]

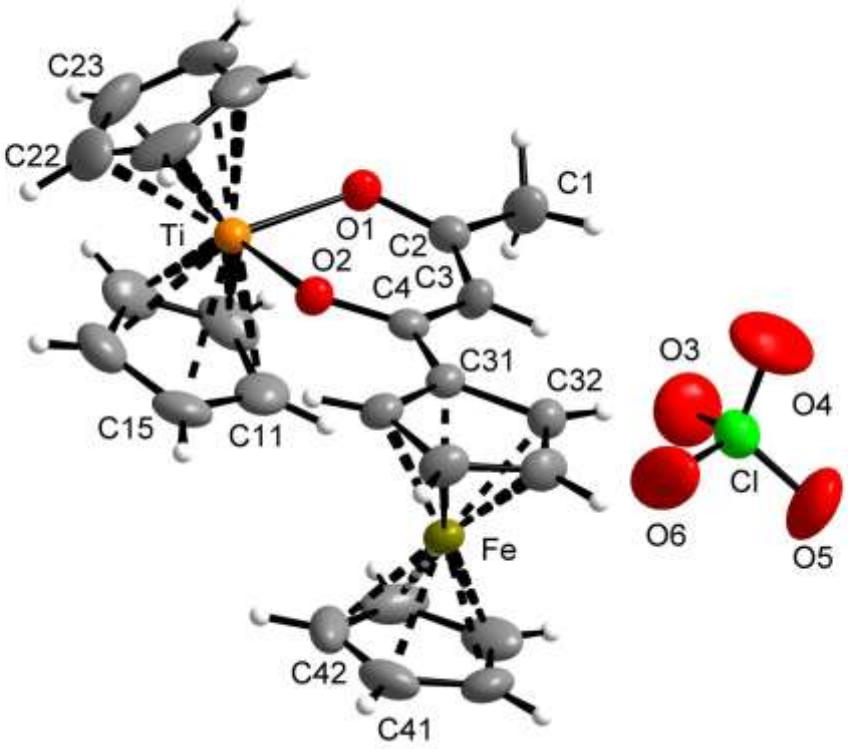

Figure 3.13. Perspective view of [$Cp_2Ti(FcCOCHCOCH_3)ClO_4$] **[18]**, showing the numbering scheme and displacement ellipsoids of 30% probability.

The DIAMOND presentation of **[18]** showing atom labelling is presented in **Figure 3.13.** Crystal data and details of data collection and refinement are given in **Table 3.9.** Selected bond lengths and angles for the molecule are listed in **Table 3.10** and **Table 3.11.**

The unit cell contains one cationic complex $[Cp_2Ti^{IV}(FcCOCHCOCH_3)]^+$ and one counter ion $[ClO_4]^-$ The titanium atom displays a distorted tetrahedral geometry. An O-Ti-O angle of between 85-88º is predicted for Ti^{IV} complexes of this type,[13] which is in agreement with the angle of 86.98º observed here. In contrast the reported[14] Ti^{III} complex $[Cp_2Ti^{III}(CH_3COCHCOCH_3)]$, revealed an O-Ti-O angle of 84.3º. The bond angles surrounding the titanium atom of **[18]** are as follows: O(1)-Ti-O(2) = 86.98º, C*(22-26)-Ti-C*(11-15) = 133.52º, O(2)-Ti-C*(22-26) = 106.21º, O(2)-Ti-C*(11-15) = 106.87º, O(1)-Ti-C*(22-26) = 107.02º and O(1)-Ti-C*(11-15) = 106.44º.

* Centroid of cyclopentadienyl ring for the given numbers.

These angles have maximum difference of 24.05º from the angles assigned to a regular tetrahedron i.e. 109.47º, which is quite a large deviation. Angles O(1)-C(2)-C(3) [123.8(4)º] and C(2)-C(3)-C(4) [124.0(4)º] vary considerably from the 120º theoretical value expected for carbon sp^2 hybridization. This is in contrast to the corresponding angles in the free β-diketone, which were much closer to ideal (**Table 3.8**). Angle O(2)-C(4)-C(3) [122.3(4)º] of compound **[18]** was also closer to the ideal 120º. The pseudo-aromatic ring is therefore distorted, implying electronic bond communication between the Ti centre, the R-group (CH_3) and the ferrocenyl group will not be optimum. **Figure 3.14** shows distortion of the titanocenyl portion.

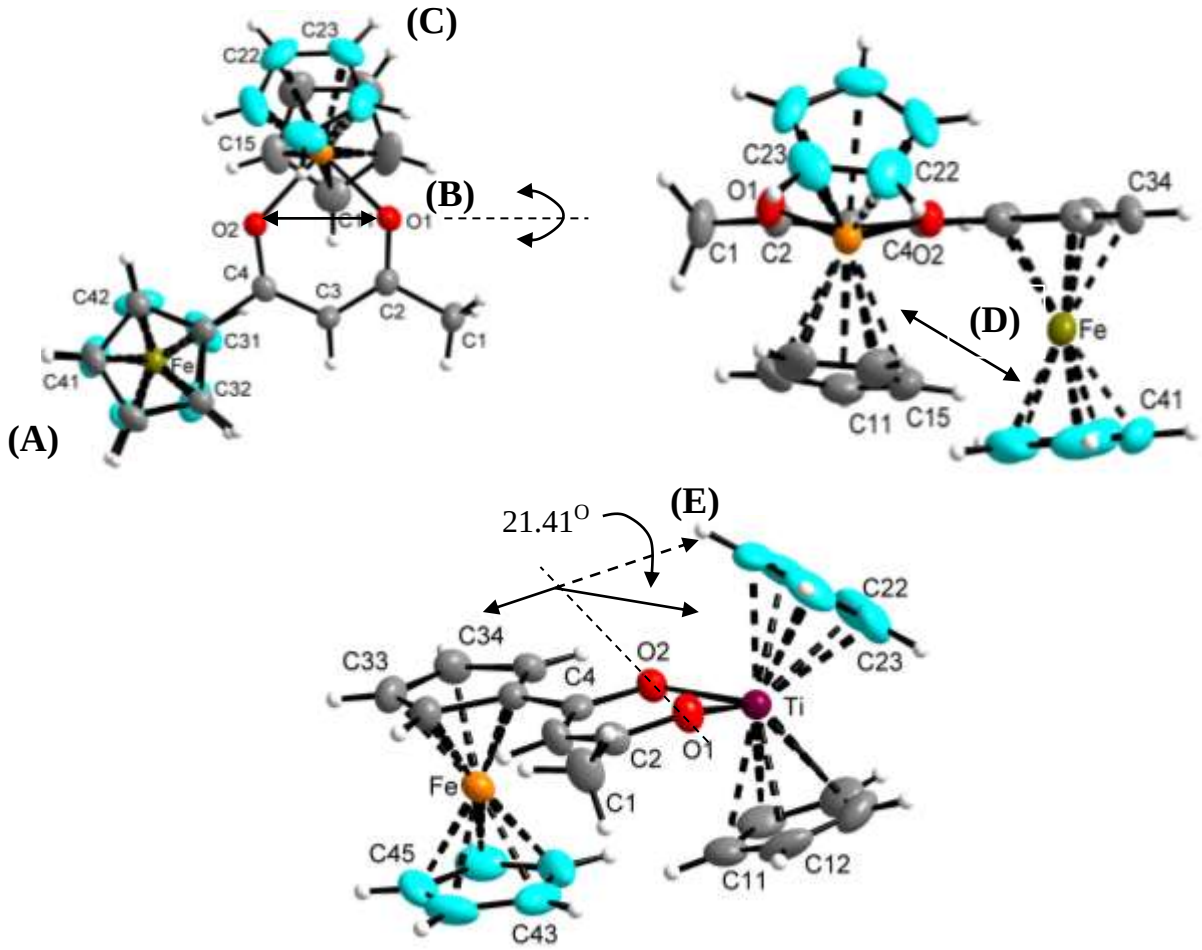

Figure 3.14. Perspective views of $[Cp_2Ti(FcCOCHCOCH_3)]^+ClO_4^-$ **[18]**. Top left: Over view, highlighting: **(A)** The eclipsed conformation of the ferrocenyl cyclopentadienyl rings; **(B)** Broadening of O(1)-O(2) distance 2.7 Å (pseudo aromatic ring) to accommodate Ti^{4+} and **(C)** Rotation of titanocenyl group about the O(1)-O(2) axis. Top right: Side view showing titanocenyl rotation around the O(1)-O(2) axis and **(D)** titanocenyl rotation has caused the bottom ferrocenyl and titanocenyl Cp rings to lie much closer to a parallel conformation than the upper Cp rings. Bottom: **(E)** Demonstrates titanocenyl group is also bowed down out of β-diketonate plane. O(1)-Ti-O(2) plane is rotated out of the β-diketonato plain defined by O(1)-C(2)-C(3)-C(4)-O(2) by 21.41(18)º.

From **Figure 3.14** (top left) an elongation of the O(1)-O(2) distance (as compared to [$FcCOCH_2CORc$] **Figure 3.11** left, where the C-O bonds are almost parallel) to accommodate the titanocenyl group can be seen. In [$FcCOCH_2CORc$] the O(1)-O(2) distance was 2.42 Å, while in the Ti complex **[18]** it is 2.70 Å. The eclipsed conformation of the ferrocenyl cyclopentadienyl rings is also clearly visible. It was expected that a similar picture would emerge for the titanocenyl Cp rings. However, rotation of the titanocenyl group around the O(1)-O(2) axis has moved the Cp orientation of the titanocenyl fragment substantially away from being symmetrical above and below the β-diketonato plane. In addition, the Ti-O(1)-O(2) plane is bending down, away from the β-diketonato plane by an angle of 21.41(18)° (**Figure 3.14** bottom). This rotation has tilted the bottom ferrocenyl Cp ring and the bottom titanocenyl cyclopentadienyl ring into close proximity (**Figure 3.14** top right), effectively blocking the molecule from nucleophilic attack from this direction (see also **Figure 3.15**).

The average distance between the Ti^{IV} centre and the β-dketonato oxygen atoms, 1.961(2) Å, is shorter than the corresponding Ti^{III}-O distances [2.068(5) Å] found for the reported [$Cp_2Ti^{III}(CH_3COCHCOCH_3)$] complex.[14] The average Ti-C bond length for the Cp ring defined by carbon atoms C(11)-C(15) is 2.365(5) Å, while that of the cyclopentadienyl ring formed by C(22)-C(26) is 2.343(5) Å. This compares well with the corresponding bond lengths of titanocene dichloride, with Ti-C bond lengths averaging 2.317(7) Å. [$Cp_2Ti^{III}(CH_3COCHCOCH_3)$] has an average Ti-C distance of 2.375(8) Å. This clearly demonstrates that the Ti^{IV} centre is noticeably more electrophilic than the Ti^{III} centre.

The Ti-O(1) bond [1.954(3) Å] is also not significantly longer than Ti-O(2) bond [1.967(2) Å]. This implies the stronger electron donating property of the ferrocenyl group (χ_{Fc} = 1.87), as compared to that of the CH_3 group (χ_{CH3} = 2.34), on the pseudo-aromatic β-diketonato ligand, does not transmit through through-bond communication to the titanium centre.

It has been mentioned in paragraph 3.2.2.1 (page 64) that a β-diketone exchange reaction is possible for complexes of this type in high yield. The structure of **[18]** explains why β-diketonato substitution is so viable. As shown in **Figure 3.15**, two of the possible approaching routes by an incoming

nucleophile (here an incoming β-diketonato ligand) are sterically hindered by the special arrangement of the Cp rings. Due to rotation about the O(1)-O(2) axis of 21.41(18)º (**Figure 3.14**) a third route for nucleophilic attack on the Ti centre has been substantially opened. This explains the high efficiency of β-diketonato substitution reactions.

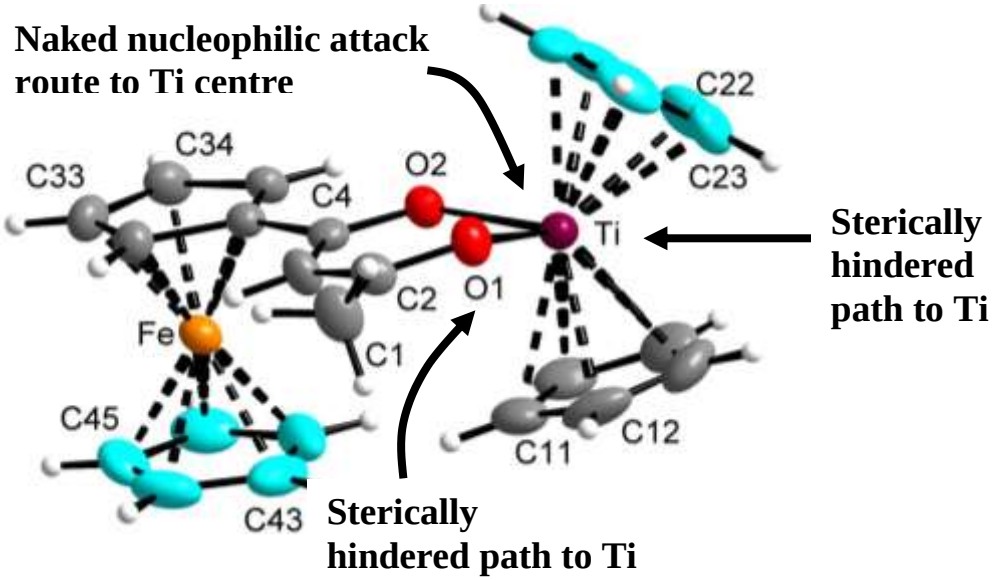

Figure 3.15. Perspective view of $[Cp_2Ti^{IV}(FcCOCHCOCH_3)]^+ClO_4^-$, demonstrating possible Ti attack pathes for incoming ligands.

Regarding the β-diketonato ligand, the bond lengths C(2)-C(3) [1.381(6) Å] and C(3)-C(4) [1.412(6) Å] do not differ significantly. This implies that the β-diketonato ligand is for all practical purposes symmetrically bound to Ti. From **Figure 3.16** it can be seen that the ferrocenyl cyclopentadienyl rings are also orientated almost parallel to one another and that the β-diketonato plane is parallel to the C(31)-C(35) cyclopentadienyl plane. The torsion angle between the plane formed by O(2)-C(4)-C(31)-C(35) and the plane formed by the C(31-35) cyclopentadienyl carbon atoms is equal to a mere 1.6º, emphasising the effective conjugation of the ferrocenyl group into the pseudo-aromatic ring of the β-diketonato side chain.

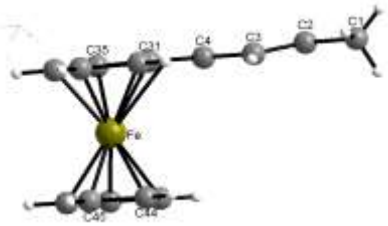

Figure 3.16. A partial view of $[Cp_2Ti(FcCOCHCOCH_3)]$ **[18]** (β-diketonato ligand shown), highlighting the eclipsed conformation of the ferrocenyl cyclopentadienyl rings.

Table 3.9. Crystal data and structure refinement for 1-Ferrocenoyl-1,3-butanedionato-κ^2O,O'-bis(η^5-cyclopentadienyl) titanium(IV) perchlorate **[18]**.

Empirical formula	C_{24} H_{23} Cl Fe O_6 Ti	**Theta range for data collection**	2.04 to 28.28°
Formula weight	546.62 g.mol^{-1}	**Index ranges**	-13<=h<=12, -26<=k<=23, -15<=l<=15
Temperature	293(2)K	**Reflections collected**	15806
Crystal size	0.34 x 0.18 x 0.03 mm^3	**Independent reflections**	5646 [R(int) = 0.0908]
Crystal system	Monoclinic	**Completeness to theta = 28.28°**	99.6 %
Space group	$P2_1/n$	**Absorption correction**	Semi-empirical from equivalents
Unit cell dimensions	a = 10.106(2) Å α= 90°. b = 20.007(4) Å β= 97.63(3)°. c = 11.402(2) Å γ = 90°.	**Max. and min. transmission**	0.9452 and 0.7261
		Refinement method	Full-matrix least-squares on F^2
Volume	2285.2(8) Å^3	**Data / restraints / parameters**	5646 / 0 / 299
Density (calculated)	1.589 Mg/m^3	**Goodness-of-fit on F^2**	0.959
Z	4	**Final R indices [I>2sigma(I)]**	R1 = 0.0566, wR2 = 0.1046
Absorption coefficient	1.140 mm^{-1}	**R indices (all data)**	R1 = 0.1814, wR2 = 0.1383
***F*(000)**	1120	**Largest diff. peak and hole**	0.353 and -0.325 e.Å^{-3}
Wavelength	0.71073 Å	**Crystal size**	0.30 x 0.22 x 0.05 mm^3

Table 3.10. Bond lengths (Å) for $[Cp_2Ti(FcCOCHCOCH_3)]^+ClO_4^-$ **[18]**. The standard deviation of the last decimal is given in parentheses.

Bond	Length(Å)	Bond	Length(Å)	Length(Å)	Length(Å)
Ti-O(1)	1.954(3)	C(11)-C(15)	1.384(7)	C(32)-C(33)	1.405(6)
Ti-O(2)	1.967(3)	C(11)-C(12)	1.394(7)	C(32)-H(32)	0.93
Ti-C(22)	2.334(5)	C(11)-H(11)	0.93	C(33)-C(34)	1.408(6)
Ti-C(23)	2.344(5)	C(12)-C(13)	1.367(7)	C(33)-H(33)	0.93
Ti-C(14)	2.344(5)	C(12)-H(12)	0.93	C(34)-C(35)	1.411(6)
Ti-C(13)	2.344(5)	C(13)-C(14)	1.387(7)	C(34)-H(34)	0.93
Ti-C(21)	2.344(5)	C(13)-H(13)	0.93	C(35)-H(35)	0.93
Ti-C(24)	2.348(5)	C(14)-C(15)	1.378(7)	C(41)-C(45)	1.369(7)
Ti-C(25)	2.348(5)	C(14)-H(14)	0.93	C(41)-C(42)	1.387(8)
Ti-C(12)	2.370(5)	C(15)-H(15)	0.93	C(41)-H(41)	0.93
Ti-C(15)	2.379(5)	C(21)-C(22)	1.352(8)	C(42)-C(43)	1.409(8)
Ti-C(11)	2.390(5)	C(21)-C(25)	1.353(8)	C(42)-H(42)	0.93
O(1)-C(2)	1.286(5)	C(21)-H(21)	0.93	C(43)-C(44)	1.397(8)
O(2)-C(4)	1.290(4)	C(22)-C(23)	1.353(8)	C(43)-H(43)	0.93
C(1)-C(2)	1.503(6)	C(22)-H(22)	0.93	C(44)-C(45)	1.358(7)
C(1)-H(1A)	0.96	C(23)-C(24)	1.347(8)	C(44)-H(44)	0.93
C(1)-H(1B)	0.96	C(23)-H(23)	0.93	C(45)-H(45)	0.93
C(1)-H(1C)	0.96	C(24)-C(25)	1.392(8)	Cl-O(4)	1.379(5)
C(2)-C(3)	1.381(6)	C(24)-H(24)	0.93	Cl-O(6)	1.382(4)
C(3)-C(4)	1.412(6)	C(25)-H(25)	0.93	Cl-O(5)	1.383(4)
C(3)-H(3)	0.93	C(31)-C(35)	1.427(6)	Cl-O(3)	1.398(4)
C(4)-C(31)	1.464(6)	C(31)-C(32)	1.431(5)		

Table 3.11. Selected angles (º) for $[Cp_2Ti(FcCOCHCOCH_3)]^+ClO_4^-$ **[18]**. The standard deviation of the last decimal is given in parentheses.

Atoms	Angle	Atoms	Angle	Atoms	Angle
O(1)-Ti-O(2)	86.98	O(1)-C(2)-C(3)	123.8(4)	O(1)-C(2)-C(1)	115.7(4)
O(1)-Ti-C(22)	135.49(18)	C(2)-C(3)-C(4)	124.0(4)	C(3)-C(2)-C(1)	120.5(4)
O(2)-Ti-C(22)	108.9(2)	O(2)-C(4)-C(3)	122.3(4)	C(15)-C(11)-Ti	72.7(3)
O(1)-Ti-C(23)	107.9(2)	O(2)-Ti-C(13)	136.80(18)	O(1)-Ti-C(13)	106.7(2)
C(22)-Ti-C(23)	33.6(2)	C(14)-Ti-C(13)	34.43(19)	**Tortion Angles**	
O(2)-Ti-C(14)	109.8(2)	H(1A)-C(1)-H(1C)	109.5	O(2)-C(4)-C(31) C(35)	1.6(4)
C(22)-Ti-C(14)	79.1(2)	H(1B)-C(1)-H(1C)	109.5	O(2)-Ti-O(1)-C(2)	29.3(4)
Angles to Centroid of Cyclopentadienyl Rings					
C*(22-26)-Ti-C*(11-15)	133.52	O(2)-Ti-C*(22-26)	106.21	O(1)-Ti-C*(11-15)	106.44
O(1)-Ti-C*(22-26)	107.02	O(2)-Ti-C*(11-15)	106.87		

* Centroid of cyclopentadienyl ring for the given numbers.

3.4. Electrochemistry

3.4.1. Introduction

Cyclic voltammetry (CV), Oster Young square wave voltammerty (SW) and linear sweep voltammetry (LSV) were conducted on selected synthesised complexes dissolved in dichloromethane in the presence of tetrabutylammonium tetrakis[pentafluorophenyl] borate ($[NBu_4][B(C_6F_5)_4]$) as supporting electrolyte. The redox active species which were studied include Ti^{4+}/Ti^{3+}, $2Rc/[2Rc^+ \rightleftharpoons (Rc_2)^{2+}]$ and Fc/Fc^+ (Rc = ruthenocenyl and Fc = ferrocenyl) metal centres within the complexes. Analysis of the formal reduction potential was performed in an attempt to quantify the electronic influence of different R-substituents (group electronegativity, χ_R) on the redox active metal centres of each of these compounds. The redox active couples vary from being electrochemically reversible (theoretically this implies $i_{pa}/i_{pc} = 1$ and $\Delta E = 59$ mV, although experimentally $\Delta E < 90$ mV was taken to imply electrochemical reversibility for this study), quasi-reversible (which for the purpose of this study is defined by 90 mV < ΔE < 150 mV) to irreversible (characterised by $\Delta E > 150$ mV and $i_{pa}/i_{pc} \neq 1$ for this study). Formal redox potentials ($E^{0/}$), peak cathodic potentials (E_{pc}) and peak anodic potentials (E_{pa}) were experimentally measured against an Ag/AgCl reference electrode but are reported *vs.* Fc/Fc^+ as an internal standard. The Fc/Fc^+ couple was found to exhibit $E^{0/}$ = 482V vs. Ag/AgCl and $i_{pa}/i_{pc} = 0.96$, under these experimental conditions.

As mentioned in chapter 2, an ideal solvent should possess electrochemical and chemical inertness over a wide potential range. It is important to predetermine this potential range or window and to establish whether all the electrochemical processes for the compounds under investigation may be resolved within this window. The potential range for the $CH_2Cl_2/[NBu_4][B(C_6F_5)_4]$ system was thus determined. As can be seen in **Figure 3.17 (A)** the experimental window for this solvent/electrolyte system is between –2000 and 1800 mV *vs.* Ag/AgCl (or ca. –2500 and 1300 mV *vs.* Fc/Fc^+). At higher or lower potentials solvent decomposition becomes evident **(B)**. **Figure 3.17 (C)** shows the cyclic voltammogram for $CH_2Cl_2/[NBu_4][B(C_6F_5)_4]$ between -2000 and 2500 mV *vs.* Ag/AgCl. By exceeding the positive maximum of the potential window by +700 mV, solvent decomposition

leads to radical formation. The new species which are formed generate peaks at approximately –700 and 400 mV (**Figure 3.17 C**). It is therefore clear, that in order to produce reliable results, the potential range, in which the solvent does not decompose, should not be exceeded.

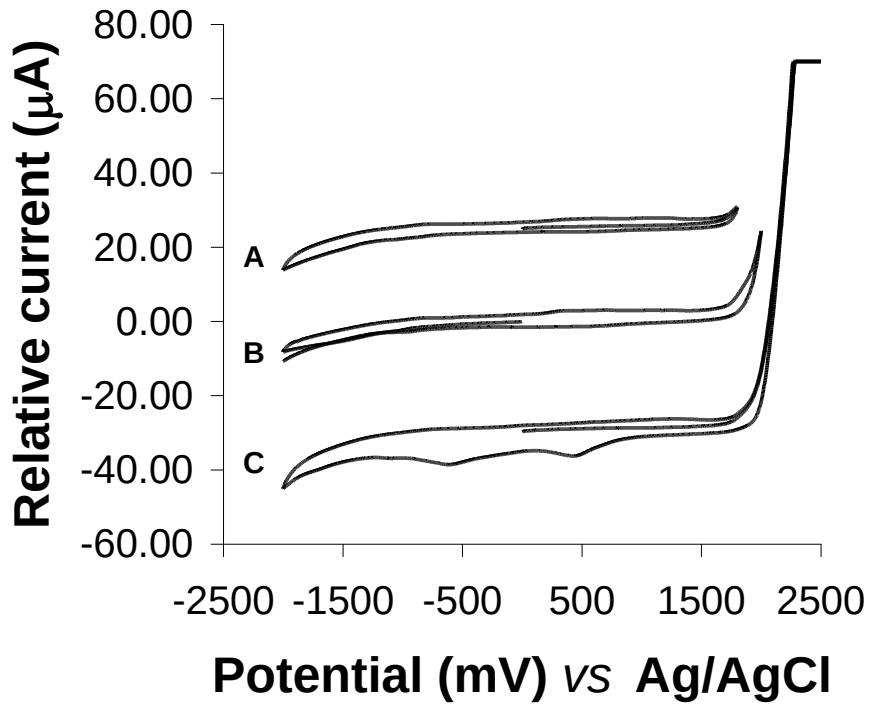

Figure 3.17. Cyclic voltammograms for $[NBu_4][B(C_6F_5)_4]$ 0.1 M in CH_2Cl_2 scan rate = 100 $mV.s^{-1}$ *vs.* Ag/AgCl at 25 °C. **(A)** Between -2000 and 1800 mV (solvent window). **(B)** Between -2000 and 2000 mV. **(C)** Between -2000 and 2500 mV.

3.4.2. Parent metallocene compounds

Since this study is focused on the use of ferrocene- and ruthenocene-containing ligands (complexed to the titanocyl group), the first step of an electrochemical study involving the present titanium complexes is a study of the parent metallocene ligands.

Figure 3.18 shows the cyclic voltammograms (CV's) of free ferrocene, ruthenocene and titanocene dichloride, as well as a CV of these redox active metal species dissolved in the same solution. It is clear from this figure that when the metallocene moeties are not bound within the same molecule, there is no communication between the redox active metal centres, because no potential shift is observed in

moving from only one compound in solution to the solution containing all the species. In forthcoming paragraphs the effects of coordination within various multi-nuclear molecules were studied.

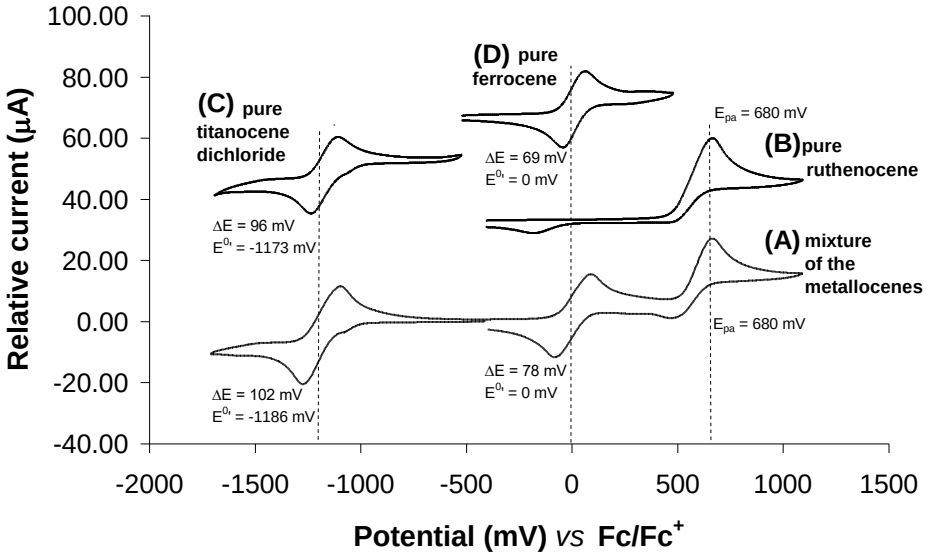

Figure 3.18. The cyclic voltammograms of 2.0 mmol.dm^{-3} solutions of **(A)** titanocene dichloride with free ferrocene and free ruthenocene added, **(B)** free ruthenocene, **(C)** titanocene dichloride and **(D)** free ferrocene in dichloromethane (supporting electrolyte is $[NBu_4][B(C_6F_5)_4]$ 0.2 mol.dm^{-3}) on a glassy carbon working electrode at 25˚C, scan rate = 100 mV.s^{-1}.

The reversible electrochemistry of ferrocene according to the reaction $Fc \rightleftharpoons Fc^+ + e^-$ is well known (**Figure 3.18 (D)**). The observed quasi-reversible Ti^{3+}/Ti^{4+} couple for titanocene dichloride in CH_2Cl_2/0.2M$[NBu_4][B(C_6F_5)_4]$ (**Figure 3.18 (C)**) is exceptional. In acetonitrile this couple is completely irreversible with ΔE = 400 mV.[15] The general titanocene dichloride electrochemistry is normally explained by the square scheme, shown in **Scheme 3.10 (**left). In the present uncoordinating $CH_2Cl_2/[NBu_4][B(C_6F_5)_4]$ system there is no solvent or counter ion which can coordinate to the Ti^{IV} species. Hence the electrochemical path simplifies to that shown in **Scheme 3.10** (right).

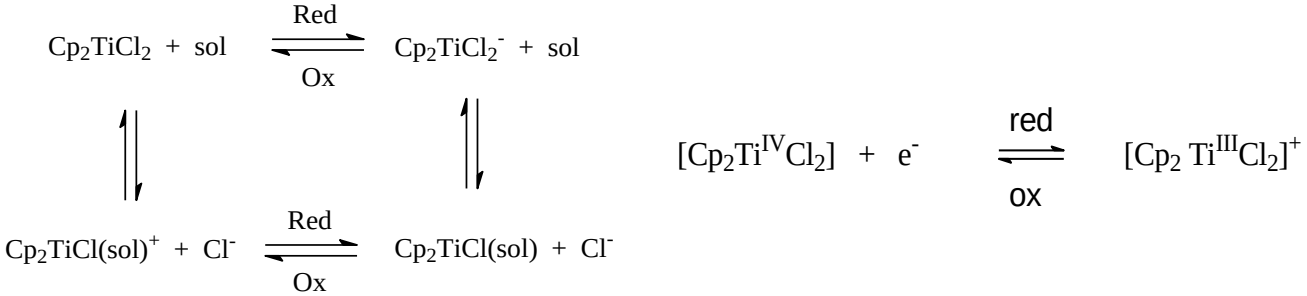

Scheme 3.10. Left: The 'square scheme' illustrating the oxidation and reduction of titanocene dichloride, sol = coordinating solvent such as CH_3CN. Right: Oxidation and reduction of titanocene dichloride in the uncoordinating $CH_2Cl_2/[NBu_4][B(C_6F_5)_4]$ system.

Ruthenocene electrochemistry (**Figure 3.19** right) has only recently been studied and partially clarified by Geiger and co-workers to be electrochemically reversible under certain conditions.[16]

3.4.2.1. Ruthenocene

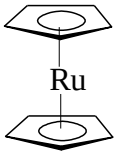

Geiger studied the electrochemistry of ruthenocene with cyclic voltammetry in $CH_2Cl_2/[NBu_4][B(C_6F_5)_4]$. They found that $RuCp_2$ **[2]** can be oxidised to $[RuCp_2]^+$ $\mathbf{[2]}^+$ and that the 17 electron ruthenocenium cation is in equilibrium with the dimeric cationic species $[RuCp_2]_2^{2+}$ $\mathbf{[2]}_2^{2+}$ at -35°C (**Figure 3.19** left).[16] Under their experimental conditions (**Figure 3.19** right)[16] the reduction of ruthenocene is observed as an irreversible cathodic wave at -181 mV (Scan rate = 200 mV.s^{-1}) *vs.* Fc/Fc^+.

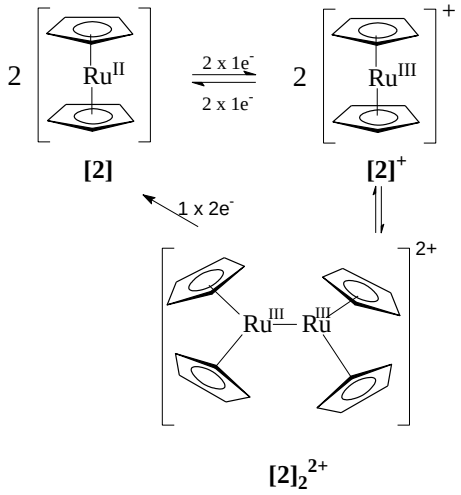

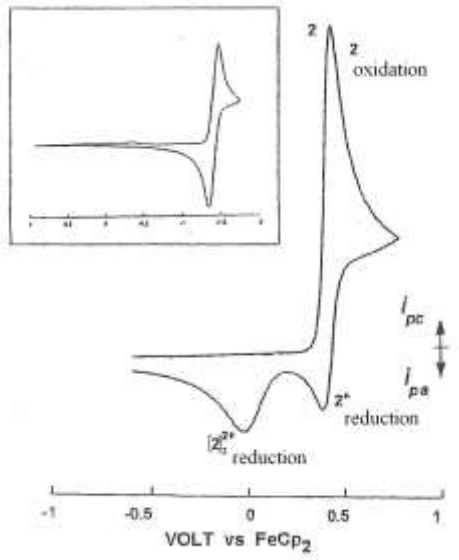

Figure 3.19. Left: Schematic representation of the redox behaviour of ruthenocene. Right: Cyclic voltammogram determined by Geiger[16] of 2 mM $[RuCp_2]$ in CH_2Cl_2/0.1 M $[NBu_4][B(C_6F_5)_4]$ at 2 mm (*d*) glassy carbon electrode. T = 243K, v = 0.2 v.s^{-1}. Inset gives scan under same conditions at ambient temperature.

The cyclic voltammetry of ruthenocene was repeated here (electrochemical data is available in **Table 3.12**). Our results (**Figure 3.20** right) were found to be mostly consistent with those found by Geiger. There is, nevertheless, a discrepancy in peak **X.** In Geiger's CV's (**Figure 3.19** right) this peak is not a dominant feature. As can be seen from **Figure 3.20** (Left), the CV of ruthenocene in CH_3CN/0.1 mol dm^{-3} $[NBu_4][PF_6]$ system is complex and electrochemically irreversible. The $RuCp_2$ oxidation wave is considered to generate a Ru^{IV} species ($Cp_2Ru^{IV}\cdot CH_3CN$) at ± 470 mV.[17] The reduction wave at -200 mV is associated with the reduction of $[Cp_2Ru^{IV}(CH_3CN)]^{2+}$.

In $CH_2Cl_2/[NBu_4][B(C_6F_5)_4]$ at -35ºC, ruthenocene oxidation is quasi-reversible with ΔE_p = 100 mV. The Rc^+ species dimerises to $(Rc_2)^{2+}$ and reduction of this dimeric species is observed at 300 mV.

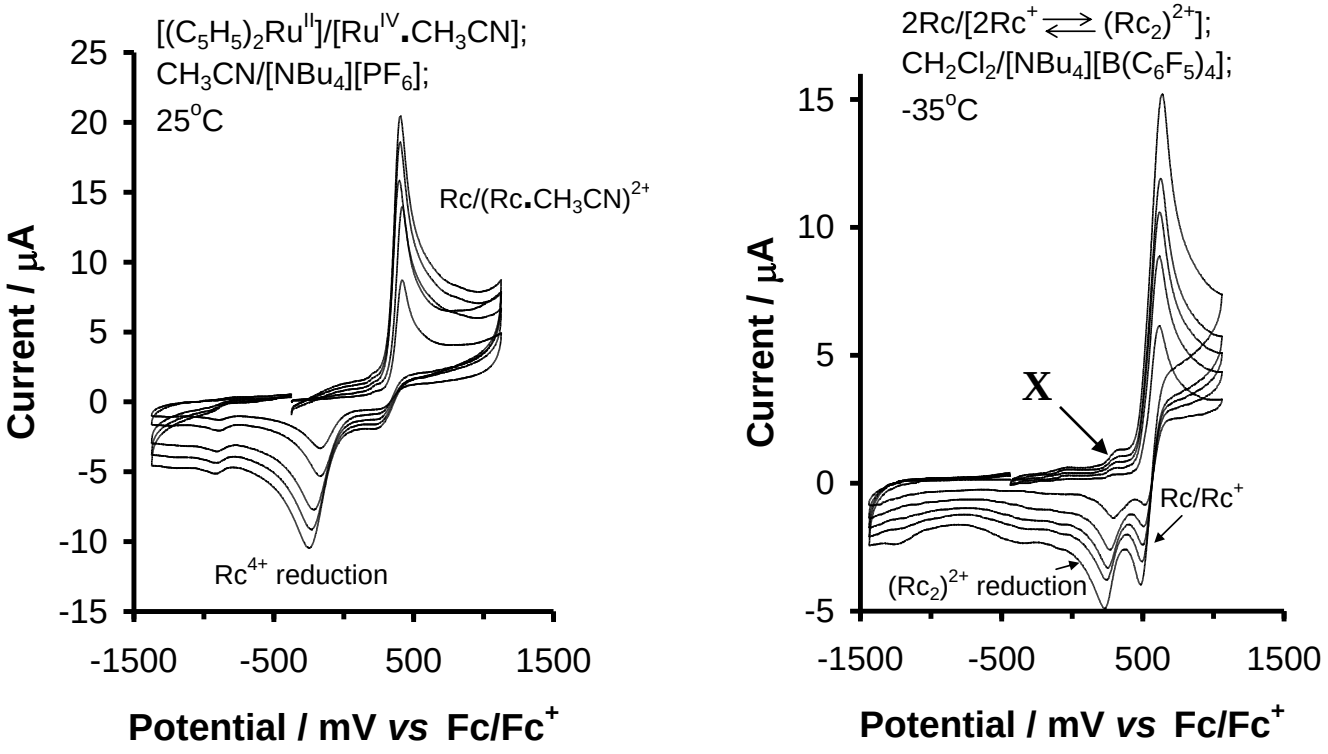

Figure 3.20. Left: CV's of ruthenocene in CH_3CN/0.1 mol dm^{-3} $[NBu_4][PF_6]$, T = 25ºC. Right: CV's of ruthenocene (Rc) in CH_2Cl_2/0.1 mol dm^{-3} $[NBu_4][B(C_6F_5)_4]$, T = -35ºC. *v* = 100, 200, 300, 400 and 500 $mV.s^{-1}$ in both cases.

Cyclic voltammograms of **[2]** in CH_2Cl_2/0.1 mol dm^{-3} $[NBu_4][B(C_6F_5)_4]$ at 25°C show $RuCp_2$ is irreversibly oxidised to $RuCp_2^+$ and reduced back to Rc (**Figure 3.21** top left). Since ΔE_p = 78 mV, full electrochemical reversibility is implied. The reduction of the dimer species $\mathbf{[2]}_2^{2+}$ is observed as a weakly broadened peak at -63 to -188 mV *vs.* Fc/Fc^+ depending on scan rate. Strikingly evident, is that at lower temperatures (-35˚C), the equilibrium $2(RuCp_2)^+ \rightleftharpoons (RuCp_2)_2^{2+}$ lies further in favour of the dimer. A key aspect lies in the fact that E_{pc} for the dimer is also shifted by ca. 380 mV to more positive potentials i.e. at + 220 mV. This shift was originally believed by Geiger to be the result of slower rate of electron transfer between electrode and Rc substrate at lower temperatures. It is also important to note that Geiger (under their conditions) did not observe the $(Rc_2)^{2+}$ cathodic reduction at 25˚C. Another key difference (which Geiger now confirms to be present via personal communications) is an additional oxidation/reduction couple **(X)**, which presents as an oxidation peak

directly before the Rc oxidation peak. The corresponding reduction peak is seen between the reduction peaks of Rc and the dimer species.

From this study it was concluded that two types of dimers exist, not just one, as reported by Geiger. We believe that the differences in dimer peak potentials may be attributed to the formation of a second dimer specie $[Cp(C_5H_4)Ru^{III}{\cdot}H]_2^{2+}$. This view is in accordance with similar findings for osmocene, where both dimer species were isolated by Taube and co-workers and characterised *via* crystallography.[18] In analogy to osmocene, the proposed structure of the second ruthenocene dimer specie is given in **Figure 3.21** (right). Electrochemical reversibility of the additional electrochemical wave, and mass balance, requires two H atoms to be part of the second dimer species **$\{[2^{/}]_2^{2+}\}$**. It is uncertain where these H atoms are located, for the sake of completeness, **Figure 3.21** shows they are associated with the Ru^{III} centre. A ^1H NMR of a solution of ruthenocene on which bulk electrolysis was performed, also confirmed the presence of a hydride species.[19] The second dimer $[Cp(C_5H_4)Ru^{III}{\cdot}H]_2^{2+}$, upon reduction, forms a hybrid hydride species which binds weakly to the surface of the electrode. This weak electrode binding was proven as follows: First the electrode was coated as heavily as possible by performing several successive CV runs i.e. by repetitive generation and reduction of the second dimer $[Cp(C_5H_4)Ru^{III}{\cdot}H]_2$. The electrode was then removed and lightly cleaned by rinsing with clean CH_2Cl_2. The analyte solution was also replaced by a solution containing only $[NBu_4][B(C_6F_5)_4]$ in CH_2Cl_2 (i.e. no ruthenocene present). The electrode was then placed back into the cell and a CV was recorded. If nothing was deposited on the electrode surface, the CV scan should show no peaks. **Figure 3.21** (bottom left) shows that weak peaks were detected in initial scans (labelled **A**). This means the electrode surface bond species must still be present. However, after 5 minutes in solution, the peak is absent (**Figure 3.21** (bottom left) **B)**. This implies the surface bond species have dissociated from the electrode surface, back into the solution, over time. The structure of this surface bond species is postulated as initially $[Cp(C_5H_4)Ru^{III}\text{-}H]$ and then after reduction $[Cp(C_5H_4)Ru^{II}\text{-}H]$. The surface bound Ru^{II} species then rearranges slowly and moves away from the electrode surface. An electrochemical/chemical scheme which corresponds with these results is shown in **Figure 3.21** (right).

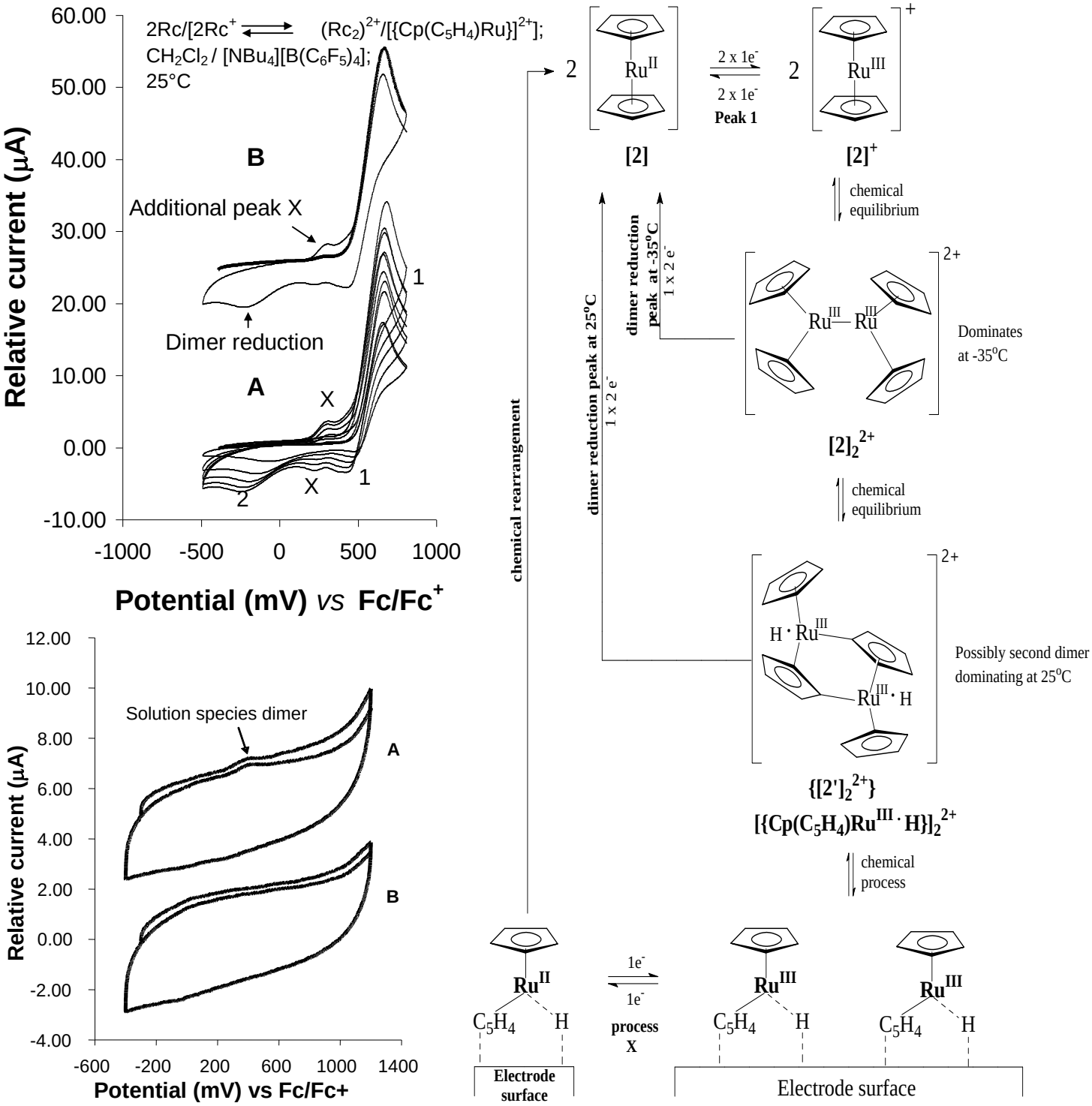

Figure 3.21. **Top left: (A)** Cyclic voltammograms of ruthenocene in CH_2Cl_2/0.1 mol dm^{-3} $[NBu_4][B(C_6F_5)_4]$, T = 25ºC. v = 100, 200, 300, 400, 500 and 1000 $mV.s^{-1}$. Scan **(B)** v = 400 $mV.s^{-1}$ highlights the absence of the "additional peak" in the initial forward scan (darker line). It only appears in the negative scan and second forward sweep (thinner line). **Right:** Schematic representation of the proposed redox behaviour of ruthenocene, incorporating the new dimer $[Cp(C_5H_4)Ru]_2^{2+}$. **Bottom left:** Cyclic voltammogram of ruthenocene dimer **$\{[2']_2^{2+}\}$** coated electrode in CH_2Cl_2/0.1 M $[NBu_4][B(C_6F_5)_4]$ on a glassy carbon electrode. T = 25°C. **(A)** Initial run, v = 1000 $mV.s^{-1}$. **(B)** After 5 minutes in solution, v = 1000 $mV.s^{-1}$.

Table 3.12. The cyclic voltammetry data obtained from voltammograms (potentials *vs.* Fc/Fc^{+}) of ruthenocene measured in CH_3CN/0.1 mol dm^{-3} $[NBu_4][PF_6]$ at 25ºCas well as CH_2Cl_2/0.1 mol dm^{-3} $[NBu_4][B(C_6F_5)_4]$ at 25ºC and at -35ºC, with a glassy carbon working electrode at different scan rates. E_{pa} (anodic peak potential), ΔE_p (difference between the anodic and cathodic peak potentials), $E^{0/}$ (formal reduction potentials), i_{pa} (anodic peak current) and i_{pa}/i_{pc} (anodic/cathodic peak current relationship) are shown. $E^{0/} = (E_{pa} + E_{pc})/2$. The concentration of the ruthenocene was 1.0 $mmol.dm^{-3}$.

v / mV s^{-1}	E_{pa} / mV	ΔE_p / mV	$E^{0/}$ / mV[a]	i_{pa} / µA	i_{pc}/i_{pa}	E_{pc} / mV	i_{pc} / µA
$[RuCp_2]$, [2]/$[RuCp_2]^+$ At 25˚C in CH_3CN/0.1 mol.dm^{-3} $[NBu_4][PF_6]$						**$[(RuCp_2)_2]^{2+}$**	
100	684		-	9.1	-	-123 [a]	4.2 [a]
200	476	-	-	11.3	-	-131 [a]	5.3 [a]
300	477	-	-	13.5	-	-139 [a]	6.5 [a]
400	482	-	-	15.7	-	-154 [a]	7.6 [a]
500	485	-	-	17.9	-	-171 [a]	8.8 [a]
v / mV s^{-1}	**E_{pa} / mV**	**ΔE_p / mV**	**$E^{0/}$ / mV[a]**	**i_{pa} / µA**	**i_{pc}/i_{pa}**	**E_{pc} / mV**	**i_{pc} / µA**
$[RuCp_2]$, [2]/$[RuCp_2]^+$ At -35˚C in CH_2Cl_2/0.1 mol.dm^{-3} $[NBu_4][B(C_6F_5)_4]$						**$[(RuCp_2)_2]^{2+}$**	
50	646	100	596	5.7	0.57	325	2.7
100	647	105	595	7.2	0.57	318	2.9
200	647	114	590	8.8	0.58	293	3.2
300	650	124	588	10.3	0.58	280	3.4
400	658	136	590	11.9	0.59	270	3.7
500	667	155	590	13.3	0.60	256	4.0
$[RuCp_2]$, [2]/$[RuCp_2]^+$ At 25˚C in CH_2Cl_2/0.1 mol.dm^{-3} $[NBu_4][B(C_6F_5)_4]$						**$[(RuCp_2)_2]^{2+}$**	
100	687	78	648	15.1	0.44	-63	0.8
200	701	87	658	21.1	0.48	-88	1.9
300	718	100	668	25.1	0.52	-113	3.1
400	728	119	668	28.3	0.55	-137	4.1
500	736	131	671	32.1	0.59	-162	7.3

a) In CH_3CN $(Ru(C_5H_5))_2^{2+}$ does not exist. Since $(Cp_2Ru^{IV}CH_3CN)^{2+}$ is known to exist, this peak is tentatively assigned to the reduction of this Ru^{IV} species.

3.4.3. Ferrocene-containing β-diketones

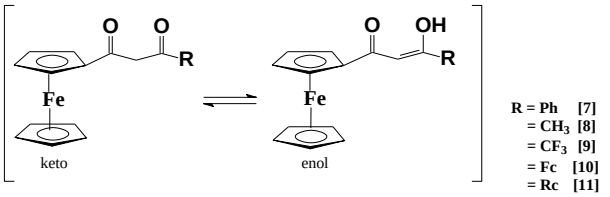

The electrochemistry of ferrocene-containing β-diketones [$FcCOCH_2COR$] (where R = Ph **[7]**, CH_3 **[8]**, CF_3 **[9]** and Fc **[10]**), in $CH_2Cl_2/[NBu_4][B(C_6F_5)_4]$, has been studied by other researchers.[20] Cyclovoltammetric analysis of the ruthenocene-containing β-diketone [$FcCOCH_2CORc$] **[11]** has been conducted for this study. Electrochemical data for β-diketones **[7]** – **[11]** is given in **Table 3.13.**

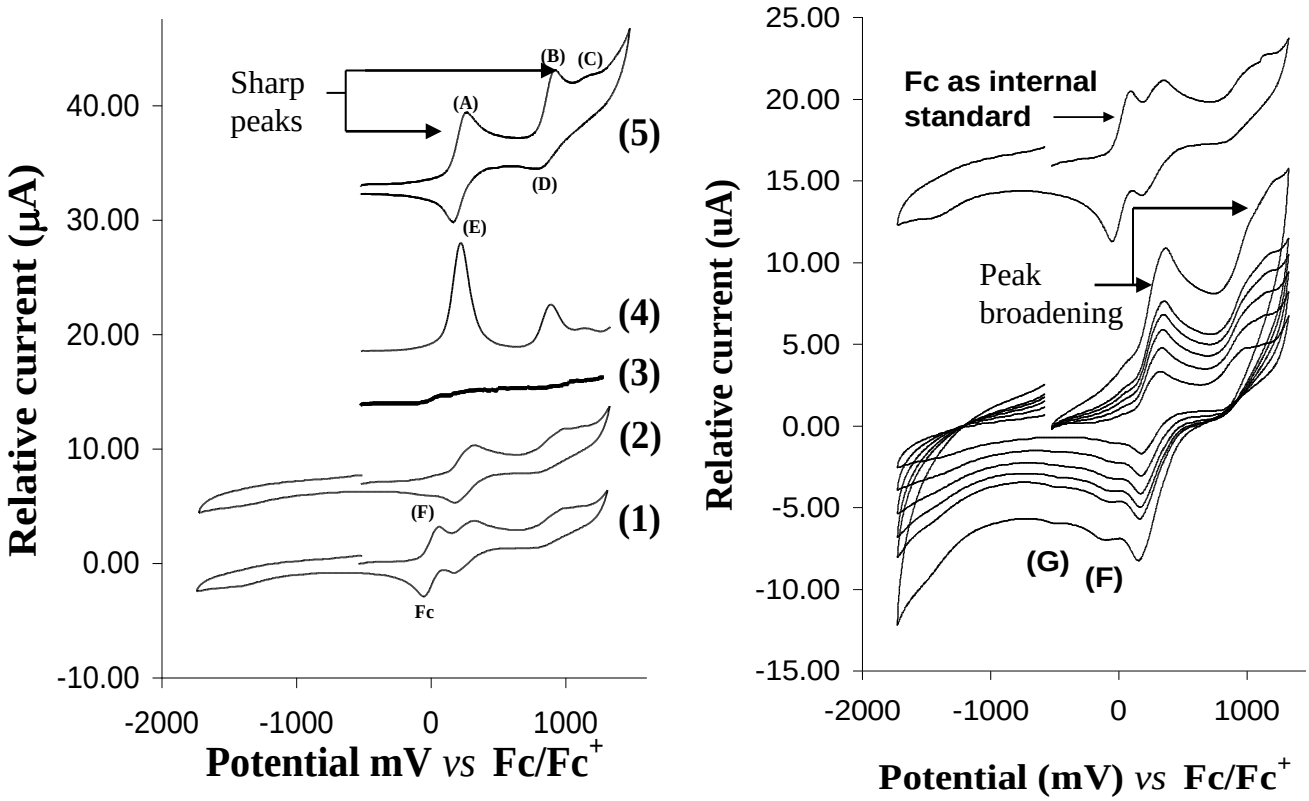

Figure 3.22. Left: Cyclic voltammograms of [$RcCOCH_2COFc$] **(1)** with added ferrocene as internal standard and **(2)** at scan rate 100 $mV.s^{-1}$, without ferrocene as internal standard. **(3)** Linear sweep voltammetry (at 2 $mV.s^{-1}$), **(4)** Oster Young square wave voltammogram (at 15 Hz) and **(5)** enlarged (I x 3) CV of a 1.0 $mmol.dm^{-3}$ solution of [$RcCOCH_2COFc$] **[11]** at 25ºC. Right/bottom: Cyclic voltammograms (at scan rates of 100, 200, 300, 400, 500 and 1000 $mV.s^{-1}$) of 1.0 $mmol.dm^{-3}$ solutions of [$RcCOCH_2COFc$] **[11]** at 25ºC. Top: Cyclic voltammogram (at scan rate = 200 $mV.s^{-1}$) of **[11]** in the presence of free ferrocene. Labels (A-G) are markers to make the text easier to follow.

Figure 3.22 (right) shows the cyclic voltammograms of 1-ferrocenyl-3-ruthenocenylpropane-1,3-dione, [$FcCOCH_2CORc$], **[11]** at different scan rates. A few observations can be made from these CV's.

Firstly, a broadening of the ferrocenyl and ruthenocenyl peaks is observable over time (compared with CV **(5)** left **Figure 3.22**). This is attributed to a shift towards the equilibrium position between enol and keto isomers of the β-diketone. This effect is identifiable because of slow keto-enol isomerisation kinetics (**Scheme 3.11**). At equilibrium in CD_2Cl_2, [$FcCOCH_2CORc$] exists as ~50% enol and ~50% keto.[21] In contrast aged samples of [$FcCOCH_2CORc$], in the solid state, exist exclusively in enol form.

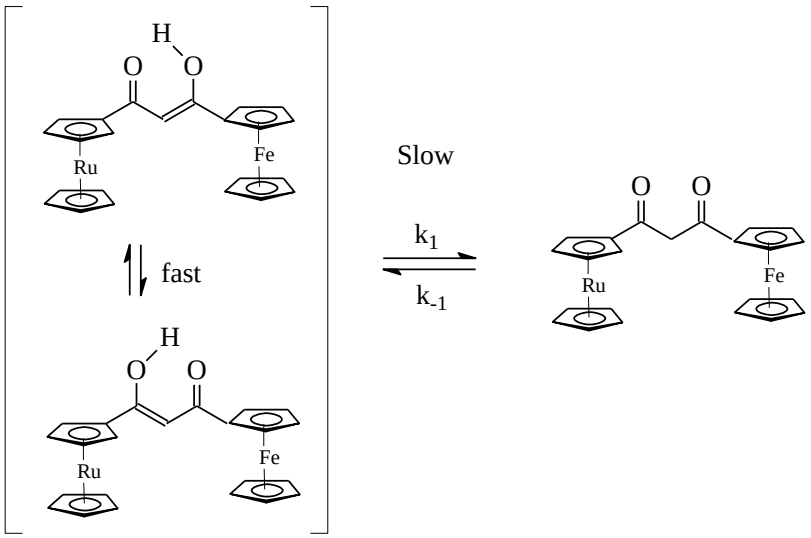

Scheme 3.11. The equilibrium between the keto- and enol-isomers of the ferrocene, ruthenocene-containing β-diketone. k_1 = rate constant for the forward reaction, k_{-1} = rate constant for the reverse reaction, $K_c = k_1/k_{-1}$ = equilibrium constant.

The fully reversible ferrocenyl-based wave is shown by the oxidation peak **(A)** at approximately 257 mV *vs.* Fc/Fc^+ internal standard and corresponding reduction peak **(E)** at 170 mV. ΔE_p = 87 mV, i_{pc}/i_{pa} = 0.84. Peaks **(B)** and **(C)** are associated with the oxidation of the keto and enol forms of the monomeric ruthenocenyl moiety respectively. A very weak reduction peak **(D)** of ($Fc^+COCH_2CORc^+$), can be seen at ~800 mV. This peak is assigned to the reduction of the ruthenocenyl fragment of monomeric **[11]**$^{2+}$. In analogy to ruthenocene itself, the anticipated dimeric ruthenium β-diketonato species is expected to have reduction waves of less positive potentials than the monomeric species. For the keto and enol isomers of [$FcCOCH_2CORc$], the peaks labelled **(F)** and **(G)** in **Figure 3.22**, right, would be consistent with the reduction of keto and enol dimers (**[11]**$_2^{4+}$). Peaks **(F)** and **(G)** are so weak in intensity that, even if this assignment is correct, it is of little practical consequence.

Table 3.13. Cyclic voltammetry data obtained from voltammograms (potentials *vs.* Fc/Fc^{+}) of ferrocene-containing β-diketones, [$FcCOCH_2COR$] (where R = Ph **[7]**, CH_3 **[8]** and CF_3 **[9]**, Fc **[10]** and Rc **[11]**. Measurements were taken in CH_2Cl_2/0.1 mol dm^{-3} $[NBu_4][B(C_6F_5)_4]$ at 25ºC, with a glassy carbon working electrode at scan rate = 100 $mV.s^{-1}$. E_{pa} (anodic peak potential), ΔE_p (difference between the anodic and cathodic peak potentials), $E^{0/}$ (formal reduction potentials), i_{pa} (anodic peak current) and i_{pc}/i_{pa} (cathodic/anodic peak current relationship) are shown. $E^{0/} = (E_{pa} + E_{pc})/2$. The concentration of the ruthenocene was 1.0 $mmol.dm^{-3}$.

β-diketone	**E_{pa} / mV**	**ΔE_p / mV**	**$E^{0/}$ / mV[a]**	**i_{pc}/i_{pa}**	**E_{pa} / mV**	**ΔE_p / mV**	**$E^{0/}$ / mV[a]**	**i_{pc}/i_{pa}**
	Ferrocenyl peak				**Ruthenocenyl or second Fc peak**			
[$FcCOCH_2COPh$][a] **[7]**	57	81	16	0.99	-	-	-	-
[$FcCOCH_2COCH_3$] [a] **[8]**	62	82	21	1.01	-	-	-	-
[$FcCOCH_2COCF_3$] [a] **[9]**	139	74	102	1.03	-	-	-	-
[$FcCOCH_2COFc$] [a] **[10]**	47	86	4	0.97	241	80	201	0.96
[$FcCOCH_2CORc$] **[11]**	257	87	213	0.99	917	88	873	2.08

[a] J.C. Swarts, Unpublished results.

3.4.4. Titanium complexes

3.4.4.1. Mono-β-diketonato titanium(IV) salts

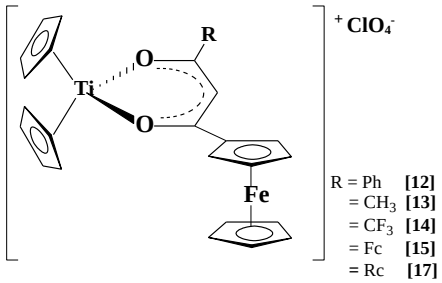

Voltammograms for the $[Cp_2Ti(FcCOCHCOR)]^+ClO_4^-$ complexes, where R = Ph **[12]**, CH_3 **[13]**, CF_3 **[14]**, Fc **[15]** and Rc **[17]**, in the $CH_3CN/[NBu_4][(PF_6)]$ solvent/electrolyte system are shown in **Figure 3.23.** The electrochemical results extracted from this study are summarised in **Table 3.14.**

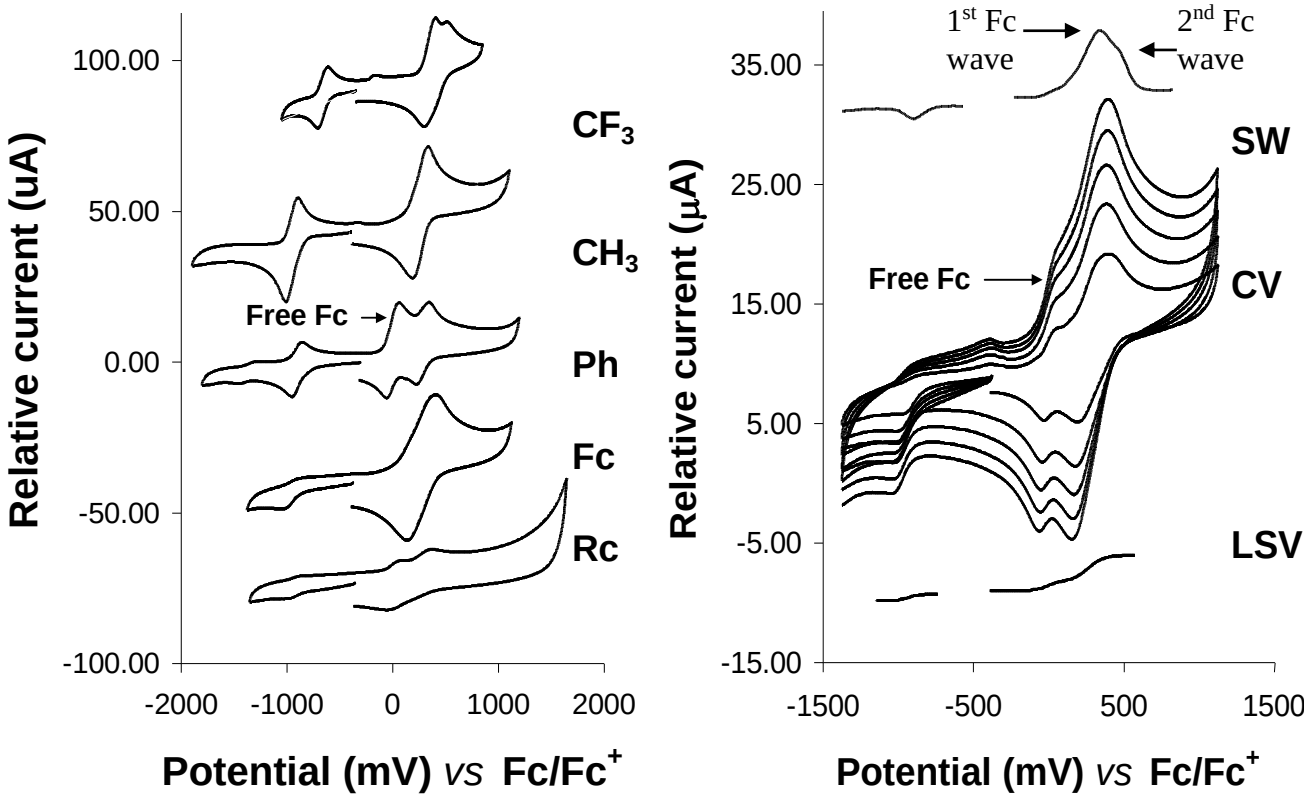

Figure 3.23. Left: The cyclic voltammograms of various 1.0 $mmol.dm^{-3}$ solutions of mono-β-diketonato titanocenyl complexes of the type $[Cp_2Ti(FcCOCHCOR)]^+ClO_4^-$, where R = Rc **[17]**, Fc **[15]**, Ph **[12]**, CH_3 **[13]** and CF_3 **[14]** (supporting electrolyte is 0.1 $mol.dm^{-3}$ $[NBu_4][PF_6]$) in CH_3CN on a glassy carbon working electrode at 25˚C. Scan rate was 500 $mV.s^{-1}$. Right: Linear sweep voltammetry (15 Hz), cyclic voltammograms (Scan rates = 100, 200, 300, 400 and 500 $mV.s^{-1}$) and Oster Young square wave voltammograms of $[Cp_2Ti(FcCOCHCOFc)]^+ClO_4^-$ **[15]** (supporting electrolyte is 0.1 $mol.dm^{-3}$ $[NBu_4][PF_6]$ in CH_3CN on a glassy carbon working electrode at 25˚C. All excepting the Oster Young square wave voltammogram contain ferrocene as internal standard.

Table 3.14. The cyclic voltammetry data obtained from voltammograms (*vs.* Fc/Fc^{+}) of various mono-β-diketonato titanocenyl complexes of the type $[Cp_2Ti(FcCOCHCOR)]^{+}ClO_4^{-}$ with R = Ph **[12]**, CH_3 **[13]**,CF_3 **[14]**, Fc **[15]** and Rc **[17].** Measured in 0.1 mol dm^{-3} tetrabuthylammonium hexafluorophosphate/CH_3CN with a glassy carbon working electrode at 25ºC, at the indicated scan rates.

v / mV s^{-1}	ΔE_{pFc} / mV	E^{01}_{Fc} / mV	i_{pc}/i_{pa} Fc	ΔE_p / mV Ti^{4+}/Ti^{3}	E^{01} / mV Ti^{4+}/Ti^{3}	i_{pa}/i_{pc} Ti^{4+}/Ti^{3}
$[Cp_2Ti(FcCOCHCOPh)]^{+}ClO_4^{-}$ [12]						
100	74	290	0.99	64	-858	0.64
200	79	291	0.99	69	-859	0.64
300	84	293	0.97	75	-858	0.67
400	91	291	0.98	83	-858	0.65
500	103	292	0.97	90	-860	0.71
$[Cp_2Ti(FcCOCHCOCH_3)]^{+}ClO_4$ [13]						
100	104	340	0.97	65	-883	0.71
200	113	342	0.96	77	-885	0.79
300	124	341	0.97	82	-882	0.74
400	131	344	0.93	89	-888	0.78
500	139	348	0.91	93	-889	0.80
$[Cp_2Ti(FcCOCHCOCF_3)]^{+}ClO_4^{-}$ [14][a]						
100	148	413	0.78	68	-640	0.80
200	156	412	0.76	75	-642	0.83
300	163	412	0.76	83	-643	0.82
400	172	414	0.78	91	-643	0.83
500	180	413	0.76	99	-644	0.84
$[Cp_2Ti(FcCOCHCOFc)]^{+}ClO_4^{-}$ [15]						
100	149	266	0.95	62	-962	0.54
200	156	268	0.93	72	-966	0.59
300	164	267	0.95	80	-963	0.54
400	171	269	0.91	88	-964	0.55
500	180	269	0.94	97	-962	0.59
$[Cp_2Ti (FcCOCHCORc)]^{+}ClO_4^{-}$[17][b]						
100	96	280	0.96	54	-928	0.39
200	99	282	0.95	64	-928	0.42
300	105	281	0.94	72	-929	0.40
400	113	282	0.93	78	-930	0.41
500	124	283	0.93	91	-927	0.42

a) Information is for aged sample (see **Figure 3.24**).

b) Due to poor resolution Rc peaks could not be quantified

The mono-β-diketonato titanium complexes containing only one ferrocenyl group in the β-diketonato ligand were found to exhibit an electrochemically reversible Ti^{4+}/Ti^{3+}couple, according to:

$$[(Cp)_2Ti^{IV}(FcCOCHCOR)]^+ + e^- \rightleftharpoons [(Cp)_2 Ti^{III}(FcCOCHCOR)]$$

$\Delta E_p \leq 90$ mV for the one-electron transfer process involved. It is known that the Ti(III) mono-β-diketonato complexes do exist and that the redox reaction does not change the coordination sphere of the complex. For example, Coutts and Wailes made the Ti(III), titanocenyl acetylacetonate complex $[Cp_2Ti^{III}(CH_3COCHCOCH_3)]$ in 1969.[22] This is in contrast to $[Cp_2Ti^{III}Cl{\bullet}CH_3CN]$ and $[Cp_2Ti^{IV}Cl_2]$ which do not have the same coordination sphere.

Complexes **[15]** and **[17]** contain two metal centres in addition to titanium. In these cases the Ti^{4+}/Ti^{3+}couple displays irreversible electrochemical behaviour, $i_{pa}/i_{pc} \neq 1$.

The complexes also exhibit a predominantly quasi-reversible Fc/Fc^+ redox couple:

$$Fc^+ + e^- \rightleftharpoons Fc \quad \text{or} \quad [(C_5H_5)Fe^{III}(C_5H_4)]^+ + e^- \rightleftharpoons [(C_5H_5)Fe^{II}(C_5H_4)]$$

The coordinated ferrocenyl ligands in the titanium complexes have an average ΔE of 114 mV for the Fc/Fc^+ couple.

Figure 3.23 right, shows a linear sweep voltammogram (15 Hz), cyclic voltammograms (Scan rate = 100, 200, 300, 400 and 500 $mV.s^{-1}$) and Oster Young square wave voltammograms of $[Cp_2Ti(FcCOCHCOFc)]^+ClO_4^-$ **[15].** The Oster Young square wave voltammogram provides better indication of the two distinct ferrocenyl moieties within the β-diketonato ligand. The LSV current of ferrocenyl ligand is 4x that of titanocenyl LSV current. The Ti^{IV}/Ti^{III} couple is irreversible (only a reduction half wave is observable). This corresponds to one Ti and two Fe within the compound. Similar observations were made for compound **[17]** with a ferrocenyl and a ruthenocenyl moiety. For all the other compounds in this series LSV showed a 1:1 electron relationship for the titanium and iron centres.

For $[Cp_2Ti(FcCOCHCORc)]^+ClO_4^-$ **[17]** the electrochemistry of the ruthenocenyl fragment is unclear in this solvent system, but is undoubtedly involved in an irreversible electrochemical process.

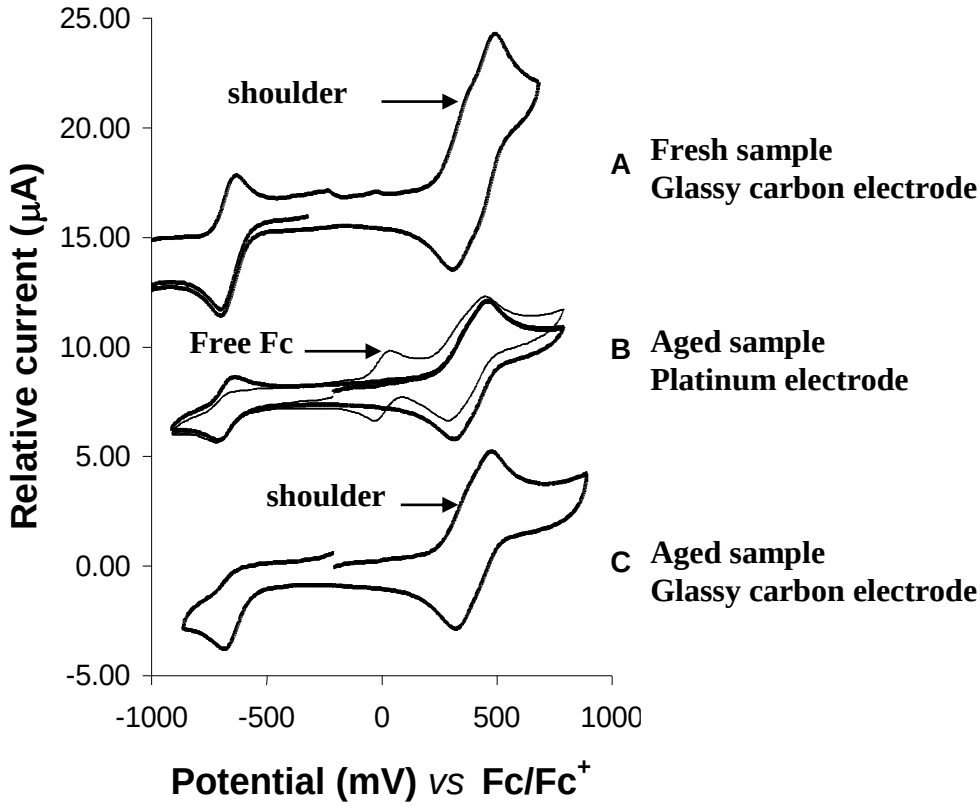

Figure 3.24. CV's of 1 mmol.dm^3 solutions of $[Cp_2Ti(FcCOCHCOCF_3)]^+ClO_4^{-1}$ **[14]**, in 0.1mol $CH_3CN/[NBu_4][(PF_6)]$ at 25˚C, scan rate = 100 mV.s$^-$**. (A)** Freshly prepared sample on a glassy carbon working electrode. **(B)** Aged sample on a platinum working electrode (overlain with scan including ferrocene as internal standard, thin line). **(C)** Aged sample on a glassy carbon working electrode.

Comparative CV's of $[Cp_2Ti(FcCOCHCOCF_3)]^+ClO_4^{-1}$ **[14]** in **Figure 3.24**, show freshly prepared samples display reversible electrochemistry for the Ti couple on a glassy carbon working electrode, this is also seen in aged samples (6 months) on a platinum working electrode. The 6-month-old sample shows virtually irreversible Ti electrochemistry on a glassy carbon electrode. The same diminishing of the Ti oxidation peak is observed upon addition of free ferrocene (see **B**). Ti oxidation recession was observed for most samples when the Fc/Fc^+ couple was added as an internal standard, as well as for samples with two ferrocenyl groups within the same molecule, as previously mentioned. Improved reversibility of the titanium wave is obtained with electrode polishing between each successive scan, all the same, full reversibility is never regained.

Also visible in **Figure 3.24** is a shoulder associated with the main ferrocenyl peak, as well as the much larger total current flow in the ferrocenyl wave as compared to the titanium couple.

This phenomenon is not seen for the other Ti(IV) salts in the $CH_3CN/[NBu_4][(PF_6)]$ system, but does become more apparent in the non-coordinating $CH_2Cl_2/[NBu_4][B(C_6F_5)_4]$ system. This is due to the exceptional electron withdrawing power of the CF_3 R-group. When coupled with an additional electron withdrawing Fc^+ group (after oxidation), electron depletion on the Ti centre is to such an extent as to require the formation of a solvent coordinated species.

In comparing the formal reduction potential for $[Cp_2Ti(FcCOCHCOR)]^+ClO_4^-$ complexes, where R = CH_3 (χ_{CH3} = 2.34); Ph (χ_{Ph} = 2.21); CF_3 (χ_{CF3} = 3.01), Fc (χ_{Fc} = 1.87) and Rc (χ_{Rc} = 1.94), both the ferrocenyl group and the Ti centre show higher $E^{0/}$ values as the group electronegativity, χ_R, of the R-group increases, see **Figure 3.25**.

This is an expected result, as an increasingly electron withdrawing R-group will result in more positive iron and titanium centres, and accordingly the reduced form will be more difficult to oxidise.

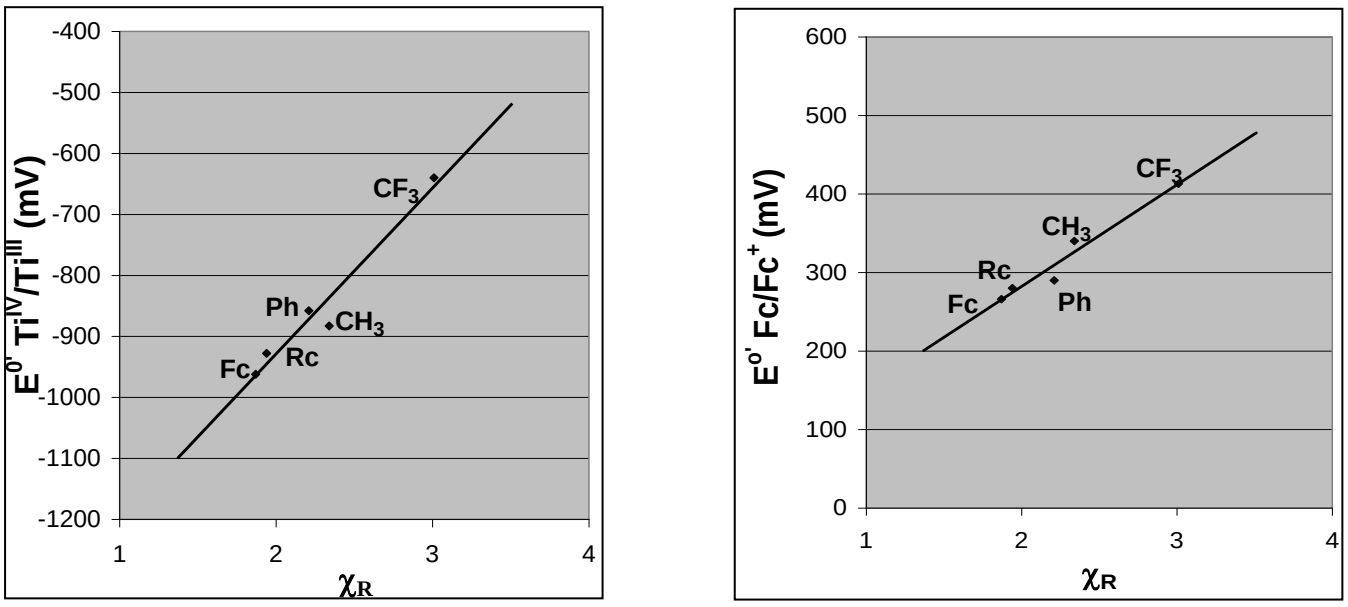

Figure 3.25. Graphs of the relationships between the formal reduction potential ($E^{0/}$) of the mono-β-diketonato titanocenyl complexes $[Cp_2Ti(FcCOCHCOR)]^+ClO_4^-$ (where R = Ph, CH_3, CF_3, Fc and Rc) and apparent group electronegativities (χ_R) of the R-groups on the β-diketonato ligands.

The cyclic voltammetric behaviour of the new mono-β-diketonato titanocenyl complexes $[Cp_2Ti(FcCOCHCOR)]^+ClO_4^-$, where R = Ph **[12]**, CH_3 **[13]**, CF_3 **[14]**, Fc **[15]** and Rc **[17]**, were studied in acetonitrile/1 mol.dm^{-3} [NBu4][(PF_6)] as well as in the non-coordinating CH_2Cl_2/0.1 mol.dm^{-3} $[NBu_4][B(C_6F_5)_4]$ system. Comparative cyclic voltammograms of $[Cp_2Ti(FcCOCHCOCH_3)]^+ClO_4^-$ in each of these solvent systems are shown in **Figure 3.26**, in both cases scan rate = 100 mV.s^{-1}.

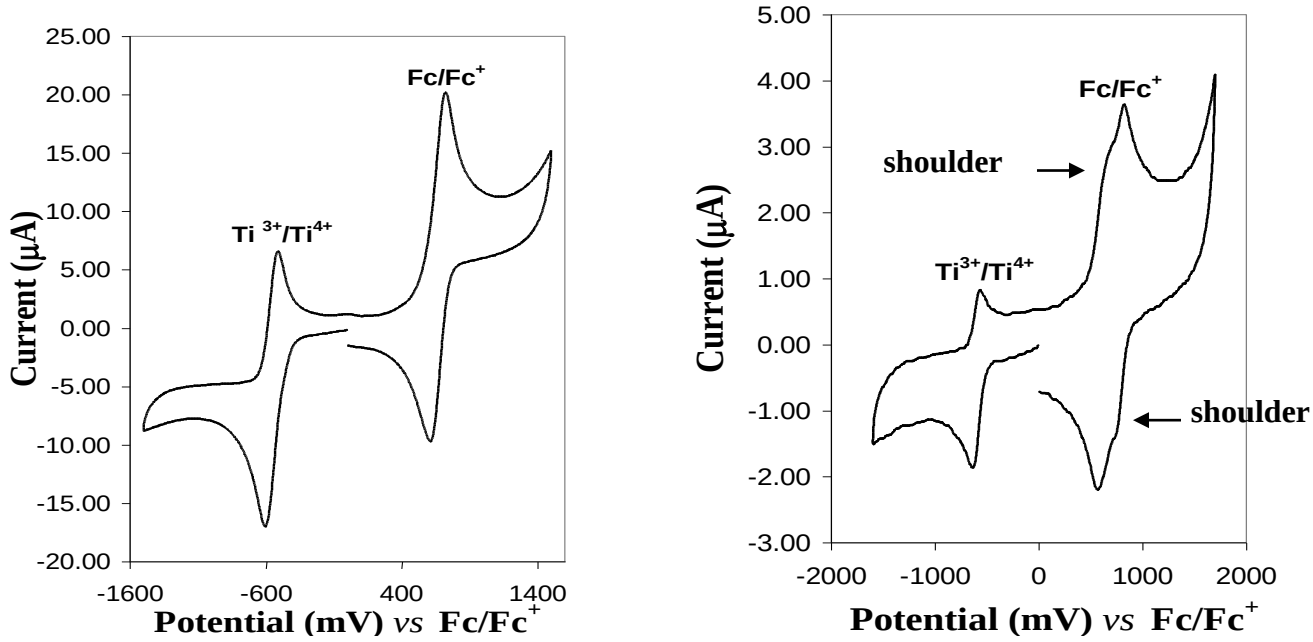

Figure 3.26. Left: Cyclic voltammogram of a 1.0 mmol.dm^{-3} $[Cp_2Ti(FcCOCHCOCH_3)]$ **[13]**, in CH_3CN solution (with supporting electrolyte 0.1 mol.dm^{-3} [NBu4][(PF_6)]) on a glassy carbon working electrode at 25˚C. Right: Cyclic voltammogram of a 1.0 mmol.dm^{-3} $[Cp_2Ti(FcCOCHCOCH_3)]$ **[13]**, in CH_2Cl_2 solution (supporting electrolyte is 0.1 mol.dm^{-3} $[NBu_4][B(C_6F_5)_4]$) on a glassy carbon working electrode at 25˚C (shouldering highlighted).

A one-electron transfer process is associated for each $Ti^{4+}/Ti^{3+}$and Fc/Fc^+ redox process. For the acetonitrile system a one electron transfer process for both the titanium and ferocene couple was confirmed by linear sweep voltammetry. Immediately noticeable in the $CH_2Cl_2/[NBu_4][B(C_6F_5)_4]$ system is the larger peak current of the ferrocene couple as compared to that of the titanocenyl fragment. In addition, the $CH_2Cl_2/[NBu_4][B(C_6F_5)_4]$ system (right) reveals a splitting of the ferrocenyl fragment into two unresolved shoulders. From this evidence it is clear that more than one ferrocene moiety is at play in this solvent/electrolyte system.

Cyclic voltammograms for the $[Cp_2Ti(FcCOCHCOR)]^+ClO_4^-$ complexes at 100 $mV.s^{-1}$ in the non-coordinating $CH_2Cl_2/[NBu_4][B(C_6F_5)_4]$ solvent/electrolyte system are shown in **Figure 3.27.** The electrochemical results extracted from this study are summarised in **Table 3.15.** In all cases the ferrocenyl wave showed two peaks (labelled 1 and 2) rather than one. This double peak is indicative of dimerisation.

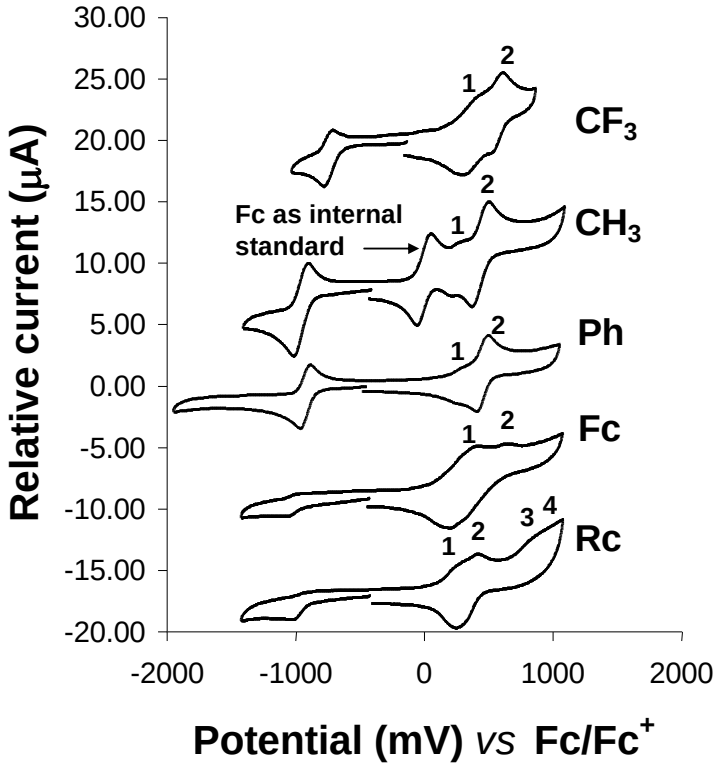

Figure 3.27. Cyclic voltammgrams for 1.0 $mmol.dm^{-3}$ solutions of mono-β-diketonato titanocenyl complexes $[(Cp_2Ti(FcCOCHCOR)]^+ClO_4^-$ where R is as indicated in the figure, recorded in CH_2Cl_2/0.1 mol dm^{-3} $[NBu_4][B(C_6F_5)_4]$ on a glassy carbon-working electrode at 25ºC and a scan rate of 100 $mV.s^{-1}$.

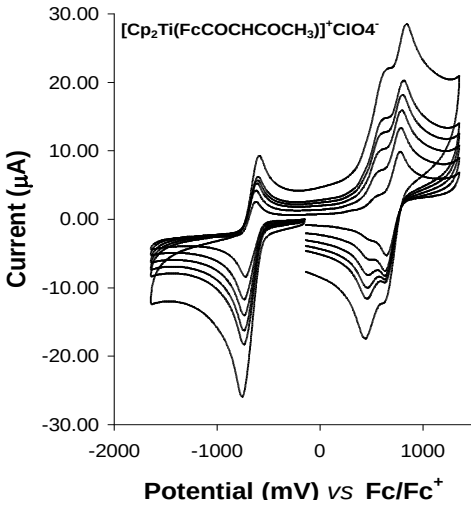

Figure 3.28. Cyclic voltammgrams for a 1.0 $mmol.dm^{-3}$ solution of $[Cp_2Ti(FcCOCHCOCH_3)]^+ClO_4^-$,complex **[13]**, recorded in CH_2Cl_2/0.1 mol dm^{-3} $[NBu_4][B(C_6F_5)_4]$ on a glassy carbon-working electrode at 25ºC. Scan rates are 100, 200, 300, 400, 500 and 1000 $mV.s^{-1}$.

Table 3.15. Cyclic voltammetry data for $[(Cp)_2Ti(RcCOCHCOR)]^+ClO_4^-$ complexes, χ_R = group electronegativity of the R-group on the β-diketonato ligand, peak anodic potentials, E_{pa} or E_{pc} (*vs.* Fc/Fc^+ couple as an internal standard); difference in peak anodic and peak cathodic potentials, ΔE_p; formal reduction potentials, $E^{0\prime}$; peak anodic currents, i_{pa}; and peak anodic/peak cathodic current ratios, i_{pa}/i_{pc}, as indicated. Concentration of samples was 1.0 $mmol.dm^{-3}$ in CH_2Cl_2/0.1 $mol.dm^{-3}$ $[NBu_4][B(C_6F_5)_4]$.

v / $mV.s^{-1}$	ΔE_p / mV	$E^{0\prime}$ / mV	i_{pc}/i_{pa}	ΔE_p / mV	$E^{0\prime}$ / mV	i_{pa}/i_{pc}	ΔE_p / mV	$E^{0\prime}$ / mV	i_{pa}/i_{pc}
	Ferrocenyl shoulder[b]			**Fc/Fc^+**			**Ti^{4+}/Ti^3**		
$[Cp_2Ti(FcCOCHCOPh)]^+ClO_4^-$ [12]; χ_{Ph} = 2.21[b]									
100	104	452	0.41	94	251	0.99	88	-922	0.91
$[Cp_2Ti(FcCOCHCOCH_3)]^+ClO_4^-$ [13]; χ_{CH3} = 2.34[b]									
100	135	431	0.53	105	268	1.01	87	-959	0.72
v / $mV.s^{-1}$	ΔE_p / mV	$E^{0\prime}$ / mV	i_{pa}/i_{pc}	ΔE_p / mV	$E^{0\prime}$ / mV	i_{pa}/i_{pc}	E_{pa} / mV	ΔE_p / mV	i_{pa}/i_{pc}
	Fc peak 1			**Fc peak 2**			**Ti^{4+}/Ti^3**		
$[Cp_2Ti(FcCOCHCOCF_3)]^+ClO_4^-$ [14]; χ_{CF3} = 3.01									
100	150	372	0.66	115	559	0.96	84	-748	0.70

v / $mV.s^{-1}$	E_{pc} / mV Fc reduction (broad peak)	E_{pa} / mV	ΔE_p / mV	i_{pa}/i_{pc}	E_{pa} / mV	ΔE_p / mV	i_{pa}/i_{pc}	E_{pc} / mV	i_{pa}/i_{pc}	E_{pa} / mV	i_{pc}/i_{pa}
		Fc oxidation peak 1			**Fc oxidation peak 2**			**Ti^{4+}/Ti^3**		**Rc**	
$[Cp_2Ti(FcCOCHCOFc)]^+ClO_4^-$ [15]; χ_{Fc} = 1.87											
100	201	414	213	1.07	626	425	1.08	1081	0	-	-
$[Cp_2Ti(FcCOCHCORc)]^+ClO_4^-$ [17]; χ_{Rc} = 1.94											
100	230	294	64	1.25	434	204	1.57	1030	0	910[a]	0

a) Not an exact value, but an estimate due to poor resolution of peak.

b) More than one peak could be identified but resolution was so poor that an individual assessment of each peak's characteristics could not be performed.

The binuclear $[Cp_2Ti(FcCOCHCOR)]^+ClO_4^-$ complexes where R = Ph **[12]**, CH_3 **[13]** and CF_3 **[14]**, were found to exhibit an electrochemically reversible Ti^{4+}/Ti^{3+} couple with ΔE < 90 mV and $i_{pa}/i_{pc} \geq 0.70$. Complexes **[15]** and **[17]** with three metal centres, show irreversible behaviour for the titanium couple and the Rc/Rc^+ couple, with ΔE > 150 mV and i_{pa}/i_{pc} approaching 0.

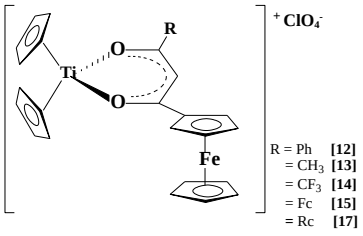

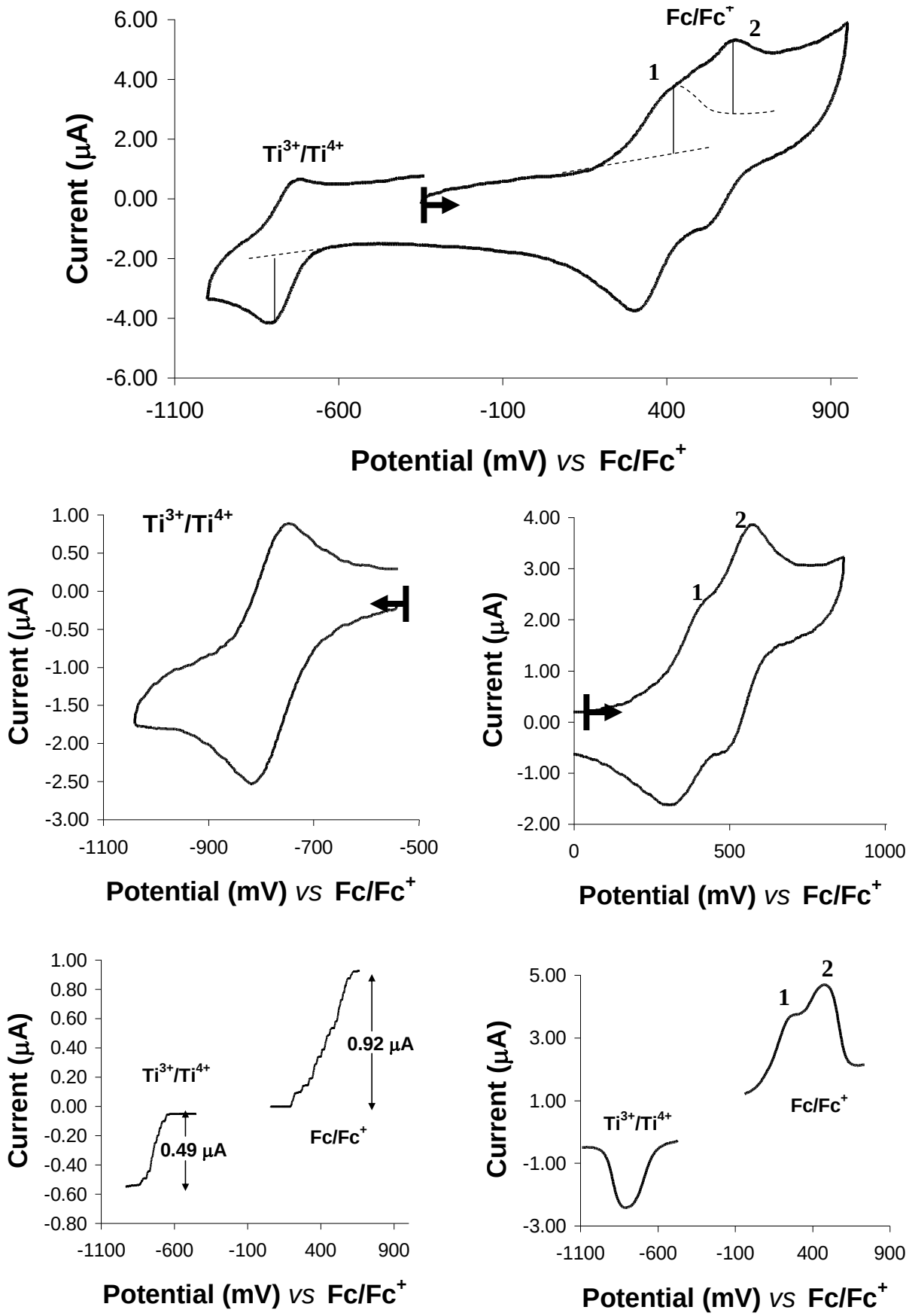

Figure 3.29. Voltammetric graphs for $[Cp_2Ti(FcCOCHCOCF_3)]^+ClO_4^-$ **[14]** (1 mmol.dm^{-3}), recorded in CH_2Cl_2/0.1 mol dm^{-3} $[NBu_4][B(C_6F_5)_4]$ on a glassy carbon-working electrode at 25ºC and a scan rate of 100 mV.s^{-1}. Above: Full CV, positive direction. Centre left: CV negative direction (titanocenyl portion). Centre right: CV positive direction (ferrocenyl portion). Below left: LSV graph. Below right: Oster Young Square Wave voltammogram.

In **Figure 3.29** (above), the "splitting" of the ferrocenyl portion of $[Cp_2Ti(FcCOCHCOCF_3)]^+ClO_4^-$ into two distinct peaks is particularly clear. In addition, for compound **[14],** the ratio of the Ti reduction peak current (i_{pc} = 2.31 μA), to the anodic peak current of the first ferrocenyl wave (i_{pa} = 2.41 μA), as well as the peak current of the second ferrocenyl wave (i_{pa} = 2.33 μA), is ca. 1:1:1. The question must be posed weather the two observed peaks at the ferrocenyl wave are not an artefact of first observing titanium transfer reactions. In **Figure 3.29** (centre) the ferrocenyl scan was obtained by initiating the CV at 0 V in the positive direction. By concentrating on only the ferrocenyl potential range it was ensured that the effect was not an artefact of electrode deposition. It was also established that even under these conditions the Ti current was much less than the total ferrocenyl current. The ferrocenyl peak splitting phenomenon was again confirmed by Oster Young square wave voltammetry (bottom right). Linear sweep voltammetry (bottom left) confirms a one electron processes for Ti and a two electron flow process for the Fe centre.

These findings are consistent with dimerisation of the molecule after ferrocenyl oxidation. Under normal conditions the ferrocenyl moiety is electron donating. This "pumping" of electrons helps to stabilise the highly electrophilic (positive) titanium(IV) centre. Upon oxidation of Fe^{2+} to Fe^{3+}, the ferrocenyl group becomes a strong electrophile itself and is therefore unable to donate electron density to the Ti^{4+} centre. The newly oxidised molecule at the surface of the electrode is hyper electrophilic which could drive a coordination reaction with any neighbouring molecule from the bulk of the solution, which is less electrophilic (i.e. not yet oxidised). In the case of the acetonitrile/$[NBu_4][(PF_6)]$ system, the nucleophilic molecules may be acetonitrile. In the absence of a coordinative solvent system, intermolecular coordination may occur between a fully oxidised, electrophilic mono-β-diketonato titanium(IV) complex and an un-oxidised ferrocenyl molecule (which is much less electrophilic) from the bulk of the solution. This result is consistent with the interpretation that a temporary dimer complex is formed (see next page, **Scheme 3.12**). The proposed dimer contains one oxidised ferrocenium centre and one ferrocenyl centre which is still in reduced form. The second ferrocenyl group from the proposed dimer must then be oxidised at a higher potential, which explains the second distinct oxidation and reduction peaks observed at ferrocenyl waves.

Once both the ferrocenyl portions of the proposed dimeric mono-β-diketonato titanium(IV) complexes have been reduced, there is no longer a shortage of electron density on the Ti centre and the dimer may fall apart. This would then result in only $[Cp_2Ti(FcCOCHCOR)]^+ClO_4^-$ type complexes remaining and explains why only one peak is observed for the Ti^{4+}/Ti^{3+} couple.

The following electrochemical scheme is consistent with the proposed interpretation of the results above, i.e. for the single Ti^{4+}/Ti^{3+} and the two observed Fc/Fc^+ waves:

$$[Cp_2Ti^{III}(FcCOCHCOR)] \underset{+\,e^-}{\overset{-\,e^-}{\rightleftharpoons}} [Cp_2Ti^{IV}(FcCOCHCOR)]^+ \underset{+\,e^-}{\overset{-\,e^-}{\rightleftharpoons}} [Cp_2Ti^{IV}(Fc^+COCHCOR)]^+ \overset{\text{Rapid chemical dimerisation with } [Cp_2Ti^{IV}(FcCOCHCOR)]^+ \text{ from the bulk of the solution}}{\rightleftharpoons}$$

$$[[Cp_2Ti^{IV}(Fc^+COCHCOR)]^+ \; ; \; [Cp_2Ti^{IV}(FcCOCHCOR)]^+] \underset{+\,e^-}{\overset{-\,e^-}{\rightleftharpoons}} [Cp_2Ti^{IV}(Fc^+COCHCOR)]_2^{2+}$$

To visualise the electrochemical scheme above, the following proposed molecular species may be considered.

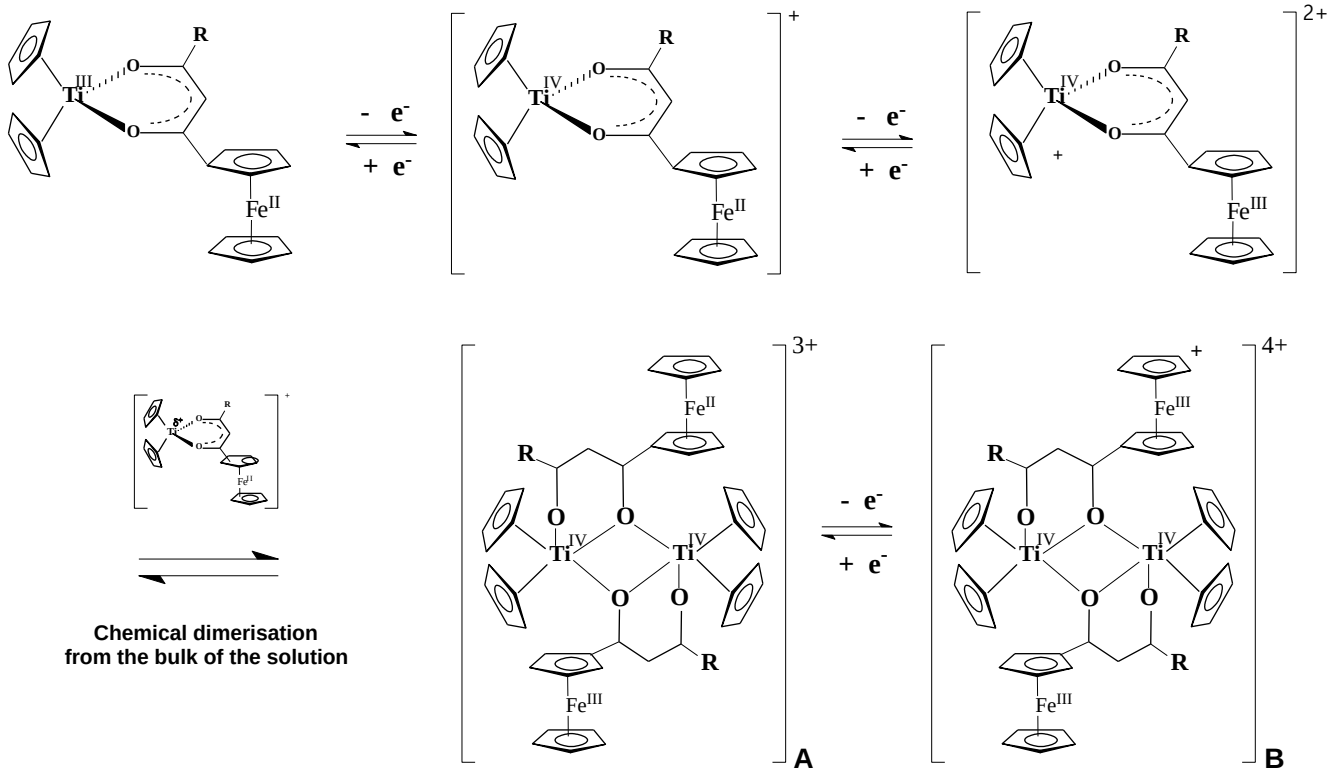

Scheme 3.12. Proposed molecular structures associated with the suggested electrochemical scheme, to explain experimental results. Structures **A** and **B** are possible because Ti^{IV} may be four, five or six coordinated. No structural evidence, from X-ray studies, for the suggested oxygen bridged complexes exists at this stage.

Further investigation is required, including isolation and crystallographic characterisation of the proposed dimer compound, before the existence of proposed species **A** and **B** can be proven.

3.4.4.2. Dichlorobis(β-diketonato)titanium(IV) complexes

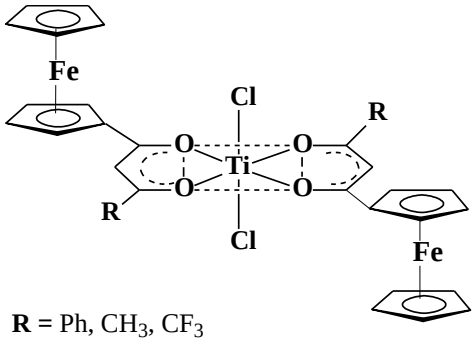

R = Ph, CH_3, CF_3

The cyclic voltammetric behaviour of the series of dichlorobis(β-diketonato)titanium(IV) complexes of the type $[(FcCOCHCOR)_2TiCl_2]$, where R = Ph **[18]**, CH_3 **[19]** and CF_3 **[20],** were studied in CH_2Cl_2/0.1 mol.dm^{-3} $[NBu_4][B(C_6F_5)_4]$. Selected cyclic voltammograms are shown in **Figure 3.30.** Electrochemical data is summarised in **Table 3.16.**

Figure 3.30 (Left) shows the comparative cyclic voltammograms of compounds **[18]**, **[19]** and **[20]**. Cyclic voltammograms at different scan rates for the phenyl compound are shown the right hand figure. Peak 5 (shows electrochemically irreversible Ti^{4+} reduction to Ti^{3+} with $\Delta E > 150$ mV. For $[(FcCOCHCOPh)_2TiCl_2]$ **[18]** especially, extreme electrode deposition is seen under reducing conditions (multiple peaks 5). Peaks 1 and 2 represent signals for the two ferrocene-containing β-diketonato ligands for compound **[18]**, R = Ph. For compounds **[19]** (R = CH_3) and **[20]** (R = CF_3) the two expected ferrocenyl waves overlap.

The multiple peaks observed for the two ferrocenyl groups of $[(FcCOCHCOPh)_2TiCl_2]$ (waves 1 and 2) are consistent with the view that mixed valent intermediates are generated during the electrochemical cycle of these complexes. An alternative explanation (but less plausible) could be that more than one isomer exists for each complex. This was also observed in the ^{1}H NMR spectra of these complexes (see **Figure 3.5**, paragraph 3.2.2.2, page 72). Possible isomers are shown in **Scheme 3.7** (pg 72). The shape of the reduction wave of Ti is typical of substrate adsorption onto the working electrode i.e. electrode coating, and the observed current fluctuations are attributed to this. The Fc/Fc^+ couple of the $[(FcCOCHCOR)_2TiCl_2]$ complexes were found to be electrochemically and chemically reversible with ΔE = 72 -75 mV and $i_{pc}/i_{pa} \approx 1.0$ (**Figure 3.30** and **Table 3.16**).

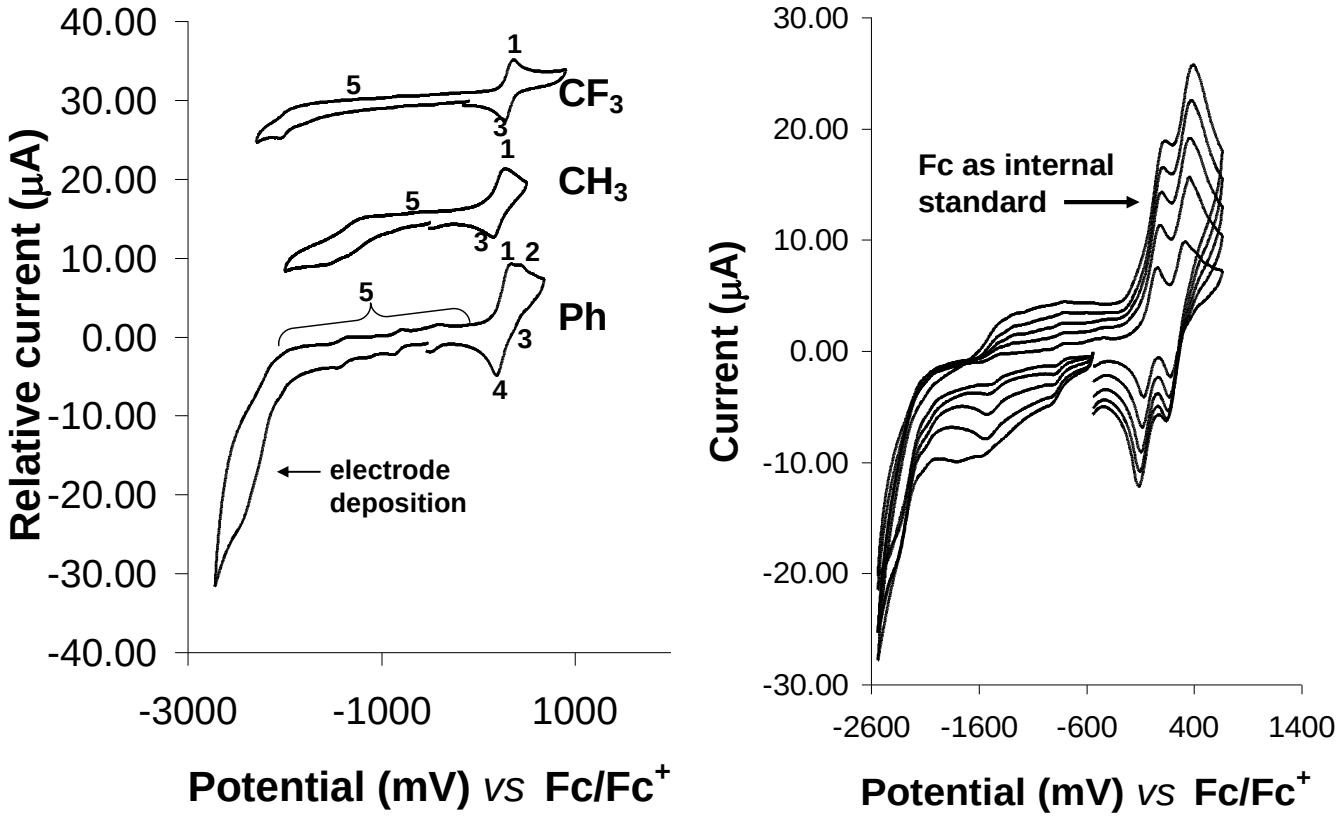

Figure 3.30. Left: Cyclic voltammograms (CV) of the 1.0 mmol.dm^{-3} solutions of $[(FcCOCHCOR)_2TiCl_2]$ where R = Ph **[18]**, CH_3 **[19]** and CF_3 **[20]**, measured in CH_2Cl_2/0.1 mol.dm^{-3} $[NBu_4][B(C_6F_5)_4]$ on a glassy carbon-working electrode at scan a rate of 100 mV s^{-1}. T = 25ºC. Right: CV's of $[(FcCOCHCOPh)_2TiCl_2]$ **[18]**, scan rate = 100, 200, 300, 400 and 500 mV.s^{-1}, in the presence of Fc as internal standard.

Table 3.16. The cyclic voltammetry data obtained from voltammograms (*vs.* Fc/Fc^+) of dichloro-bis(β-diketonato)titanium(IV) complexes of the type $[(FcCOCHCOR)_2TiCl_2]$ with R = Ph **[18]**, CH_3 **[19]**,CF_3 **[20]** were measured in 0.1 mol dm^{-3} $[NBu_4][B(C_6F_5)_4]$ /CH_2Cl_2 with a glassy carbon working electrode at 25ºC and a scan rate of 100 mV s^{-1}. The concentration of for all complexes was 1.0 mmol.dm^{-3}.

Tc complex	**No.**	**ΔE_p / mV** Fc/Fc^+	**E_{pa} / mV** Fc/Fc^+	**$E^{0/}$ / mV** Fc/Fc^+	**i_{pc}/i_{pa}** Fc/Fc^+	**E_{pc} / mV** Ti^{4+}/Ti^3	**i_{pa}/i_{pc}** Ti^{4+}/Ti^3
$[(FcCOCHCOPh)_2TiCl_2]$	**[18]**	72[a] 166[b]	350[a] 444[b]	314[a] 361[b]	0.99[a] 1.02[b]	-2470	0
$[(FcCOCHCOCH_3)_2TiCl_2]$	**[19]**	75	291	253	0.97	-1576	0
$[(FcCOCHCOCF_3)_2TiCl_2]$	**[20]**	73	397	360	0.78	-2041	0

a) Peak 1

b) Peak 2

Possibly due to electrode deposition, no meaningful relationship could be found between the E_{pc} of Ti^{4+}/Ti^{3+} couple and χ_R, probably because E_{pc} is not a thermodynamic quantity. The general trend for the relationship between the apparent group electronegativity of the R-group and the formal reduction potentials of the Fc/Fc^+ couple appears to be, as χ_R increases $E^{0/}$ of the Fc/Fc^+ couple increases (**Figure 3.31**). This is expected because of the relatively larger positive charge which is induced on the titanium(IV) and ferrocenyl centres as χ_R increases, making the ferrocenyl group more difficult to oxidise.

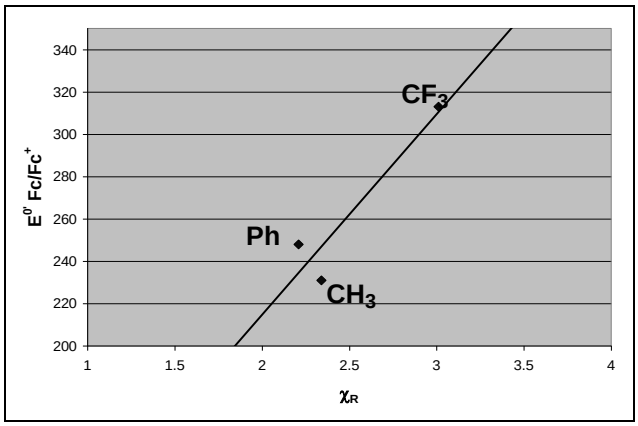

Figure 3.31. Left: Graph of relationship between $E^{0/}$ Fc/Fc^+ and apparent group electronegativities of the R-groups on the β-diketonato ligands.

3.4.4.3. Di(1-oxyethyl-1-ferrocenyl)bis(β-diketonato)titanium(IV) complexes

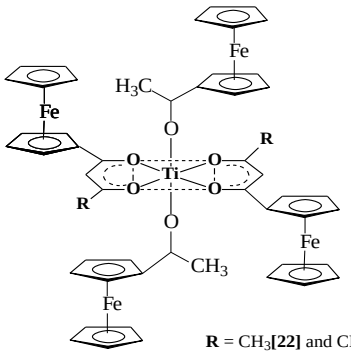

R = CH_3**[22]** and CF_3 **[23]**

The cyclic voltammetric behaviour of the series of di(1-oxyethyl-1-ferrocenyl) bis(β-diketonato)titanium(IV) complexes $[(FcCOCHCOR)_2Ti(O\text{-}CH(CH_3)\text{-}Fc)_2]$, where R = CH_3 **[22]** and CF_3 **[23]**, were studied in CH_2Cl_2/0.1 mol dm^{-3} $[NBu_4][B(C_6F_5)_4]$. Cyclic voltammograms for these compounds are shown in **Figure 3.32** and **Figure 3.33.** Electrochemical data is summarised in **Table 3.17**.

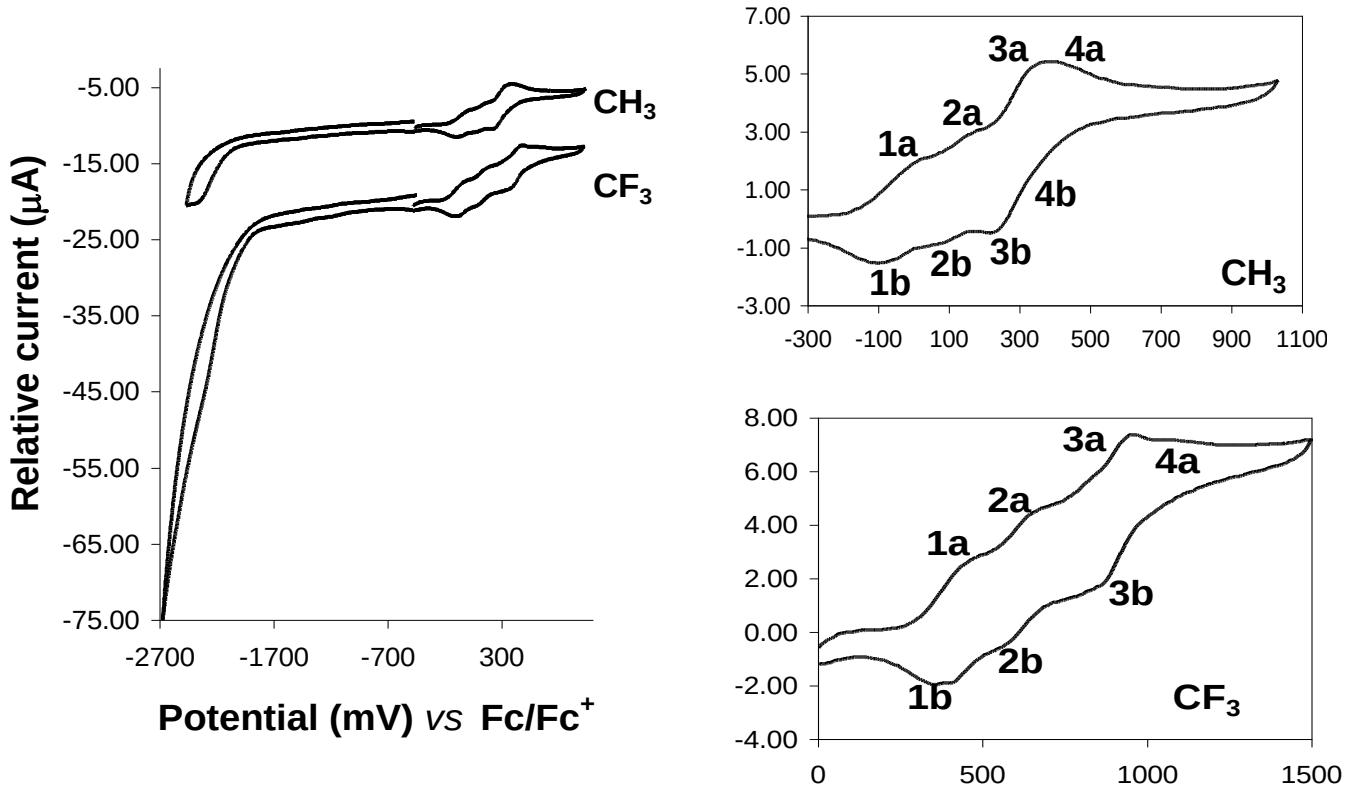

Figure 3.32. Left: Cyclic voltammograms of 1.0 mmol.dm^{-3} solutions of complexes of the type [FcCOCHCOR)$_2$Ti(O-CH(CH$_3$)-Fc)$_2$], where R = CH$_3$ **[22]** and CF$_3$ **[23]**, measured in CH$_2$Cl$_2$/0.1 mol dm^{-3} [NBu$_4$][B(C$_6$F$_5$)$_4$] at a glassy carbon-working electrode, 25ºC and a scan rate of 50.mV.s^{-1}. Right: Highlighted ferrocenyl couples of compounds **[22]** and **[23]**.

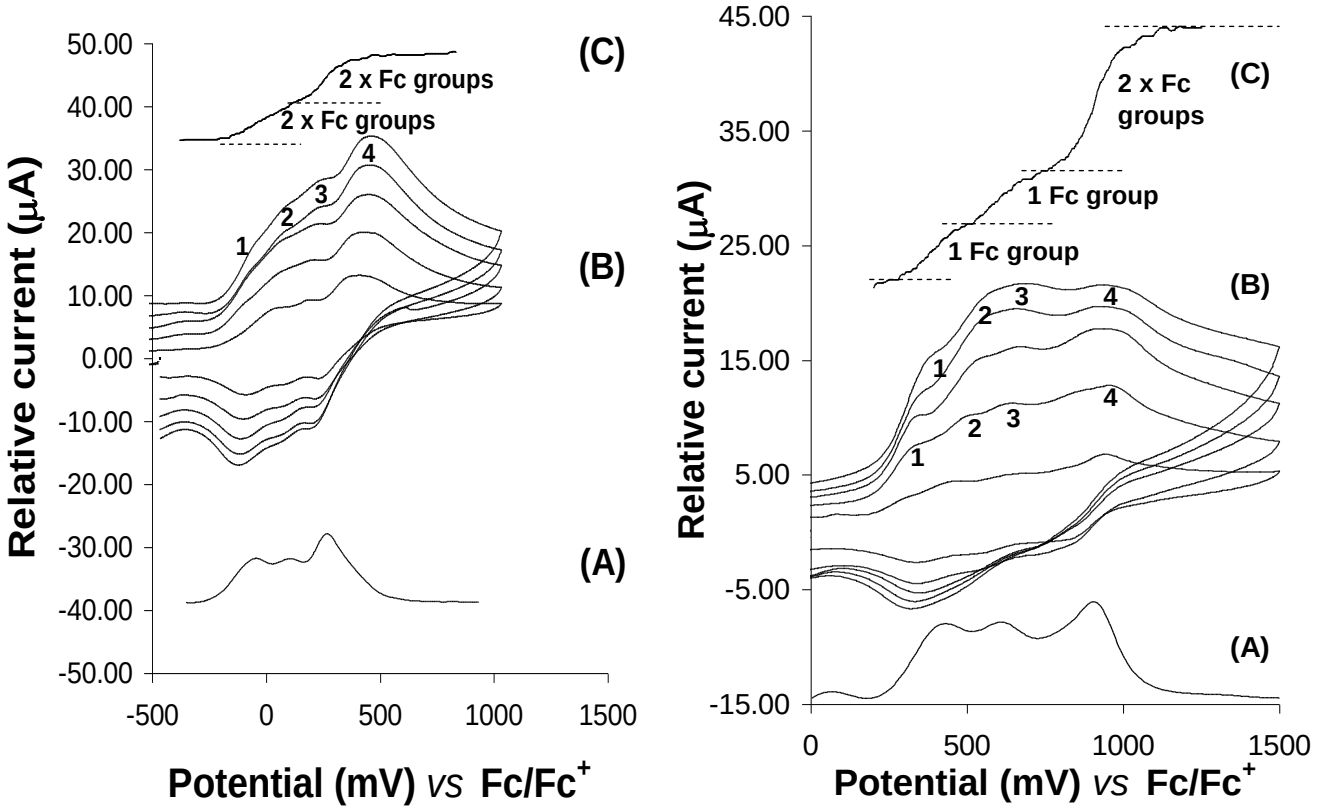

Figure 3.33. **(A)** Oster Young Square wave voltammogram, **(B)** Cyclic voltammograms at scan rates 100, 200, 300, 400 and 500 mV s^{-1} and **(C)** Linear sweep voltammogram of ferrocenyl portion of Left: [FcCOCHCOCH$_3$)$_2$Ti(O-CH(CH$_3$)-Fc)$_2$] **[22]** and Right: [FcCOCHCOCF$_3$)$_2$Ti(O-CH(CH$_3$)-Fc)$_2$] **[23]** (LSV current magnified 5 X).

Table 3.17. The cyclic voltammetry data obtained from voltammograms (*vs.* Fc/Fc^{+}) of various Di(1-oxyethyl-1-ferrocenyl)bis(β-diketonato)titanium(IV) complexes $[(FcCOCHCOR)_2Ti(O\text{-}CH\text{-}(CH)\text{-}Fc)_2]$, where R = Ph **[21]**, CH_3 **[22]** and CF_3 **[23]** measured in 0.1 mol dm^{-3} $[NBu_4][B(C_6F_5)_4]$ /CH_2Cl_2 with a glassy carbon working electrode at 25ºC and a scan rate of 50 mV s^{-1}. The concentration of for all complexes was 1.0 mmol.dm^{-3}.

v/ mV.s^{-1}	ΔE_p / mV	$E^{0/}$ / mV	i_{pa}/i_{pc}	ΔE_p / mV	$E^{0/}$ / mV	i_{pa}/i_{pc}	ΔE_p / mV	$E^{0/}$ / mV	i_{pa}/i_{pc}	ΔE_p / mV	$E^{0/}$ / mV	i_{pa}/i_{pc}	E_{pc} / mV Ti^{4+}/Ti^{3+}
	Peak 1			Peak 2			Peak 3			Peak 4			
$[(FcCOCHCOCH_3)_2Ti(O\text{-}CH(CH_3)\text{-}Fc)_2]$ [22]													
50	114	-27	0.65	105	28	0.68	92	127	0.86	120	284	1.33	-2314
100	120	-30	0.69	106	30	0.70	100	130	0.84	124	280	1.30	-
200	133	-29	0.65	119	31	0.72	111	128	0.85	133	283	1.35	-2344
300	142	-31	0.70	130	29	0.69	123	131	0.69	142	287	1.05	-2344
400	151	-28	0.70	136	32	0.73	134	129	0.88	149	289	1.33	-2259
500	162	-32	0.75	141	33	0.76	142	128	0.75	152	285	1.10	-
$[(FcCOCHCOCF_3)_2Ti(O\text{-}CH(CH_3)\text{-}Fc)_2]$ [23]													
50	102	-59	0.30	96	95	0.55	102	140	0.83	108	410	1.80	-2354
100	112	-59	0.35	98	100	0.50	109	137	0.86	112	434	1.85	-2305
200	119	-63	0.33	100	101	0.70	123	141	0.76	139	489	1.91	-
300	132	-60	0.34	112	99	0.55	129	152	0.88	121	501	1.95	-
400	140	-62	0.35	119	105	0.61	135	149	0.90	154	513	1.97	-
500	149	-64	0.37	130	121	0.64	152	148	0.90	162	532	2.01	-

In complexes **[22]** and **[23]** there are five redox active centres. The first is the Ti^{4+}/Ti^{3+} couple, which is an electrochemically irreversible process. An interesting point that can be seen in **Figures 3.32** (left) is that the Ti reduction peak is very large. The shape of this reduction wave is typical of excessive electrode deposition taking place. The other four poorly resolved waves are from the ferrocenyl groups of the two $(O\text{-}CH(CH_3)\text{-}Fc)$ axial ligands and the two ferrocenyl groups of the β-diketonato ligands. These four processes are associated with peaks **1 - 4** in **Figure 3.32** (right) and **figure 3.33**. On the cathodic half wave, peaks 1 – 4 overlap to different degrees at different scan rates. All are electrochemically quasi-reversible since $\Delta E > 90$ mV and chemically reversible, i_{pa}/i_{pc} approaches 1. **(A)** depicts the Oster Young square voltammograms for compounds **[22]** and **[23]**, which clearly shows the alkoxy peaks which are unequivalent yet equal in magnitude. The larger β-diketonato ferrocenyl peaks are also clearly visible; although in the Oster Young square voltammograms they overlap to a very large extent making them indistinguishable from one another.

The electrochemical portion of this study was by far the most challenging and exciting part of this research. Countless late nights lead to many interesting and novel findings.

3.5. Cytotoxic results

3.5.1. Introduction

The complexes of this study were synthesised with the purpose of investigating their physical properties, but also to investigate possibilities of their application in terms of anticancer activity. The latter was probed by determining the cytotoxicity of selected compounds against cancer cells. Mrs. Margo Nell of the Department of Pharmacology at the University of Pretoria is acknowledged for performing the cytotoxic tests and for constructing the survival curves of the obtained results. The cytotoxicity of ferrocene-containing titanium(IV) compounds of the type $[Cp_2Ti(FcCOCHCOR)]^+ClO_4^-$ **[12] – [15]** & **[17]**, were determined by observing their effects *in vitro* on cultured HeLa (a human cervix epitheloid cancer) and CoLo (a human colorectral) cell lines for 1 and/or 7 days of continued drug exposure. After incubation at 37°C, cell survival was measured as a percentage of living cells in relation to a control that was not exposed to the drug. This was done by means of the colorometric 3-(4,5-dimethylthiazol-2-yl)-diphenyltetrazodium bromide (MTT) assay. Survival curves indicate percentage cell survival plotted as a function of drug dose, with concentration expressed in μmol.dm^{-3}. IC_{50} values (drug dose required for 50% cell death) were estimated by extrapolation. As the new complexes in this study were derived from titanocene dichloride, a drug which is currently in phase II clinical trials, the IC_{50} value under our testing conditions for $[Cp_2TiCl_2]$ was determined for reference purposes. Survival curves are shown in **Figure 3.34**, the IC_{50} values obtained from these curves were 39.37 μmol.dm^{-3} for HeLa and 84.51 μmol.dm^{-3} for CoLo cells respectively (see also **Table 3.18**).

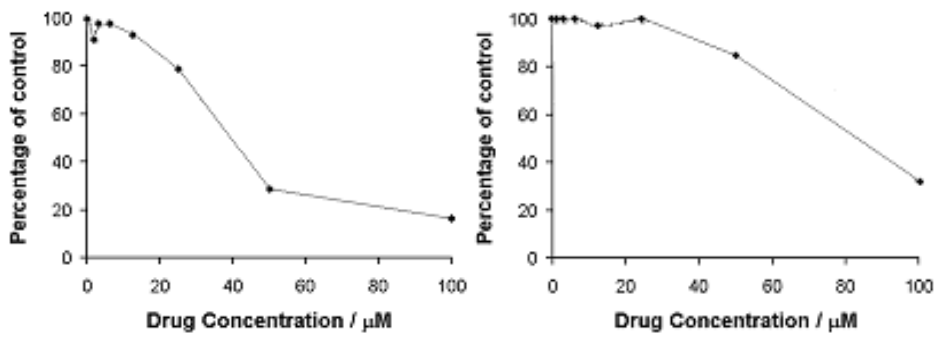

Figure 3.34. Plots of percentage survival curves for HeLa (left) and CoLo (right) cells against concentration (μmol.dm^{-3}) of titanocene dichloride $[Cp_2TiCl_2]$, currently in Phase II clinical trials.

3.5.2. Cytotoxicity of $[Cp_2Ti(FcCOCHCOR)]^+ClO_4^-$ complexes

The chloride ligands of $[Cp_2TiCl_2]$ were substituted with various β-diketonates to give $[Cp_2Ti(FcCOCHCOR)]^+ClO_4^-$ derivatives. The results of the cytotoxic analysis are summarised in **Table 3.18**. Complex $[Cp_2Ti(FcCOCHCOFc)]^+ClO_4^-$ **[15]** could not be used in the survey due to difficulties dissolving the compound in appropriate concentrations. As the IC_{50} value represents the concentration needed for the potential drug to produce 50% cell death, the lower this value, the better. The cytotoxic reactivity of the titanocene complexes increased approximately three - seven times for the HeLa cells and two - six times for the CoLo cells as compared to $[Cp_2TiCl_2]$, (**Table 3.18** and **Figure 3.35**).

Table 3.18. IC_{50} values of mono-β-diketonato titanium complexes of the type $[Cp_2Ti(FcCOCHCOR)]^+ClO_4^-$, in *in vitro* cancer cells after 7 days incubation utilising HeLa and CoLo cell lines. χ_R and IC_{50} values for the free β-diketonate are also given.

Titanium complex	**No.**	**IC_{50} ($\mu mol.dm^{-3}$)**		**Free β-diketonato Ligand**	**χ_R**	**IC_{50} ($\mu mol.dm^{-3}$)**	
		HeLa	**CoLo**			**HeLa**	**CoLo**
$[Cp_2TiCl_2]$	**[3]**	84.5	39.4	-	-	-	-
$[Cp_2Ti(FcCOCHCOPh)]^+ClO_4^-$	**[12]**	25.8	16.8	$[FcCOCH_2COPh]$	2.21	54.2	85.1
$[Cp_2Ti(FcCOCHCOCH_3)]^+ClO_4^-$	**[13]**	12.6	6.5	$[FcCOCH_2COCH_3]$	2.34	66.6	57.1
$[Cp_2Ti(FcCOCHCOCF_3)]^+ClO_4^-$	**[14]**	11.4	14.1	$[FcCOCH_2COCF_3]$	3.01	6.8	7.3
$[Cp_2Ti(FcCOCHCOFc)]^+ClO_4^-$	**[15]**	…[a]	…[a]	$[FcCOCH_2COFc]$	1.87	54.2	64.3
$[Cp_2Ti(FcCOCHCORc)]^+ClO_4^-$	**[17]**	16.2	38.4	$[FcCOCH_2CORc]$	1.94	54.7	67.4
Cisplatin	-	2.3	4.9	-	-	-	-

[a] Solubility was too low, IC_{50} values could not be determined.

The best results were obtained for the $[Cp_2Ti(FcCOCHCOCH_3)]^+ ClO_4^-$ complex, against CoLo cells. IC_{50} values decreased from 84.51 (Cp_2TiCl_2) to 12.614 $\mu mol.dm^{-3}$ for HeLa cells and from 39.37 for titanocene dichloride to 6.483 $\mu mol.dm^{-3}$ for CoLo cells.

This is in contrast to reports by Keppler and Heim, whose findings suggest that the titanocene complex with a β-diketonato ligand containing an aromatic (phenyl) group should in fact be most effective against cancer cells.[23] Keppler and Heim, however, did not study any complexes where the β-diketonato ligand contained a ferrocenyl group.

The higher cytotoxicity of $[Cp_2Ti(\beta\text{-diketonato})]^+$ complexes is not attributable to the ClO_4^- counter anion, separate tests utilising $NaClO_4$ as cytotoxic agent, showed $[NaClO_4]$ has IC_{50} values substantially higher than those of the titanocenyl derivatives ($IC_{50,\ NaClO4} > 100\ \mu mol.dm^{-3}$).

No clear cytotoxic trend could be linked to the group electronegativity of the R-group of the $[Cp_2Ti(FcCOCHCOCH_3)]^+\ ClO_4^-$ complexes. The general trend appears to be, an increase in group electronegativity of the R-group on the β-diketonato ligand, leads to an decrease in IC_{50} values (**Figure 3.35**).

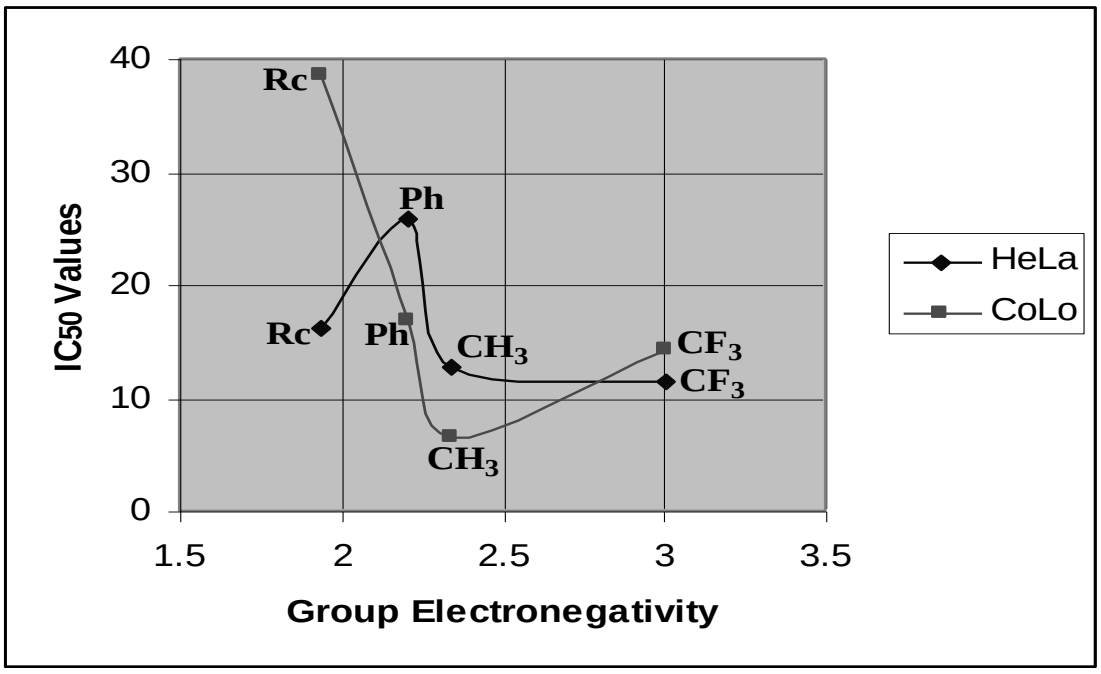

Figure 3.35. Graph of IC_{50} values of HeLa and CoLo cells *vs.* group electronegativity of the R-groups of the β-diketonato ligand in $[Cp_2Ti(FcCOCHCOR)]^+ClO_4^-$, R = Rc, Ph, CH_3 and CF_3.

Cisplatin [$Pt(NH_3)_2Cl_2$] has long been considered the benchmark when it comes to metal-containing antineoplastic compounds. None of the complexes tested here were as effective as cisplatin in killing cancer cells. Although, as an anti-cancer drug, cisplatin suffers from many detrimental side effects (including extreme nephrotoxicity) limiting its clinical use.

Titanium complexes such as titanocene dichloride [Cp_2TiCl_2] are known to exhibit far less harmful side effects than cisplatin. The present class of compounds are therefore also expected to have less toxic side effects. This is currently under investigation. All tested [$Cp_2Ti(\beta\text{-diketonato})]^+ClO_4^-$ complexes showed enhanced cytotoxic activity when compared with titanocene dichloride (currently in stage II clinical trials) see **Table 3.18**. In separate studies performed in this laboratory, IC_{50} for the free β-diketones were determined. Results are shown in **Table 3.18**, with the exception of the CF_3-containing
β-diketone, all the Ti complexes showed increased cytotoxicity.

This is a clear indication that a combination of more than one type of antineoplastic moiety in the same molecule. Here, titanium and the iron-containing ferrocenyl group leads to enhanced anti-cancer activity.

Multidrug resistance by cancer cells is another problem encountered by potential anti-cancer drugs. Each of the drug fragments are expected to have differing mechanisms of action, therefore potentially making this series of drugs less prone to resistance build up. Further research is required to clarify the exact mechanism by which the titanocenyl fragment attacks and destroys cancer cells. The ferrocenyl group was shown to operate *via* a free radical mechanism.[24]

Furthermore, the ionic nature of the complexes increases aqueous compatibility. Any drug that can be dissolved in the body's aqueous environment will ultimately be beneficial with respect to administrative techniques.

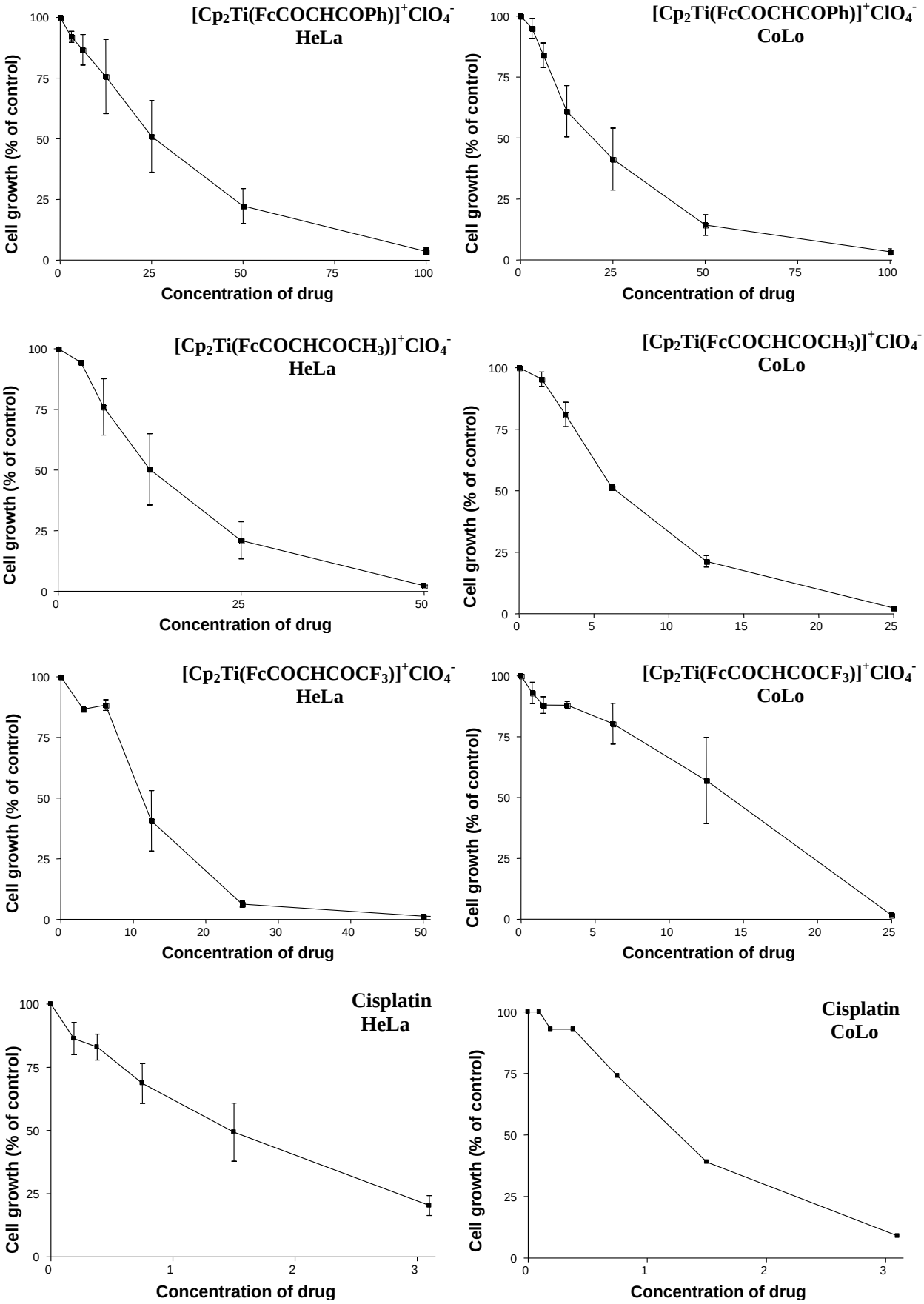

Figure 3.36. Plots of percentage survival of cells for HeLa (left) and CoLo (right) against concentration (μmol.dm^{-3}) of selected mono-β-diketonato titanium(IV) complexes.

Comparison of the electrochemical data with the IC_{50} values revealed no direct relationship but the general trend, for non phenyl-group-containing complexes, appears to be that as the formal reduction potential for the ferrocenyl group ($E^{0/}$) increases the IC_{50} decreases.

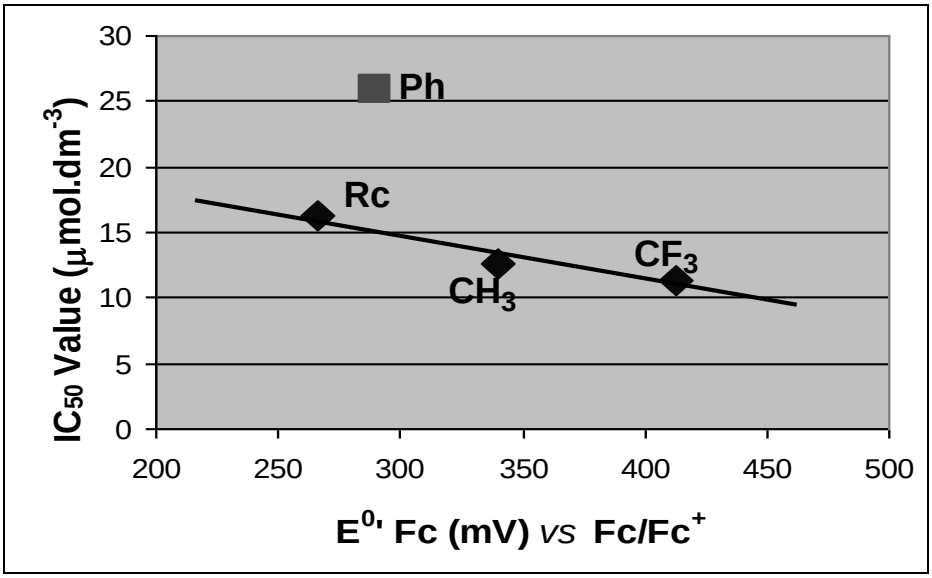

Figure 3.37. Graph of IC_{50} values of HeLa cells *vs.* $E^{0/}$ ferrocenyl group of the $[Cp_2Ti(FcCOCHCOR)]^+ClO_4$ complexes, where R = Rc, Ph, CH_3 and CF_3.

Since no clear trend between IC_{50} values for CoLo and HeLa cells and $E^{0/}$ values for the Ti^{4+}/Ti^{3+} couple could be identified in complexes of the type $[Cp_2Ti(\beta\text{-diketonato})]^+ClO_4^-$ either, doubt exists as to whether an electron transfer mechanism is very dominant in the mechanism of action of these particular complexes. It is more likely that the leaving capabilities of the β-diketonato ligand are so much better than that of the Cl^- ligands in $[Cp_2TiCl_2]$, that the β-diketonato complexes may operate at least in part by a substitution mechanism with DNA. This possibility is currently under investigation in this laboratory.

The heightened cytotoxicity of these complexes could therefore be traced to synergistic effects between the two cytotoxic moieties of each molecule.

In conclusion, the ferrocene-containing mono-β-diketonato titanium(IV) series show promise as anti-cancer agents, but further testing is required to evaluate their potential use in cancer clinics.

3.6. References

[1] W.R. Cullen, S.J. Rettig and F.B. Wickenheiser, *J. Mol. Catal.*, 251, **66** (1991).

[2] W.C. du Plessis, T. Vosloo and J.C. Swarts, *J.C.S. Dalton Trans.*, 2507 (1998).

[3] A.H. Lowrey, P.D. D'Antonio and J. Karle, *J. Am. Chem. Soc.*, 6399, **93** (1971).

[4] W.C. du Plessis, W.L. Davis, S.J. Cronje and J.C. Swarts, *Inorg. Chim. Acta*, 97**, 314** (2000).

[5] G. Doyle and R.S. Tobias, *Inorg. Chem.*, 1111, **6** (1967).

[6] K.C. Kemp, J.C. Swarts, Unpublished results (2004).

[7] P.C. Bharara, *J. Organomet. Chem.*, 199, **121** (1976).

[8] R.C. Weast, Editor, *Handbook of Chemistry and Physics*, 65th Edition, CRC Press, Boca Raton, Florida, p F-176 (1984).

[9] R.C. Fay and R.N. Lowry, *J. Inorg. Chem.*, **8**, 1512 (1967).

[10] K.F. Purcell and J.C. Kotz, *Inorganic Chemistry*, Holt-Saundres International Editions, Everbest Printing Co.,Ltd., Hong Kong, p 883 (1977).

[11] http://wulfenite.fandm.edu/Data%20/Table_6.html

[12] Ferguson, G., Glidewell, C. and Zakaria, C.M., *Acta Cryst.*, 1673, **C50** (1994).

[13] K. Prout, T.S. Cameron, R.A. Forder, S.R. Critchley, B. Denton and G.V. Rees, *Acta Crystllogr., Sect B*, 2290, **30** (1974).

[14] A.M. Bond, R. Colton, U. Englert, H. Hugel and F. Marken, *Inorg. Chim. Acta.*, 117, **235** (1995).

[15] N. El Murr, A. Chaloyard and J. Tirouflet, *J. Chem. Soc. Chem. Comm.*, 446 (1980).

[16] S. Trupia, A. Nafady and W.E. Geiger, *Inorg. Chem. Comm.*, 5480, **42** (2003).

[17] M.G. Hill, W.M. Lamanna and K.R. Mann, *Inorg. Chem.*, 4690, **30** (1991).

[18] M.W. Droege, W.D. Harman and H. Taube, *Inorg. Chem.*, 1309, **26** (1987).

[19] J.C. Swarts, Unpublished results.

[20] P.T.N. Nonjola, Unpublished results (2006).

[21] E. Erusmus, J.C. Swarts, Unpublished results (2005).

[22] R.S.P. Coutts and P.C. Wailes, *Aust. J. Chem.*, 1547, **22** (1969).

[23] B.K. Keppler and M.E. Heim, *Drugs of the Future*, 638, **3** (1988).

[24] D. Osella, M. Ferrali, P. Zanello, F. Laschi, M. Fontani, C. Nervi and G. Cavigiolio, *Inorg. Chim. Acta*, 42, **306** (2000).

Chapter 4

Experimental

4.1. Introduction

This chapter describes the chemicals, apparatus as well as techniques (experimental procedures and reaction conditions) utilized to obtain data for chapter 3.

4.2. Materials and Techniques

4.2.1. Chemicals

Ferrocene (Strem) and most other solid reagents (Merck, Aldrich) were employed directly without further purification. Liquid reagents and solvents were distilled prior to use. Water was doubly distilled. Organic solvents (ether, hexane, DCM and $CHCl_3$) were dried according to published procedures[1] and distilled directly before use. Reactions requiring an inert atmosphere were performed in either nitrogen or argon by using standard Shlenk techniques and vacuum-line methods. Column chromatography was performed on Kieselgel 60 (Merck, grain size 0.063-0.2 mm, eluent ether/hexane 2:3 by volume).

4.2.2. Characterization

Melting points (m.p.) were determined with a Reichert Thermopan microscope with a Koffler hot-stage and are uncorrected. The instrument can only detect melting points lower than or equal to 200°C. All ^1H NMR spectra were recorded in deuterated solvents on a Bruker Advance DPX 300 NMR spectrometer at 289 K. Chemical shifts were presented as δ-values, referenced to $SiMe_4$ at 0.00 parts per million (ppm).

4.3. Synthesis

4.3.1. Precursors for ferrocene-containing β-diketones

4.3.1.1. Acetylferrocene [$FcCOCH_3$], [4]

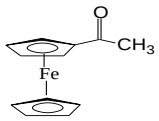

Ferrocene (9.3g / 0.05 mol) and acetic anhydride (40 cm^3) were added to a beaker and stirred for 12 minutes. Phosphoric acid 85% (5 cm^3) was then added drop wise. The exothermic reaction was kept between 100-105˚C for 10 minutes. The mixture was then cooled to 80˚C, poured over ice and left to stand over-night (16 hrs). The solution was first neutralized and then brought to pH 10 with cold NaOH solution (20 $mol.dm^{-3}$). The resulting orange/brown pasty mass was cooled in an ice bath and filtered with water. The crude tan/brown product was washed with water (3 x 100 cm^3 portions) and allowed to air dry. Recrystallization from hexane gave solid orange product in 84% (9.6 g) yield. M.p. 85-86˚C; δ_H(300MHz, $CDCl_3$)/ppm 2.41 (s, 3H, CH_3), 4.22 (s, 5H, C_5H_5), 4.52 (t, 2H, ½ x C_5H_4) and 4.80 (t, 2H, ½ x C_5H_4).

4.3.1.2. Methyl ferrocenoate, ($FcCOOCH_3$), [5]

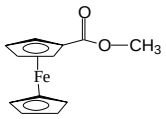

Ferrocenoic acid was prepared with the 2-chlorobenzoylchloride method as described in published results.[2] Ferrocenoic acid (1.7 g / 5.98 mmol) was then esterified by refluxing in methanol (100 cm^3) in the presence of concentrated H_2SO_4 (0.04 cm^3), under a nitrogen atmosphere, for 48 hrs. The resulting liquid was poured over ice (150 g) and extracted with ether (3 x 100 cm^3 portions). The combined ether extracts were washed with water, aqueous NaOH (0.5 $mol.dm^{-3}$) and again with water. The solution was then dried over $NaSO_4$ and the solvent removed under reduced pressure to give solid tan product[3] in 81.4% (1.19 g) yield. M.p. 69˚C; δ_H(300MHz, $CDCl_3$)/ppm 3.82 (s, 3H, OCH_3), 4.22 (s, 5H, C_5H_5), 4.41 (t, 2H, ½ x C_5H_4) and 4.8 (t, 2H, ½ x C_5H_4).

4.3.1.3. Acetylruthenocene, ($RcCOCH_3$), [6]

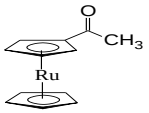

Ruthenocene (1.156 g / 5 mmol) and acetic anhydride (10 cm^3) were added to a beaker and stirred for 1 hour. Phosphoric acid 85% (0.5 cm^3) was then added drop wise. The exothermic reaction was kept between 100-105˚C for 2 hrs. The mixture was then cooled to 80˚C, poured over ice and left to stand 48 hrs. The solution was first neutralized and then brought to pH 10 with cold NaOH solution (20 $mol.dm^{-3}$). The resulting yellow/brown pasty mass was cooled in an ice bath and filtered with water. The crude tan product was washed with water (3 x 100 cm^3 portions) and allowed to air dry. Recrystallization from hexane gave solid yellow product in 36% (0.494 g) yield. M.p. 85-86˚C; δ_H(300MHz, $CDCl_3$)/ppm 2.30 (s, 3H, CH_3), 4.59 (s, 5H, C_5H_5), 4.78 (t, 2H, ½ x C_5H_4) and 5.09 (t, 2H, ½ x C_5H_4).

4.3.2. Ferrocene-containing β-diketones

4.3.2.1. 1-ferrocenyl-3-phenyl-1,3-propanedione, [$FcCOCH_2COPh$], [7]

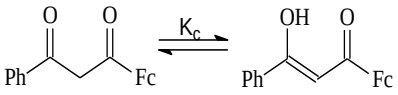

The lithium diisopropylamide method: Rigorous Schlenk conditions were adhered to. Lithium diisopropylamide ($LiNPr^i_2$) solution (l cm^3 / 1.8 $mol.dm^{-3}$) was added to a solution of acetylferrocene (0.39 g / 1.7 mmol) in THF (2 cm^3) and stirred at room temperature for 30 min before dry methyl benzoate (0.34 g / 2.5 mmol) was added. Stirring of the resulting reaction mixture continued for 16 hrs before the β-diketonate salt was precipitated with ether/hexane 3:2 (5 cm^3). The precipitate was then separated by suction filtration. Both portions (precipitate and filtrate) were immediately shaken with HCl (50 cm^3 / 0.5 $mol.dm^{-3}$) and extracted with ether/hexane 3:2 (5 x 80 cm^3). The combined ether extracts were thoroughly washed with water, dried ($MgSO_4$) and the solvent removed under reduced pressure.

Flash chromatography of the residue (R_f = 0.58) afforded [$FcCOCH_2COCPh$] in yields of 30% (0.17 g); (Found: Fe, 16.6. $C_{19}H_{16}FeO_2$ requires 16.81%); m.p. 107^{0}C (lit.,[4] 106 - 107 ^{0}C); ν_{max}(KBr)/cm^{-1} 1640 and 1710 (C=O); δ_H(300 MHz, $CDCl_3$)/ppm: keto form - 3.91 (s, 2H, CH_2), 4.13 (s, 5H, C_5H_5), 4.53 (t, 2H, ½ x C_5H_4), 4.85 (t, 2H, ½ x C_5H_4); enol form - 4.23 (s, 5H, C_5H_5), 4.58 (t, 2H, ½ x C_5H_4), 4.91 (t, 2H, ½ x C_5H_4), 6.40 (s, 1H, CH) and 7.48 - 7.53, 7.89 - 8.16 (m, 5H, C_6H_5) keto / enol forms indistinguishable; K_c = 10.4.

4.3.2.2. 1-ferrocenylbutane-1,3-dione, [$FcCOCH_2COCH_3$], [8]

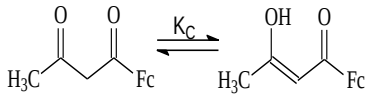

[$FcCOCH_2COCH_3$] was prepared in yields up to 35% (0.16 g) according to *the lithium diisopropylamide method* as described for [$FcCOCH_2COPh$], by replacing methyl benzoate with dried ethyl acetate (0.19 g / 2.5 mmol); (Found: Fe, 20.6. $C_{14}H_{14}FeO_2$ requires 20.68%); m.p. 98 ^{0}C; (lit.,[5] 97 – 97.5 ^{0}C); ν_{max}(KBr)/cm^{-1} 1620 (C=O); δ_H(300 MHz, $CDCl_3$)/ppm: Keto form - 2.32 (s, 3H, CH_3), 3.85 (s, 2H, CH_2), 4.25 (s, 5H, C_5H_5), 4.60 (t, 2H, ½ x C_5H_4), 4.81 (t, 2H, ½ x C_5H_4); enol form - 2.10 (s, 3H, CH_3), 4.22 (s, 5H, C_5H_5), 4.52 (t, 2H, ½ x C_5H_4), 4.80 (t, 2H, ½ x C_5H_4), and 5.74 (s, 1H, CH); K_c = 3.4.

4.3.2.3. 1-ferrocenyl-4,4,4-trifluorobutane-1,3-dione, [$FcCOCH_2COCF_3$], [9]

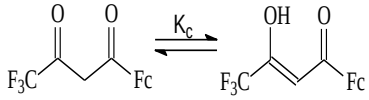

Once again *the lithium diisopropylamide method* was utilised. Equivalents remained unchanged, however, a larger scale reaction was attempted. $LiNPr^i_2$ solution (2 cm^3 / 3.6 mmol) was added to acetylferrocene (0.78 g / 3.5 mmol) in THF (4 cm^3) ice cooled solution. After 30 minutes stirring at room temperature, dry ethyl-triflouracetate (0.71 g / 5 mmol) was added dropwise. This solution was left to stir for 16 hrs after which the product was acquired in the usual way. Recrystallisation with hexane afforded spectroscopically pure maroon [$FcCOCH_2COCF_3$] crystals, yield 40% (0.46 g); (Found: Fe, 17.3. $C_{14}H_{14}F_3FeO_2$ requires 17.23%); m.p. 102^{0}C; ν_{max}(KBr)/cm^{-1} 1620 (C=O); δ_H(300

MHz, $CDCl_3$)/ppm: keto form - 4.34 (s, 5H, C_5H_5), 4.68 (t, 2H, ½ x C_5H_4), 4.83 (t, 2H, ½ x C_5H_4), 6.07 (s, 2H, CH_2); enol form - 4.25 (s, 5H, C_5H_5), 4.70 (t, 2H, ½ x C_5H_4), 4.88 (t, 2H, ½ x C_5H_4) and 6.11 (s, 1H, CH); K_c = 30.

4.3.2.4. 1,3-diferrocenylpropane-1,3-dione, [FcCOCH$_2$COFc], [10]

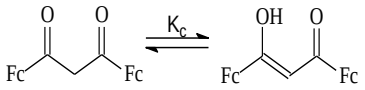

Rigorous Schlenk conditions were applied. A light yellow $LiNPr^i_2$ solution (0.5 cm^3 / 0.9 mmol) was added to an ice-cooled solution of acetylferrocene (0.23 g / 1.0 mmol) in THF (2.5 cm^3) and stirred at room temperature for 30 minutes. To this a solution of methyl ferrocenoate (0.36 g / 1.5 mmol) dissolved in THF (2.5 cm^3) was added. Stirring of the resulting reaction mixture continued for 18 hrs before it was shaken with HCl (50 cm^3 / 0.5 mol dm^{-3}) and immediately extracted with ether (5 x 50 cm^3 portions). The combined ether extracts were thoroughly washed with water, dried ($MgSO_4$) and the solvent removed under reduced pressure. Flash chromatography of the residue (R_f = 0.54) afforded [FcCOCH$_2$COFc] in 26% (0.12 g) yield. (Found: Fe, 25.2. $C_{23}H_{20}Fe_2O_2$ requires 25.38%); m.p. 157 ^{0}C; ν_{max}(KBr)/cm^{-1} 1640 and 1710 (C=O); δ_H(300 MHz, $CDCl_3$)/ppm: keto form – 4.21 (s, 10H, 2 x C_5H_5), 4.58 (t, 4H, 2 x (½ x C_5H_4)), 4.95 (t, 4H, 2 x (½ x C_5H_4)), 4.11 (s, 2H, CH_2); enol form - 4.22 (s, 10H, 2 x C_5H_5), 4.53 (t, 4H, 2 x (½ x C_5H_4)), 4.85 (t, 4H, 2 x (½ x C_5H_4)) and 5.99 (s, 1H, CH); K_c = 2.0.

4.3.2.5. 1-ferrocenyl-3-ruthenocenylpropane-1,3-dione, [FcCOCH$_2$CORc], [11]

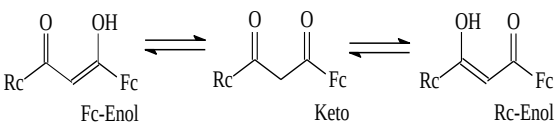

The reaction was performed under rigorous Schlenk conditions with an inert N_2 atmosphere maintained throughout. Lithium diisopropylamide solution (0.5 cm^3 / 0.9 mmol) was added to an ice-cooled solution of acetylruthenocene (0.15 g / 0.55 mmol) in THF (2.5 cm^3) and stirred at room temperature for 30 minutes. To this a solution of methyl ferrocenoate (0.30 g, 1.2 mmol) dissolved in THF (2.5 cm^3) was

added drop wise, over ice. Stirring of the resulting reaction mixture continued for 18 hrs before it was immediately shaken with HCl (50 cm^3, 0.5 mol dm^{-3}) and extracted with ether (5 x 50 cm^3 portions). The combined ether extracts were thoroughly washed with water, dried ($MgSO_4$) and the solvent removed under reduced pressure, affording the ferrocenyl-ruthenocenyl β–diketone, yield = 12% (0.03 g); (Found: C, 56.80; H, 4.16 $C_{23}FeH_{20}O_2Ru$ requires C, 56.77%; H, 4.14%); m.p.178°; δ_H (300MHz; $CDCl_3$)/ppm: Fc-enol form (48.43 %), 4.20 (s, 5H, C_5H_4 Fc), 4.51 (t, 2H, ½ x C_5H_4 Fc), 4.60 (s, 5H, C_5H_4 Rc), 5.19 (t, 2H, ½ x C_5H_4 Rc), 5.9 (s, 1H, CH); Rc-enol form (13.95 %), 3.99 (s, 5H, C_5H_4 Fc), 4.56 (s, 5H, C_5H_4 Rc), 4.72 (t, 2H, ½ x C_5H_4 Fc), 5.14 (t, 2H, ½ x C_5H_4 Rc); keto form (37.62%), 2.28 (s, 2H, CH_2), 4.23 (s, 5H, C_5H_5 Fc), 4.61 (s, 5H, C_5H_4 Rc), 5.10 (t, 2H, ½ x C_5H_4 Fc) and 5.24 (t, 2H, ½ x C_5H_4 Rc); K_c = 1.94.

4.3.3. Mono-β-diketonato titanium(IV) salts

4.3.3.1. 1-ferrocenyl-3-phenyl-1,3-propanedionato-κ^2O,O' bis-(η^5cyclopentadienyl) titanium(IV) perchlorate, $[Cp_2Ti(FcCOCHCOPh)]^+ClO_4^-$, [12]

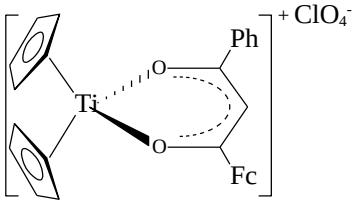

Dichlorobiscyclopentadienyltitanium(IV) (titanocene dichloride), (0.25 g / 1.0 mmol) was suspended in water/THF, 1:1 mixture (8 cm^3) and stirred, under nitrogen, in a black flask for an hour. Silver perchlorate (0.41 g / 1.98 mmol) dissolved in water (0.5 cm^3) was added and the mixture stirred for 40 minutes. Silver chloride, a white precipitate, was filtered off and washed with water/THF (2 cm^3). The bright yellow filtrate was cooled on an ice-bath and [$FcCOCH_2COPh$] (0.67 g / 1.50 mmol) dissolved in cold THF (1.5 cm^3, c.a. 4˚C) was added drop wise while stirring. The solution was left to stir for 3 hrs, after which the ox-blood red precipitate was filtered off and washed with water and ether. Recrystallisation from DCM/hexane afforded purple product. Yield 35% (0.22 g); m.p. >200^0C; δ_H(300 MHz, acetone-d_6)/ppm 4.49 (s, 5H, C_5H_5 Fc), 4.92 (t, 2H, ½ x C_5H_4 Fc), 5.30 (t, 2H, ½ x C_5H_4 Fc), 7.02 (s, 10H, 2 x C_5H_4 Cp_2Ti), 7.32 (s, 1H, CH), 7.60-7.71 (d of t) and 8.18 (d) (5H, $C_6H_5^-$).

4.3.3.2. 1-Ferrocenoyl-1,3-butanedionato-κ^2O,O'-bis(η^5-cyclopentadienyl) titanium(IV) perchlorate, $[Cp_2Ti(FcCOCHCOCH_3)]^+ClO_4^-$, [13]

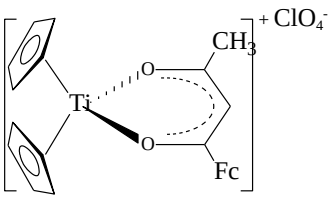

Titanocene dichloride (0.18 g / 0.717 mmol) was suspended in water (6 cm^3) and stirred under nitrogen for 1 hr. Silver perchlorate (0.3 g / 1.42 mmol) was added and the mixture was stirred for 30 minutes. Silver chloride (white precipitate) was filtered off and washed with water (2 cm^3). The filtrate was cooled on an ice-bath and ferrocenoylacetone (0.15 g / 0.717 mmol) dissolved in cold THF (1.5 cm^3, c.a. 4˚C) was added drop wise while stirring. A red-brown precipitate formed immediately, which was filtered off and washed with water and ether. Yield 46% (0.15 g); (Found C, 52.7%, H 4.2% and found C, 53.5%, H 4.4%); m.p. >200˚C; *v* (C=O)/cm^{-1} = 1509; δ_H(300 MHz, acetone-d_6)/ppm 2.28 (s, 3H, CH_3), 4.41 (s, 5H, C_5H_5 Fc), 4.84 (s, 2H, ½ x C_5H_4 Fc), 5.08 (s, 2H, ½ x C_5H_4 Fc), 6.65 (s, 1H, CH) and 6.93 (s, 10H, 2 x C_5H_5 Cp_2Ti)..

4.3.3.3. 1-ferrocenyl-4,4,4-trifluoro-1,3-butanedionato-κ^2O,O'-bis(η^5cyclopentadienyl) titanium(IV) perchlorate, $[Cp_2Ti(FcCOCHCOCF_3)]^+ClO_4^-$, [14]

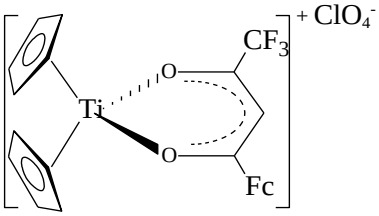

Titanocene dichloride (0.25 g / 1mmol) was dissolved in water (5 cm^3) and stirred for 90 minutes. Silver perchlorate (0.4 g / 1.98 mmol) dissolved in water (1 cm^3) was added and the mixture was left to stir at room temperature for 30 minutes. The resulting bright orange liquid was filtered to remove silver chloride and washed with a water/THF 2:3 mixture (2 cm^3). [$FcCOCHCOCF_3$] was dissolved in THF (5 cm^3) then quickly added to the titanocene solution. The reaction vessel was loosely covered and left to stir for 3 hrs. Water (100 cm^3) was added, the solid was allowed to settle and the liquid decanted. The crude product was washed with ether (4 x 50 cm^3portions), dissolved in DCM (10 cm^3) and recrystallised with ether (≈ 200 cm^3) to afford the navy blue product in 35% (0.21 g) yield; m.p. >200^0C; δ_H(300 MHz, acetone-d_6)/ppm 4.57 (s, 5H, C_5H_5 Fc), 5.17 (t, 2H, ½ x C_5H_4 Fc), 5.36 (t, 2H, ½ x C_5H_4 Fc), 6.92 (s, 1H, CH) and 7.09 (s, 10H, 2 x C_5H_5 Cp_2Ti).

4.3.3.4. 1,3-diferrocenylpropane-1,3-dionato-κ²O,O'-bis-(η⁵cyclopentadienyl) titanium(IV) perchlorate, [Cp₂Ti(FcCOCHCOFc)]⁺ClO₄⁻, [15]

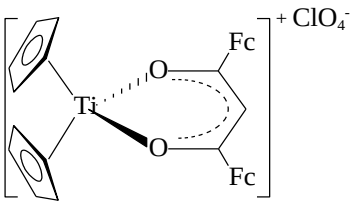

Titanocene dichloride (0.25 g / 1 mmol) was added to water/THF 1:1 mixture (8 cm^3) in a blackened flask and stirred for 1 hr. A slight excess of silver perchlorate (0.41 g / 1.98 mmol) was dissolved in water (0.7 cm^3) then added to the ice cooled titanocene mixture. The resulting solution was left to stir for 40 minutes after which solid silver chloride was filtered off and washed with water/THF 1:1 (3 cm^3). [$FcCOCH_2COPh$] (0.67 g / 1.5 mmol) was dissolved in THF (8 cm^3) and added drop wise to the titanocene filtrate (c.a. 4˚C). The reaction mixture was left to stir for 16 hrs. Filtration yielded a dark brown solid, which was dissolved in DCM (8 cm^3) and precipitated with ether (200 cm^3) giving the purple/brown product in 25% (0.15 g) yield. M.p. >200^{0}C; δ_H(300 MHz, acetone-*d_6*)/ppm 4.41 (s, 10H, 2 x C_5H_5 Fc), 4.82 (H, 2 x (½ x C_5H_4) Fc), 5.19 (s, 2H, 2 x (½ x C_5H_4) Fc), 6.85 (s, 1H, CH) and 8.96 (s, 10H, 2 x C_5H_5 Cp_2Ti).

4.3.3.5. 2,4-Pentanedionato-κ²O,O'-bis-(η⁵-cyclopentadienyl)titanium(IV) perchlorate, [Cp₂Ti(CH₃COCHCOCH₃)]⁺ClO₄⁻, [16]

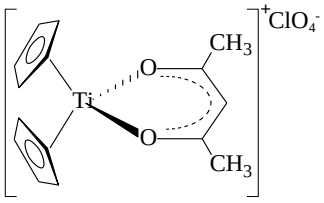

Titanocene dichloride (0.12 g, 0.48 mmol) was suspended in water (3 cm^3) and stirred under nitrogen for an hour. Silver perchlorate (0.198 g / 0.95 mmol) was added and the mixture was stirred for about 30 minutes maintaining a nitrogen atmosphere. Silver chloride (white precipitate) was filtered off and washed with water (2 cm^3). The filtrate was cooled on an ice-bath and cold acetylacetone (2 cm^3, c.a. 4˚C) was added drop wise while stirring. A grey-purple precipitate formed immediately, which was filtered off and washed with water and ether giving 86% (0.15 g) yield. M.p. >200˚C; *ν* (C=O)/cm^{-1} = 1524; δ_H(300 MHz, $CDCl_3$)/ppm 2.29 (s, 6H, 2 x CH_3), 6.14 (s, 1H, CH) and 6.73 (s, 10H, 2 x C_5H_5); δ_H(300 MHz, acetone-*d_6*)/ppm 2.32 (s, 6H, 2 x CH_3), 6.38 (s, 1H, CH) and 6.92 (s, 10H, 2 x C_5H_5).

4.3.3.5. 1-ferrocenyl-3-ruthenocenylpropane-1,3-dionato-κ^2O,O'-bis-(η^5cyclopentadienyl) titanium(IV) perchlorate, $[Cp_2Ti([FcCOCHCORc)]^+ClO_4^-$, [17]

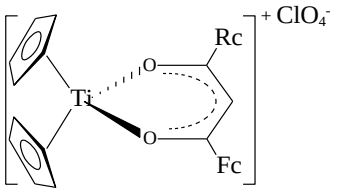

$[Cp_2Ti(CH_3COCHCOCH_3)]^+ClO_4^-$ (0.38 g / 1.0 mmol) and $[FcCOCH_2CORc]$ (0.27 g / 0.55 mmol) were dissolved in acetonitrile (50 cm^3). The solution was then refluxed for 3 hrs. At this point the condenser was removed and the solvent reduced to approx. 6 cm^3. Excess water (50 cm^3) was then added to precipitate the product. The precipitate was filtered off and washed with ether (3 x 50 cm^3portions). A solid, tan product was obtained, yield 20 % (0.085 g); m.p. 78^0C; δ_H(300 MHz, acetone-*d_6*)/ppm 4.40 (s, 5H, C_5H_5 Rc), 4.78 (s, 5H, C_5H_5 Fc), 4.80 (H, ½ x C_5H_4 Rc), 5.03 (H, ½ x C_5H_4 Fc), 5.12 (s, 2H, ½ x C_5H_4 Fc), 5.48 (s, 2H, ½ x C_5H_4 Rc), 6.78 (s, 1H, CH) and 6.93 (s, 10H, 2 x C_5H_5 Cp_2Ti).

4.3.4. Dichlorobis-β-diketonato titanium(IV) complexes

4.3.4.1. Dichlorobis-(1-ferrocenyl-3-phenyl-1,3-propanedionato) titanium(IV), $[(FcCOCHCOPh)_2TiCl_2]$, [18]

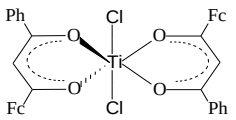

A N_2 atmosphere was maintained throughout the ensuing reaction and all glassware was flame dried. $[FcCOCH_2COPh]$ (0.44 g / 1.3mmol) was dissolved in dry DCM (5 cm^3). Titanium tetrachloride (0.1246 g / 0.65 mmol) was dissolved in dry DCM (2 cm^3) and added to the $[FcCOCH_2COPh]$ solution. The solution volume was then reduced to 1/3 by heating (NB! not N_2 evaporation) in a water bath. Excess dry hexane (100 cm^3) was then added to form a precipitate. The precipitate was then collected by filtration under N_2. Finally the bottle green product was obtained *via* recrystallisation from DCM/hexane. Yield 79% (0.4 g); m.p. >200^0C; δ_H(300 MHz, CD_3CN)/ppm 4.10–4.64 and 4.64–5.59 (m, 18H, 2 x Fc of different isomers), 7.27 (s, 2H, 2 x CH), 7.43–7.85 and 8.99–8.48 (m, 10H, 2 x $C_6H_5^-$).

4.3.4.2. Dichlorobis-(1-Ferrocenoyl-1,3-butanedionato) titanium(IV), [(FcCOCHCOCH$_3$)$_2$TiCl$_2$], [19]

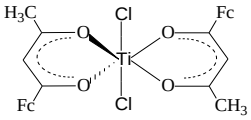

[FcCOCH$_2$COCH$_3$] (0.135 g / 0.5 mmol) was placed in a flame-dried flask and degassed with N_2 for 30 minutes. Dry DCM (3 cm^3) was added and stirring begun. [TiCl$_4$] (0.0475 g / 0.25mmol) was diluted in DCM (1 cm^3) and added to the solution. The solution volume was then reduced to approximately 1/3 by heating. Dry hexane (excess) was then added to form a precipitate. The solid product was then collected by filtration and washed with dry hexane under N_2. The emerald green product was immediately stored in an airtight container under argon. Yield 78% (0.128 g); m.p. >200^{0}C; δ_H(300 MHz, CD$_3$CN)/ppm 2.02–2.24 (m, 6H, 2 x CH$_3$), 4.14–4.59 and 4.70–5.22 (m, 18H, 2 x Fc of different isomers), 6.28–6.50 (m, 2H, 2 x CH of different isomers).

4.3.4.3. Dichlorobis-(1-ferrocenyl-4,4,4-trifluorobutane-1,3-dionato) titanium(IV), [(FcCOCHCOCF$_3$)$_2$TiCl$_2$], [20]

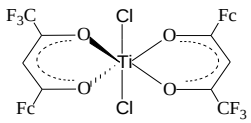

Throughout the reaction a flow of N_2 was maintained. [FcCOCH$_2$COCF$_3$] (0.162 g / 0.5 mmol) was placed in a flame dried three-neck flask, thereafter the flask and contents were degassed for 30 minutes. Dry / distilled DCM (5 cm^3) was added and stirred resulting in a very dark maroon colour. [TiCl$_4$] (0.1 g / 0.527 mmol) was dissolved in DCM (2 cm^3) and added to the [FcCOCH$_2$COCF$_3$] solution. After evaporating 2/3 of the solvent, with a hot water bath, excess dry hexane (50 cm^3) was added to precipitate the product. The solid was filtered under N_2 and washed with hexane. The product was blue-green, yield 72% (0.275 g); m.p. >200^{0}C; δ_H(300 MHz, CD$_3$CN)/ppm 3.72–4.66 and 4.66–5.57 (m, 18H, 2 x Fc of different isomers), 6.18–6.67 (m, 2H, 2 x CH of different isomers).

4.3.5. Di(1-oxyethyl-1-ferrocenyl)bis(β-diketonato)titanium(IV)Complexes

Reaction vessels where flame dried and all reactions were performed under N_2. The author acknowledges Prof. J. C. Swarts of the University of the Free State for providing ample quantities of the ferrocenyl alcohol 1-ferrocenylethan-1-ol ([$FcCH_3(CH)OH$]) used in the following syntheses.

4.3.5.1. Di(1-oxyethyl-1-ferrocenyl)bis(1-ferrocenyl-3-phenyl-1,3-)titanium(IV), [$(FcCOCHCOPh)_2Ti(O\text{-}CH\text{-}(CH_3)\text{-}Fc)_2$], [21]

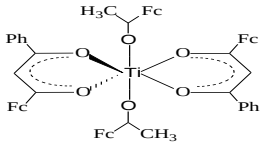

1-ferrocenylethan-1-ol [$FcCH_3(CH)OH$] (0.069 g / 0.27 mmol) dissolved in chloroform (4 cm^3), was added to a solution of [$(FcCOCHCOPh)_2TiCl_2$] (0.1 g / 0.13 mmol) in dry $CHCl_3$ (10 cm^3). The resulting mixture was left to stir overnight, (16 hrs), at ambient temperature. The solvent was then removed under reduced pressure. The residue was dissolved in DCM (10 cm^3) and precipitated with hexane and filtration was performed under N_2. The precipitated product was black/green and found to be 29% (0.06 g) yield; m.p. 116-120^{0}C; δ_H(300 MHz, CD_3CN)/ppm 1.26–1.50 (m, 6H, 2 x CH_3), 3.51–5.38 (m, 38H, 2 x H $CH_{ferrocenyl\ alcohol}$ and 4 x Fc of many isomers) and 5.43–5.85 (m, 2H, 2 x $CH_{\beta\text{-}diketones}$).

4.3.5.2. Di(1-oxyethyl-1-ferrocenyl)bis(1-Ferrocenoyl-1,3-butanedionato)titanium(IV), [$(FcCOCHCOCH_3)_2Ti(O\text{-}CH(CH_3)\text{-}Fc)_2$], [22]

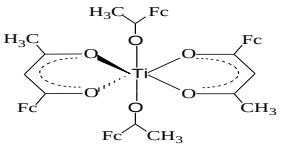

To a solution of [$(FcCOCHCOCH_3)_2TiCl_2$](0.1 g / 0.15 mmol) in chloroform (4 cm^3), was added [$FcCH_3(CH)OH$] (0.7 g / 0.31mmol) dissolved in $CHCl_3$ (5 cm^3). The reaction mixture was stirred for 16 hrs at room temperature after which the solvent was removed under reduced pressure. This residue was dissolved in DCM (10 cm^3) and precipitated with hexane (≈200 cm^3). In this case the dark green product was collected by removal of solvent (under reduced pressure, O_2 free conditions) from the filtrate. Yield 38% (0.048 g); m.p. 165^{0}C; δ_H(300 MHz, CD_3CN)/ppm 0.74–1.38 (m, 6H, 2 x CH_3),

1.66–1.90 (m, 2H, 2 x CH_3 suspect 4H hidden under solvent signal) 3.60–5.88 (m, 38H, 2 x H $CH_{ferrocenyl\ alcohol}$ and 4 x Fc of many isomers) and 6.41 (s, 2H, 2 x $CH_{\beta\text{-diketones}}$).

4.3.5.3. Di(1-oxyethyl-1-ferrocenyl)bis(1-ferrocenyl-4,4,4-trifluoro-butane-1,3-dionato)titanium(IV), $[(FcCOCH_2COCF_3)_2Ti(O(CH)CH_3Fc)_2]$, [23]

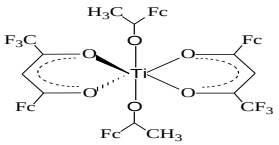

$[(FcCOCHCOCF_3)_2TiCl_2]$ (0.1 g / 0.13 mmol) was dissolved in $CHCl_3$ (10 cm^3) and 1-ferrocenylethan-1-ol (0.069 g / 0.27 mmol) dissolved in $CHCl_3$ (4 cm^3) were added to a flame dried two-neck flask. The mixture was stirred at room temperature for 16 hrs. Thereafter the solvent was removed under reduced pressure and the viscous blue residue was washed with ether (4 x 50 cm^3 portions), followed by washing with excess dry hexane (500 cm^3). A blue/black product was obtained in 45% (0.07 g) yield. M.p. 145^0C; δ_H(300 MHz, CD_3CN)/ppm 0.97–1.50 (m, 6H, 2 x CH_3), 3.96–5.23 (m, 38H, 2 x H $CH_{ferrocenyl\ alcohol}$ and 4 x Fc of many isomers) and 6.30–6.55 (m, 2H, 2 x $CH_{\beta\text{-diketones}}$).

4.3.6. Supporting electrolyte

4.3.6.1. Tetrabutylammonium tetrakis[pentaflourophenyl] borate, $[N(^nBu)_4][B(C_6F_5)_4]$, (BARF), [25]

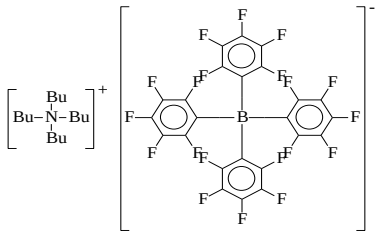

$[LiB(C_6F_5)_4 \bullet 3H_2O]$ (10 g / 0.0182 mol, Boulder Scientific) was dissolved in MeOH (AR, 20 cm^3). A $[N(Bu)_4Br]$ (5.1 g / 0.0158 mol) in MeOH (AR, 10 cm^3) solution was also prepared. The two solutions were combined and left to stir for 15 minutes at room temperature. The reaction vessel was then sealed and left to stand overnight (16 hrs, ca. -25^0C). An off-white precipitate formed, which was filtered, washed with MeOH (AR, 10 cm^3, ca. -25^0C) and left to air dry. The residue was dissolved in excess CH_2Cl_2 (30 cm^3) and dried ($MgSO_4$). All solvent was removed under reduced pressure, producing a solid white product. Yield 62% (9.0 g); m.p. bla^{0}C; δ_H(300 MHz, $CDCl_3$)/ppm 0.98 (t, 12H, 4 x CH_3), 1.36 (m, 8H, 4 x CH_2), 1.57 (m, 8H, 4 x CH_2) and 3.03 (t, 8H, 4 x CH_2).

4.4. Crystallography

The author acknowledges Dr. A.J. (Fanie) Muller from the Department of Chemistry, University of the Free State, for determining and solving the crystal structure.

4.4.1. Structural determination of 1-ferrocenyl-3-ruthenocenylpropane-1,3-dione, [FcCOCH$_2$CORc], [11].

Crystals of [FcCOCH$_2$CORc], **[11]** were obtained by recrystallizing from ether/hexane (1:5 by volume).

A tan coloured crystal was mounted on a glass fiber and intensity data was collected on a Rigaku AFC5R diffractometer using graphite monochromated Cu-K_α radiation and a rotating anode generator. Cell constants and an orientation matrix for data collection were obtained from a least-squares refinement using the setting angles of 25 carefully centered reflections in the range $62.88° < 2\theta < 74.41°$. Data was corrected for Lorentz and polarization effects. Correction for secondary extinction was also applied. The structure was solved by direct methods[6] and expanded using Fourier techniques.[7] Non-hydrogen atoms were refined anisotropically, hydrogen atoms were included but not refined. Neutral atom scattering factors were taken from Cromer and Waber.[8] Anomalous dispersion effects were included in F_{calc};[9] the values for $\Delta f'$ and $\Delta f''$ were obtained from Creagh and McAuley.[10] The values for the mass attenuation coefficients are those of Creagh and Hubell.[11] All calculations were performed using the teXsan[12] crystallographic software packages from the Molecular Structure Corporation.

4.4.2. Structural determination of 1-Ferrocenoyl-1,3-butanedionato κ^2O,O'-bis(η^5-cyclopentadienyl) titanium(IV) perchlorate, [$Cp_2Ti(FcCOCHCOCH_3)ClO_4$] [18].

[$Cp_2Ti(FcCOCHCOCH_3)ClO_4$], **[18]** crystals were obtained by recrystallizing from DCM/heptane (1:3 by volume). A bright red crystal was mounted on a glass fibre and intensity data was collected on a Rigaku AFC5R diffractometer using graphite monochromated Cu-Kα radiation and a rotating anode generator. Cell constants and an orientation matrix for data collection were obtained from the least-squares refinement. Setting angles of 25 carefully centred reflections in the range $62.88^o < 2\theta < 74.41^o$ were used. Data was corrected for Lorentz and polization effects. A correction for secondary extinction was also applied. The structure was solved *via* direct methods[6] and expanded using Fourier techniques.[7] Non-hydrogen atoms were refined anisotropically and hydrogen atoms are included but not refined. Neutral atom scattering factors were taken from Cromer and Waber.[8] Anomalous dispersion effects were included in F_{calc};[9] the values for $\Delta f'$ and $\Delta f''$ were obtained from Creagh and McAuley.[10] The values for the mass attenuation coefficients are those of Creagh and Hubell.[11] All calculations were performed using the teXsan[12] crystallographic software packages from the Molecular Structure Corporation.

4.5. Electrochemistry

Cyclovoltammetric measurements were performed on ca. 1.0 mmol.dm^{-3} solutions of the complexes. The solvent was DCM (spectroscopic grade, HPCL) containing 0.1 mmol.dm^{-3} [N(^{n}Bu)$_4$B(C_6F_5)$_4$] (BARF, see paragraph 4.3.6.) as supporting electrolyte. The measurements were conducted under a blanket of purified argon at 25.0˚C utilizing a BAS 100 B/W electrochemical workstation interfaced with a personal computer. A three-electrode cell, comprised of a Pt auxiliary electrode, a glassy carbon (surface area 0.0707 cm^2) working electrode and an Ag/AgCl reference electrode[13] was utilised.[14,15] All temperatures were kept constant to within 0.5˚C. Successive experiments under similar experimental conditions showed that all formal reduction and oxidation potentials were reproducible to within 5 mV.

Measurements on ca. 1.0 mmol.dm^{-3} mono- β-diketonato titanium(IV) salt solutions were repeated in acetonitrile with 0.1 mol.dm^{-3} tetra-*n*-butylammonium hexafluorophosphate ([N(Bu)$_4$][PF_6^-], Fluka, electrochemical grade) as supporting electrolyte. All other experimental conditions and apparatus remained unchanged.

The Ag/AgCl reference electrode was prepared as follows. A 0.1M HCl solution was prepared and added to an Erlenmeyer flask. A separate Ag wire was then placed in a swizzle stick and immersed in the HCl solution. A DC power supply was then connected, (-) to wire in swizzle stick and (+) to the wire which is to be coated. This wire is also immersed in the bulk of the HCl solution in the Erlenmeyer. A potential of ca. 1.2 V was then applied for 10 minutes. A thin white coat (which turns black over time) forms on the wire. The reference electrode is now ready for use.

Electrodes were cleaned by polishing with METADI® II diamond polishing compounds (1 μm and ¼ μm), rinsed with ethanol, acetonitrile/DCM, then with water and finally dried before each experiment. All measurements were referenced against an Ag/AgCl electrode. Scan rates were between 50 and 1000 mV/s. Data, uncorrected for junction potentials, was collected with BAS 100 software and analysed with Microsoft® Exel 2000.

4.6. Cytotoxicity tests

The author acknowledges Prof. Connie Medlin, head of the Department of Immunology, Institute for Pathology at the University of Pretoria and especially, Mrs. Margo Nell, for performing these experiments.

Sample preparations: Mono-β-diketonato titanium(IV) salts, **[17] – [22]**, were dissolved in DMSO, giving stock concentrations of 10 $mg.cm^{-3}$. The samples were then diluted in the appropriate growth medium and supplemented with fetal calf serum (FCS), giving final concentrations not exceeding 0.5% and drug concentrations of 1-3000 $\mu g.cm^{-3}$ prior to cell experiments.

Cell cultures: A human colorectal cell line, CoLo DM320 (ATCC CCL-220), was grown as a suspended culture in RPMI 1640. The human cervix epitheloid cancer cell line, HeLa (ATCC CCL-2), was grown as a monolayer culture in MEM. Growth media were incubated at 37°C under 5% CO_2 and fortified with 10% FCS, and 1% penicillin and streptomycin. Appropriate solvent control systems were included. Cells were seeded at 2000 cells/well for 24 hr incubation experiments and 400 cells/well, 7 day, incubation experiments. The experiments were performed in 96 well microtiter plates with a final volume of 200 μl of growth medium, with different concentrations of experimental drugs, either present or absent. Wells with and without cells but devoid of drugs were included as controls. After incubation at 37°C for 1 day or 7 days, cell survival was measured by means of the colometric 3-(4,5-dimethylthiazol-2-yl)-diphenyltetrasodium bromide (MMT) assay.[16]

4.7. References

[1] B.S. Furniss, A.J. Hannaford, P.W.G. Smith and A.R. Tatchell, *Vogel's Textbook of Practical Organic Chemistry* 4th Edition, Longman, New York, p 264-318 (1989).

[2] P.C. Reeves, *Org.Synth.*,28, *Chem*,850., **28** (1963).

[3] W.C. Du Plessis, T.G. Vosloo and J.C. Swarts, *J. Chem. Soc., Dalton Trans.*, p 2512 (1998).

[4] Hauser, C.R. and Lindsay, J.K., *J. Org. Chem.*, 482, **22** (1957).

[5] C.F. Cain, T.A. Mashburn and C.R. Hauser, *J. Org. Chem.*, 1030, **26** (1961).

[6] A. Altomare, M. Cascarano, C. Giacovazzo and A. Guagliardi, *J. Appl. Crystallogr*., 343, **26** (1993).

[7] P.T. Beurskens, G. Admiraal, G. Beurskens, W.P. Bosman, R. de Gelder, I. Israel, and J.M.M. Smits, *The DIRDIF-94 program system. Technical Report of the Crystallography Laboratory*, University of Nijmegen, The Netherlands (1994).

[8] D.T. Cromer and J.T. Waber, , *International tables for X-ray crystallography*, **Vol. IV**, The Kynoch Press, Birmingham, Table 2.2 A (1974).

[9] J.A. Ibers and W.C. Hamilton, *Acta Cryst*., 781, **17** (1964).

[10] D.C. Creagh and W.J. McAuley, *International tables for crystallography*, **Vol. C**, Edited by A.J.C. Wilson, Kluwer Academic Publishers, Boston, Table 4.2.6.8, p. 219 (1992).

[11] D.C. Creagh and J.H. Hubbell, *International tables for crystallography*, **Vol. C**, Edited by A.J.C. Wilson, Kluwer Academic Publishers, Boston, Table 4.2.4.3, p.200 (1992).

[12] *TeXan for windows: crystal structure analysis package*. Molecular Structure Corporation, The Woodlands, Tex. (1997).

[13] D.T. Sawyer and J.L. Roberts Jr, *Experimental electrochemistry for chemists*, Wiley, New York, p 54 (1974).

[14] D.H. Evans, K.M. O'Connell, R.A. Peterson and M.J. Kelly, *J. Chem. Educ.*, 291, **60** (1983).

[15] G.A. Mabbott, *J. Chem. Educ.*, 697, **60** (1983).

[16] B. K. Keppler, M. Henn, U. M. Juhl, M. R. Berger, R. Niebl and F. E. Wagner, *Progress in Clinical Biochemistry and Medicine*, 41, **10** (1989).

Chapter 5

Summary, conclusions and future perspectives

In this study, 5 ferrocene-containing β-diketones (one of which also contains ruthenocene) and 11 new ferrocene-containing titanium(IV) complexes were synthesised in multi-step reactions. These compounds are shown in **Figure 5.1.** To achieve this, in certain cases, known synthetic protocols were optimised to enhance synthetic yields and for titanium complexes new synthetic procedures had to be developed. The newly synthesised complexes were characterised by ^{1}H NMR and single crystal crystallographic techniques. Physical properties were investigated electrochemically. The effects of varying electron density on metal centres were also quantified. The cytotoxicity (IC_{50} values on CoLo and HeLa human cancer cell lines) of selected compounds was also evaluated to determine their use as potential new anti-cancer drugs.

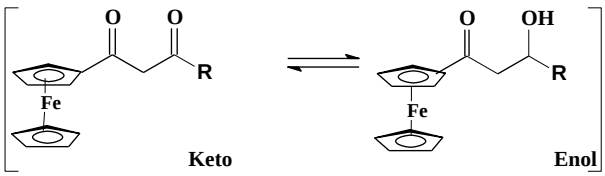

Ferrocene-containing β-diketones
R = Ph [7], CH_3 [8], CF_3 [9], Fc [10] and Rc [11]

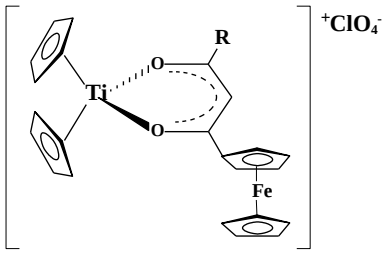

Mono-β-diketonato titanium(IV) salts
R = Ph [12], CH_3 [13], CF_3 [14], Fc [15] and Rc [17]

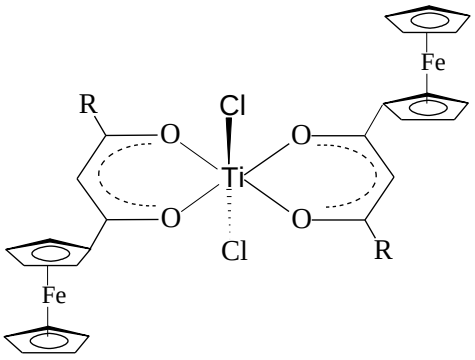

Dichlorobis-β-diketonato titanium(IV) complexes
R = Ph [18], CH_3 [19]and CF_3 [20]

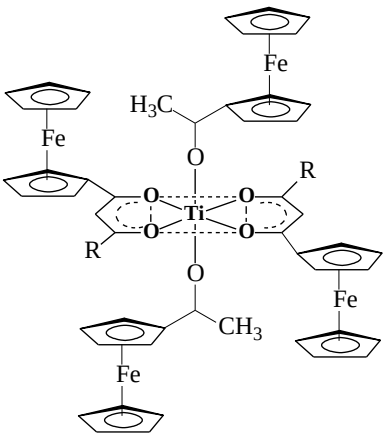

Di(1-oxyethyl-1-ferrocenyl)bis(β-diketonato) titanium(IV) complexes
R = Ph [21], CH_3 [22]and CF_3 [23]

Figure 5.1. Structures of the compounds synthesized in this study. R-groups vary from the highly electron withdrawing CF_3 group to the electron donating Fc group. Fc = ferrocenyl and Rc = ruthenocenyl.

The five ferrocene-containing β-diketones were synthesised *via* Claisen condensation reactions between acetylferrocene and the appropriate monocarboxylic ester.

A variety of new tetrahedral mono-β-diketonato titanium(IV) complexes of the type $[Cp_2Ti(FcCOCHCOR)]^+ClO_4^-$ were obtained *via* two different routes; the known route which utilises titanocene dichloride as reactant and a new route, developed in this laboratory. This new method involves the substitution of $CH_3COCHCOCH_3^-$ from $[Cp_2Ti(CH_3COCHCOCH_3)]^+ClO_4^-$ with the desired β-diketone. The substitution route was utilised for the $[Cp_2Ti(FcCOCHCORc)]^+ClO_4^-$ complex where the titanocene dichloride approach had failed. It was found that this β-diketone exchange reaction is dependent on the group electronegativity of the R-group of the incoming β-diketone as well as on the bulkiness of the R-group. The method is especially synthetically successful when the incoming β-diketone contains groups which are less electronegative than those of the leaving ligand.

Three new octahedral complexes of the form $[(FcCOCHCOR)_2TiCl_2]$ with R = Ph, CH_3 and CF_3 were also prepared. For these complexes titanium tetrachloride was used as starting material and reacted with 2 equivalents of β-diketone to give the desired product. ^1H NMR studies of the bis-β-diketonato complexes established that these compounds exist as more than one isomer in solution. Multiple solution isomers were also detected electrochemically, utilising cyclic voltammetry.

The ferrocene-containing alkoxy complexes of the type $[(FcCOCHCOR)_2Ti\{O\text{-}CH(CH_3)\text{-}Fc\}_2]$ with R = Ph, CH_3 and CF_3 were prepared by reacting the appropriate bis-β-diketonatodichloro titanium complex with the ferrocenyl alcohol, 1-ferrocenylethan-1-ol ($[FcCH(OH)CH_3]$). The % yield obtained for the complexes was seen to increase in direct relation to an increasing group electronegativity of the R-group on the β-diketonato ligand.

Electrochemical studies were initially performed in a weakly coordinating $CH_3CN/[NBu_4][PF_6]$ medium. However, better understanding of results was obtained utilising the non-coordinating solvent/supporting electrolyte medium $CH_2Cl_2/[NBu_4][B(C_6F_5)_4]$. Electrochemical studies on all synthesised complexes were thus performed in dichloromethane utilising $[NBu_4][B(C_6F_5)_4]$ as

electrolyte. Cyclic voltammetry, linear sweep voltammetry and Oster Young square wave voltammetry were preformed.

The ferrocene/ruthenocene-containing β-diketone exhibited multiple cathodic (reduction) waves due to the formation of a dimerized ruthenocium species $(Rc^{III}\text{-}Rc^{III})^{2+}$. The Ru^{3+}/Ru^{2+} couple displayed irreversible electrochemistry while the Fc/Fc^{+} couple was reversible. Peak broadening over short time periods is attributed to a kinetic process whereby enol isomers in solution slowly convert to keto isomers until a solution keto/enol equilibrium has set in.

The mono-β-diketonato titanocenyl(IV) complexes containing only two metal centres, namely one ferrocene and titanium, revealed chemical and electrochemically reversible Ti^{4+}/Ti^{3+} couples, with the Fc/Fc^{+} couples of the complexes showing predominantly quasi-reversible electrochemistry. For the complexes containing three metals i.e., a second ferrocene or an additional ruthenocene fragment, the Ti^{4+}/Ti^{3+} couple becomes irreversible. The formal reduction potentials of the Ti^{4+}/Ti^{3+} and Fc/Fc^{+} couples are influenced by the group electronegativity of the R-group of the β-diketonato ligand. With an increase in group electronegativity of the R-group of the β-diketonato ligand, titanium(IV) reduction becomes easier and ferrocenyl oxidation is increasingly difficult. The un-coordinative $CH_2Cl_2/[NBu_4][B(C_6F_5)_4]$ medium cast more light on the quasi-reversible behaviour of the Fc/Fc^{+} couple. Splitting of the ferrocenyl fragment into two unresolved peaks was detected and current ratios of Ti^{4+}/Ti^{3+}: Fe^{3+}/Fe^{2+} approaching 1:2 in the extreme case where R = CF_3, compound **[14]** was observed. From this evidence it was clear that more than one ferrocene moiety is at play. These results were interpreted to be electrochemical evidence for the formation of a temporary mixed valent dimer complex. The second distinct oxidation and reduction peak is attributed to ferocenyl oxidation of this mixed valent dimer complex. The following electrochemical scheme is consistent with the obtained results:

$$[Cp_2Ti^{III}(FcCOCHCOR)] \underset{+\,e^-}{\overset{-\,e^-}{\rightleftharpoons}} [Cp_2Ti^{IV}(FcCOCHCOR)]^+ \underset{+\,e^-}{\overset{-\,e^-}{\rightleftharpoons}} [Cp_2Ti^{IV}(Fc^+COCHCOR)]^+ \overset{\text{Rapid chemical dimerisation with } [Cp_2Ti^{IV}(FcCOCHCOR)]^+ \text{ from the bulk of the solution}}{\rightleftharpoons}$$

$$[[Cp_2Ti^{IV}(Fc^+COCHCOR)]^+ \; ; \; [Cp_2Ti^{IV}(FcCOCHCOR)]^+] \underset{+\,e^-}{\overset{-\,e^-}{\rightleftharpoons}} [Cp_2Ti^{IV}(Fc^+COCHCOR)]_2^{2+}$$

The bis-β-diketonato complexes generally revealed Ti^{4+}/Ti^{3+} couples to be chemically and electrochemically irreversible while the Fc/Fc^{+} couple was found to be chemically reversible and electrochemically reversible to quasi-reversible. In addition, the multiple oxidation and reduction peaks observed for the ferrocenyl portions provide evidence for the exsistance of multiple isomers in solution for all the octahedral complexes.

The crystal structures for [$FcCOCH_2CORc$] and $[Cp_2Ti(FcCOCHCOCH_3)]^{+}ClO_4^{-}$ were also reported. The crystal structure for [$FcCOCH_2CORc$] revealed that, unlike other known ferrocene-containing β-diketones, enolisation does not occur exclusively in the direction away from the ferrocene group. Results were consistant with the conclusion that equal amounts of both enol forms are present in the solid state. The structure of the mono-β-diketonato titanium(IV) complex $[Cp_2Ti(FcCOCHCOCH_3)]^{+}ClO_4^{-}$ displays the expected distorted tetrahedral geometry around the Ti centre. Effective conjugation of the ferrocenyl group into the pseudo-aromatic ring of the β-diketonato side chain was observed. The structure revealed one particular unhindered access route to the titanium centre, which explains why β-diketone substitution reactions for complexes of this type are so effective.

The cytotoxic properties of the new mono-β-diketonato titanium(IV) complexes were studied to investigate possibilities of their application in terms of anti-cancer activity. The cytotoxicity of the ferrocene-containing titanium(IV) compounds was determined by observing their effects *in vitro* on cultured HeLa (a human cervix epitheloid cancer) and CoLo (a human colorectral) cell lines. The tested complexes were not as effective as the benchmark, cisplatin, in killing cancer cells. All tested $[Cp_2Ti(\beta\text{-diketonato})]^{+}ClO_4^{-}$ complexes did, however, show enhanced cytotoxic activity when compared with titanocene dichloride (currently in stage II clinical trials). Titanocene dichloride is known to exhibit far less harmful side effects than cisplatin. It is hoped that the present series of Ti complexes will also show decreased side effects compared to cisplatin. Research to establish this is

currently underway. The combination of more than one type of antineoplastic moiety in the same molecule (titanocyl and ferrocenyl fragments) leads to enhanced anti-cancer activity over titanocene dichloride i.e. synergistic effects were detected. Furthermore the ionic nature of the complexes increases aqueous compatibility, ultimately benefiting administrative and cell absorptive processes. The exact mechanism by which each drug fragment attacks and destroys cancer cells is currently under investigation.

Perspectives for future studies are varied. In this study, a series of ferrocene-containing mono-β-diketonato and bis-β-diketonato complexes were synthesised and ferrocene containing alcohols were also coordinated. In addition bi-, tri and tetrametallocene-containing alkoxy complexes could be synthesised. Different metallocene alcohols of the type $Mc(CH)_nOH$ with Mc = Fc, Rc and Oc (osmocenyl) and n = 1, 2, 3 and 4 may replace $FcCH(OH)CH_3$ in the complex $[(FcCOCHCOR)_2Ti\{O\text{-}CH(CH_3)\text{-}Fc\}_2]$ to probe the influence of different metallocenes and alcoxy chain length on electrochemical and anti-cancer behaviour. The central titanium(IV) metal could also be replaced with Zr, Hf, V, Nb or Mo. Quantification of trends within a group (Ti, Zr and Hf) or a certain period (Ti and V; Zr, Nb and Mo complexes) of the periodic table may be made. Future studies could also be extended to the use of either ruthonocene-, osmocene- or cobalticenium-containing β-diketones instead of ferrocene. The new complexes may be subjected to electrochemical and crystallographic studies. Ligand exchange, substitution kinetics and hydrolysis kinetics could be investigated. Similar studies could also be extended toward the other metallocene complexes.

Application of the complexes synthesised in this study in terms of catalysis and anti-cancer activity should be addressed. A clarification study as to the mode of action of the complexes in killing cancer cells needs to be performed. Cytotoxic properties with respect to HeLa and CoLo cancer cell lines were reported in this study. The toxicity on healthy cells in comparison with cancer cells should also be investigated. Possible upgrades to tests on rats and phases I, II and III clinical trials could be initiated. Cytotoxic tests on the bis-β-diketonato complexes are pending.

These complexes as well as the mono-β-diketonato compounds can also be complexed to other transition metals such as rhodium, iridium and platinum to find possible synergistic antineoplastic effects as well as catalytic properties. A series of new cobalticenium-containing β-diketones, ferrocene and/or ruthenocene-containing enaminones as well as a new series of titanocene-containing β-diketones and ruthenocene-containing β-ketoesters may also be designed.

Organomettalic chemistry represents one of the fastest growing fields to date and the vastly different application possibilities for metallocenes present unlimited opportunities for further research.

Appendix A

^{1}H NMR Spectra

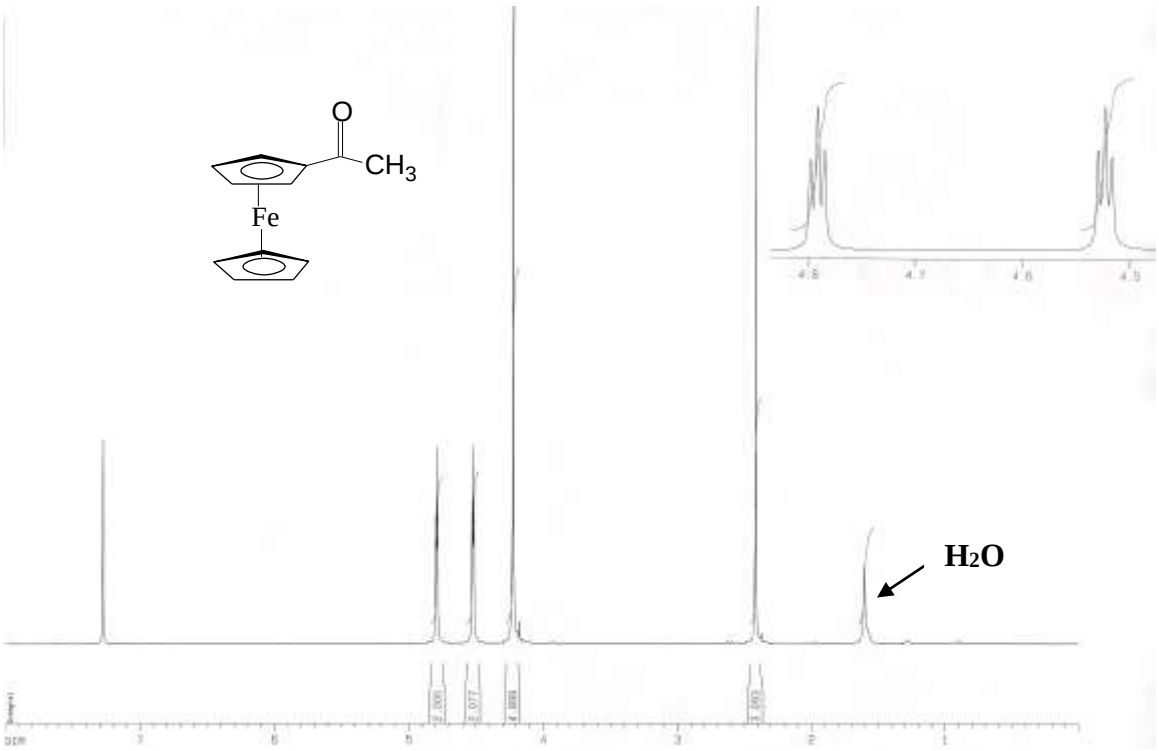

Spectrum 1: Acetylferrocene [$FcCOCH_3$], [4]

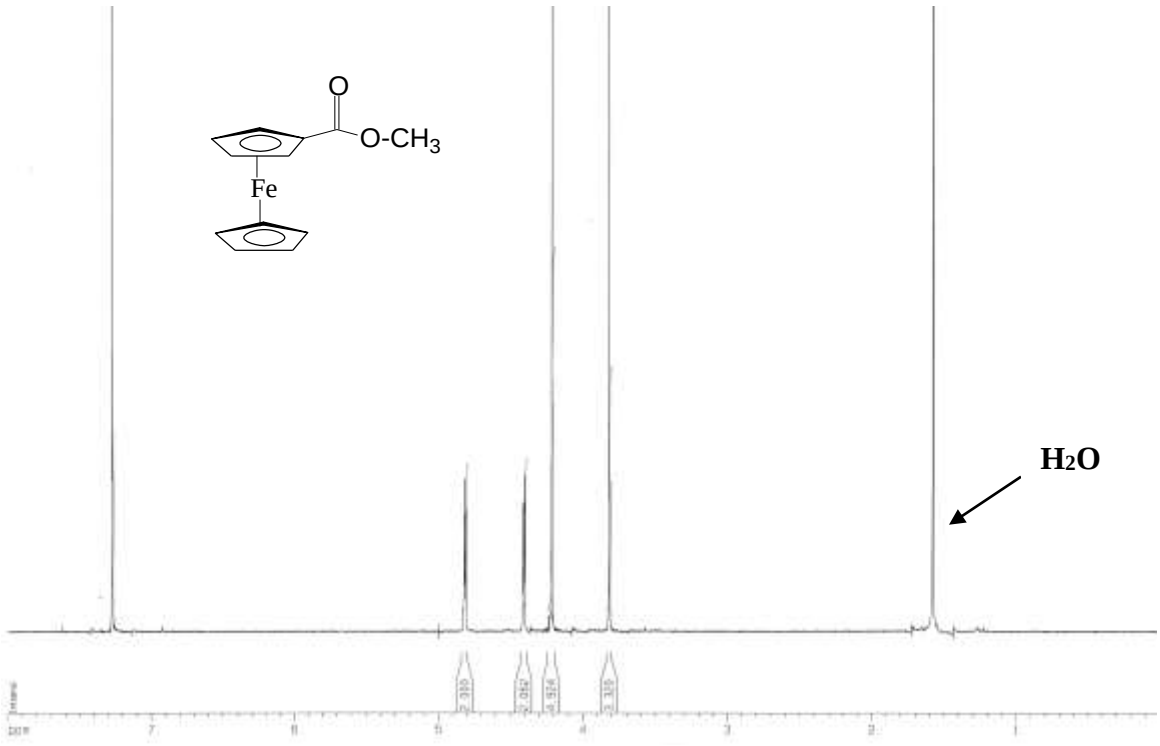

Spectrum 2: Methyl ferrocenoate, ($FcCOOCH_3$), [5]

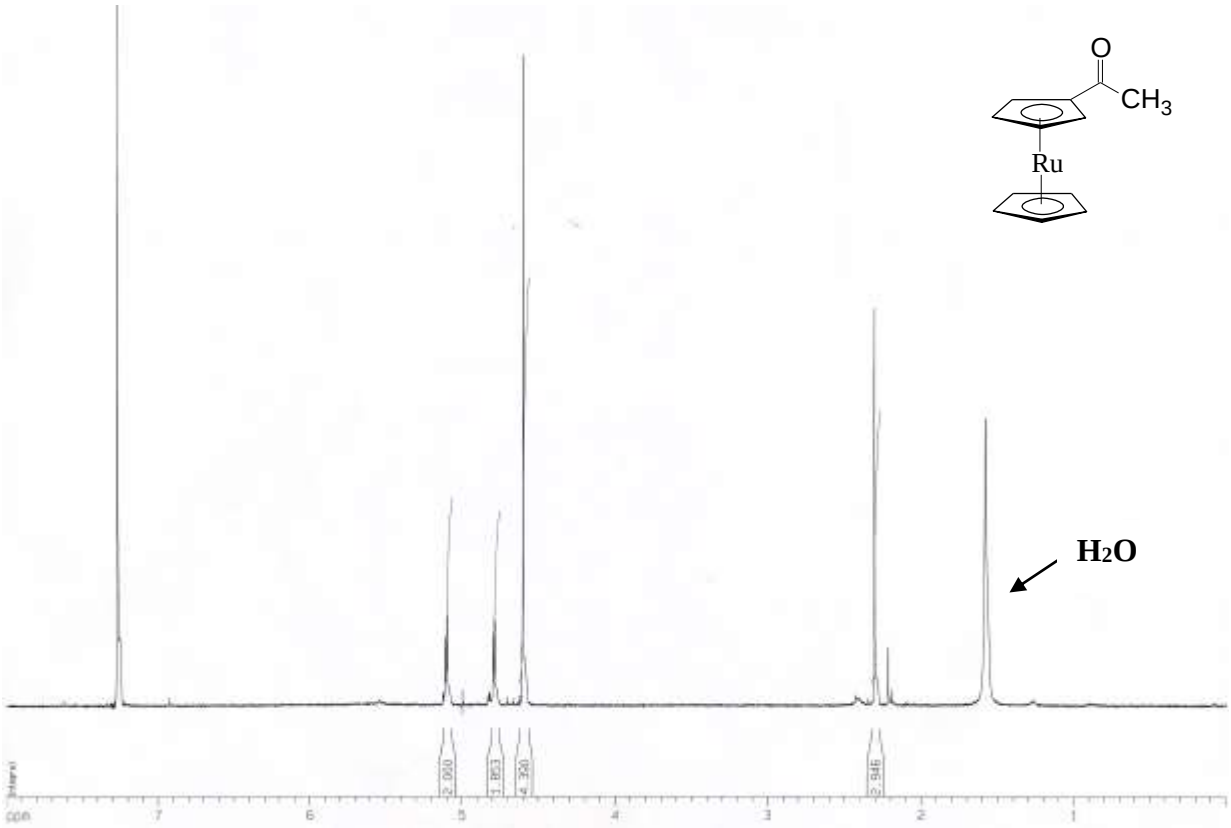

Spectrum 3: Acetylruthenocene, ($RcCOCH_3$), [6]

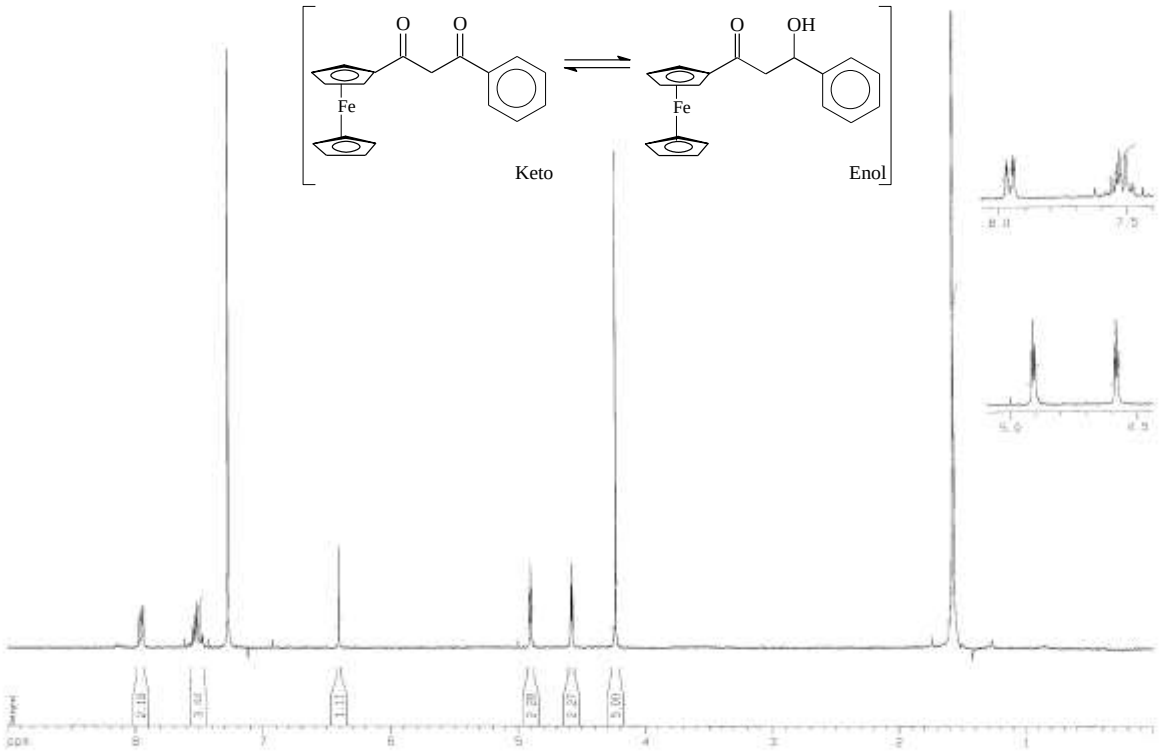

Spectrum 4: 1-ferrocenyl-3-phenyl-1,3-propanedione, [$FcCOCH_2COPh$], [7]

Spectrum 5: 1-ferrocenylbutane-1,3-dione, [$FcCOCH_2COCH_3$], [8]

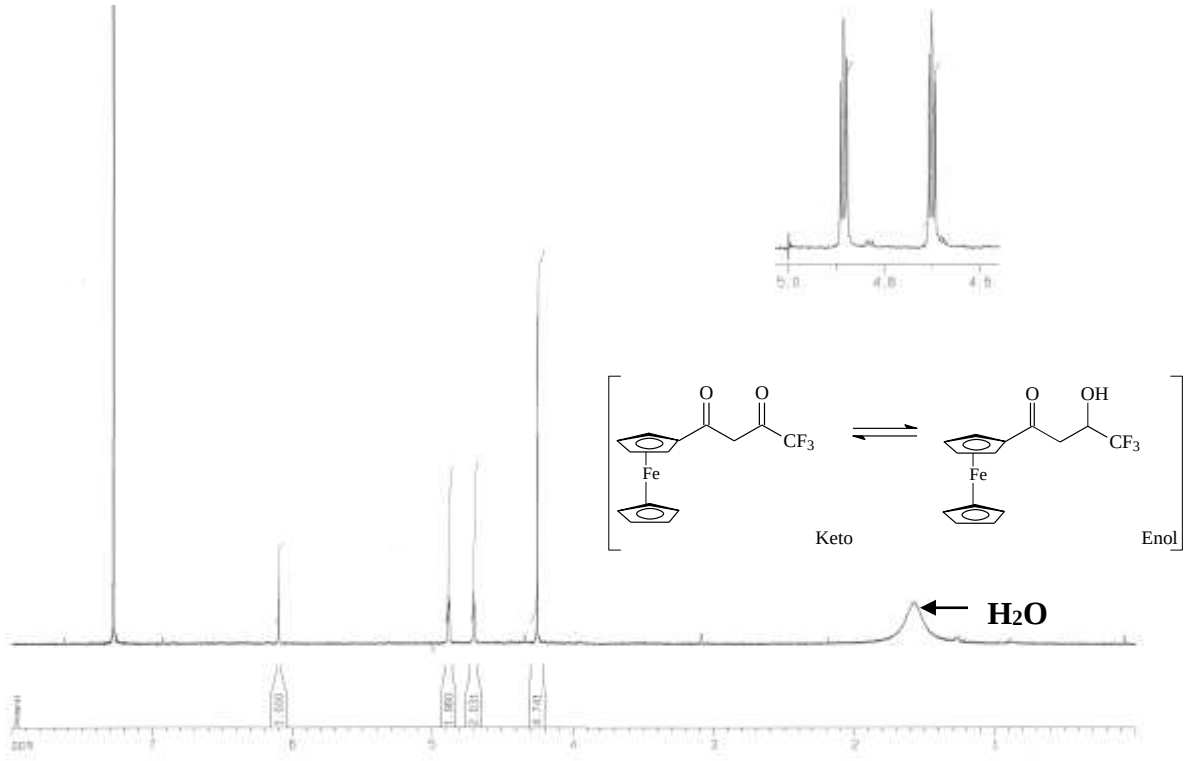

Spectrum 6: 1-ferrocenyl-4,4,4-trifluorobutane-1,3-dione, [$FcCOCH_2COCF_3$], [9]

^{1}H NMR Spectra

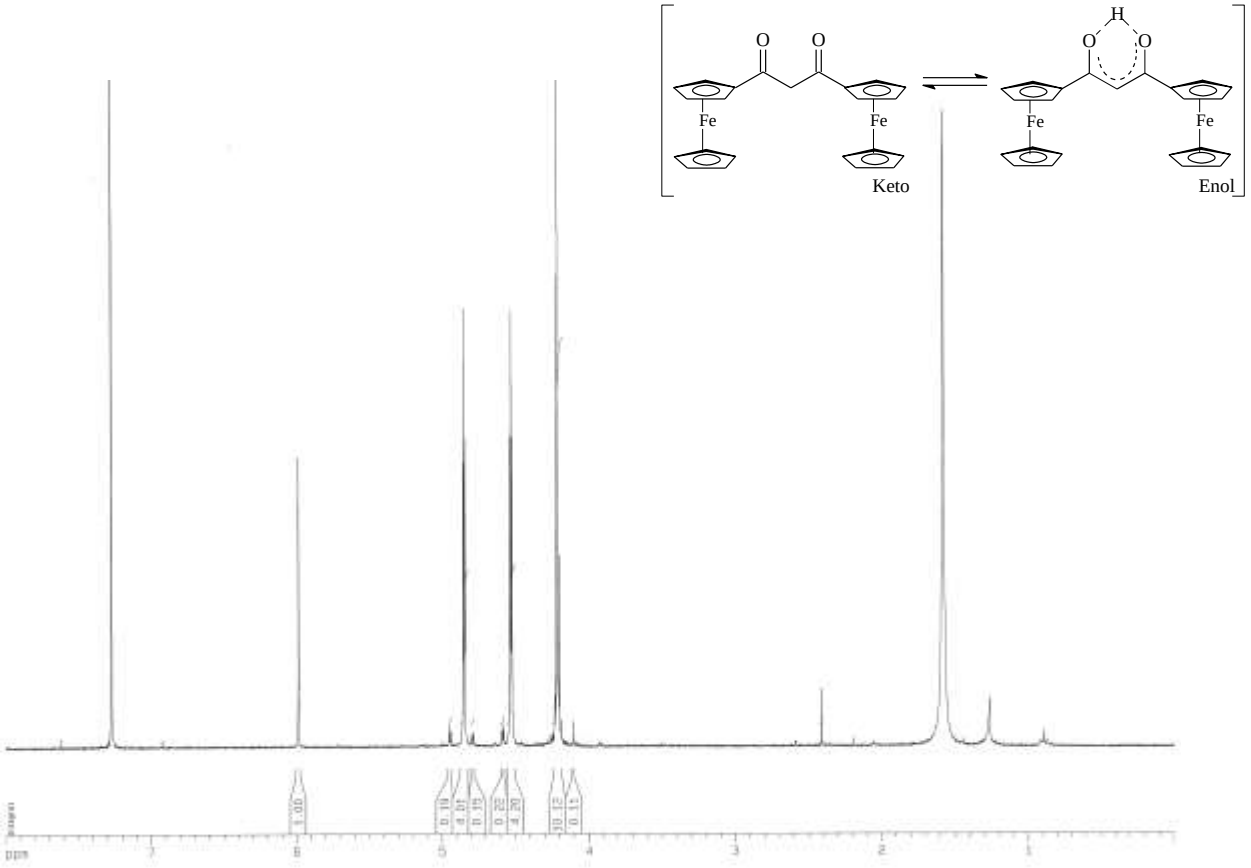

Spectrum 7: 1,3-diferrocenylpropane-1,3-dione, [FcCOCH$_2$COFc], [10]

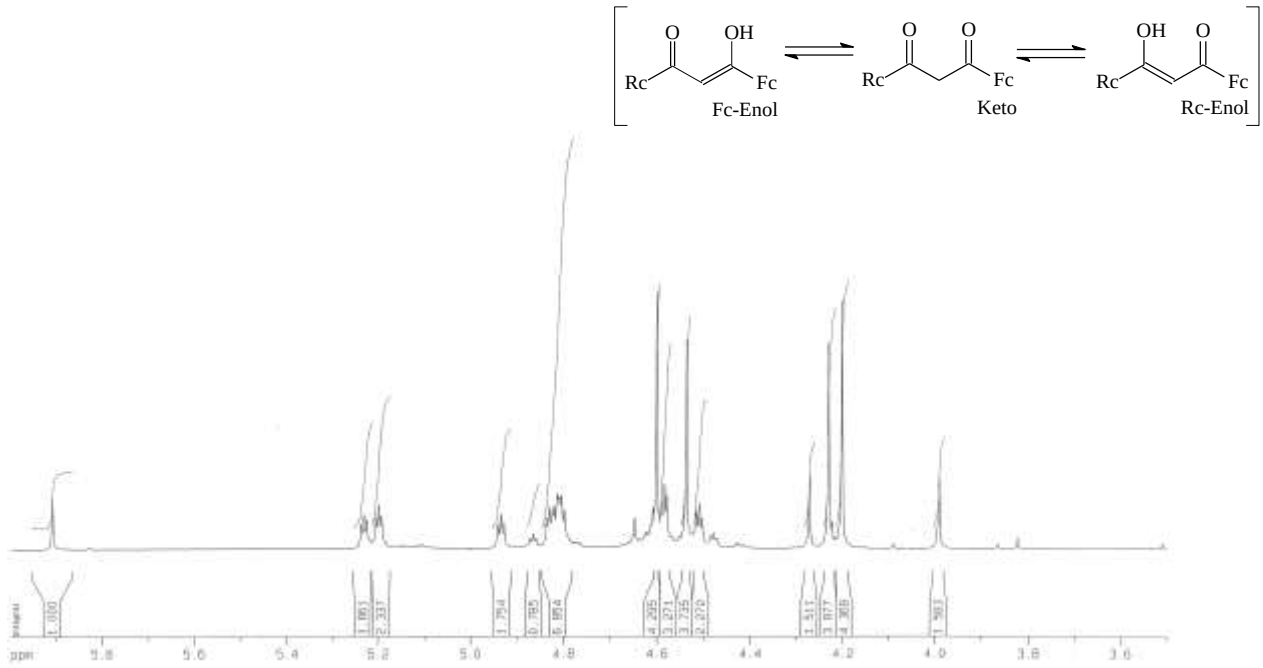

Spectrum 8: 1-ferrocenyl-3-ruthenocenylpropane-1,3-dione, [FcCOCH$_2$CORc], [11]

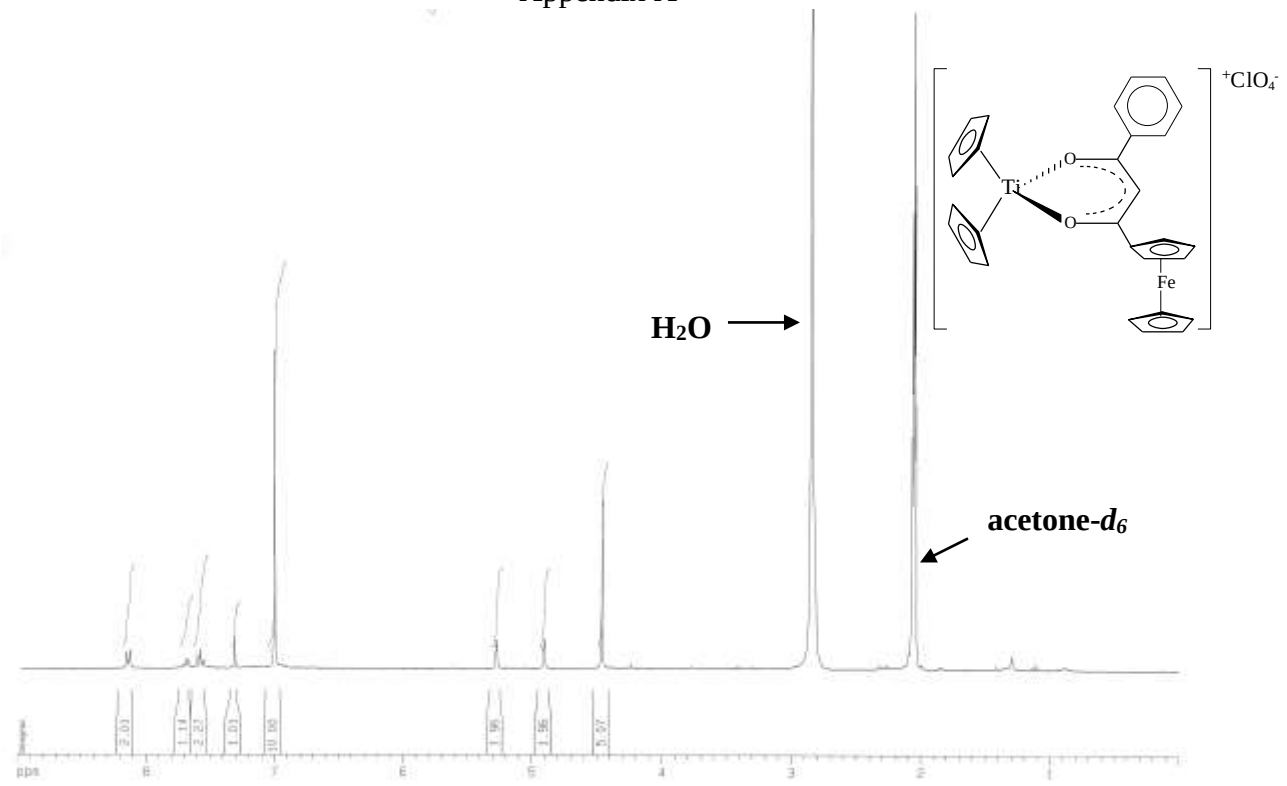

Spectrum 9: 1-ferrocenyl-3-phenyl-1,3-propanedionato-κ^{2}O,O'bis-(η^{5}cyclopentadienyl) titanium(IV) perchlorate, [Cp$_2$Ti(FcCOCHCOPh)]$^+$ClO$_4^-$,[12]

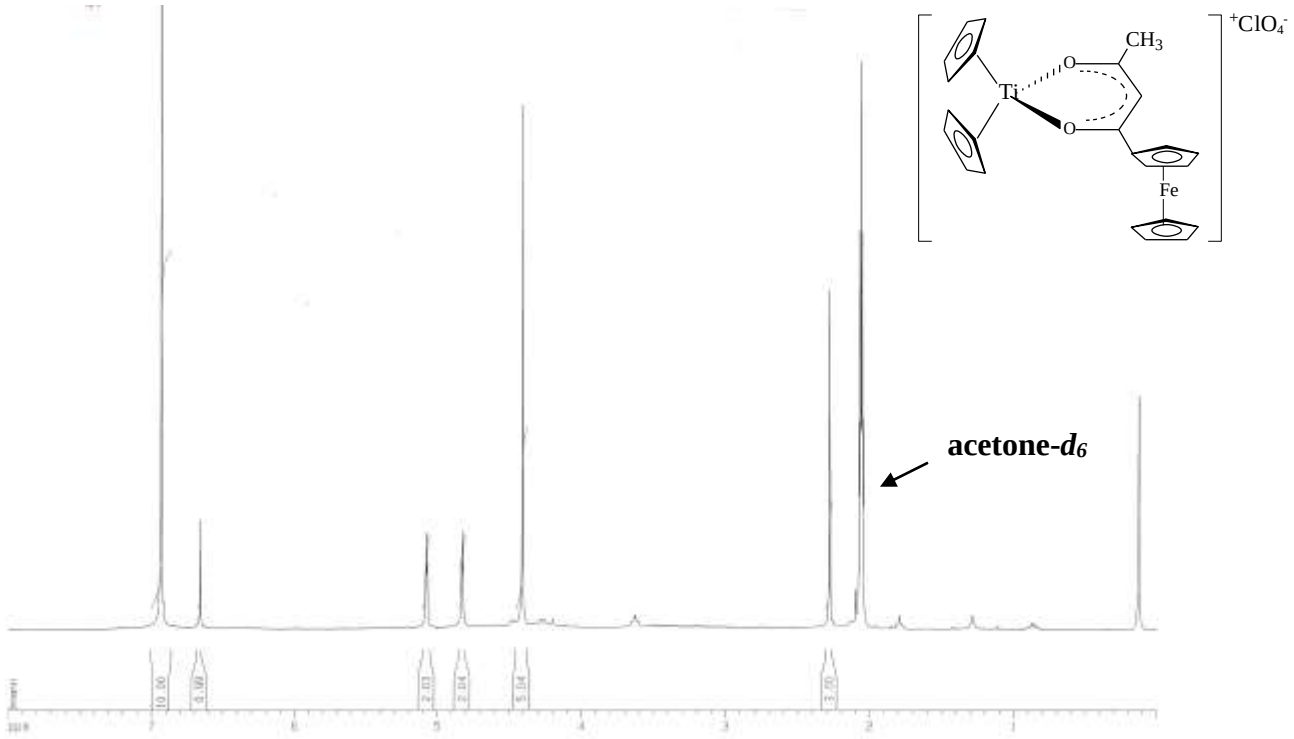

Spectrum 10: 1-Ferrocenoyl-1,3-butanedionato-κ^{2}O,O'-bis(η^5-cyclopentadienyl) titanium(IV) perchlorate, [Cp$_2$Ti(FcCOCHCOCH$_3$)]$^+$ClO$_4^-$, [13]

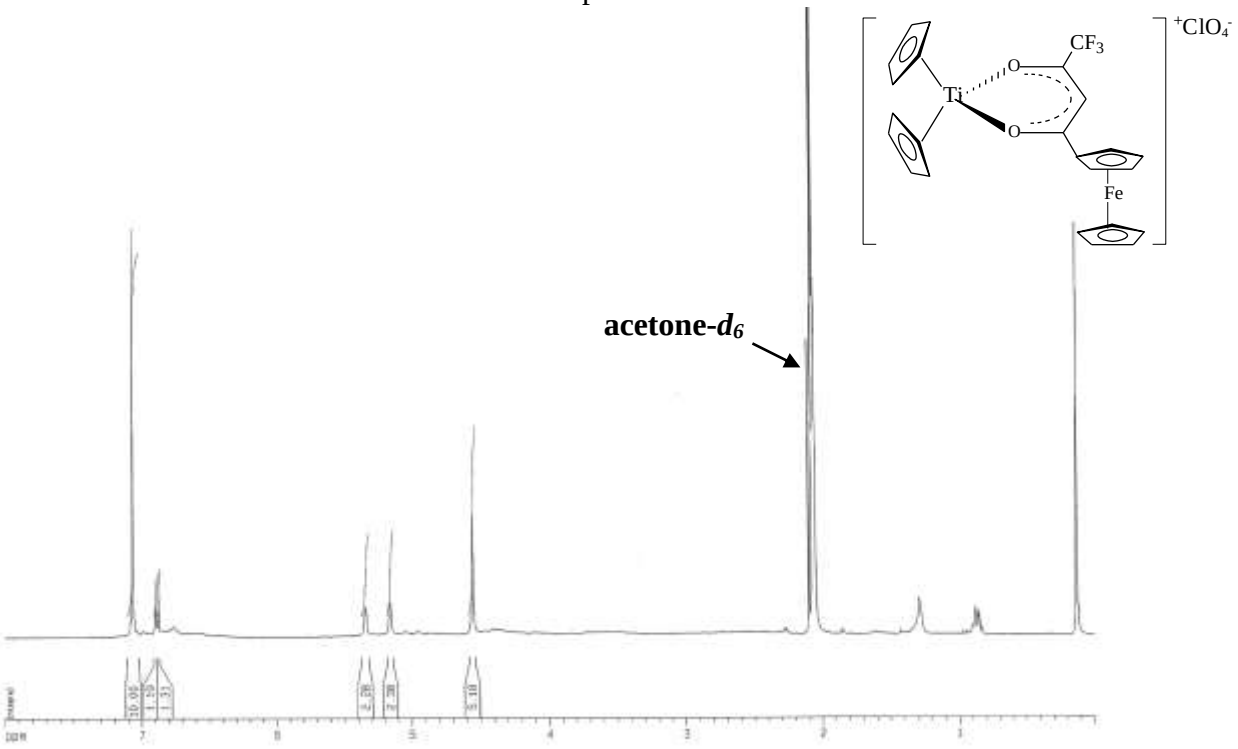

Spectrum 11: 1-ferrocenyl-4,4,4-trifluoro-1,3-butanedionato-κ^{2}O,O'-bis (η^{5}cyclopentadienyl) titanium(IV) perchlorate, [Cp$_2$Ti(FcCOCHCOCF$_3$)]$^+$ClO$_4^-$, [14]

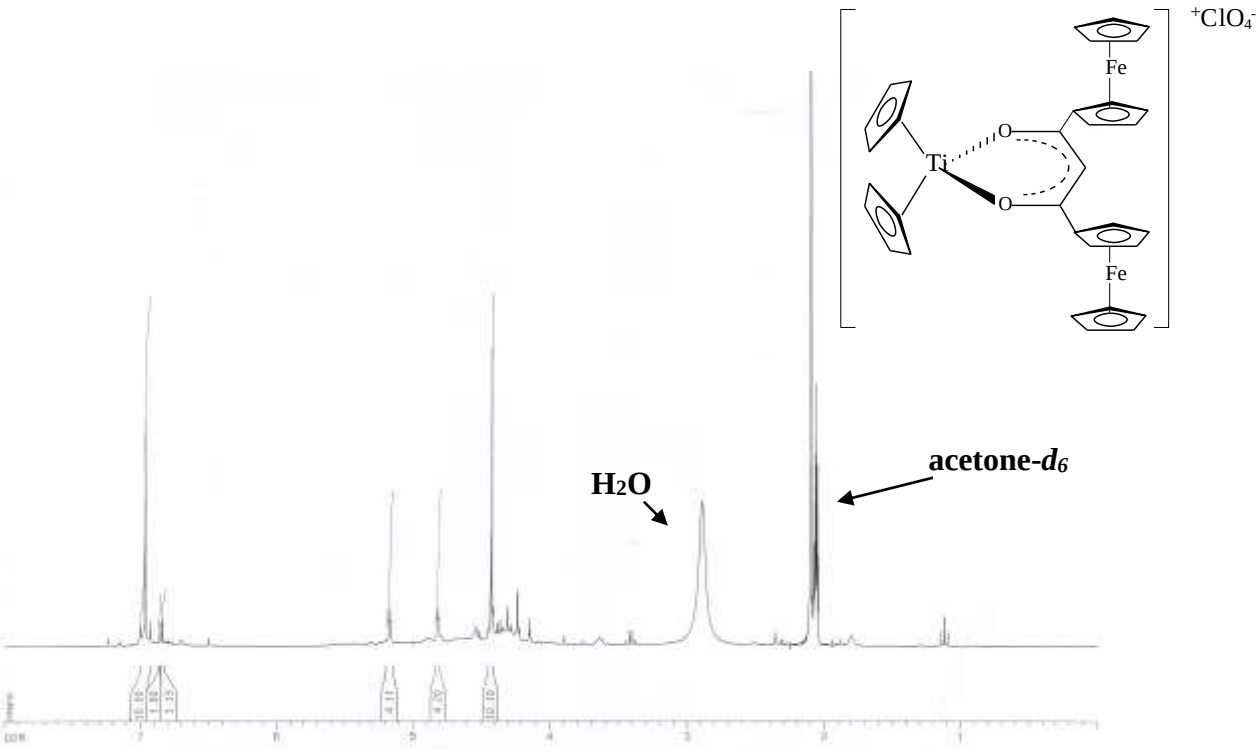

Spectrum 12: 1,3-diferrocenylpropane-1,3-dionato-κ^{2}O,O'-bis-(η^{5}cyclopentadienyl) titanium(IV) perchlorate, [Cp$_2$Ti(FcCOCHCOFc)]$^+$ClO$_4^-$, [15]

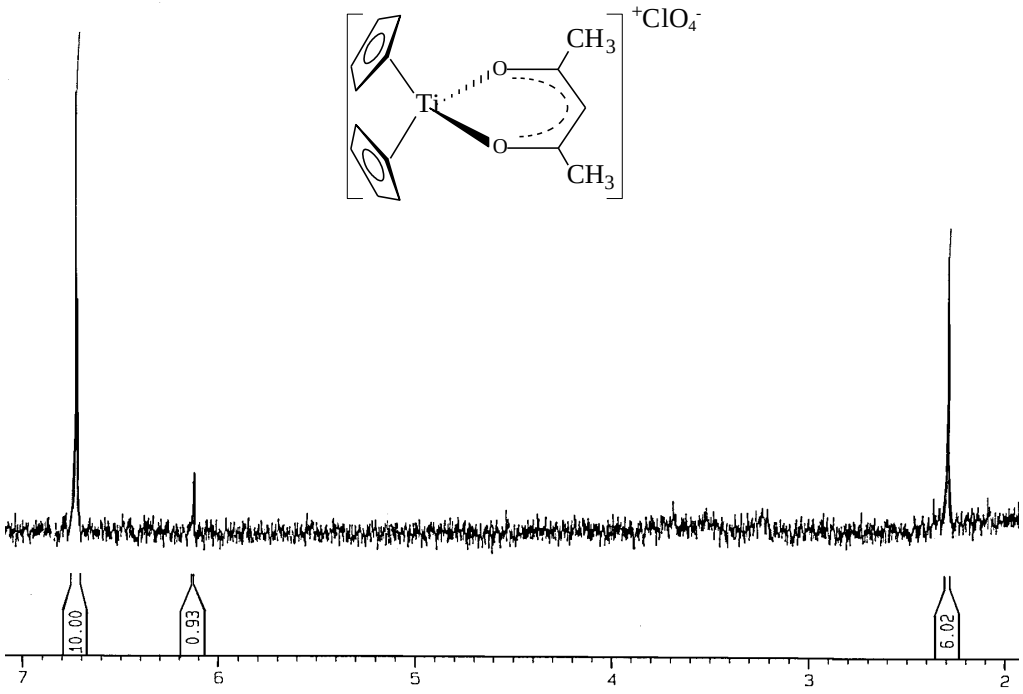

Spectrum 13: 2,4-Pentanedionato-κ^2O,O'-bis-(η^5-cyclopentadienyl) titanium(IV) perchlorate, $[Cp_2Ti(CH_3COCHCOCH_3)]^+ClO_4^-$, [16]

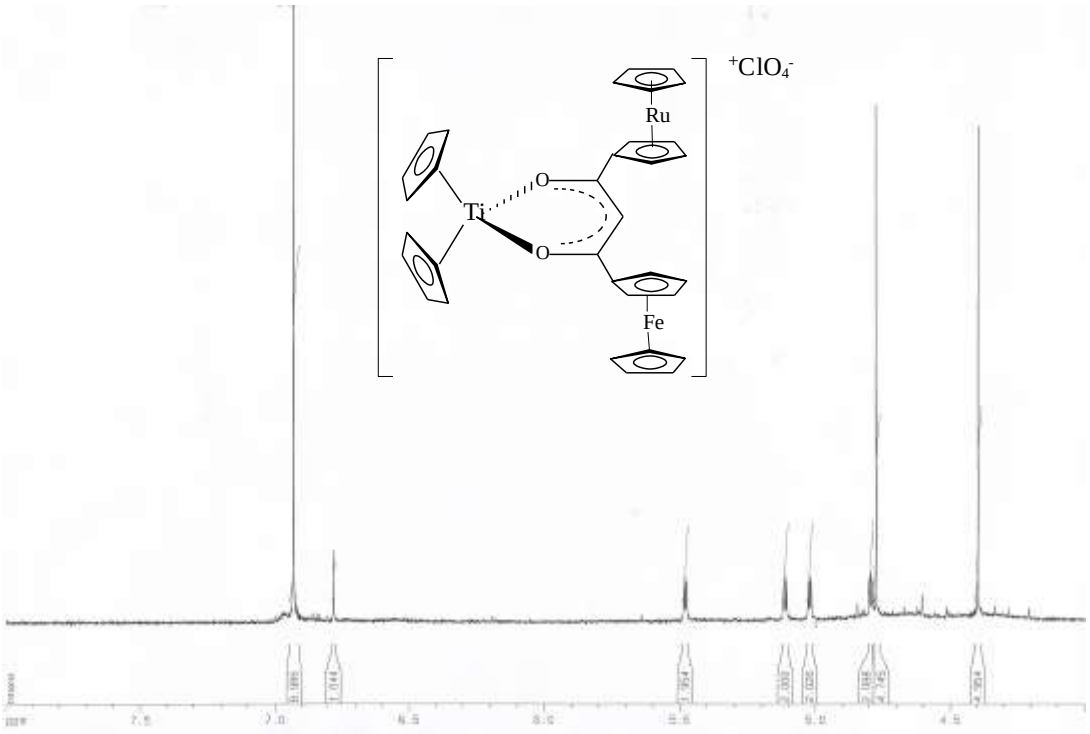

Spectrum 14: 1-ferrocenyl-3-ruthenocenylpropane-1,3-dionato-κ^2O,O'-bis-(η^5cyclopentadienyl) titanium(IV) perchlorate, $[Cp_2Ti([FcCOCHCORc)]^+ClO_4^-$, [17]

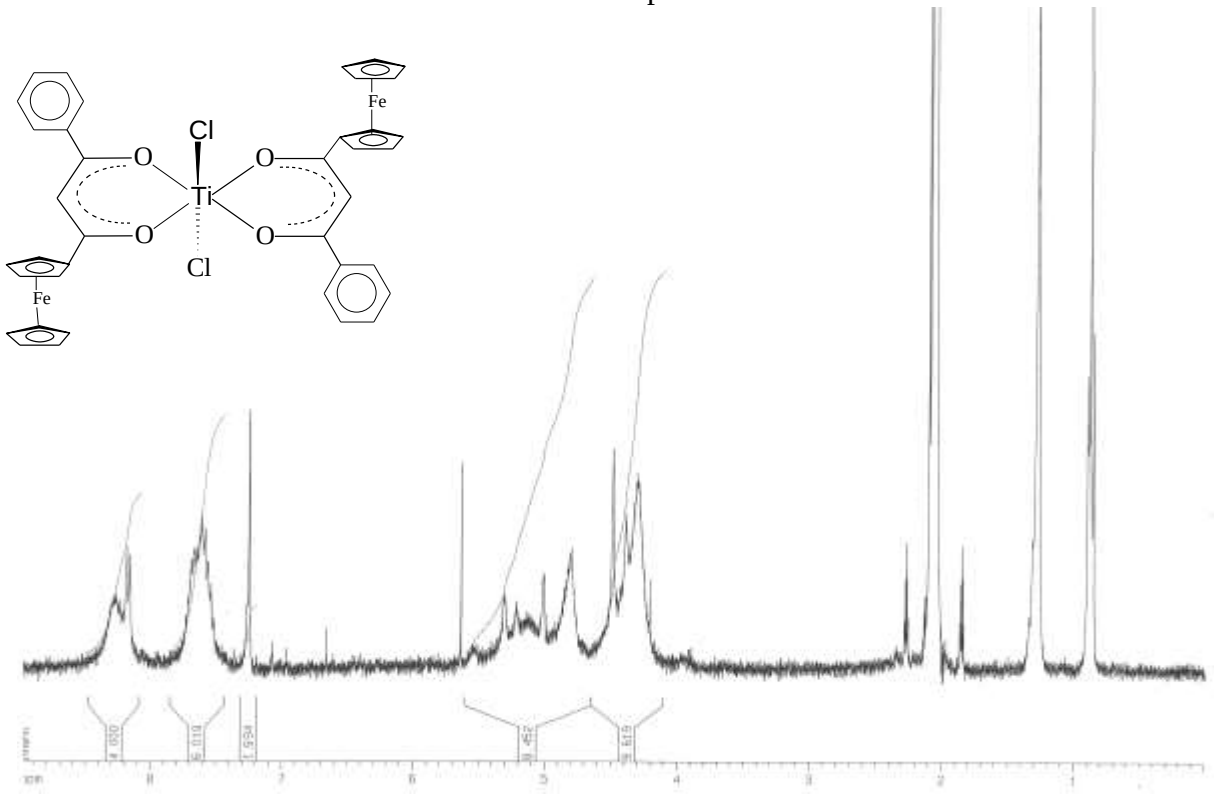

Spectrum 15: Dichlorobis-(1-ferrocenyl-3-phenyl-1,3-propanedionato) titanium(IV), [(FcCOCHCOPh)$_2$TiCl$_2$], [18]

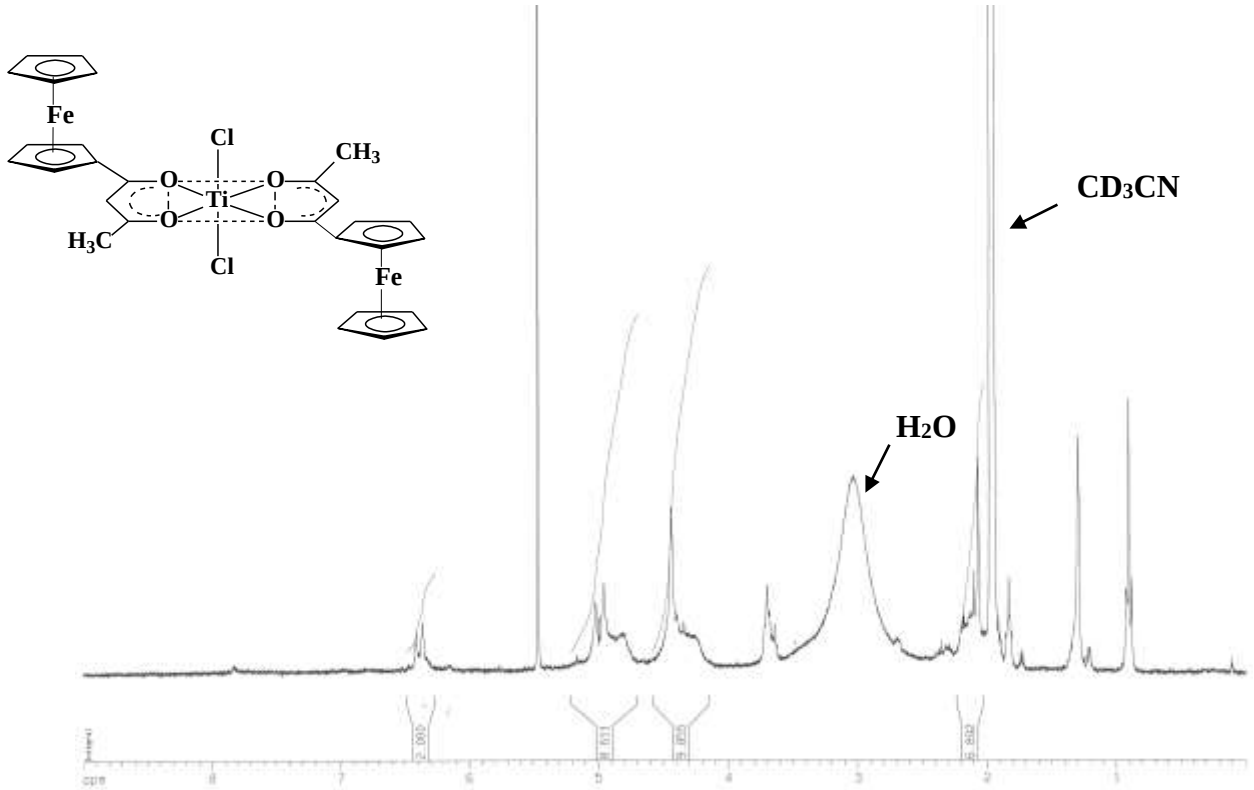

Spectrum 16: Dichlorobis-(1-Ferrocenoyl-1,3-butanedionato) titanium(IV), [(FcCOCHCOCH$_3$)$_2$TiCl$_2$], [19]

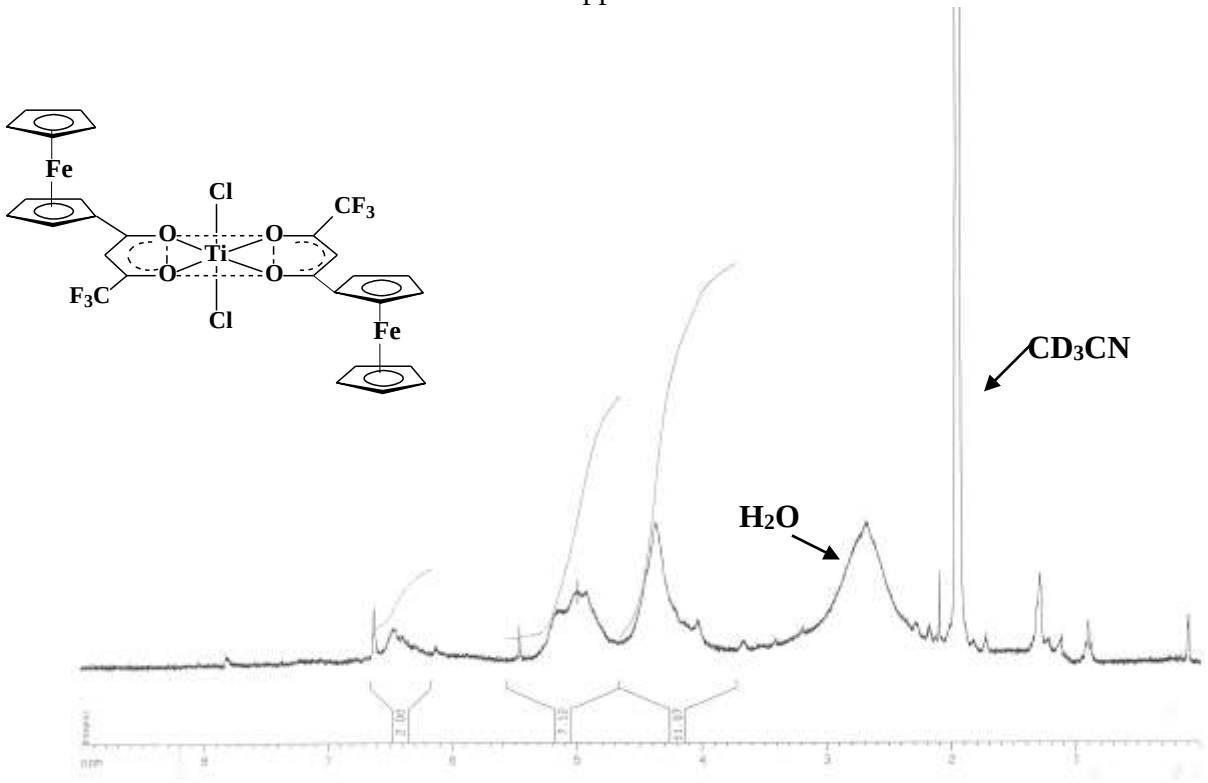

Spectrum 17: Dichlorobis-(1-ferrocenyl-4,4,4-trifluorobutane-1,3-dionato) titanium(IV), $[(FcCOCHCOCF_3)_2TiCl_2]$, [20]

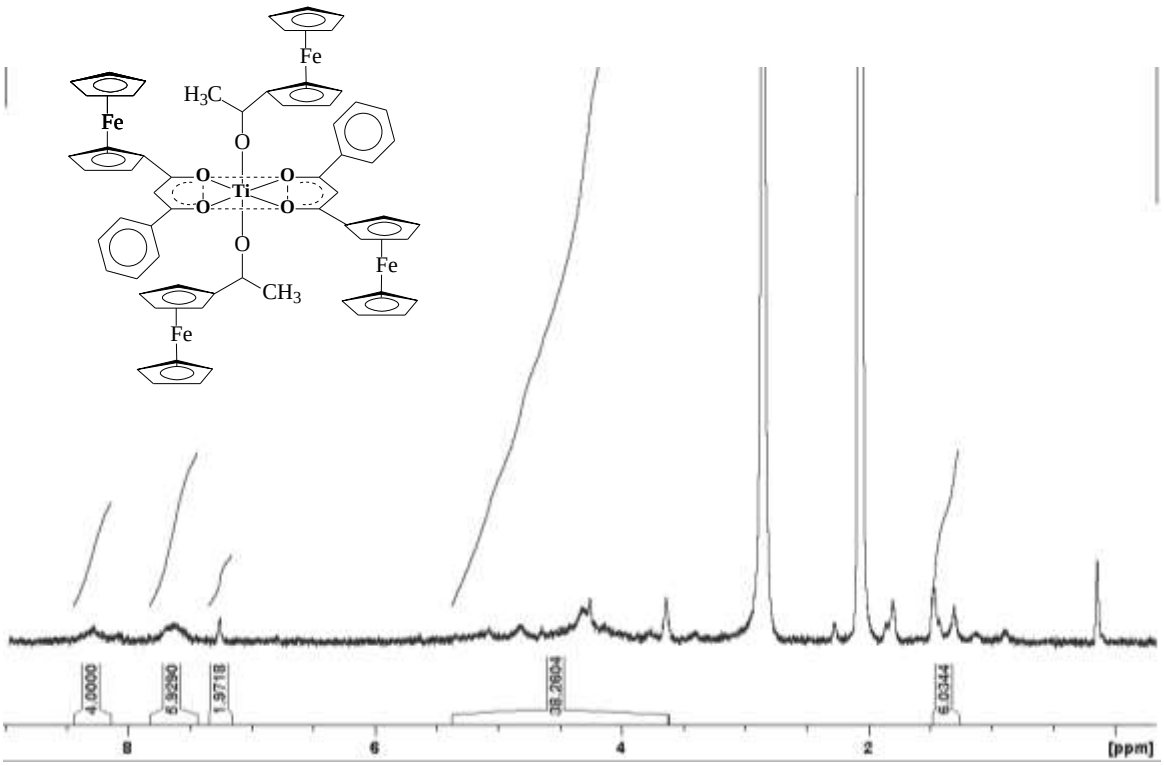

Spectrum 18: Bis-(1-oxyethyl-1-ferrocenyl)-bis-(1-ferrocenyl-3-phenyl-1,3-) titaniun(IV), $[(FcCOCHCOPh)_2Ti(O\text{-}CH\text{-}(CH_3)\text{-}Fc)_2]$, [21]

^{1}H NMR Spectra

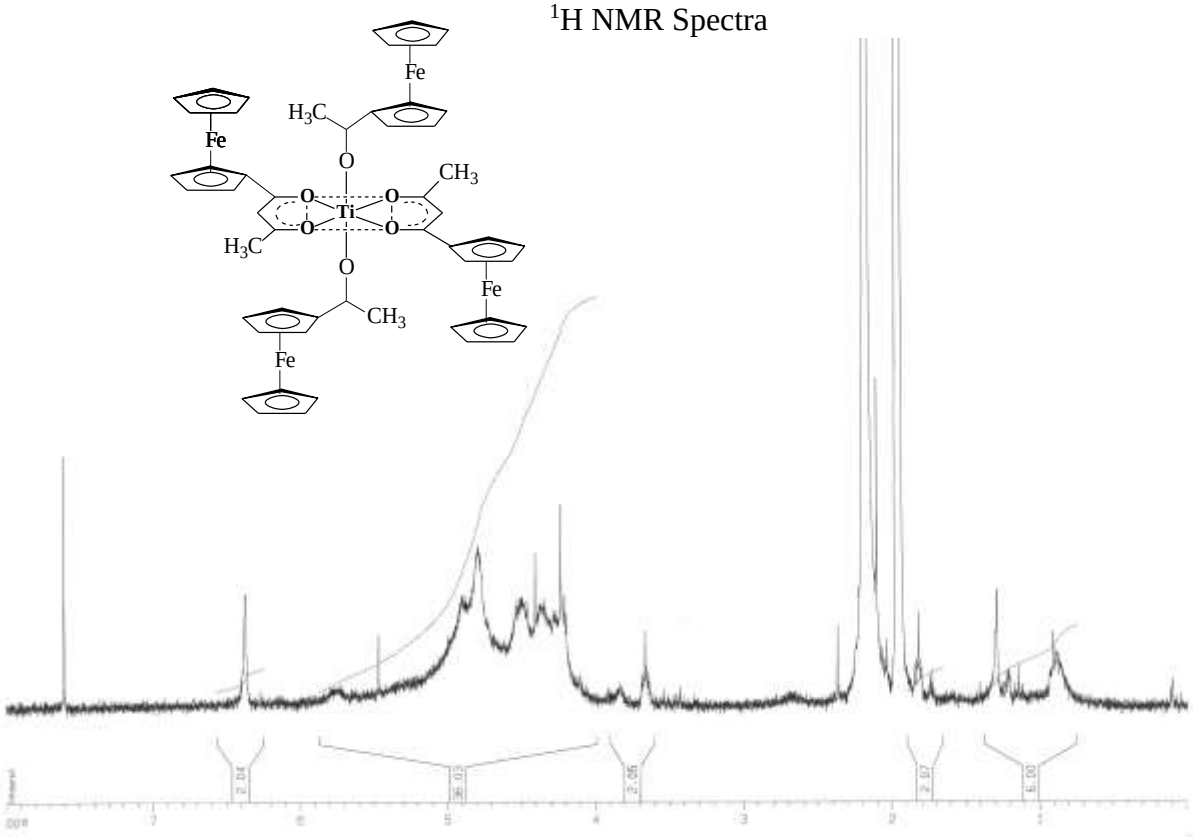

Spectrum 19: Bis-(1-oxyethyl-1-ferrocenyl)-bis-(1-Ferrocenoyl-1,3-butanedionato) titaniun(IV), [(FcCOCHCOCH$_3$)$_2$Ti(O-CH(CH$_3$)-Fc)$_2$], [22]

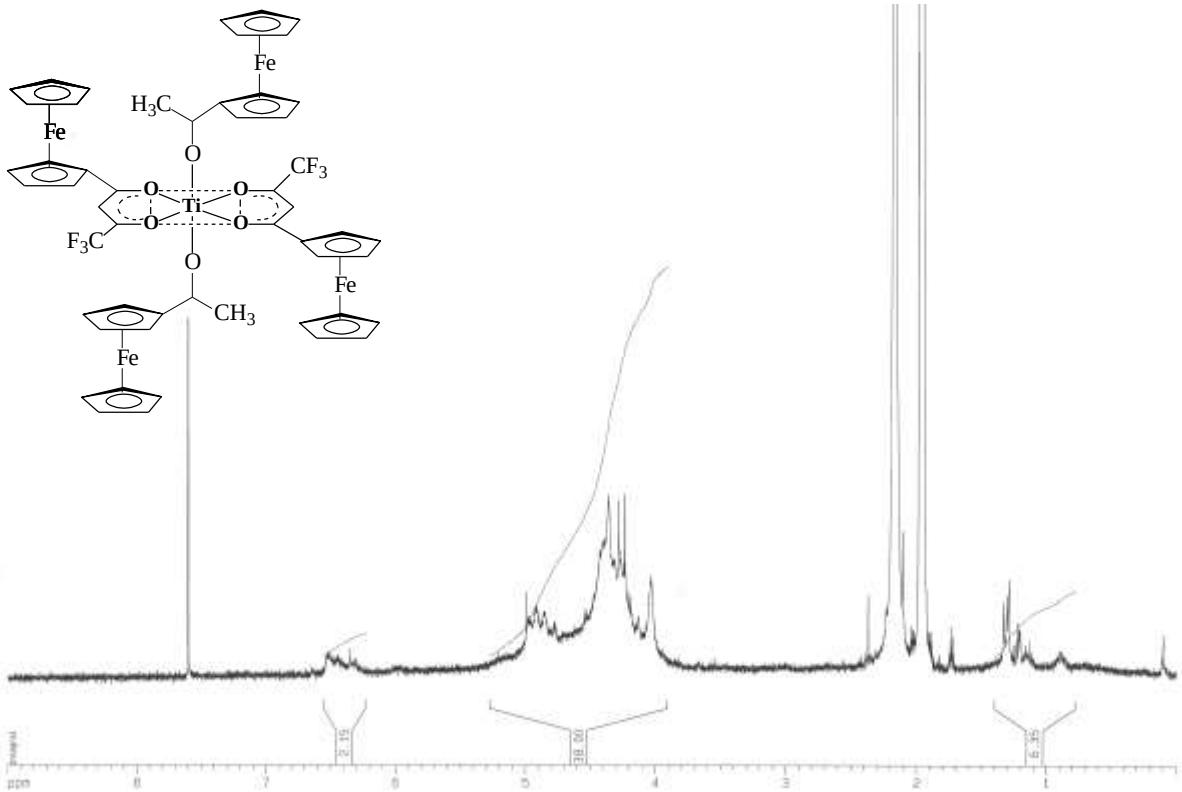

Spectrum 20: Bis-(1-oxyethyl-1-ferrocenyl)-bis-(1-ferrocenyl-4,4,4-trifluoro-butane-1,3-dionato) titaniun(IV), [(FcCOCH$_2$COCF$_3$)$_2$Ti(O(CH)CH$_3$Fc)$_2$, [23]

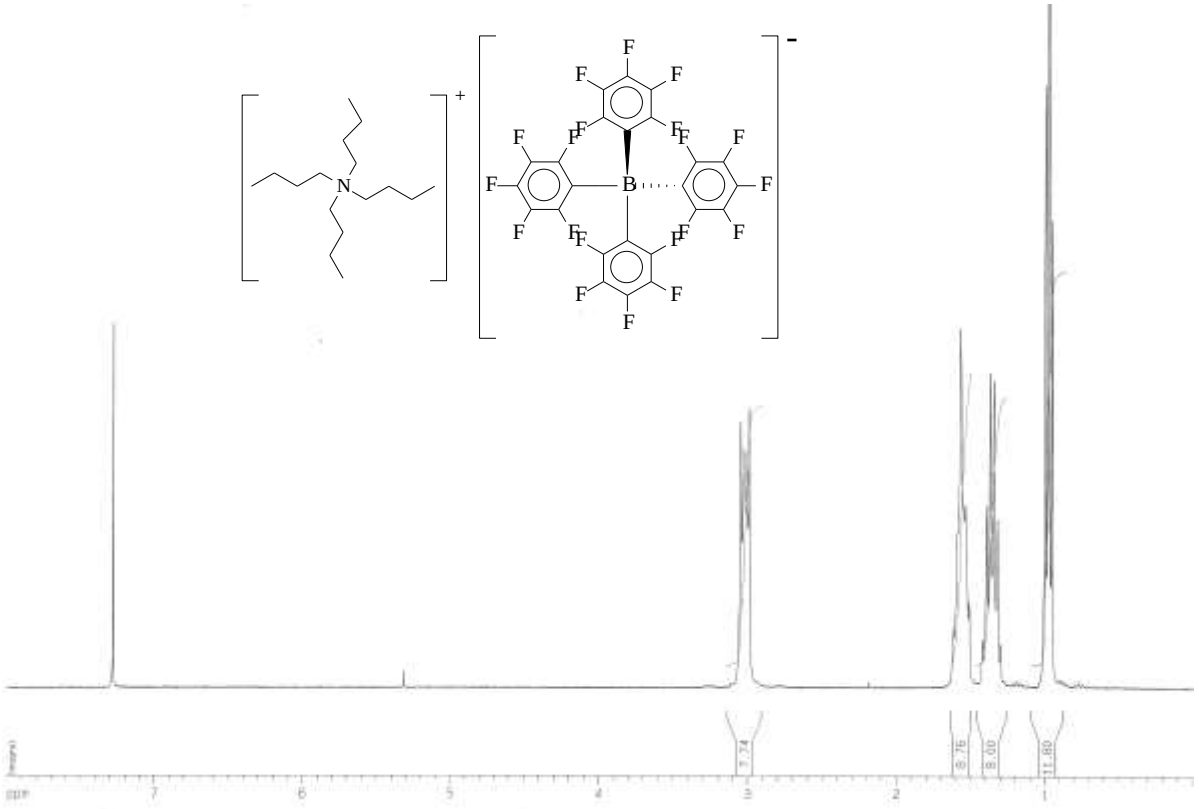

Spectrum 21: Tetrabutylammonium tetrakis[pentaflourophenyl] borate, $[N(^{n}Bu)_4][B(C_6F_5)_4]$, (BARF), [25]

Abstract

In this study ferrocene-containing β-diketones of the type [$FcCOCH_2COR$] where R = Ph, CH_3, CF_3, Fc and Rc (Fc = ferrocenyl and Rc = ruthenocenyl) and β-diketonato titanium(IV) complexes of the type [$Cp_2Ti(FcCOCHCOR)]^+ClO_4^-$, [(β-diketonato)$_2TiCl_2$] and [(β-diketonato)$_2$Ti(Fc-$CH(CH_3)O)_2$] were synthesised. Eleven of these compounds were previously unknown.

Complexes were characterised by ^{1}H NMR spectroscopy and the structures of [$RcCOCH_2COFc$] and [$Cp_2Ti(FcCOCHCOCH_3)]^+ClO_4^-$, as representative examples of two of the synthesised classes of complexes, were determined using single crystal crystallographic techniques.

Electrochemical studies were conducted in dichloromethane in the presence of [NBu_4][$B(C_6F_5)_4$] as uncoordinating supporting electrolyte. Dimerization of the ruthenocenium fragment of the β-diketone [$RcCOCH_2COFc$] was not as prominent as that of free ruthenocene. The Ru^{3+}/Ru^{2+} couple displayed irreversible electrochemistry while the Fc/Fc^+ couple was electrochemically reversible. For the Ti complexes, electrochemically quazi-reversible to irreversible behaviour was observed for the Ti^{4+}/Ti^{3+} couple, while the Fc/Fc^+ couples were mostly found to be electrochemically quasi-reversible and chemically reversible. In addition, for the mono-β-diketonato titanium(IV) salts, a splitting of the ferrocenyl peaks was discernable. This phenomenon is exceptional. A unique monomer/dimer equilibrium was proposed as a possible explanation for this observation. Intra-molecular communication between the iron centres of [$(FcCOCHCOPh)_2$Ti(Fc-$CH(CH_3)O)_2$] allowed electrochemical detection of all four ferrocenyl centres.

Cytotoxic studies revealed that complexes [$Cp_2Ti(FcCOCHCOR)]^+ClO_4^-$, which contain the titanium and ferrocenyl antineoplastic moieties, were more effective in killing CoLo and HeLa cancer cell lines than the parent titanocene dichloride compound which is currently in phase II clinical trials. These results are attributed to a synergistic effect between different fragments possessing anti-cancer activity in the same molecule.

***Keywords*:** Titanium, ferrocene, ruthenocene, β-diketones, electrochemistry and cytotoxicity.

Opsomming

In hierdie studie is ferroseen-bevattende β-diketone van [$FcCOCH_2COR$] vorm met R = Ph, CH_3, CF_3, Fc en Rc (Fc = ferroseniel en Rc = rutenoseniel) as ook β-diketonato titanium(IV) komplekse van vorm [$Cp_2Ti(FcCOCHCOR)]^+ClO_4^-$, [(β-diketonato)$_2TiCl_2$] en [(β-diketonato)$_2$Ti(Fc-$CH(CH_3)O)_2$] gesintetiseer. Elf van hierdie verbindings was tot nou toe onbekend.

Die komplekse was gekarakteriseer met behulp van ^{1}H KMR spektroskopie. Die strukture van [$RcCOCH_2COFc$] en [$Cp_2Ti(FcCOCHCOCH_3)]^+ClO_4^-$, as verteenwoordigend van twee van die gesintetiseerde kompleksklasse was ook deur enkelkristal kristalografiese tegnieke bepaal.

Elektrochemiese studies was uitgevoer in diclorometaan in die teenwoordigheid van [NBu_4][$B(C_6F_5)_4$] as nie-koördinerende ondersteuningselektroliet. Dimerisasie van die rutenosenium fragment van die [$RcCOCH_2COFc$] β-diketoon was minder prominent as vir vry rutenoseen. Onomkeerbare elektrochemie was vir die Ru^{2+}/Ru^{3+} koppel waargeneem terwyl elektrochemiese omkeerbaarheid vir die Fc/Fc^+ koppel waargeneem was. Vir die Ti komplekse was elektrochemiese kwasi-omkeerbaarheid tot onomkeerbaarheid is vir die Ti^{4+}/Ti^{3+} koppel gevind, terwyl die Fc/Fc^+ koppels elektrochemiese kwasi-omkeerbaarheid en chemiese omkeerbare gedrag getoon het. Die Fc/Fc^+ koppels het ook splyting in die mono-β-diketonato titanium(IV) soute getoon. Die verskynsel is buite gewoon. ‘n Unieke monomeer/dimeer ewewig is as ‘n moontlike verduideliking vir hierdie waarneming voorgehou. Intra-molekulêre komunikasie tussen die ysterkerne van [$(FcCOCHCOPh)_2$Ti(Fc-$CH(CH_3)O)_2$] het elektrochemiese waarneming van al vier ferroseniel groepe toegelaat.

Sitotoksiese studies het getoon dat die antineoplastiese titanium- en ferrosenielbevattende [$Cp_2Ti(RcCOCHCOR)]^+ClO_4^-$ komplekse, meer effektief CoLo en HeLa kankersellyne vernietig as titanoseendicloried wat huidiglik in fase II kliniese proewe is. Hierdie resultaat is toegeskryf aan ‘n sinergistiese effek wat tussen die verskillende kankerbestrydende molekulêre fragmente bestaan.

Sleutelwoorde: Titanium, ferroseen, rutinoseen, β-diketone, elektrochemie en sitotoksisiteit.